frontiers | Research Topics

Case reports in neuromuscular disorders and peripheral neuropathies, volume III, 2023

Edited by
Giovanni Meola

Published in
Frontiers in Neurology

ISSN 1664-8714
ISBN 978-2-8325-4825-7
DOI 10.3389/978-2-8325-4825-7

About Frontiers

Frontiers is more than just an open access publisher of scholarly articles: it is a pioneering approach to the world of academia, radically improving the way scholarly research is managed. The grand vision of Frontiers is a world where all people have an equal opportunity to seek, share and generate knowledge. Frontiers provides immediate and permanent online open access to all its publications, but this alone is not enough to realize our grand goals.

Frontiers journal series

The Frontiers journal series is a multi-tier and interdisciplinary set of open-access, online journals, promising a paradigm shift from the current review, selection and dissemination processes in academic publishing. All Frontiers journals are driven by researchers for researchers; therefore, they constitute a service to the scholarly community. At the same time, the *Frontiers journal series* operates on a revolutionary invention, the tiered publishing system, initially addressing specific communities of scholars, and gradually climbing up to broader public understanding, thus serving the interests of the lay society, too.

Dedication to quality

Each Frontiers article is a landmark of the highest quality, thanks to genuinely collaborative interactions between authors and review editors, who include some of the world's best academicians. Research must be certified by peers before entering a stream of knowledge that may eventually reach the public - and shape society; therefore, Frontiers only applies the most rigorous and unbiased reviews. Frontiers revolutionizes research publishing by freely delivering the most outstanding research, evaluated with no bias from both the academic and social point of view. By applying the most advanced information technologies, Frontiers is catapulting scholarly publishing into a new generation.

What are Frontiers Research Topics?

Frontiers Research Topics are very popular trademarks of the *Frontiers journals series*: they are collections of at least ten articles, all centered on a particular subject. With their unique mix of varied contributions from Original Research to Review Articles, Frontiers Research Topics unify the most influential researchers, the latest key findings and historical advances in a hot research area.

Find out more on how to host your own Frontiers Research Topic or contribute to one as an author by contacting the Frontiers editorial office: frontiersin.org/about/contact

Case reports in neuromuscular disorders and peripheral neuropathies, volume III, 2023

Topic editor
Giovanni Meola — University of Milan, Italy

Citation
Meola, G., ed. (2024). *Case reports in neuromuscular disorders and peripheral neuropathies, volume III, 2023*. Lausanne: Frontiers Media SA.
doi: 10.3389/978-2-8325-4825-7

Table of contents

frontiers | Frontiers in Neurology

TYPE Case Report
PUBLISHED 02 June 2023
DOI 10.3389/fneur.2023.1170071

OPEN ACCESS

EDITED BY
Serdar Ceylaner,
Intergen Genetic Diagnosis and Research Center, Turkey

REVIEWED BY
Per Harald Jonson,
University of Helsinki, Finland
Afagh Alavi,
University of Social Welfare and Rehabilitation Sciences, Iran

*CORRESPONDENCE
Dario Ronchi
✉ dario.ronchi@unimi.it

RECEIVED 20 February 2023
ACCEPTED 16 May 2023
PUBLISHED 02 June 2023

CITATION
Velardo D, Antognozzi S, Rimoldi M, Pagliarani S, Cogiamanian F, Barbieri S, Corti S, Comi GP and Ronchi D (2023) Case report: Clinical and molecular characterization of two siblings affected by Brody myopathy. *Front. Neurol.* 14:1170071. doi: 10.3389/fneur.2023.1170071

Case report: Clinical and molecular characterization of two siblings affected by Brody myopathy

Daniele Velardo[1], Sara Antognozzi[2], Martina Rimoldi[3], Serena Pagliarani[2], Filippo Cogiamanian[4], Sergio Barbieri[4], Stefania Corti[2,3], Giacomo Pietro Comi[1,3] and Dario Ronchi[3]*

[1]Fondazione IRCCS Ca' Granda Ospedale Maggiore Policlinico, Neuromuscular and Rare Disease Unit, Milan, Italy, [2]Fondazione IRCCS Ca' Granda Ospedale Maggiore Policlinico, Neurology Unit, Milan, Italy, [3]Dino Ferrari Center, Department of Pathophysiology and Transplantation, University of Milan, Milan, Italy, [4]Fondazione IRCCS Ca' Granda Ospedale Maggiore Policlinico, Neurophysiology Unit, Milan, Italy

Exercise-induced muscle stiffness is the hallmark of Brody disease, an autosomal recessive myopathy due to biallelic pathogenic variants in *ATP2A1*, encoding the sarcoplasmic/endoplasmic reticulum Ca^{2+} ATPase SERCA1. About 40 patients have been reported so far. Our knowledge about the natural history of this disorder, genotype–phenotype correlations and the effect of symptomatic treatment is partial. This results in incomplete recognition and underdiagnosis of the disease. Here, we report the clinical, instrumental, and molecular features of two siblings presenting childhood-onset exercise-induced muscle stiffness without pain. Both the probands display difficulty in climbing stairs and running, frequent falls, delayed muscle relaxation after exertion. Cold temperatures worsen these symptoms. No myotonic discharges were observed at electromyography. Whole Exome Sequencing analysis in the probands revealed the presence of two *ATP2A1* variants: the previously reported frameshift microdeletion c.2464delC and the likely pathogenic novel splice-site variant c.324+1G>A, whose detrimental effect was demonstrated in *ATP2A1* transcript analysis. The bi-allelic inheritance was verified by Sanger sequencing in the unaffected parents. This study expands the molecular defects associated with Brody myopathy.

KEYWORDS

Brody myopathy, SERCA1, *ATP2A1*, WES, neuromuscular disorder

1. Introduction

Brody Myopathy (BM, MIM # 601003) is a muscle disorder characterized by childhood onset exercise-induced progressive impairment of muscle relaxation, stiffness, cramps, and myalgia, predominantly in upper and lower limbs and face (eyelids). Symptoms generally improve after a few minutes of rest and may be exacerbated by cold. This disorder is recessively inherited and associated with pathogenic variants in the *ATP2A1* gene encoding for the Sarco(Endoplasmic) Reticulum Calcium ATPase protein SERCA1 (1–3).

SERCA1 catalyzes the ATP-dependent uptake of Ca^{2+} from the cytosol to sarcoplasmic reticulum taking part in the regulation of calcium levels in the sarcoplasmic reticulum and therefore muscle contraction (4, 5). In Brody myopathy patients, the activity of SERCA1 in type II muscle fibres is reduced, resulting in delayed muscle relaxation, silent cramps, muscle weakness and muscle atrophy. The reduction of SERCA1 activity has been documented in

available muscle samples from affected patients, supporting at biochemical and histochemical level the diagnosis of Brody myopathy. Since SERCA1 is uniquely expressed in type II (fast-twitch) skeletal muscle fibres, exercise-induced muscle stiffness in Brody disease is primarily triggered by phasic (rapid and intense contractions), but not tonic (slow movements), activity (3).

Although about 40 patients from 28 different families affected with Brody myopathy have been reported so far, since the first description in 1969 (6), our knowledge about disease progression and pathogenesis are far from being exhaustive (2, 4, 7–12).

Here we report two siblings with clinical symptoms suggestive of Brody myopathy. Whole Exome Sequencing analysis (WES) allowed the identification of two *ATP2A1* variants, one of which was novel. Clinical, instrumental, and molecular findings are discussed in view of previous literature in the field.

2. Case reports

2.1. Patient 1

Patient 1 is a 19-years-old boy, second-born to non-consanguineous and healthy parents of Italian origin. Family history is uneventful and negative for neuromuscular problems (see Figure 1).

The prenatal and perinatal history is unremarkable. His psychomotor development was regular.

Since his first childhood, he showed difficulty climbing and descending stairs and running, with frequent falls. At the age of 5 years, he experienced transient upper limb tremors with spontaneous resolution (Table 1).

At the age of 12, a neurological examination revealed mild running impairment and delayed muscle relaxation after closing fists. His serum creatine kinase (CK) levels were normal. In addition, to exclude a GLUT1 deficiency syndrome with infantile onset, he underwent *SLC2A1* gene sequencing, which was negative.

At the age of 18 years, the proband was referred to our center for neurological examination.

The clinical evaluation showed a negative neurological examination, except for an awkward running with lower limbs muscle stiffness. After repeated movements, such as fist opening and closing, wrist and ankle flexion and extension, delayed muscle relaxation phenomenon became evident bilaterally.

Electromyography (EMG) and nerve conduction studies (NCS) results were normal. In addition, a short and long exercise test on bilateral deep finger flexor muscles was performed, which was unremarkable. Specifically, both before and after repeated voluntary contractions, in basal condition and after limb cooling, there were no myotonic discharges, however the patient clinically demonstrated delay of muscle relaxation after repetitive efforts (silent contractures).

During the diagnostic assessment at our Center, the patient underwent *SCN4A* gene sequencing to exclude a Non-Dystrophic Myotonia (NDM, specifically the Paramyotonia Congenita of von Eulenburg, MIM #168300). This analysis turned out negative.

The patient currently reports a feeling of muscle stiffness during exercise, not accompanied by pain, which forces him to stop and rest to resume the physical activity; he does not report cramps, nor myoglobinuria. He regularly practices sports activity.

Notably, proband's symptoms worsen upon exposure to cold temperatures but are stable over time.

2.2. Patient 2

Patient 2 is Patient 1's 23 years old sister. She was born by induced delivery at 30 weeks of gestation after spontaneous pregnancy complicated by gestosis. Perinatal period was characterized by two episodes of pneumothorax. Her psychomotor development was regular.

Clinical symptoms, including age and onset modalities, overlap those observed in her brother (Table 1).

At the age of 15, she was referred to another Institute for neurological evaluation: the CK dosage and NCS/EMG analysis were normal. After genetic counseling, she underwent a Next Generation Sequencing (NGS) analysis targeted on genes related to metabolic conditions, which gave negative results. A carb-free diet was started with no benefit.

Lastly, she was referred to our Institute at the age of 22 years. Her neurological evaluation was overlapping with her brother's. The NCS/EMG was again normal; the short and long exercise test performed on deep finger flexor muscles and on quadriceps, before and after effort, revealed silent contractures (prolonged involuntary muscle contractions) following voluntary phasic contractions, without electrical activity detected by needle.

To date, she reports difficulties in walking, running, and climbing stairs. She complains of a sensation of motor impairment as soon as the muscle activity begins (muscle stiffness at the start of exercise). She currently practices physical activity.

3. Methods

3.1. DNA analysis

After obtaining signed written informed consent, genomic DNA was extracted from peripheral blood obtained from the patients and their parents, on a QiaSymphony Automated Nucleic Acid Extraction Platform (QIAGEN).

Whole Exome Sequencing was performed starting from 100 ng of high-quality DNA of the two affected siblings and the parents by using Agilent SureSelectXT Human All Exon V8 library preparation and target enrichment kit. The libraries underwent paired-end sequencing on a NextSeq2000 Illumina platform. The variants included in the generated VCF files were annotated (according to the genome assembly of hg19) and classified according to an internal analysis pipeline (13) and by using the bioinformatic tool eVai Expert Variant Interpreter v2.7.

Filtering criteria applied were: (i) variants with a Quality Score > 30, (ii) variants with allele frequency < 0.1 (gnomAD), (iii) variants shared by affected subjects, (iv) variants presenting biallelic inheritance, and (v) variants presenting a coding impact or in conserved splice sites. The candidate variants in the *ATP2A1* gene were validated by using PCR amplification followed by Sanger sequencing (Thermo Fisher Big Dye Terminator v3.1) on an ABI Prism 3,130 automated DNA analyzer.

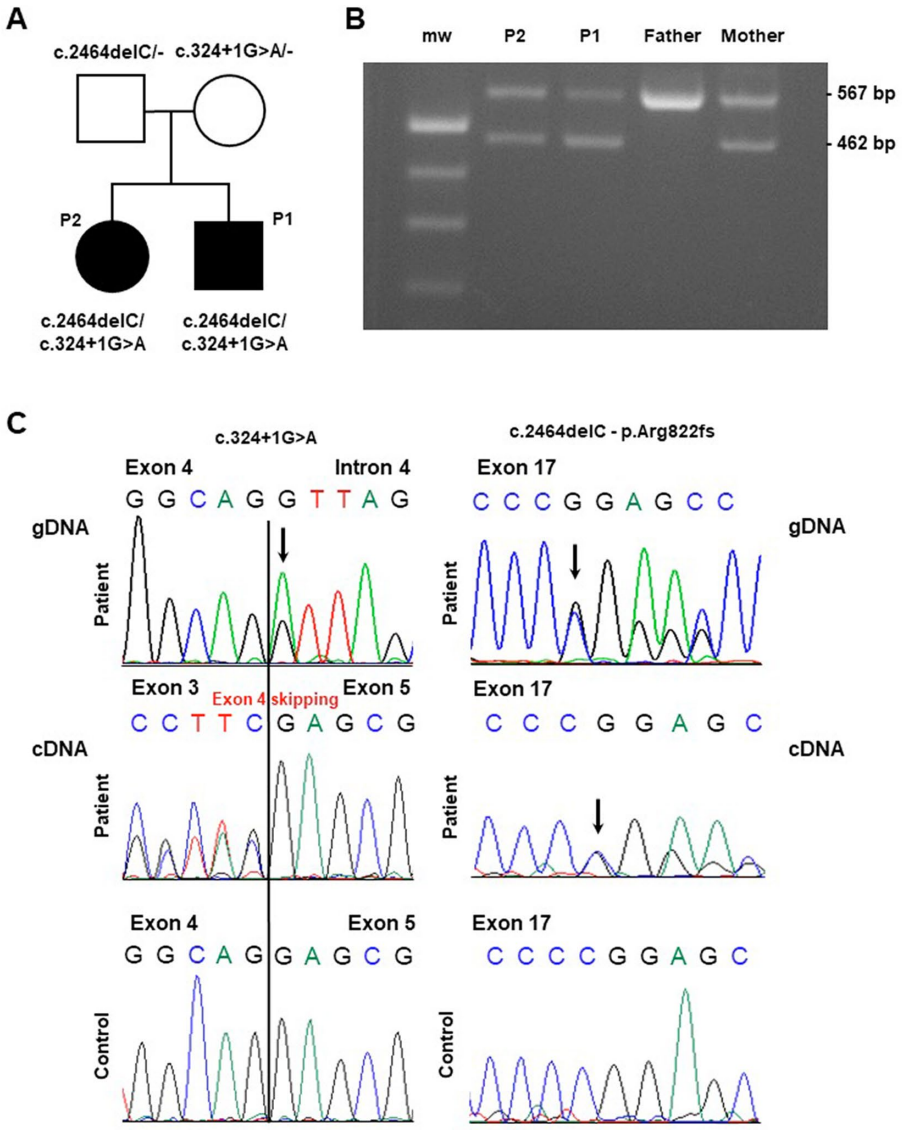

FIGURE 1
Molecular findings in the investigated pedigree. **(A)** Pedigree of the family. Black symbols indicate the affected probands (patient 1: "P1" and patient 2: "P2") carrying the described *ATP2A1* variants. **(B)** Gel agarose showing RT-PCR products encompassing exons 1 and 6, obtained by blood extracted cDNA showing, besides the wild-type band, a smaller fragment compatible the skipping of part of the *ATP2A1* transcript in the affected siblings and their mother ("mw" indicates the molecular weight). **(C)** Sequence electropherogram of genomic (gDNA) and complementary (cDNA) DNA products showing the effect of the c.324+1G>A variation in the alteration of physiological splicing of *ATP2A1*. The heterozygous deletion c.2464delC, resulting in the loss of *ATP2A1* reading frame, is observed at genomic and cDNA level.

3.2. Transcript analysis

Total RNA was extracted from peripheral blood obtained from the subjects investigated by using Thermo Fisher Tempus Spin RNA Isolation Kit. RNA was retrotranscribed into cDNA using Maxima Reverse Transcriptase (Thermo Scientific). For the analysis of *ATP2A1* transcript, specific primers were designed to amplify the regions corresponding to exons 1–6 and 17 (available upon request) based on the reference sequence NM_ 004320. Resulting Polymerase Chain Reaction (PCR) products were stained with ethidium bromide and visualized on 2% agarose gels and then were sequenced as described above.

4. Results

Whole Exome Sequencing analysis identified two *ATP2A1* (NM_004320.6) variants in the affected siblings: the microdeletion chr16:28913640C/– corresponding to c.2464delC (p.Arg822Glyfs*49) and the single nucleotide variant chr16:28892341G/A corresponding to c.324 + 1G > A. The two variants segregated from father and mother, respectively (see Figure 1A).

The c.2464delC variant is rare (GnomAD 2.1 frequency in non-Finnish European population is 0.003%) and has been previously reported as a likely pathogenic variant in the ClinVar database (Accession VCV000464084.5).

10.3389/fneur.2023.1170071

TABLE 1 Patients timelines.

Patient 1				
2008 Childhood	2015 12 yo	January 2022 18 yo+1 mo	May 2022 18 yo+5 mos	October 2022 18 yo+10 mos
First signs and symptoms	1st neurological evaluation; *SLC2A1* seq. (neg)	Referral to our Institute and clinical evaluation; *SNC4A* seq. (neg)	CK dosage (normal); EMG and S/L exercise tests; Informed consent for WES	WES confirms the diagnosis of BM

Patient 2				
2005 Childhood	2015 15 yo	January 2022 22 yo	May 2022 22 yo+4 mos	October 2022 22 yo+9 mos
First signs and symptoms	1st neurological evaluation; NGS (metabolic diseases) (neg); CK dosage (normal); EMG	Referral to our Institute and clinical evaluation	EMG and S/L exercise tests; Informed consent for WES	WES confirms the diagnosis of BM

NGS, next generation sequencing; WES, whole exome sequencing; yo, years old; mo/mos, month/months; neg, negative; seq., sequencing; S/L, short/long.

The c.324 + 1G > A variant is not reported in population databases. This variant, affecting the conserved donor splice site downstream Exon 4, is predicted to alter physiological splicing. By using Reverse Transcription PCR analysis on proband's blood-extracted RNA, we observed the skipping of the whole Exon 4 as demonstrated by gel agarose electrophoresis (Figure 1B) and sequencing (Figure 1C). This alteration is expected to preserve the reading frame. Both the variants are classified as Likely Pathogenic (class 4), according ACMG criteria (PVS1, PM2) (14).

5. Discussion

Here we report the clinical and molecular features of two siblings in which a diagnosis of Brody myopathy was clinically suspected and confirmed by Whole Exome Sequencing applied to the patients pedigree. These findings were compared with those reported in a recent publication investigating a cohort of 40 patients affected with Brody disease (7).

BM is known to typically manifest in the first decade of life, even though patients usually do not present to a physician until their third decade (7).

In our patients, the first evidence of exercise induced muscle stiffness occurred during childhood. Anyway, the siblings were referred to our Institute for neurological examination and received a molecular diagnosis only at the age of 18 (patient 1) and 22 (patient 2). Among the probands to date reported, only 7 patients have been diagnosed before age 22, even though symptoms had emerged relatively early, during childhood or before the age of 10 years.

Both our patients suffer from exercise-induced muscle stiffness with delayed muscle relaxation, predominantly affecting the lower limbs, with symptoms emerging after explosive, short, and repetitive contractions: this is coherent with the selective type II muscle fiber involvement usually observed in BM. The high percentage of type II muscle fibres in orbicularis oculi muscle also explains the eyelid involvement reported in 63% of probands. Anyway, facial muscles, and eyelids were preserved in our patients.

Similarly to the majority of Brody myopathy patients to date reported (25 out of 36, 70%), our patients mention an increase of symptoms upon exposure to cold temperatures.

Both our probands can currently practice sports (including strength exercises) regularly. On the Modified Rankin Scale (MRS), we could assign a patients disability score of 1/5, corresponding to "no significant disability despite symptoms, able to perform all usual activities and tasks." Our patients do not need any symptomatic treatment and they never underwent physical therapy. In addition, their symptoms do not show a progression and are stable over time. Considering the 40 BM patients so far reported, symptoms were progressive in 23% of them but did not become debilitating: the MRS was performed in 23 of them and scored "1" and "2" (mild disability: no longer able to carry out all the previous activities but independent in walking/daily life activities) in 10 (43%) and 13 probands (57%), respectively (7).

Regarding the EMG findings, none of the patients previously described had myotonic discharges on EMG, while silent contractures were present in 18/28 patients (64%) (7). Even in our two patients, the EMG was normal and short and long exercise tests showed silent contractures.

Except for the EMG findings, the symptoms described in BM are commonly reported in many other neuromuscular disorders, so that Brody myopathy might resemble other hereditary conditions genetically determined, such as myotonic dystrophies or sodium/chloride channelopathies. For this reason, Patient 1 underwent *SCN4A* gene sequencing at the age of 18, since a Paramyotonia Congenita of von Eulenburg was suspected (2, 15–19).

In inherited neuromuscular disorders, a comprehensive clinical assessment contributes to achieve a molecular diagnosis (i.e., by addressing the most appropriate genetic testing). This concept is easily applied to Brody disease where the following cardinal clinical features are associated with the disorder: muscle stiffness consequent to short,

repetitive, and explosive movements, the presence of symptoms manifesting on vigorous exercise, the absence of a warm-up phenomenon (2, 19).

WES analysis, our current choice for the diagnosis of familial forms of neuromuscular presentations, revealed the presence of the previously unreported c.324 + 1G > A variant in *ATP2A1*. This variant is classified as likely pathogenic and results in the skipping of Exon 4 coding for a region encompassing SERCA1 transmembrane domain M2. This region helps to anchor the actuator domain to the rest of the protein (1), and its absence likely results in protein instability and impairment of SERCA1 function. The second variant, c.2464delC, has been previously reported in independent ClinVar submissions associated with Brody Myopathy. No obvious correlation between genotype and phenotype has so far emerged.

To date, there is no specific treatment and cure for BM. Some therapeutic strategies have been considered such as the use of drugs promoting Ca^{2+} efflux from the cytosol or aiming to reduce proteasomal SERCA1 disposal (20, 21).

In conclusion, our report expands the clinical and molecular features associated with *ATP2A1* variants in Brody Myopathy. Our findings contribute to define the clinical presentation associated with this condition.

Data availability statement

The datasets presented in this article are not readily available because of ethical and privacy restrictions. Requests to access the datasets should be directed to the corresponding author.

Ethics statement

The studies involving human participants were reviewed and approved by Comitato Etico Milano Area 2 Fondazione IRCCS Ca' Granda Ospedale Maggiore Policlinico (Milan, Italy). The patients/participants provided their written informed consent to participate in this study. Written informed consent was obtained from the individual(s) for the publication of any potentially identifiable images or data included in this article.

Author contributions

DV, MR, and DR interpreted the results, conceived the idea, revised the literature, and wrote the manuscript. SA and SP performed genetic analysis. DV, MR, and SC made the clinical evaluation. FC and SB performed neurophysiological assessment. SC and GPC performed a critical revision of the manuscript for important intellectual content. All authors contributed to the article and approved the submitted version.

Funding

This study was (partially) funded by Italian Ministry of Health – Current research IRCCS Ca′ Granda Ospedale Maggiore Policlinico and by SEQMD project (IRCCS Cà Granda Ospedale Maggiore Policlinico, PI: Giacomo Comi).

Acknowledgments

This work was promoted within the European Reference Network (ERN) for Rare Neuromuscular Diseases. The authors thank the Association Centro Dino Ferrari for its support, the patients and their family members who participated in this study.

Conflict of interest

The authors declare that the research was conducted in the absence of any commercial or financial relationships that could be construed as a potential conflict of interest.

Publisher's note

References

1. Barbot T, Beswick V, Montigny C, Quiniou É, Jamin N, Mouawad e L. Deciphering the mechanism of inhibition of SERCA1a by sarcolipin using molecular simulations. *Front Mol Biosci*. (2021) 7:606254. doi: 10.3389/fmolb.2020.606254

2. Braz L, Soares-dos-Reis R, Seabra M, Silveira F, Guimarães e J. Brody disease: when myotonia is not myotonia. *Pract Neurol*. (2019) 19:417–9. doi: 10.1136/practneurol-2019-002224

3. Guglielmi V, Vattemi G, Gualandi F, Voermans NC, Marini M, Scotton C, et al. SERCA1 protein expression in muscle of patients with Brody disease and Brody syndrome and in cultured human muscle fibers. *Mol Genet Metab*. (2013) 110:162–9. doi: 10.1016/j.ymgme.2013.07.015

4. Benders AA, Veerkamp JH, Oosterhof A, Jongen PJ, Bindels RJ, Smit LM, et al. Ca2+ homeostasis in Brody's disease. A study in skeletal muscle and cultured muscle cells and the effects of dantrolene and verapamil. *J Clin Invest*. (1994) 94:741–8. doi: 10.1172/JCI117393

5. Benders AA, Wevers RA, Veerkamp e JH. Ion transport in human skeletal muscle cells: disturbances in myotonic dystrophy and Brody's disease. *Acta Physiol Scand*. (1996) 156:355–67. doi: 10.1046/j.1365-201X.1996.202000.x

6. Brody Irwin A. (1969). Muscle contracture induced by exercise. A syndrome attributable to decreased relaxing factor – PubMed. 24 luglio 1969. Available at: https://pubmed.ncbi.nlm.nih.gov/4239835/.

7. Molenaar JP, Verhoeven JI, Rodenburg RJ, Kamsteeg EJ, Erasmus CE, Vicart S, et al. Clinical, morphological and genetic characterization of Brody disease: an international study of 40 patients. *Brain*. (2020) 143:452–66. doi: 10.1093/brain/awz410

8. Mussini J-M, Magot A, Hantaï D, Sternberg D, Chevessier F, Péréon e Y. Atypical nuclear abnormalities in a patient with Brody disease. *Neuromuscul Disord*. (2015) 25:773–9. doi: 10.1016/j.nmd.2015.07.005

9. Novelli A, Valente EM, Bernardini L, Ceccarini C, Sinibaldi L, Caputo V, et al. Autosomal dominant Brody disease cosegregates with a chromosomal (2;7)(p11.2;p12.1) translocation in an Italian family. *Eur J Hum Genet*. (2004) 12:579–83. doi: 10.1038/sj.ejhg.5201200

10. Odermatt A, Barton K, Khanna VK, Mathieu J, Escolar D, Kuntzer T, et al. The mutation of Pro789 to Leu reduces the activity of the fast-twitch skeletal muscle sarco(endo)plasmic reticulum Ca2+ ATPase (SERCA1) and is associated with Brody disease. *Hum Genet*. (2000) 106:482–91. doi: 10.1007/s004390000297

11. Sambuughin N, Zvaritch E, Kraeva N, Sizova O, Sivak E, Dickson K, et al. Exome analysis identifies Brody myopathy in a family diagnosed with malignant hyperthermia susceptibility. *Mol Genet Genomic Med*. (2014) 2:472–83. doi: 10.1002/mgg3.91

12. Vattemi G, Gualandi F, Oosterhof A, Marini M, Tonin P, Rimessi P, et al. Brody disease: insights into biochemical features of SERCA1 and identification of a novel mutation. *J Neuropathol Exp Neurol*. (2010) 69:246–52. doi: 10.1097/NEN.0b013e3181d0f7d5

13. Ronchi D, Monfrini E, Bonato S, Mancinelli V, Cinnante C, Salani S, et al. Dystonia-ataxia syndrome with permanent torsional nystagmus caused by ECHS1 deficiency. *Ann Clin Transl Neurol*. (2020) 7:839–45. doi: 10.1002/acn3.51025

14. Richards S, Aziz N, Bale S, Bick D, Das S, Gastier-Foster J, et al. Standards and guidelines for the interpretation of sequence variants: a joint consensus recommendation of the American College of Medical Genetics and Genomics and the Association for Molecular Pathology. *Genet Med*. (2015) 17:405–24. doi: 10.1038/gim.2015.30

15. Brugnoni R, Maggi L, Canioni E, Verde F, Gallone A, Ariatti A, et al. Next-generation sequencing application to investigate skeletal muscle Channelopathies in a large cohort of Italian patients. *Neuromuscul Disord*. (2021) 31:336–47. doi: 10.1016/j.nmd.2020.12.003

16. Kuntzer T. Electrophysiological testing in muscle channelopathies. *Rev Neurol*. (2004) 160:49–54. doi: 10.1016/s0035-3787(04)71006-1

17. Matthews E, Fialho D, Tan SV, Venance SL, Cannon SC, Sternberg D, et al. The non-dystrophic myotonias: molecular pathogenesis, diagnosis and treatment. *Brain*. (2010) 133:9–22. doi: 10.1093/brain/awp294

18. Miller TM. Differential diagnosis of myotonic disorders: AANEM monograph. *Muscle Nerve*. (2008) 37:293–9. doi: 10.1002/mus.20923

19. Trip J, Drost G, Ginjaar HB, Nieman FHM, van der Kooi AJ, de Visser M, et al. Redefining the clinical phenotypes of non-dystrophic myotonic syndromes. *J Neurol Neurosurg Psychiatry*. (2009) 80:647–52. doi: 10.1136/jnnp.2008.162396

20. Anderson DM, Anderson KM, Chang C-L, Makarewich CA, Nelson BR, McAnally JR, et al. A micropeptide encoded by a putative long noncoding RNA regulates muscle performance. *Cells*. (2015) 160:595–606. doi: 10.1016/j.cell.2015.01.009

21. Bianchini E, Testoni S, Gentile A, Calì T, Ottolini D, Villa A, et al. Inhibition of ubiquitin proteasome system rescues the defective sarco(endo)plasmic reticulum Ca2+−ATPase (SERCA1) protein causing Chianina cattle pseudomyotonia *◆. *J Biol Chem*. (2014) 289:33073–82. doi: 10.1074/jbc.M114.576157

frontiers | Frontiers in Neurology

TYPE Case Report
PUBLISHED 07 August 2023
DOI 10.3389/fneur.2023.1212497

OPEN ACCESS

EDITED BY
Giovanni Meola,
University of Milan, Italy

REVIEWED BY
Luis Del Carpio-Orantes,
Instituto Mexicano del Seguro Social,
Delegación Veracruz Norte, Mexico
Joseph George Verbalis,
Georgetown University, United States

*CORRESPONDENCE
Thorsten Lenhard
✉ Thorsten.lenhard@med.uni-heidelberg.de

RECEIVED 26 April 2023
ACCEPTED 17 July 2023
PUBLISHED 07 August 2023

CITATION
Rudolph AM, Doubrovinskaia S, Knabbe J, Seliger C and Lenhard T (2023) Case report: A 33 years-old alcoholic male with diarrhea and progressive muscle weakness mimicking Guillain–Barré syndrome.
Front. Neurol. 14:1212497.
doi: 10.3389/fneur.2023.1212497

Case report: A 33 years-old alcoholic male with diarrhea and progressive muscle weakness mimicking Guillain–Barré syndrome

Anja M. Rudolph, Sofia Doubrovinskaia, Johannes Knabbe, Corinna Seliger and Thorsten Lenhard*

Department of Neurology, Heidelberg University Hospital, Heidelberg, Germany

Background: A subacute manifestation of muscle weakness in temporal association with a diarrheal intestinal infection is always suspicious of Guillain–Barré syndrome (GBS). GBS is characterized as an acute inflammatory polyneuroradiculopathy, mediated by cross-reacting autoantibodies and typically triggered by various infections, vaccinations or other causes. Hyponatremia can be associated with GBS and is usually seen in more severe cases. However, the presence of relevant hyponatremia in a case suspicious of GBS can lead to a diagnostic dilemma. We here describe an intriguing and initially misleading case of hyponatremia mimicking GBS, where repeated and thorough electrophysiology was the key to the correct diagnosis.

Case presentation: A 33 years-old man with a history of severe alcohol dependence and schizophrenia developed progressive muscle weakness in the course of a preceding episode of diarrhea. Neurological examination revealed a leg-accentuated tetraplegia with global areflexia. There was also a complex oculomotor dysfunction. Laboratory tests showed hyponatremia of 110 mM. Cerebrospinal-fluid analysis showed a normal cell count and cytological evaluation, protein concentration within the normal range. Electroneurography showed severe proximal nerve conduction block as evidenced by prolonged F-wave latency and distal nerve conduction block as evidenced by prolonged distal motor latencies and reduced motor nerve conduction velocities (NCV) in all peripheral nerves examined. GBS-associated ganglioside autoantibodies were absent. After compensation of hyponatremia alone, muscle weakness improved rapidly and nerve conduction velocity improved similarly. These dynamics are not consistent with GBS and unnecessary immunoglobulin treatment could be avoided.

Conclusion: Suspicion of GBS in the presence of relevant hyponatremia can be misleading as hyponatremia is able to mimic GBS. We demonstrate that repeated and accurate nerve conduction studies together with F-wave diagnostics is helpful to make the correct diagnosis. We discuss the mechanisms of the causes of hyponatremia in GBS and contrast these with the electropyhsiological changes caused by hyponatremia itself. The correct diagnosis will prevent the uncritical use of intravenous immunoglobulins and save unnecessary costs. Also, a possible aggravation of the hyponatremia by immunoglobulin treatment can be averted.

KEYWORDS

hyponatremia, Guillain–Barré syndrome, nerve conduction blockade, albuminocytological dissociation, Wernicke encephalopathy

Introduction

Guillain–Barré syndrome (GBS) is a common cause of acute flaccid paralysis, characterized by symmetric limb weakness and hyporeflexia or areflexia, reaching maximum severity within 4 weeks (1, 2). GBS typically occurs after an infection in which the immune response produces autoantibodies that cross-react with gangliosides on nerve membranes. This autoimmune response leads to a functional blockade of nerve conduction and to subsequent nerve damage. The most common cause of antecedent infection is *Campylobacter jejuni*, but other pathogens such as Epstein-Barr virus, cytomegalovirus, SARS-CoV-2, *Mycoplasma pneumoniae, Haemophilus influenzae* and influenza A virus and many others can also cause GBS (3, 4).

Nerve conduction studies show signs of demyelination, including prolonged distal motor latency (dmL), reduced nerve conduction velocity (NCV), prolonged F-wave latency, increased temporal dispersion and intermediate conduction block (5).

Cerebrospinal-fluid (CSF) analysis reveals a combination of elevated protein levels and normal CSF cell counts (called albuminocytological dissociation), which is considered a hallmark of GBS. In addition, testing for autoantibodies to ganglioside epitopes has been established for the diagnosis of GBS, but has limited positive predictive value because antiganglioside antibodies are also present in other diseases. Exceptions to this rule are anti-GQ1b antibodies, which are present in the serum of at least 90% of patients with Miller–Fisher syndrome as a variant with cranial nerve involvement, and anti-GM1/-GD1a antibodies, which are frequently found in patients with pure motor GBS (1, 6).

In GBS, mild hyponatremia may develop during the course of the disease. Hyponatremia in these patients is more common when mechanical ventilation is required and occurs around day 10 after intubation. Fluid restriction normalizes sodium levels, suggesting a syndrome of inappropriate antidiuresis as the underlying cause. Only a subgroup of GBS patients with severe autonomic dysregulation and extremely high blood pressure have elevated atrial natriuretic protein levels, which may indicate an underlying salt-wasting syndrome (7).

We report a case of severe hyponatremia mimicking features of GBS. However, careful nerve conduction studies revealed an alternative pathogenesis of subacute flaccid tetraparesis despite a history of diarrhea.

Case description

A 33 years-old man with a history of severe alcohol dependence and schizophrenia was seen by a neurology consultant in the emergency department of a hospital in northern Baden-Württemberg, Germany. The patient reported diarrhea for at least 2 weeks and progressive muscle weakness. He denied fever and associated myalgias or painful paresthesias. He had stopped drinking (6–10 × 0.5 L bottles of beer per day) 2 days before admission. Neurological examination revealed leg-accentuated tetraplegia with global areflexia. Muscle strength was 0/5 for foot and toe flexors and extensors, 2/5 for pelvic girdle muscles and 4/5 for shoulder girdle muscles. Sensory examination revealed a stocking-like hypesthesia of the feet. There was also a complex oculomotor dysfunction with an immured left eye, abduction deficiency of the right eye and a vertical skew deviation. Cognitive assessment revealed mild mental impairment.

Blood analysis showed elevated transaminases, γ-glutamyltransferase, lipase, slightly decreased thiamine level (26 µg/L; *n*: 28–85) and severe hyponatremia (110 mM; *n*: 135–145). Other electrolytes and renal function were within the normal range or borderline (K^+ 4.4 mM, *n*: 3.3–5.1; Ca^{2+} 1.15 mM, *n*: 1.15–1.35; GFR 57 mL/min, *n*: >60). The CSF on admission showed a normal cell count and cytological assessment, protein concentration within the normal range and an intact blood-CSF barrier. Control lumbar puncture at day 6 after admission showed no changes except an increase in CSF protein (78.2 mg/L, *n*: 15–46). MRI of the entire spine and a CT-scan of the head showed no abnormalities.

Nerve conduction studies (NCS) revealed severe proximal nerve conduction block, as evidenced by greatly increased F-wave latency, and distal nerve conduction block, as evidenced by increased dmL and decreased motor NCV in all peripheral nerves studied. Chronodispersion of the tibial nerve compound muscle action potential (CMAP) was also evident. No intermediate conduction block was observed. Figures 1A,B and Figures 2A,B show representative recordings of the ulnar and tibial nerves. Table 1 summarizes the absolute values on admission.

Some of the electrophysiological findings are reminiscent of GBS. However, GBS typically has an NCV of less than 30 m/s and often intermediate conduction blocks. Therefore, we concluded that GBS may not be the underlying pathology and that hyponatremia may be the more important underlying pathology. Therefore, we refrained from treatment with intravenous immunoglobulin (IVIG) and compensated the hyponatremia only by slowly increasing the sodium concentration with intravenous sodium infusion. We also replaced the mild thiamine deficiency (200 mg/day intravenously). Within 24 h after admission and the start of sodium replacement [$(Na^+)_{0h}$ 110 mM; $(Na^+)_{24h}$ 125 mM; $(Na^+)_{48h}$ 132 mM; $(Na^+)_{72h}$ 137 mM], the oculomotor dysfunction and mental abnormalities improved completely. Muscle strength also improved. At the same time, follow-up electroneurography showed an impressive improvement in NCVs and conduction blocks (Figures 1C,D, Figures 2C,D and Table 1).

Further analysis in the course revealed negative results for autoantibodies against gangliosides (IgG + IgM immunoblotting, all negative for GD1a, GD1b, GM1, GM2, GM3, GQ1b, GT1a, GT1b;) and antibodies against *Campylobacter jejuni* (IgM + IgA ELISA: 5.7 and 6.3 U/mL, $n < 20$), making GBS even less likely. The following pathogens were also excluded: *Salmonella-, Yersinia-* and *Shigella species* and *Treponema pallidum, Borrelia burgdorferi*, Hepatitis A, B, C virus and SARS-CoV-2.

The patient's symptoms improved as described above and he was transferred to a neurological rehabilitation clinic.

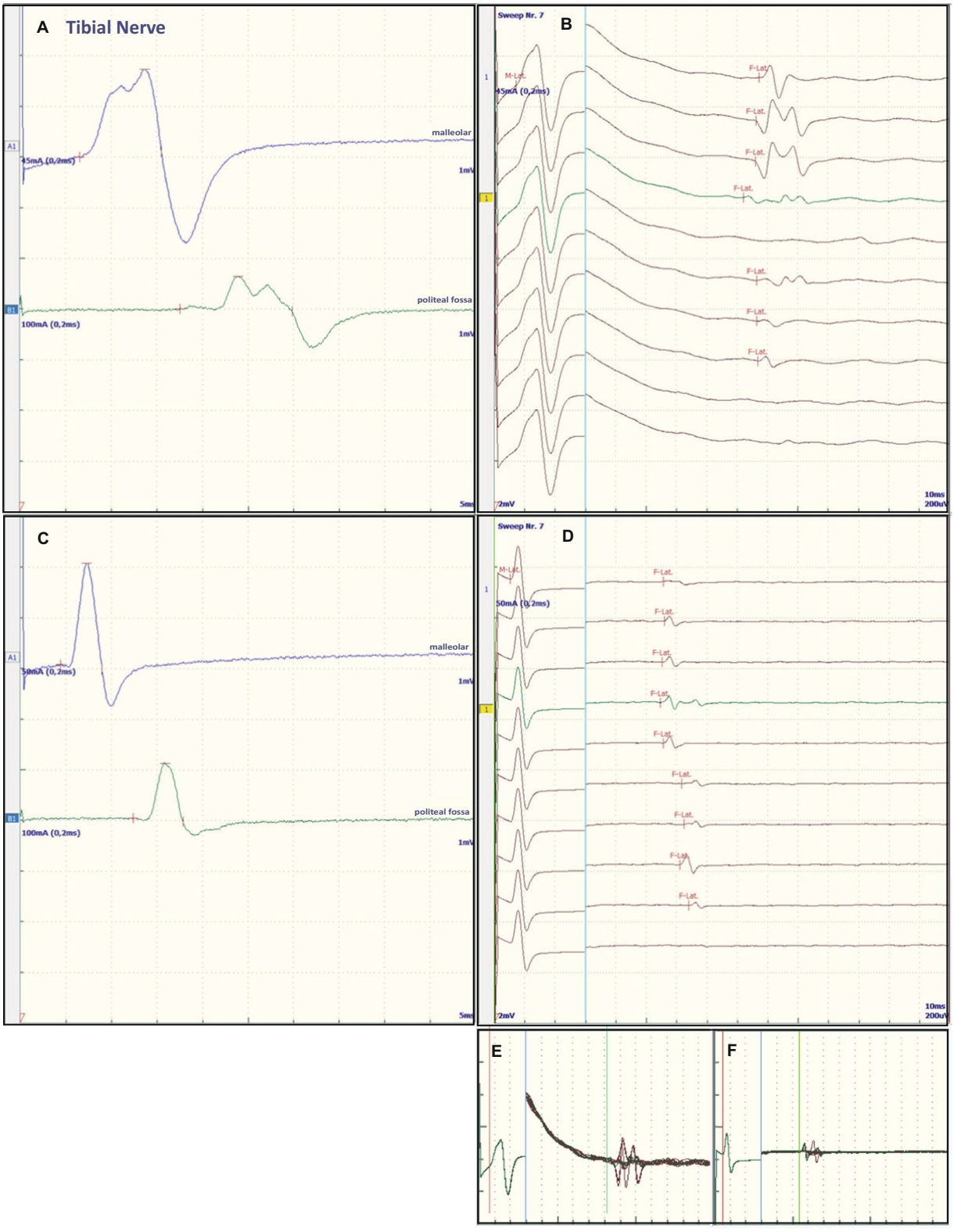

FIGURE 1
Representative electroneurographic findings for the tibial nerve. **(A,C)** Show nerve conduction velocities with corresponding F-wave latencies **(B,D)**. **(A,B)** Show the findings on admission, **(C,D)** the changes after correction of hyponatremia, 4 days after admission. The small boxes below the F-wave recordings show an overlay of **(B)** F-wave recordings at admission **(E)** and an overlay of **(D)** recordings after sodium corrections **(F)**.

Discussion

This case illustrates severe hyponatremia mimicking GBS. Diarrhea, ascending paresis and mild hypesthesia would strongly remind neurologists of an underlying GBS (1, 2). Although mild sensory deficits may be seen in GBS, more severe sensory deficits, e.g., of the posterior funiculus, are uncommon, whereas muscle pain or painful paresthesias are often associated with GBS. Oculomotor

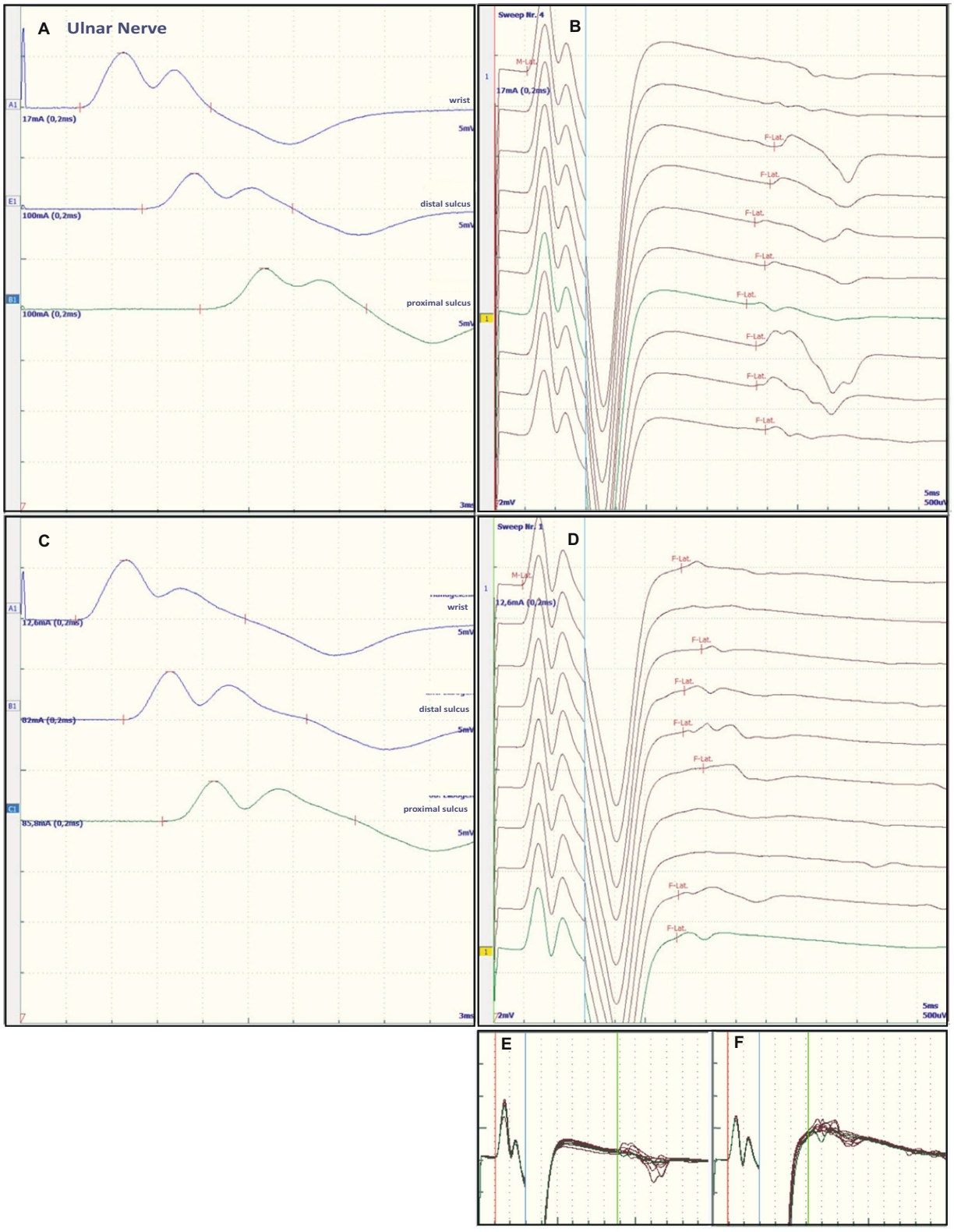

FIGURE 2
Representative electroneurographic findings for the ulnar nerve. **(A,C)** Show nerve conduction velocities with corresponding F-wave latencies **(B,D)**. **(A,B)** Show the findings on admission, **(C,D)** the changes after correction of hyponatremia, 4 days after admission. The small boxes below the F-wave recordings show an overlay of **(B)** F-wave recordings at admission **(E)** and an overlay of **(D)** recordings after sodium corrections **(F)**.

involvement is seen in Miller–Fisher syndrome as a rare variant of GBS (1). Areflexia may also be caused by alcoholic polyneuropathy. Cognitive impairment and oculomotor dysfunction are seen in Wernicke encephalopathy. Other differential diagnoses include myopathies, infectious diseases, malignancies or paraneoplastic neuropathies and disorders of the neuromuscular junction (1). Table 2

TABLE 1 Summary of electroneurographic findings for ulnar and tibial nerve.

Nerve	Hyponatremia (timepoint)	dmL (msec)	CMAP (mV)	NCV (m/s)	1st F-WL (msec)	MF-W (msec)	F-WCV (m/s)
Ulnar nerve (UN)	Admission[a]	3.9	5.4	39.1	41.6	44.0	5.1
	Compensation[b]	3.6	5.9	44.0	31.6	32.6	7.1
	% changes	−8	+9	+13	−24	−26	+39
Tibial nerve (TN)	Admission[a]	6.6	1.7	33.6	82.2	85.9	2.4
	Compensation[b]	4.4	2.1	44.1	54.7	58.3	4.0
	% changes	−33	+24	+31	−33	−32	+67

dmL, distal motor latency; CMAP, compound muscle action potential; NCV, nerve conduction velocity; F-WL, F-wave latency; MF-W, mean F-wave latency; F-WCV, mean F-wave conduction velocity. Normal values: dmL: UN <4.5 msec, TN <5.4 msec; CMAP: UN >4 mV, TN >5 mV; NCV (age adjusted): UN >42 m/s, TN >40 m/s; 1st F-wave: UN <33 msec, TN <58 msec (leg length adjusted) (8). [a]Admission, [Na^+] 110 mM. [b]Compensation, at day 4 after admission, [Na^+] 136 mM.

TABLE 2 Clinical comparison of GBS/Miller–Fisher syndrome, hyponatremia and Wernicke encephalopathy with reference to the patient's particular symptoms at admission.

Clinical symptom / observation	GBS / Miller–Fisher's variant	Hyponatremia	Wernicke encephalopathy	Patient
Flaccid paresis	Typical	Impaired motor function, gait instability	Gait instability caused by ataxia, but not flaccid paresis	Present at admission
Ophthalmoplegia	Typical	Not reported	Horizontal gaze nystagmus, INO, abducens nerve paresis	Present at admission
Areflexia	Typical	Reduced tendon reflexes	Not typical[b]	Present at admission
Ataxia	Typical	Rarely reported (9)	Typical	Absent
Cognitive impairment	Not typical	Typical, consciousness disturbance[a]	Typical, consciousness disturbance[a]	Present at admission; not present[a]
Distal hypesthesia	Not typical	Not typical	Not typical	Present at admission
Previous diarrhea	Possible (*C. Jejuni* infection)	Possible as underlying pathology	Not associated	Present at admission
Hyponatremia	In the course possible	intrinsic to disorder	Not associated	Present at admission
Slowed NCV	Typical	Has been described (10, 11)	Not reported[b]	Present at admission
Prolonged F-WL	Typical	Has been described (10, 11)	Not reported[b]	Present at admission
Prolonged dmL	Typical	Has been described (11)	Not reported[b]	Present at admission
Thiamine deficiency	Not associated	Not associated	intrinsic to disorder	Borderline
Albuminocytological dissociation	Typical in the course, often not present at the time of admission	Not associated	Not associated	Present in the course

INO, internuclear ophthalomoplegia; NCV, nerve conduction velocity; F-WL, F-wave latency; dmL, distal motor latency. [a]Refers to a symptom mentioned within a cell of the same line. [b]Axonal neuropathy has been described in beriberi (19, 20), but exact data on NCV, F-WL, dmL are not available.

summarizes the differential clinical signs and observations in GBS–Miller–Fisher syndrome, Wernicke encephalopathy and hyponatremia with reference to the patient's particular symptoms on admission.

Sodium disturbances, an important laboratory finding in our patient, are known to be associated with GBS (12). A syndrome of inappropriate antidiuresis is discussed as the underlying pathology in most cases, and a salt-wasting syndrome has been reported in isolated cases (7, 13, 14). However, to our knowledge, hyponatremia mimicking GBS in clinical signs and some electroneurographic patterns has not been published (15), yet.

In most cases, hyponatremia in GBS is mild and is associated with a severe course of the disease and mechanical ventilation or with IVIG treatment (7, 13, 16). In our patient, however, the hyponatremia was severe (110 mM) and was already present on admission. It is most likely due to massive beer consumption in the sense of dilutional hyponatremia. As the symptoms in our patient resemble Miller–Fisher syndrome, which is strongly associated with *C. jejuni* or other pathogens and GQ1b and GT1a ganglioside autoantibodies, the absence of these antibodies in our patient did not support this diagnosis (17); nor did the absence of albuminocytological dissociation at admission. Other causative agents of GBS were also excluded. Finally, convincing evidence was provided by the rapid improvement in oculomotor dysfunction and muscle weakness with sodium replacement,

which occurred much faster than would be expected in GBS with IVIG treatment.

The NCS showed changes that are common in GBS. However, some features raised differential diagnostic considerations. There were severe proximal conduction blocks, but only a slightly reduced NCV, which was still faster than 30 m/s, and no intermediate conduction blocks. Therefore, after sodium correction, there was also a rapid improvement in follow-up NCS, as shown for proximal nerve conduction blocks and NCV (Figures 1C,D and Figures 2C,D). These electroneurographic changes usually improve much more slowly (if at all) in GBS. They are associated with severe disease progression (e.g., mechanical ventilation) and delayed improvement (2).

Most neurological manifestations of hyponatremia are neurocognitive and mental status changes (confusion, disorientation, seizures, syncope, coma) and not necessarily neuromuscular, with the exception of unsteady gait (18). The most likely cause of unsteadiness leading to falls is decreased reaction latency, secondary to decreased NCV and F-wave latencies (10), as were also present in our patient at admission (see Table 1, Figures 1A,B and Figures 2A,B). Previous publications have shown reversibility of NCV and F-wave latencies in hyponatremia with correction of sodium levels (10, 11). However, our patient had a pre-existing relevant axonal polyneuropathy, which was still evident in reduced CMAP even after compensation for hyponatremia, and this finding was particularly accentuated in the tibial nerve (see Table 1 and Figures 1A,B). Here, the NCV slowing and the F-Wave and dmL extension were particularly pronounced [compare changes in percentage (%) in tibial nerve versus ulnar nerve, Table 1]. This suggests that the pre-damaged nerve is particularly susceptible to hyponatremia, which clinically results more in a manifesting flaccid paresis than just gait instability. This is supported by the fact that the effect was particularly evident in the tibial nerve, where the CMAP remained pathologically reduced, whereas the ulnar nerve had a normal CMAP at baseline but also showed an increase in CMAP with sodium correction (Table 1). These results are consistent with the measurements made by Vandergheynst et al. (10), who discuss in their paper the effect of pre-existing polyneuropathy on patients' symptoms and electrophysiological changes in hyponatremia.

The contribution of thiamine deficiency to the severity of symptoms, particularly ocular motor dysfunction, needs to be discussed. Since thiamine levels were only slightly decreased, we believe that thiamine deficiency may have had some effect, but the main pathology was due to hyponatremia. A contribution of osmotic demyelination to the observed ophthalmoplegia could be ruled out by evaluation of the clinical course. A CT-scan of the head at day 6 showed normal brainstem structures including pons. In chronic thiamine deficiency (beriberi) in alcoholic patients or pregnant women rapid improvement of neurological symptoms including muscle weakness has been reported after replacement of thiamine (19, 20). One study reports patients predominantly presenting with axonal polyneuropathy (19). The other reports women exclusively presenting with axonal polyneuropathy (20). However, neither study mentions quantitative values of electrophysiological measurements or of thiamine concentrations. Rather, as discussed above, the pre-existing alcoholic polyneuropathy in our patient may have exacerbated the effects of hyponatremia on the peripheral nerves rather than a relevant thiamine effect, showing reversible proximal and distal nerve blockades as so-called "demyelinating features" (Figures 1, 2 and Table 1). The rapid improvement of these "demyelinating features" with sodium replacement shows that the changes are reversible and not due to substantial damage to the nerve fibres, further supporting the hyponatremia hypothesis.

Our key message is that if severe hyponatremia is present already on admission, the diagnosis of GBS should be questioned. An attempt to treat the sodium balance alone may be indicated, as IVIG treatment can further exacerbate the hyponatremia (2, 21). In addition, other IVIG-associated side effects may be avoided and costs saved. Furthermore, the case is very instructive because it illustrates the nature of the multifactorial causality (hyponatremia, pre-existing alcoholic neuropathy, thiamine deficiency) of the entire clinical picture. Developing a multifactorial mindset is critical to formulating optimal differential diagnoses, a medical skill rarely taught in textbooks.

Data availability statement

The original contributions presented in the study are included in the article/supplementary material, further inquiries can be directed to the corresponding author.

Ethics statement

Ethical review and approval was not required for the study on human participants in accordance with the local legislation and institutional requirements. The patients/participants provided their written informed consent to participate in this study.

Author contributions

TL conducted and evaluated the electrophysiological studies and drafted the manuscript. AR, SD, and JK conducted the clinical and laboratory examinations and proofread the manuscript. CS performed a second evaluation of the electrophysiological examinations and proofread the manuscript. All authors contributed to the article and approved the submitted version.

Conflict of interest

The authors declare that the research was conducted in the absence of any commercial or financial relationships that could be construed as a potential conflict of interest.

Publisher's note

References

1. Leonhard SE, Mandarakas MR, Gondim FAA, Bateman K, Ferreira MLB, Cornblath DR, et al. Diagnosis and management of Guillain–Barre syndrome in ten steps. *Nat Rev Neurol*. (2019) 15:671–83. doi: 10.1038/s41582-019-0250-9

2. van den Berg B, Walgaard C, Drenthen J, Fokke C, Jacobs BC, van Doorn PA. Guillain–Barre syndrome: pathogenesis, diagnosis, treatment and prognosis. *Nat Rev Neurol*. (2014) 10:469–82. doi: 10.1038/nrneurol.2014.121

3. Sansone P, Giaccari LG, Aurilio C, Coppolino F, Esposito V, Fiore M, et al. Post-infectious Guillain–Barre syndrome related to SARS-CoV-2 infection: a systematic review. *Life*. (2021) 11:167. doi: 10.3390/life11020167

4. Jacobs BC, Rothbarth PH, van der Meche FG, Herbrink P, Schmitz PI, de Klerk MA, et al. The spectrum of antecedent infections in Guillain–Barre syndrome: a case-control study. *Neurology*. (1998) 51:1110–5. doi: 10.1212/WNL.51.4.1110

5. Hadden RD, Cornblath DR, Hughes RA, Zielasek J, Hartung HP, Toyka KV, et al. Electrophysiological classification of Guillain–Barre syndrome: clinical associations and outcome. Plasma exchange/sandoglobulin Guillain–Barre syndrome trial group. *Ann Neurol*. (1998) 44:780–8. doi: 10.1002/ana.410440512

6. Fokke C, van den Berg B, Drenthen J, Walgaard C, van Doorn PA, Jacobs BC. Diagnosis of Guillain–Barre syndrome and validation of Brighton criteria. *Brain*. (2014) 137:33–43. doi: 10.1093/brain/awt285

7. Lenhard TBM, Schwab S. Disorders of salt and fluid balance: diabetes insipidus, cerebral salt-wasting syndrome, and syndrome of inappropriate antidiuresis In: DW Pfaff, AM Etgen, SE Fahrbach and RT Rubin, editors. *Hormones, brain and behavior*. *2nd* ed. San Diego: Academic Press (2009). 3235–65.

8. Stöhr M, Pfister R. Kapitel: 1.3 Motorische Neurographie und 1.4 Reflex- und F-Wellen-Untersuchungen In: *Klinische Elektromyographie und Elektroneurographie—Lehrbuch und Atlas*. Stuttgart, Germany: W. Kohlhammer (2014) doi: 10.17433/978-3-17-028373-2

9. Asokumar P, Gogate YV, Gangadhar P, Bhansali A. Reversible cerebellar ataxia: a rare presentation of depletional hyponatremia. *Neurol India*. (2011) 59:631–2. doi: 10.4103/0028-3886.84356

10. Vandergheynst F, Gombeir Y, Bellante F, Perrotta G, Remiche G, Melot C, et al. Impact of hyponatremia on nerve conduction and muscle strength. *Eur J Clin Investig*. (2016) 46:328–33. doi: 10.1111/eci.12597

11. Aranyi Z, Kovacs T, Szirmai I, Vastagh I. Reversible nerve conduction slowing in hyponatremia. *J Neurol*. (2004) 251:1532–3. doi: 10.1007/s00415-004-0574-1

12. Griffin D, Asad H, Patel P, Gohar A. Flaccid paralysis with hyponatremia: think Guillain–Barre syndrome. *Cureus*. (2020) 12:e7113. doi: 10.7759/cureus.7113

13. Cooke CR, Latif KA, Huch KM, Wall BM. Inappropriate antidiuresis and hyponatremia with suppressible vasopressin in Guillain–Barre syndrome. *Am J Nephrol*. (1998) 18:71–6. doi: 10.1159/000013309

14. Lenhard T, Grimm C, Ringleb PA. Renal salt wasting as part of dysautonomia in Guillain–Barre syndrome. *J Neurol Neurosurg Psychiatry*. (2011) 82:1051–3. doi: 10.1136/jnnp.2009.192369

15. Nagler EV, Vanmassenhove J, van der Veer SN, Nistor I, Van Biesen W, Webster AC, et al. Diagnosis and treatment of hyponatremia: a systematic review of clinical practice guidelines and consensus statements. *BMC Med*. (2014) 12:1. doi: 10.1186/s12916-014-0231-1

16. Rumalla K, Reddy AY, Letchuman V, Mittal MK. Hyponatremia in Guillain–Barre syndrome. *J Clin Neuromuscul Dis*. (2017) 18:207–17. doi: 10.1097/CND.0000000000000157

17. Rocha Cabrero F, Morrison EH. *Miller Fisher syndrome*. Treasure Island (FL): StatPearls (2021).

18. Renneboog B, Musch W, Vandemergel X, Manto MU, Decaux G. Mild chronic hyponatremia is associated with falls, unsteadiness, and attention deficits. *Am J Med*. (2006) 119:71.e1–8. doi: 10.1016/j.amjmed.2005.09.026

19. Saini M, Lin W, Kang C, Umapathi T. Acute flaccid paralysis: do not forget beriberi neuropathy. *J Peripher Nerv Syst*. (2019) 24:145–9. doi: 10.1111/jns.12297

20. Ahmad S, Ahmad S, Jan A. Thiamine deficiency related peripheral neuropathy in peripartum women of Kashmir, India: a hospital based study. *Int J Adv Med*. (2019) 6:662–7. doi: 10.18203/2349-3933.ijam20191498

21. Nguyen MK, Rastogi A, Kurtz I. True hyponatremia secondary to intravenous immunoglobulin. *Clin Exp Nephrol*. (2006) 10:124–6. doi: 10.1007/s10157-006-0416-9

frontiers | Frontiers in Neurology

TYPE Case Report
PUBLISHED 14 August 2023
DOI 10.3389/fneur.2023.1232199

OPEN ACCESS

EDITED BY
Giovanni Meola,
University of Milan, Italy

REVIEWED BY
Hai Zhang,
Shanghai First Maternity and Infant Hospital, China
Juan Wu,
Western Theater General Hospital, China

*CORRESPONDENCE
Qian Wang
✉ wangqian_9186@163.com
Hui Tang
✉ tanghui1110@163.com

RECEIVED 31 May 2023
ACCEPTED 24 July 2023
PUBLISHED 14 August 2023

CITATION
Su Y, Li Z, Wang Q and Tang H (2023) Local subcutaneous lidocaine injection for the treatment of complex regional pain syndrome: a case report and literature review. *Front. Neurol.* 14:1232199. doi: 10.3389/fneur.2023.1232199

Local subcutaneous lidocaine injection for the treatment of complex regional pain syndrome: a case report and literature review

Yaping Su[1,2], Zhenyu Li[1], Qian Wang[1]* and Hui Tang[1,3]*

[1]Department of Pharmacy, Shandong Provincial Hospital Affiliated to Shandong First Medical University, Jinan, China, [2]Department of Pharmacy, The People's Hospital of Xin Tai City, Taian, China, [3]Stem Cell Clinical Institute, Shandong Provincial Hospital Affiliated to Shandong First Medical University, Jinan, China

A 14-year-old child was diagnosed with complex regional pain syndrome (CRPS) after bromhidrosis surgery. She experienced a stinging, knife-like, and intermittent attack pain, accompanied by numbness of both upper limbs and limited movements. Ultrasound-guided radiofrequency surgery on the peripheral nerve did not reduce pain. Then, gabapentin 300 mg three times a day and 2% lidocaine by local subcutaneous injection once a day for 3 days were administrated. After the local subcutaneous injection of lidocaine, the pain was significantly relieved, and the pain induced by skin touch at the scar disappeared. No pain recurred after the 1-month follow-up. An evidence-based literature review showed that local or systemic intravenous lidocaine was used to reduce adult CRPS symptoms but less has been reported in children. In our case, a local subcutaneous injection of 2% lidocaine in a child for CRPS treatment was reported to be effective in relieving complex local pain with favorable outcomes. Though further high-quality randomized controlled trials are needed to investigate the effects and safety of local subcutaneous lidocaine injection on pain relief in children with CRPS, it could still provide a relatively safe and effective adjuvant therapy for minor patients.

KEYWORDS

lidocaine, local subcutaneous injection, complex regional pain syndrome, analgesic therapy, case report

1. Introduction

Complex regional pain syndrome (CRPS) is usually secondary to primary trauma and may be a syndrome of severe intractable, polytropic pain following fracture, postoperative or unintentional minor trauma, characterized by malnutrition and dysfunction (1). The fourth edition of the Diagnosis and Treatment Guidelines for CRPS in 2013 pointed out that the main clinical features are acute pain inconsistent with the original trauma, and clinical manifestations are pain, edema, erythema, hyperthermia, hypofunction, and so on. There are two typical types of sympathetic pain disorders: CRPS type I, which has no nerve damage, and CRPS type II, which has definite nerve damage and typical neuropathic pain features (2). The incidence of CRPS was 5–25 per 1,00,000, the ratio of male to female was 1:2-3, and the ratio of upper limb to lower limb was 2:1 (3), but the pathological pathogenesis of CRPS was still unknown.

The primary treatment of CRPS is multimodal pain management, which includes bisphosphonates, glucocorticoids, non-steroidal anti-inflammatory drugs, tricyclic antidepressants, antiepileptics, NMDA receptor antagonists, and drugs such as calcitonin

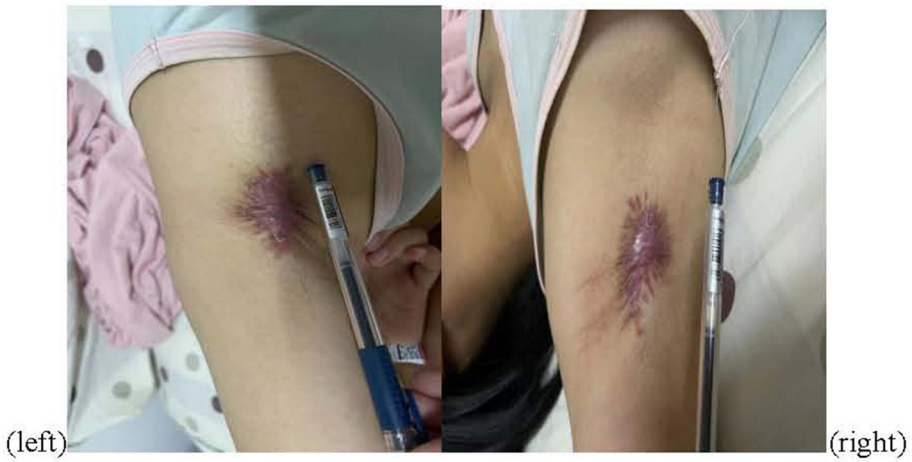

FIGURE 1
Postoperative figure.

and Botox. In addition, there are also other options such as psychological therapy, physical therapy, surgery, and interventional therapy. Minimally invasive interventional therapy mainly includes sympathetic nerve block, spinal cord electrical stimulation, and ultrasound-guided pulsed radiofrequency. Surgical treatment mainly includes lesion of dorsal root of spinal cord and neurolytic sympathetic procedures (1, 2).

We present a unique case of a child detailing the use of local subcutaneous lidocaine injection, which is poorly documented in the literature. An evidence-based literature review was conducted to help us scientifically analyze and grasp the safety and effectiveness of analgesic drugs.

2. Case presentation

A 14-year-old child (168 cm, 58 kg) had been diagnosed with complex regional pain syndrome (CRPS) on 28 October 2022. Two months after a bromhidrosis surgery, the patient developed axillary pain with numbness in both upper limbs. The pain site was the axillary region, radiating to both upper limbs with pain numbness and limited movements. The numerical rating scale (NRS) was 8 points. The patient reported pain as stinging, knife-like, and intermittent attacks, with a frequency of 6–8 episodes per day, each lasting 10–20 min. The pain was worse at night than during the day, occasionally interfering with sleep. The child had no significant weight loss and denied a history of chronic medical conditions such as high blood pressure.

The patient received one local injection of scar softening needle on 14 October 2022 and then applied mupirocin ointment and human epidermal growth factor gel to the scar. The color of the scar deepened and the contracture improved, but the pain did not improve significantly. Physical examination revealed bilateral axillary surgical scars of 5 * 2 cm (Figure 1), peripheral skin contracture, local tenderness (++), limited movement of both upper limbs, abductor lift of 120°, forward flexion lift of 150°, back extension test to the medial margin of scapula, random contact of both upper limbs on the ulnar side caused pain, and no atrophy of the skin, tissues, and muscles of both upper limbs. The ulnar touch induced pain in both upper limbs (+), severe pain in the left armpit, numbness in the bilateral axilla of both upper limbs, and contracture of the hands and feet during the attack. The electromyography-evoked potential report showed no significant abnormalities in nerve motor conduction, sensory conduction, F-wave, or muscles (Table 1). Bilateral axillary ultrasound, blood, urine, and stool tests were normal. The patient met the Budapest diagnostic criteria for CRPS established by Harden in 2007 (4).

3. Therapeutic intervention and results

The patient was admitted to the hospital on 30th October and was given oral ibuprofen. Flurbiprofen ester gel ointment was applied to her right armpit for pain relief. On 1st November, radiofrequency surgery was performed on the left periaxillary nerve under ultrasound guidance, and 1 ml anti-inflammatory analgesic solution (2% lidocaine l ml +0.9% sodium chloride solution 2 ml + dexamethasone 5 mg) was given. The patient reported unbearable pain during the surgery. On the 1st day after the surgery, the patient reported increased pain in the left axilla, with no significant improvement in pain duration and attack frequency. The NRS score was 9 points. The patient was given gabapentin 300 mg, three times a day. However, after taking gabapentin, the child experienced dizziness and drowsiness. Considering that gabapentin was highly correlated with adverse reactions, the patient refused to continue taking gabapentin. After a comprehensive evaluation by clinical pharmacists and doctors, the patient was given a 3 ml local subcutaneous injection of 2% lidocaine. On 5th November, the patient reported significant relief in bilateral axillary pain, and the NRS score decreased from 8 to 3 points at the onset of pain. No adverse reactions were observed during the administration. The patient was discharged immediately. After 1 month of discharge, the patient was followed up by the clinical pharmacist, and the frequency and duration of the pain were significantly relieved. The

10.3389/fneur.2023.1232199

pain disappeared completely with the subsequent application of lidocaine gel patches.

4. Discussion

Lidocaine was used as an adjunct to CRPS, and local subcutaneous injection was rarely published (5–9). To date and to the best of our knowledge, only eight cases of CRPS with different lidocaine administration methods were retrieved (Table 2), of which six were adults and two were children The history of CRPS was more than 1 month, and the longest duration was 7 years. The pain was mainly concentrated in the upper and lower limbs and affected the patients' normal life. Of the two children, one received a 5% lidocaine local patch (10) and the other received a local block of 0.5% lidocaine 15 mL and 0.25% bupivacaine 20 mL, followed by an intravenous infusion of 250 mg lidocaine (11). Among the six adult patients, a 26-year-old patient was given intravenous medication at 1–2mg/kg/h for 4 h (12), one patient was given 5% lidocaine ointment three times a day (13), and four patients were given a local block therapy with combination medication (11, 14–16). Except for one patient who received a systemic infusion of lidocaine and ketamine without any pain relief (17), all the other patients achieved varying degrees of pain relief, of which two patients did not achieve sustained pain relief (11, 12).

In addition, we retrieved seven clinical trials of lidocaine for CRPS (Table 3), including three observational studies and four prospective studies. Intravenous lidocaine was administered in two clinical trials, one sustained subcutaneous infusion of lidocaine 3–5μg/ml (18), and one intravenous infusion of lidocaine 5mg/L for 5 days (19). There were three trials of lidocaine combined with other agents for regional block (5, 7, 8), and one lidocaine patch as an additional analgesic (6). With the exception of 49 patients, mentioned in a study by Schwartzman et al. (19), who relapsed after 6 months of pain relief, all patients in these trials achieved significant pain relief and no recurrence. Moreover, the duration of remission was not associated with mean lidocaine levels or highest measured lidocaine levels but was significantly associated with baseline pain intensity. There was a randomized controlled double-blind trial of lidocaine for regional block. Taskaynatan et al. found that in 22 patients with CRPS, 2% lidocaine combined with 40 mg methylprednisolone did not provide lasting pain relief and only relieved pain for 1 h (9).

In terms of safety, we found that high concentrations of systemic lidocaine were more likely to cause adverse effects, including nausea, dizziness, fatigue, bradycardia, tachycardia, and atrial arrhythmias (Table 3) (12, 19). The adverse reactions in patients using lidocaine patches were mild, mainly skin reactions, which could be recovered after drug withdrawal (6). Patients who received lidocaine regional block had few adverse reactions, mainly mild dizziness (9, 11, 16).

In our case, the patient was a 14-year-old child who developed CRPS in both arms after surgery with increased pain following peripheral nerve radiofrequency therapy similar to the case reported by Frost et al. in (10). The patient experienced significant adverse reactions after taking gabapentin. The pain was significantly relieved 3 days after a local subcutaneous injection

TABLE 1 Electromyography/evoked potential report: the results of electromyography.

Muscle name	Left/right	Insertion potential	Fibrillation potential	Positive sharp wave	Beam flutter potential	Myotonia	Amplitude	Polyphase wave	Time limit	Strong recruitment	Strong recruitment potential (mv)
Musculi interossiae I	L	Normal	0	0	0	0	Normal	Normal	Normal	Interference phase	1.2
Radial hip flexors	L	Normal	0	0	0	0	Normal	Normal	Normal	Interference phase	1.9
Biceps	L	Normal	0	0	0	0	Normal	Normal	Normal	Interference phase	1.1
Deltoid	L	Normal	0	0	0	0	Normal	Normal	Normal	Interference phase	2.0

TABLE 2 Case report of different lidocaine administration modes for CRPS.

First author	Patients	Age	Lidocaine administration	NRS	Pain relief	Duration of CRPS	Position and type	Previous treatments	ADR
Rickard et al. (12)	1	26	Intravenous administration 1–2 mg/kg/h for 4 h	8	NRS decreased from 8 to 6, but did not persist and recurred 2 months later	7 years	Left upper limb was injured, affecting the contralateral function	Glucocorticoids + opioids + gabapentin 0.3 g/tid	Mild dizziness
Frost (10)	1	10	5% Lidocaine patch (12 h/d, 1 month)	(-)	Sustainable pain relief	5 years	Left lower limb CRPS I	Gabapentin 0.3 g/tid, Amitriptyline 25 mg qn, Tramadol 50 mg/q8h Baclofen 10 mg/bid, Carbamazepine 200 mg/bid, Clonazepam 0.5 mg qn In October, it was changed to Doxazosinzaleplone1 mg/d, mesylate 5 mg	(-)
Hanlan et al. (13)	1	65	5% Lidocaine ointment tid	9	Sustainable pain relief	>2 months	Traumatic cervical spinal cord injury resulting in restriction of the right hand CRPS II	Pregabalin 600 g/d, Prednisolone 50 mg, Calcitonin 200 IU	(-)
Herschkowitz and Kubias (17)	1	47	Lidocaine and ketamine infusion therapy	6–7	No relief	>6 years	Right forearm CRPS I	Regional block + opioids + gabapentin 0.3 g/tid	(-)
Patel and Aiello (14)	1	65	0.5 ml 1% lidocaine and 20 mg dexamethasone were injected into the flexor tendon sheath	(-) Acute pain	Sustainable pain relief	>3 years	Right hand right forearm CRPS I	Multimodal therapy: occupational and desensitization therapy; Medication: nortriptyline 60 mg Oxycodone acetaminophen 5/325 mg Duloxetine 60 mg/bid	Not found
Wang et al. (15)	1	32	Betamethasone + 0.5% lidocaine was injected locally into the right carpal tunnel and pain point	10	Complete pain relief, NRS decreased to 1	>1 month	Right wrist and upper limb CRPS I	Multimodal therapy: occupational and desensitization therapy; Medication: oral corticosteroid, opioid agonist, and antidepressant	Not found
Toda et al. (16)	1	35	10 regional blocks of 1% lidocaine at 0.5 mL/kg were administered in the dorsal vein of the wrist	10	Complete pain relief	>1 years	Right hand CRPS I	Transcutaneous electrical nerve stimulation, occupational therapy and carbamazepine	Mild dizziness
Maneksha et al. (11)	1	12	15 mL 0.5% lidocaine + 20 mL 0.25% Bupivacaine+ 250 mg lidocaine iv	10	Mild pain relief, NRS decreased to 7	>5 months	Right foot and lower limb CRPS I	Physical therapy, regional nerve block and medication: Tramadol 50 mg Gabapentin 0.3 g/tid Amitriptyline 10 mg	Mild toxic symptoms with perioral tingling and some slurred speech occurred during intravenous administration

NRS, numerical rating scale; tid, three times a day; bid, twice a day; iv, intravenous injection; ADR, adverse drug reaction.

10.3389/fneur.2023.1232199

TABLE 3 Clinical trials of different lidocaine administration modes for CRPS.

First author	Patients	Age	Lidocaine administration	NRS (VAS)	Pain relief	Duration of CRPS	Position and type	Previous treatments	ADR
Linchitz and Raheb (18); observational study	5	37–63	Serum concentration is maintained by continuous subcutaneous infusion with infusion pump for 3-5μg/mL	7–10	Sustainable pain relief	3–8 years	(-)	Conventional treatment is invalid (standard medical therapy and physical therapy)	(-)
Schwartzman et al. (19); observational study	49	18–62	Intravenous administration was titrated slowly to 5 mg/L for 5 days	5–10	NRS decreased to 3.4 after 1 month and slightly decreased after 6 months	0.5–25 years	Upper and lower limbs and spread to the chest, back, and feet	Conventional treatment is invalid (standard medical therapy and physical therapy)	No serious complications were found. Mild side effects include nausea, fatigue, bradycardia, tachycardia, and atrial arrhythmia
Varitimidis et al. (5); observational study	168	19–78	25 ml 0.5% lidocaine +125 mg methylprednisolone for hand venous regional block	NRS >4, 81 patients; NRS 6.5–10	148 patients reported only mild pain (0–2) and 20 reported pain relief	>1 month	Double upper limbs CRPS I	Conventional treatment is invalid (standard medical therapy and physical therapy)	Not found
Calderón et al. (6); single-center, prospective, observational study	10	28–91	5% lidocaine ointment for additional analgesia	7.9	Sustainable pain relief, NRS decreased to 3.9.	>6 months	(-)	Anticonvulsants, antidepressants, non-steroidal anti-inflammatory drugs, opioids, and nerve blocks and radiofrequency	Local skin reactions (itching, redness, or dry skin)
Singh et al. (7); single-center, prospective, observational study	33	48–62	Regional block: Shoulder joint: 40 mg methylprednisolone +5 ml 2% lidocaine; radial, median, and ulnar nerve: 10 mg methylprednisolone + 1.5 ml of 2% lidocaine	7–10 (VAS)	Sustainable pain relief, VAS decreased to 2.7.	>1 month <1years	Double upper limbs	No other treatment	(-)
Paraskevas et al. (8); single-center, prospective study	17	33–72	Dorsal venous block of hand 15 mg guanethidine +1 mg/kg lidocaine twice a week for 5 weeks; 10 mg guanethidine +1 mg/kg lidocaine, once every 2 days, 20 times	8–10 (VAS)	Sustainable pain relief	5–67 months	Left and right hand	NSAIDs + opioids + calcitonin injection and physical therapy	(-)
Taskaynatan et al. (9); prospective, randomized, placebo study	22	20–25	40 mg methylprednisolone +10 ml 2% lidocaine for cubital regional block three times	>5	Relieved 1 h later, but no significant difference between 1 week and 1.5 months later	>3 months	Unilateral upper limb	(-)	Nausea, dizziness, tinnitus, flushing, and pruritus. All symptoms resolved spontaneously in a few hours

NRS(VAS), numerical rating scale (visual analog scale); tid, three times a day; bid, twice a day; ADR, adverse drug reaction; NSAIDs, non-steroidal anti-inflammatory drugs.

10.3389/fneur.2023.1232199

of 2% lidocaine, and no adverse reactions were observed during the administration.

Based on the above findings, a 5% lidocaine patch appears to have a significant analgesic effect on CRPS. Intravenous lidocaine could provide temporary relief, but it does not last long term. The usual dose of lidocaine for local block is 0.5–2%, and the pain relief is obvious, which is similar to the case we reported. It is suggested that topical lidocaine might relieve the pain of CRPS better and has a favorable safety. However, these clinical trials have been conducted on adults, and there have been few studies on adolescents.

By reviewing the literature, we attempted to analyze and speculate the reasons why local subcutaneous injection of lidocaine could relieve the pain of CRPS. A large number of ion channels related to pain regulation, such as voltage-gated sodium channel, potassium channel, and calcium channel, are distributed in the central and peripheral nervous system, which are closely related to pain perception (20, 21). Lidocaine is a selective Na+ channel blocker with strong membrane stabilization. It can selectively block the inward flow of Na+, block the K+ channel, prevent depolarization of damaged and dysfunctional nerves that are implicated in chronic pain (20, 21), increase the cellular efflux of glutamic acid and potassium, decrease excitability, and diminish neuronal transmission of pain signals, achieving the purpose of pain treatment (21, 22). Subcutaneous injection of lidocaine creates a high drug content in the spinal ganglia through the intradermal nerve terminal receptor pathway, severing the ring of pain stimulation, and thereby relieving pain (23).

In summary, we reported a case of a child treated with a local subcutaneous injection of 2% lidocaine for CRPS pain. At present, there is still no specific treatment for juvenile CRPS at home and abroad. There are also few clinical studies and systematic analyses on CRPS. Through a review of evidence-based literature, we concluded that local administration or local block used to treat CRPS pain in adults provided more pain relief than systemic administration of lidocaine. Our case and review of the literature suggested that local subcutaneous injection of lidocaine might be a convenient and effective treatment for CRPS in children. However, due to the small number of clinical cases collected and the lack of rigorous randomized controlled trials, the safety of CRPS in the treatment of adolescents remains uncertain. Therefore, further high-quality randomized controlled studies are needed to investigate the effect of local subcutaneous injection of lidocaine on pain relief in children with CRPS.

Data availability statement

The original contributions presented in the study are included in the article/supplementary material, further inquiries can be directed to the corresponding authors.

Ethics statement

The studies involving humans were approved by Shandong Provincial Hospital Ethics Committee. The studies were conducted in accordance with the local legislation and institutional requirements. The participants provided their written informed consent to participate in this study. Written informed consent was obtained from the individual(s), and minor(s)' legal guardian/next of kin, for the publication of any potentially identifiable images or data included in this article.

Author contributions

QW and HT contributed to the conception and design of the study and proofread all drafts. YS wrote the first draft of the manuscript. ZL wrote sections of the manuscript. HT provided guidance on the article. All authors contributed to the revision of the article, read, and approved the submitted version.

Funding

This study was supported by the National Natural Science Foundation of China (82102372) and the Natural Science Foundation of Shandong Province (ZR2020MC060 and ZR2020MH399).

Conflict of interest

The authors declare that the research was conducted in the absence of any commercial or financial relationships that could be construed as a potential conflict of interest.

Publisher's note

All claims expressed in this article are solely those of the authors and do not necessarily represent those of their affiliated organizations, or those of the publisher, the editors and the reviewers. Any product that may be evaluated in this article, or claim that may be made by its manufacturer, is not guaranteed or endorsed by the publisher.

References

1. Harden RN, McCabe CS, Goebel A, Massey M, Suvar T, Grieve S, et al. Complex regional pain syndrome: practical diagnostic and treatment guidelines, 5th edition. *Pain Med.* (2022) 23:S1–S53. doi: 10.1093/pm/pnac046

2. Mangnus TJP, Bharwani KD, Dirckx M, Huygen FJPM. From a symptom-based to a mechanism-based pharmacotherapeutic treatment in complex regional pain syndrome. *Drugs.* (2022) 82:511–31. doi: 10.1007/s40265-022-01685-4

3. Field J. Complex regional pain syndrome: a review. *J Hand Surg Eur Vol.* (2013) 38:616–26. doi: 10.1177/1753193412471021

4. Harden RN, Bruehl S, Stanton-Hicks M, Wilson PR. Proposed new diagnostic criteria for complex regional pain syndrome. *Pain Med.* (2007) 8:326–31. doi: 10.1111/j.1526-4637.2006.00169.x

5. Varitimidis SE, Papatheodorou LK, Dailiana ZH, Poultsides L, Malizos KN. Complex regional pain syndrome type I as a consequence of trauma or surgery to upper extremity: management with intravenous regional anaesthesia, using lidocaine and methyloprednisolone. *J Hand Surg Eur Vol.* (2011) 36:771–7. doi: 10.1177/1753193411413852

6. Calderón E, Calderón-Seoane ME, García-Hernández R, Torres LM. 5% Lidocaine-medicated plaster for the treatment of chronic peripheral neuropathic pain: complex regional pain syndrome and other neuropathic conditions. *J Pain Res.* (2016) 9:763–70. doi: 10.2147/JPR.S113517

7. Singh NJ, Khanna M, Gupta A, Haldar P. Effectiveness of peripheral median, radial, and ulnar nerve block at wrist along with intra-articular steroid injection in shoulder joint in management of complex regional pain syndrome of upper limb: 1-week follow-up study. *Neurol India.* (2022) 70:1064–8. doi: 10.4103/0028-3886.349618

8. Paraskevas KI, Michaloglou AA, Briana DD, Samara M. Treatment of complex regional pain syndrome type I of the hand with a series of intravenous regional sympathetic blocks with guanethidine and lidocaine. *Clin Rheumatol.* (2006) 25:687–93. doi: 10.1007/s10067-005-0122-0

9. Taskaynatan MA, Ozgul A, Tan AK, Dincer K, Kalyon TA. Bier block with methylprednisolone and lidocaine in CRPS type I: a randomized, double-blinded, placebo-controlled study. *Reg Anesth Pain Med.* (2004) 29:408–12. doi: 10.1016/j.rapm.2004.05.007

10. Frost SG. Treatment of complex regional pain syndrome type 1 in a pediatric patient using the lidocaine patch 5%: a case report. *Curr Ther Res Clin Exp.* (2003) 64:626–9. doi: 10.1016/j.curtheres.2003.09.010

11. Maneksha FR, Mirza H, Poppers PJ. Complex regional pain syndrome (CRPS) with resistance to local anesthetic block: a case report. *J Clin Anesth.* (2000) 12:67–71. doi: 10.1016/s0952-8180(99)00126-9

12. Rickard JP, Kish T. Systemic intravenous lidocaine for the treatment of complex regional pain syndrome: a case report and literature review. *Am J Ther.* (2016) 23:e1266–1269. doi: 10.1097/MJT.0000000000000345

13. Hanlan AKL, Mah-Jones D, Mills PB. Early adjunct treatment with topical lidocaine results in improved pain and function in a patient with complex regional pain syndrome. *Pain Physician.* (2014) 17:E629–635.

14. Patel M, Aiello M. Successful treatment of acute worsening complex regional pain syndrome in affected dominant right-hand from secondary pathology of new onset third and fourth digit trigger finger. Case reports. *Plast Surg Hand Surg.* (2022) 9:123–5. doi: 10.1080/23320885.2022.2063871

15. Wang LK, Chen HP, Chang PJ, Kang FC, Tsai YC. Axillary brachial plexus block with patient controlled analgesia for complex regional pain syndrome type I: a case report. *Reg Anesth Pain Med.* (2001) 26:68–71. doi: 10.1053/rapm.2001.9879

16. Toda K, Muneshige H, Asou T. Intravenous regional block with lidocaine for treatment of complex regional pain syndrome. *Clin J Pain.* (2006) 22:222–4. doi: 10.1097/01.ajp.0000169666.17159.8f

17. Herschkowitz D, Kubias J. Wireless peripheral nerve stimulation for complex regional pain syndrome type I of the upper extremity: a case illustration introducing a novel technology. *Scand J Pain.* (2018) 18:555–60. doi: 10.1515/sjpain-2018-0014

18. Linchitz RM, Raheb JC. Subcutaneous infusion of lidocaine provides effective pain relief for CRPS patients. *Clin J Pain.* (1999) 15:67–72. doi: 10.1097/00002508-199903000-00010

19. Schwartzman RJ, Patel M, Grothusen JR, Alexander GM. Efficacy of 5-day continuous lidocaine infusion for the treatment of refractory complex regional pain syndrome. *Pain Med.* (2009) 10:401–12. doi: 10.1111/j.1526-4637.2009.00573.x

20. Zagon A. Innervation of serotonergic medullary raphe neurons from cells of the rostral ventrolateral medulla in rats. *Neuroscience.* (1993) 55:849–67. doi: 10.1016/0306-4522(93)90446-m

21. Kosharskyy B, Almonte W, Shaparin N, Pappagallo M, Smith H. Intravenous infusions in chronic pain management. *Pain Physician.* (2013) 16:231–49.

22. Tully J, Jung JW, Patel A, Tukan A, Kandula S, Doan A, et al. Utilization of intravenous lidocaine infusion for the treatment of refractory chronic pain. *Anesth Pain Med.* (2020) 10:e112290. doi: 10.5812/aapm.112290

23. Zhang YH, Sun ZX, Chen GH, et al. Observation on retrograde neural tracing of nerve ending receptor passage with lidocaine tracer through intradermal injection. *Zhongguo Linchuang Kangfu.* (2006) 10:128–30. doi: 10.3321/j.issn:1673-8225.2006.04.054

frontiers | Frontiers in Neurology

TYPE Case Report
PUBLISHED 12 September 2023
DOI 10.3389/fneur.2023.1230889

OPEN ACCESS

EDITED BY
Giovanni Meola,
University of Milan, Italy

REVIEWED BY
Riccardo Masson,
IRCCS Carlo Besta Neurological Institute Foundation, Italy
Hideyuki Iwayama,
Aichi Medical University, Japan
Aravindhan Veerapandiyan,
Arkansas Children's Hospital, United States

*CORRESPONDENCE
Elisa Nigro
elisa.nigro@sickkids.ca

RECEIVED 29 May 2023
ACCEPTED 15 August 2023
PUBLISHED 12 September 2023

CITATION
Nigro E, Grunebaum E, Kamath B, Licht C, Malcolmson C, Jeewa A, Campbell C, McMillan H, Chakraborty P, Tarnopolsky M and Gonorazky H (2023) Case report: A case of spinal muscular atrophy in a preterm infant: risks and benefits of treatment.
Front. Neurol. 14:1230889.
doi: 10.3389/fneur.2023.1230889

Case report: A case of spinal muscular atrophy in a preterm infant: risks and benefits of treatment

Elisa Nigro[1]*, Eyal Grunebaum[2], Binita Kamath[3], Christoph Licht[4], Caroline Malcolmson[5], Aamir Jeewa[6], Craig Campbell[7], Hugh McMillan[8], Pranesh Chakraborty[9], Mark Tarnopolsky[10] and Hernan Gonorazky[1]

[1]Division of Neurology, The Hospital for Sick Children (SickKids), Toronto, ON, Canada, [2]Division of Immunology, The Hospital for Sick Children (SickKids), Toronto, ON, Canada, [3]Division of Gastroenterology, Hepatology and Nutrition, The Hospital for Sick Children (SickKids), Toronto, ON, Canada, [4]Division of Nephrology, The Hospital for Sick Children (SickKids), Toronto, ON, Canada, [5]Division of Hematology/Oncology, The Hospital for Sick Children (SickKids), Toronto, ON, Canada, [6]Division of Cardiology, The Hospital for Sick Children (SickKids), Toronto, ON, Canada, [7]Department of Pediatrics, Children's Hospital, London Health Sciences Centre, Western University, London, ON, Canada, [8]Department of Pediatrics, Children's Hospital of Eastern Ontario Research Institute, Ottawa, ON, Canada, [9]Department of Pediatrics, Newborn Screening Ontario, Children's Hospital of Eastern Ontario Research Institute, Ottawa, ON, Canada, [10]Department of Pediatrics, McMaster Children's Hospital, Hamilton, ON, Canada

Spinal muscular atrophy (SMA) is a neuromuscular genetic disorder caused by the loss of lower motor neurons leading to progressive muscle weakness and atrophy. With the rise of novel therapies and early diagnosis on newborn screening (NBS), the natural history of SMA has been evolving. Earlier therapeutic interventions can modify disease outcomes and improve survival. The role of treatment in infants born preterm is an important question given the importance of early intervention. In this study, we discuss the case of an infant born at 32 weeks who was diagnosed with SMA on NBS and was treated with Spinraza® (Nusinersen) and Zolgensma® (Onasemnogene abeparvovec-xioi) within the first 2 months of life. With the scarce evidence that currently exists, clinicians should be aware of the efficacy and safety impact of early therapy particularly in the preterm infant.

KEYWORDS

spinal muscular atrophy, preterm, newborn screening, gene therapy, Zolgensma

Introduction

Spinal muscular atrophy (SMA) is a neuromuscular disease characterized by the degeneration of lower motor neurons caused predominantly by defects in the *SMN1* gene encoding the survival motor neuron protein (SMN). SMA is an autosomal recessive disorder that results in progressive muscle weakness and atrophy leading to significant morbidity and mortality. Approximately 70% of all cases are severe, with a median survival of 7 months and a mortality rate of 95% by 18 months of age (1, 2).

SMN is highly expressed during the gestation period and in the first few months of life. Between the fetal and postnatal phases, SMN protein content in the spinal cord declines 6.5-fold from its peak abundance during the embryonic period (2, 3). The loss of the lower motor neurons starts before the infant presents clinically and without any physical signs of SMA. Ramos et al. described a potential therapeutic window, encompassing the last trimester

of gestation and the first 3 months after birth when SMN protein decreases rapidly (4). Given this biology, early diagnosis and intervention have a critically important impact on the natural course of the disorder. Since 2017, various novel therapies have been approved which have changed the natural history of SMA.

Newborn screening (NBS) is completed shortly after birth to identify treatable diseases in the pre-symptomatic period. SMA can be detected using NBS, allowing for early diagnosis and potential intervention prior to, or early on in symptom onset. In Ontario, Canada, NBS was first implemented in clinical settings in 2006, and SMA was included in the screening as of 2020. Since then and until this study was submitted, approximately 394,299 patients have been screened, and 24 cases have been diagnosed in Ontario (5).

The implementation of NBS has led to an increase in pre-symptomatic therapy in the management of SMA (6). However, none of these therapies have been approved to treat preterm infants nor are there any available data to suggest the optimal time to treat a preterm infant safely. This has led to the question of when is the safest time to treat a preterm infant given the physiology of SMA and the potential risk associated with these interventions.

According to the WHO, the definition of a preterm infant is a baby born <37 weeks gestation (7). The combination of NBS and uncharted territory in the preterm world has led to a pathway of uncertainty. Lee et al. provided a recommendation to not treat preterm infants with SMA until the 37th week of gestational age (GA) because concomitant treatment with corticosteroids may adversely impact neurological development (8). They examine two cases with the use of gene replacement therapy on a 34 + 6-week GA infant and another of 34 + 1 weeks GA and made this recommendation given the potential complications of gene therapy in a younger infant.

In Canada, two therapies are currently approved for newborns who are <6 months of age with two or three copies of *SMN2*. The first is nusinersen, an antisense oligonucleotide therapy. The second is a gene replacement therapy, onasemnogene abeparvovec-xioi. A third medication called risdiplam (evrysdi®) is approved by Health Canada for infants older than 2 months of age.

Here, we will examine the outcome of a pre-symptomatic preterm infant diagnosed with SMA through the NBS program in Ontario and review the current evidence around the risk of therapy on this pediatric population.

Case

A 32-week-old baby boy was born via spontaneous vaginal delivery due to premature rupture of membranes after an uncomplicated pregnancy. His neonatal course was complicated by respiratory distress secondary prematurity requiring 3 days of continuous positive airway pressure (CPAP) in the neonatal intensive care unit (NICU) and phototherapy for neonatal jaundice. He was screened positive for SMA on NBS and had confirmatory genetic testing for homozygous loss of *SMN1* and two copies of *SMN2*. There was no family history of SMA or neuromuscular disease. Physical examinations at birth and during his first few weeks of life were normal, including good neurological and motor functioning. He scored 2/26 on the Hammersmith Infant Neurological Examination (HINE) at birth. He was seen by an occupational therapist on day 10 of life and was deemed safe for swallowing.

With respect to potential therapeutic interventions, his parents were counseled on all the therapies available in the treatment of SMA as well as the option to not treat with a therapy and allow for the natural course of the disease. Parents were interested in treating early and preferred to proceed with gene replacement therapy as this would be a one-time infusion. Risdiplam was not yet approved in Ontario at the time of this patient's birth but was discussed and not favored as an option to wait to treat until he was eligible. Given his premature age, there was no clear evidence to suggest that gene therapy would be safe before 39 weeks GA. As a result, we opted to administer nusinersen before 40 weeks of age due to the localized effects of the drug and less potential for systemic effects that may impact a premature infant. As such, he received three loading doses of nusinersen at 36, 38, and 40 weeks GA until he was able to be administered onasemnogene abeparvovec-xioi. He tolerated nusinersen well with no complications, and we did not observe any neurological abnormalities.

He later received onasemnogene abeparvovec-xioi at 10 weeks of age. He was monitored weekly as an outpatient for 2 months postinfusion to ensure no adverse events would occur. His baseline liver biochemical tests including serum transaminase levels and abdominal ultrasound (US) were normal. He was started on prednisone (1 mg/kg) the day before onasemnogene abeparvovec-xioi infusion and remained on prednisone at the same dose for 4 weeks. At this time, the prednisone was slowly tapered over the course of an additional 4 weeks. This was performed in conjunction with weekly bloodwork, assessing liver biochemistry and hematology and then changed to biweekly and then monthly for 6 months post-prednisone completion. At the onset of prednisone weaning, his serum transaminases were elevated but steadily improved during the remainder of the tapering period (Figures 1A, B).

Along with our physical examinations and neurological examinations regularly, he was assessed by a physiotherapist who obtained motor scores following onasemnogene abeparvovec-xioi administration. He obtained head control at 4 months of age and achieved independent walking at 18 months both of which are delayed even for his preterm age. Presently, at 20 months of age, he is currently pulling to stand, walk, and sit independently, is reaching for objects, and has good head control (Figure 2). He is eating orally, is gaining weight, has no respiratory concerns, and can say up to 10 words. In a recent EMG study, we detected high-amplitude motor unit potentials with no signs of denervation which might suggest some degree of chronic motor neuron involvement, while nerve conduction studies were normal (Figure 3).

Discussion

In our patient, the mild motor milestone delay plus the electrophysiological findings might suggest the requirement of initiation of treatment as soon as possible to improve the outcome.

The importance of early intervention in the diagnosis and management of infants with SMA is becoming increasingly clear

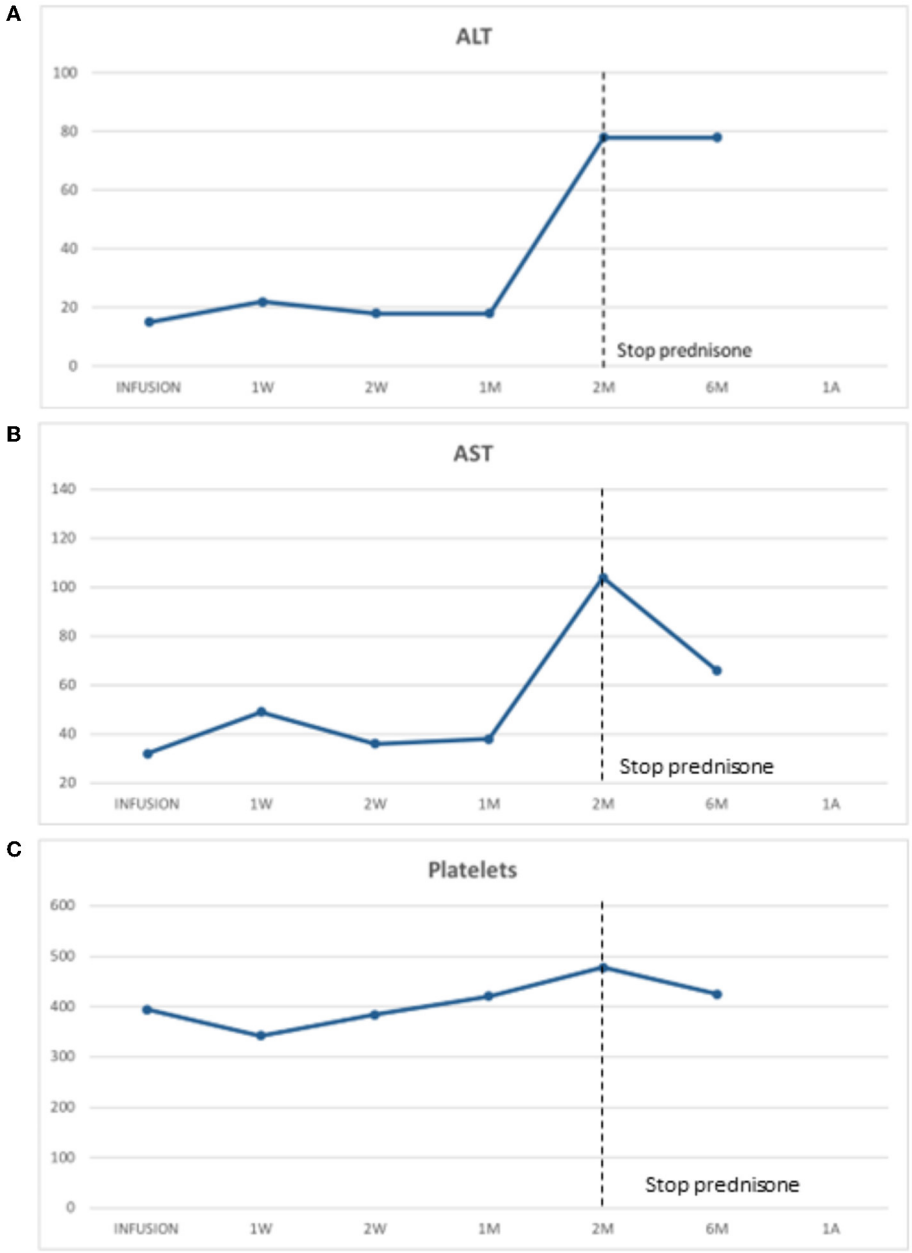

FIGURE 1
(A) Alanine transaminase (ALT) was stable post-gene therapy infusion during prednisone and initially elevated upon prednisone wean but later stabilized. **(B)** Aspartate transaminase (AST) was stable post-gene therapy infusion with prednisone daily. It was initially elevated and then stabilized post-prednisone weaning. **(C)** Platelet post-gene therapy infusion. There was a typical drop in platelet level post-gene therapy with a nadir at day 7 postinfusion which later recovered.

to save motor neurons and prevent declines in motor functioning. Signs and symptoms of SMA often begin in the first 6 months of life (1). Given this and the potential adverse effects that novel therapies play in SMA management, impacts to a preterm infant come with many considerations where a balance of implementing early treatment while considering the physiology of a preterm infant is necessary. As mentioned before, we will be focusing on the use of gene replacement therapy in preterm infants and the currently available evidence.

Impact of steroid use on the immune system

Currently, the use of onasemnogene abeparvovec-xioi requires the use of systemic corticosteroids (prednisone) at 1 mg/kg for at least 1-month posttherapy with the 2nd month tapering the dose to help with the management of the adverse effect of liver inflammation that comes with gene therapy. According to the FDA, onasemnogene abeparvovec-xioi is not recommended

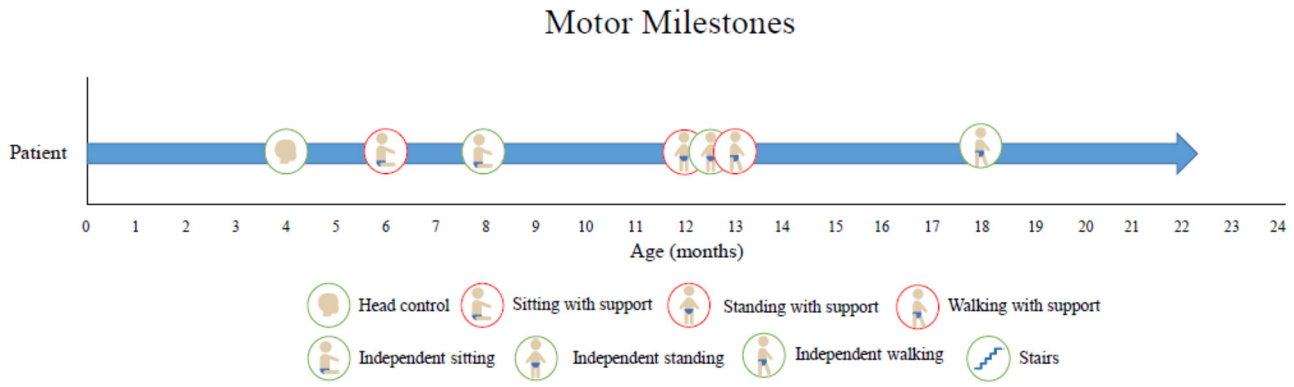

FIGURE 2
Motor milestone development. At 4 months of age, he obtained head control, at 8 months, he achieved sitting independently, and at 12 months, he was able to stand with support. Presently, at 20 months of age, he is currently walking short distances, can stand independently, reaches for objects, and has good head control.

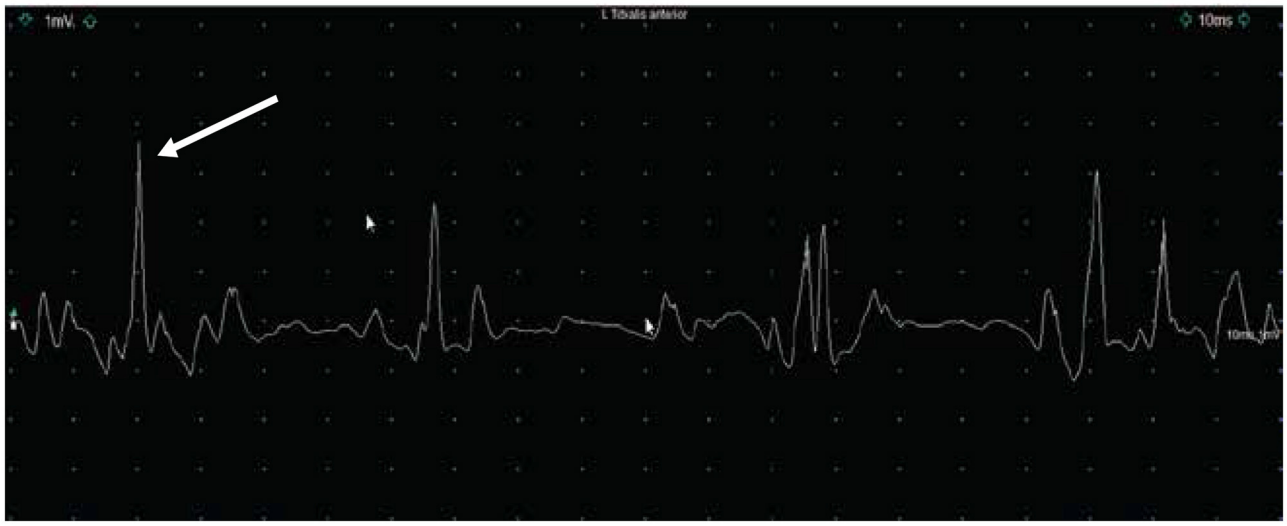

FIGURE 3
Electromyography (1mv/Div; 10 ms/Div) (EMG) with a concentric needle over the left tibialis anterior muscle showing the presence of high-amplitude motor unit potential between 2.5mV and 4mV at 20 months of age. We did not observe any spontaneous activity.

until preterm infants reach full-term gestational age because the use of corticosteroids can affect neurological development (9). However, in a study of preterm infants with bronchopulmonary dysplasia (BPD), the primary management strategy is a course of systemic corticosteroids for a short period of time (10). The primary risks are adrenal insufficiency and growth failure, but with close monitoring and recognition, these adverse effects could be managed accordingly or prevented. Similar to onasemnogene abeparvovec-xioi in preterm infants with SMA, the benefits of having the corticosteroid and recovering from the disorder have a far greater impact on the outcome of the disease than the adverse effects of corticosteroid use.

Regarding immunosuppression in a preterm infant, the immune system is not fully developed from an embryological standpoint and is not exposed to prior antigens. The use of corticosteroids in addition to adeno-associated virus 9 vector (AAV9) needed in onasemnogene abeparvovec-xioi adds to the stress of the immune system. Corticosteroids lead to further immunosuppression in the preterm infant that is already weakened. Several immune pathways have reduced involvement, and immune immaturity is present in premature neonates in proportion to their age (10). Fragile skin, moderate-to-severe hypogammaglobulinemia, decreased lymphocyte counts, plasma complement, and antimicrobial peptide levels are also seen in premature babies (10). Extreme preterm children lack trans-placental transfer of maternal antibodies, which occurs primarily during the third trimester of pregnancy. Given the specific susceptibility of preterm newborns' developing organs, it is probable that a lower inflammatory response during fetal life protects against the potentially harmful consequences of an overactive immune system (10). Most of the adverse effects related to AAV9 expressing SMN therapy have been related to the immune response toward the viral infection. Thus, it might be that preterm infants will have an advantage at the time of receiving therapies

where AAV is the vector. Moreover, AAV infection has not been directly connected to any specific disease, thus reducing the need of high-dose steroids for a prolonged period of time (10).

Steroids and the developing brain

With the administration of onasemnogene abeparvovec-xioi, infants are started on low-dose prednisone for the management of liver inflammation post-onasemnogene abeparvovec-xioi. There is growing concern and evidence that the use of corticosteroids can impact the developing brain in a preterm infant. Most of the evidence of the impact of corticosteroids on neurodevelopment comes from the use of steroids in chronic lung disease, and the risk of short-term corticosteroid use outweighs the potential benefits in particular when considering SMA (8). An example is in the treatment of BPD, where infants are given dexamethasone for earlier weaning and extubation of mechanical ventilation. However, studies have now shown that the administration of dexamethasone within the 1st week of life has been associated with an increased risk for adverse effects including speech, cognitive, and learning impairments (11). This is concerning when these infants are on steroids post-onasemnogene abeparvovec-xioi for at least 1 month before they are weaned off, and these infants are often still in their first 3 months of life. In a multicenter cohort study examining the use of steroids on preterm infants with BPD, infants given prednisone or methylprednisolone had less impact on the developing brain compared with infants given dexamethasone in neurodevelopment (12). This suggests that considering an alternative systemic corticosteroid may be a solution to minimizing the risk of neurodevelopmental health. Further studies are required to continue to evaluate this risk in particular preterm infants post-onasemnogene abeparvovec-xioi.

Pediatric liver and early steroid use

The liver continues to mature right after birth regardless of gestational age, and full liver maturity takes up to 2 years to be achieved (6). Although this liver immaturity has little effect on a healthy full-term infant, preterm infants are particularly susceptible to the effect of an immature liver (6, 13). Preterm infants have a higher risk of bleeding, cholestasis, hypoglycemia, and impaired drug metabolism. This can lead to significant concerns with the metabolism of onasemnogene abeparvovec-xioi as it is encapsulated in an AAV9 vector that has been shown to cause liver inflammation and chronically elevated transaminases in patients with SMA post-gene therapy (14). Liver insufficiency is a major concern post-gene therapy administration, and onasemnogene abeparvovec-xioi has a black box warning for the potential to cause acute serious liver injury and acute liver failure (9). There have also been reported two deaths in children following onasemnogene abeparvovec-xioi administration due to liver failure (9).

In addition to liver immaturity, preterm infants are 80% more likely to have neonatal jaundice. This is a result of increased red cell breakdown and decreased bilirubin excretion and leads to unconjugated hyperbilirubinemia. There is currently no contraindication or safety data of onasemnogene abeparvovec-xioi administration and neonatal jaundice, but in a preterm infant who is at increased risk with a longer time to recover from jaundice, it is uncertain if this would be a reason to delay gene therapy.

With weekly bloodwork, the impact on the liver was assessed in our preterm infant regularly, and this allowed for early recognition of liver injury. His neonatal jaundice had resolved prior to the administration of onasemnogene abeparvovec-xioi, therefore this did not place him at higher risk.

Pediatric nephrogenesis

Nephrogenesis is completed by 34–36 weeks of gestation, and kidney function continues to mature during the postnatal period (15). Thus, a preterm infant whose kidney development and function are delayed and immature at birth poses particular susceptibility in the preterm infant to kidney injury and long-term impacts on kidney functioning (16). This is particularly concerning in preterm infants' post-onasemnogene abeparvovec-xioi as cases of thrombotic microangiopathy (TMA) were reported post-onasemnogene abeparvovec-xioi that have led to kidney failure (9). Post onasemnogene abeparvovec-xioi preterm infants may be especially susceptible to any possible exogenous disturbance causing fluid and electrolyte management to be more challenging.

Pediatric thrombocytopenia

Platelet count is an important consideration for infants receiving onasemnogene abeparvovec-xioi since thrombocytopenia and TMA have been previously reported in patients who received gene replacement therapy (9). Premature infants have a higher incidence of thrombocytopenia often due to multiple risk factors including small for gestational age, maternal preeclampsia, infection, and disseminated intravascular coagulation (17). Thrombocytopenia in neonates may also relate to an inability of platelet precursors or megakaryocytes to increase in size in response to increased platelet demands or thrombopoietin stimulation (18). This, therefore, decreases the ability of the neonatal hematopoietic system to respond to the need for platelets in a situation of consumption or destruction as seen with TMA or infection, which can be particularly challenging for the premature infant.

In our patient, we observed a typical decrease in platelet levels with a nadir at day 7 postinfusion which later recovered (Figure 1C). It is not clear which patients will naturally improve their platelet levels or which ones might be heading to an episode of TMA. Further investigations and better guidelines are needed in future to clarify this important question.

Cardiac involvement in the pediatric infant

Due to cardiac immaturity, preterm newborns are subject to myocardial structural and functional maladaptation after

delivery (3). The elevation of troponin I has been reported in patients post-onasemnogene abeparvovec-xioi; however, no clinically significant cardiac events have been reported (9). Animal studies have shown cardiac involvement in mice following intravenous injection of onasemnogene abeparvovec-xioi, including mild mononuclear infiltration, mild fibrosis, and scattered cardiomyocytes degeneration and regeneration (19). The use of corticosteroids in the preterm infant can also lead to thickening or hypertrophy of the left ventricle (20). This is a common side effect of corticosteroid that was reported in premature infants that were on the medication for as long as 42 days or as short as 3 days (21). It is thus recommended that preterm infants are closely monitored for cardiac involvement secondary to steroid exposure until they are discontinued. Included in our weekly bloodwork was troponin I levels which remained stable in our preterm infant without signs of elevation post-onasemnogene abeparvovec-xioi and with prednisone.

Conclusion

With the rise in early identification of SMA through newborn screening programs, more infants are diagnosed with SMA prior to symptoms appearing allowing for clinicians to initiate treatment with a novel therapy early in the course of the disease leading to improved outcomes and saving motor neurons. With this early identification, there is a rise in identifying preterm infants who may be impacted by SMA. Although their physiologic immaturity, increased risk of gene therapy, and corticosteroid use post-gene therapy pose an increased risk to the preterm infant, waiting to treat until the infant is 39-week gestation also poses a risk of losing motor neurons and leads to symptoms. Knowing that time is a muscle and with careful monitoring and guidance from a multidisciplinary team, it is valuable to consider early treatment even in a preterm infant. Opting to bridge with nusinersen administration as a local impact rather than the systemic effects seen in onasemnogene abeparvovec-xioi may be one method to ensuring the best outcome. It is also imperative to consider that each individual case may differ, and thus, evaluating each clinical presentation on a case-by-case basis may also be warranted until there are enough data to suggest otherwise. We recognize that this is one case of a preterm infant and to investigate this further, we would require more data to suggest the risk and benefits of early treatment in the preterm infant. We hope to bring awareness to this clinical predicament and acknowledge the advent of medicine and change in the natural history of SMA with the rise of novel therapies, as well as the need to still treat the preterm infant early is imperative for the best possible outcome of the disease.

Data availability statement

The raw data supporting the conclusions of this article will be made available by the authors, without undue reservation.

Ethics statement

The studies involving humans were approved by the SickKids Hospital Ethics Committee. The studies were conducted in accordance with the local legislation and institutional requirements. Written informed consent for participation was not required from the participants or the participants' legal guardians/next of kin in accordance with the national legislation and institutional requirements. Written informed consent was obtained from the minor(s)' legal guardian/next of kin for the publication of any potentially identifiable images or data included in this article. Written informed consent was obtained from the participant/patient(s) for the publication of this case report.

Author contributions

EN and HG drafted the manuscript and analyzed the data. All other authors reviewed their respective specialties and revised it critically for publication. All authors contributed to the article and approved the submitted version.

Conflict of interest

EN has been a speaker for Biogen, Novartis, and Roche and on the advisory board for Novartis. HG has been a speaker and on the advisory board for Biogen, Novartis, and Roche. CC has been site investigator for Biogen and Roche clinical trials and on advisory board for Biogen, Roche and Novartis. AJ is on an advisory board for Ultragenyx and Merck and has received an unrestricted educational grant from Abbott.

The remaining authors declare that the research was conducted in the absence of any commercial or financial relationships that could be construed as a potential conflict of interest.

Publisher's note

All claims expressed in this article are solely those of the authors and do not necessarily represent those of their affiliated organizations, or those of the publisher, the editors and the reviewers. Any product that may be evaluated in this article, or claim that may be made by its manufacturer, is not guaranteed or endorsed by the publisher.

References

1. Arnold WD, Kassar D, Kissel JT. Spinal muscular atrophy: diagnosis and management in a new therapeutic era. *Muscle Nerve.* (2005) 51:157–67. doi: 10.1002/mus.24497

2. Finkel RS, McDermott MP, Kaufmann P, Darras BT, Chung WK, Sproule DM, et al. Observational study of spinal muscular atrophy type I and implications for clinical trials. *Neurology.* (2014) 83:810–7. doi: 10.1212/WNL.0000000000000741

3. Aslesh T, Yokota T. Restoring SMN expression: an overview of the therapeutic developments for the treatment of spinal muscular atrophy. *Cells.* (2022) 11:417. doi: 10.3390/cells11030417

4. Ramos DM, d'Ydewalle C, Gabbeta V, Dakka A, Klein SK. Age-dependent SMN expression in disease-relevant tissue and implications for SMA treatment. *J Clin Invest.* (2019) 129:4817–831. doi: 10.1172/JCI124120

5. *Newborn Screening Ontario Program 2022. Spinal Muscular Atrophy*. Ottawa: CHEO (2022).

6. Nault JC, Datta S, Imbeaud S, Franconi A, Mallet M. Recurrent AAV2-related insertional mutagenesis in human hepatocellular *carcinomas. Nature Genetics.* (2015) 47:1187–1193. doi: 10.1038/ng.3389

7. Preterm Birth. (2022). Available online at: https://www.who.int/news-room/fact-sheets/detail/preterm-birth (accessed May 10, 2023).

8. Lee BH, Waldrop MA, Connolly AM, Ciafaloni E. Time is muscle: a recommendation for early treatment for preterm infants with spinal muscular atrophy. *Muscle Nerve.* (2001) 64:153–5. doi: 10.1002/mus.27261

9. *Highlights of Prescribing Information for Zolgensma*. Durham: Novartis Gene Therapies, Inc (2021).

10. Htun ZT, Schulz EV, Desai RK, Marasch JL, McPherson CC, Mastrandrea LD, et al. Postnatal steroid management in preterm infants with evolving bronchopulmonary dysplasia. *J Perinatol Off J Perin Assoc.* (2021) 41:1783–96. doi: 10.1038/s41372-021-01083-w

11. Barrington KJ. The adverse neuro-developmental effects of postnatal steroids in the preterm infant: A systemic review of RCTs. *BMC Pediatric.* (2001) 1:1. doi: 10.1186/1471-2431-1-1

12. Puia-Dumitrescu M, Wood TR, Comstock BA, Law JB, German K, Perez KM, et al. Dexamethasone, prednisolone, and methylprednisolone use and 2-year neurodevelopmental outcomes in extremely preterm infants. *JAMA network open.* (2022) 5:e221947. doi: 10.1001/jamanetworkopen.2022.1947

13. Chand D, Mohr F, McMillan H, Tukov FF, Montgomery K, Kleyn A, et al. Hepatotoxicity following administration of onasemnogene abeparvovec (AVXS-101) for the treatment of spinal muscular atrophy. *J Hepatol.* (2021) 74:560–6. doi: 10.1016/j.jhep.2020.11.001

14. Black MJ, Sutherland MR, Gubhaju L, Kent AL, Dahlstrom JE, Moore L, et al. When birth comes early: effects on nephrogenesis. *Nephrology.* (2013) 18:180–2. doi: 10.1111/nep.12028

15. Corrêa LP, Gatto FR, Bressani GYS, Lanza K, Simões E. Nephrogenesis, renal function, and biomarkers in preterm newborns. *Curr Med Chem.* (2022) 25:4097–112. doi: 10.2174/0929867328666211101102227

16. Beiner ME, Simchen MJ, Sivan E, Chetrit A, Kuint J, Schiff E, et al. Risk factors for neonatal thrombocytopenia in preterm infants. *Am J Perinatol.* (2003) 20:49–54. doi: 10.1055/s-2003-37948

17. Davenport P, Liu ZJ, Sola-Visner M. Changes in megakaryopoiesis over ontogeny and their implications in health and disease. *Platelets.* (2020) 31:692–9. doi: 10.1080/09537104.2020.1742879

18. Estcourt LJ. Platelet transfusion thresholds in premature neonates (PlaNeT-2 trial). *Transf Med.* (2019) 29:20–2. doi: 10.1111/tme.12587

19. Woodgate P, Jardine LA. Neonatal jaundice. *BMJ Clin Evid.* (2011) 2011: 0319.

20. Vrselja A, Pillow JJ, Black MJ. Effect of preterm birth on cardiac and cardiomyocyte growth and the consequences of antenatal and postnatal glucocorticoid treatment. *J Clin Med.* (2021) 10:3896. doi: 10.3390/jcm10173896

21. Brozanski BS, Jones JG, Gilmour CH, Balsan MJ, Vazquez RL, Israel BA, et al. Effect of pulse dexamethasone therapy on the incidence and severity of chronic lung disease in the very low birth weight infant. *J Pediatr.* (1995) 126:769–76. doi: 10.1016/S0022-3476(95)70410-8

frontiers | Frontiers in Neurology

TYPE Case Report
PUBLISHED 14 September 2023
DOI 10.3389/fneur.2023.1227505

OPEN ACCESS

EDITED BY
Giovanni Meola,
University of Milan, Italy

REVIEWED BY
Henry Hrdlicka,
Gaylord Hospital, United States
Nakul Katyal,
Stanford Healthcare, United States

*CORRESPONDENCE
Pengfei Wang
✉ wpf5287598@163.com
Yong Zhang
✉ 48259958@qq.com

RECEIVED 23 May 2023
ACCEPTED 14 August 2023
PUBLISHED 14 September 2023

CITATION
Geng N, Wang P and Zhang Y (2023) Acute motor-sensory axonal polyneuropathy variant of Guillain-Barré syndrome with a thalamic lesion and COVID-19: a case report and discussion on mechanism.
Front. Neurol. 14:1227505.
doi: 10.3389/fneur.2023.1227505

Acute motor-sensory axonal polyneuropathy variant of Guillain-Barré syndrome with a thalamic lesion and COVID-19: a case report and discussion on mechanism

Na Geng, Pengfei Wang* and Yong Zhang*

Department of Neurology, Weihai Municipal Hospital, Weihai, China

Background: Severe acute respiratory syndrome coronavirus 2 (SARS-CoV-2) primarily affects the respiratory system. During the global coronavirus disease (COVID-19) pandemic, COVID-19-associated neurological diseases have been increasingly reported, including peripheral nervous system diseases, such as Guillain–Barré syndrome (GBS). Acute motor-sensory axonal polyneuropathy (AMSAN), is a GBS variant associated with COVID-19. To date, there are no reports of GBS cases with thalamic injury and dynamic evolution with fluctuating GBS symptoms. In this report, we describe the first case of COVID-19-associated AMSAN accompanied by a thalamic lesion and discuss the magnetic resonance imaging (MRI) findings.

Case presentation: A 76-year-old woman, with known co-morbid type 2 diabetes mellitus, presented to the emergency room with complaints of weakness and paraesthesia in both her legs and arms for 4 days, and fever and dry cough for the past 5 days. A nasopharyngeal swab for SARS-CoV-2 returned positive. The patient had not received specific treatment for COVID-19 infection. Neurological examination disclosed symmetric weakness (Medical Research Council grade upper limbs 4/5, lowers limbs 2/5) and areflexia in both the legs and feet. No cranial nerves were involved. Following a neuro-electro-physiology study to evaluate neurological symptoms, AMSAN was suggested. Cerebrospinal fluid (CSF) analysis showed elevated protein levels that confirmed the diagnosis of GBS. The patient was subsequently treated with intravenous immune globulin (IVIG), which improved her neurological symptoms (upper limbs 4/5, lowers limbs 4/5). However, urinary retention, dysarthria, dysphagia, bilateral facial paralysis, facial diplegia, bucking, and motor alalia gradually appeared, followed by aggravated paralysis (upper limbs 3/5, lowers limbs 1/5). After being hospitalized for 16 days, the patient underwent continuous plasma exchange (PE) treatment for a duration of 3 days. Following treatment, the patient's neurological symptoms and paralysis gradually improved (upper limbs 4/5, lowers limbs 4/5) over 2 weeks. Meanwhile, we observed that the patient's cerebral magnetic resonance imaging (MRI) findings dynamically evolved along with the fluctuation of her GBS symptoms, mainly in terms of the changes in T2 hyperintensity in the right thalamus accompanied by microhaemorrhages. The inflammation index was normal. We considered a wide range of possible causes including hypoxia, drugs, toxins, and metabolic derangements but these were excluded.

Conclusion: The AMSAN variant of GBS secondary to COVID-19 infection is severe and can cause extensive damage to the peripheral nerves system. The deterioration

of symptoms in the patient after early immunotherapy may indicate treatment-related fluctuation (TRF) and could be attributed to immune rebound. Moreover, an excessive immune response post-COVID-19 infection may trigger concurrent damage to the central nervous system, indicating secondary harm to brain small blood vessels and nerve units. For suspected cases of GBS complicated by COVID-19, it is essential to conduct early brain MRI examinations in addition to routine peripheral nervous system evaluations to promptly detect any intracranial lesions. This facilitates appropriate immunotherapy and improves patient prognosis.

KEYWORDS

Guillain-Barré syndrome, COVID-19, neuro-electrophysiological characteristics, MRI findings, thalamic lesion

Introduction

Severe acute respiratory syndrome coronavirus 2 (SARS-CoV-2), which causes the coronavirus disease 2019 (COVID-19), primarily affects the respiratory system. During the global COVID-19 pandemic, neurological complications of COVID-19 have been increasingly reported, including Guillain–Barré syndrome (GBS) (1). GBS is an acute poly radiculo-neuropathy characterized by rapid progression, symmetrical limb weaknesses, areflexia, sensory symptoms, and, in some patients, facial weakness. GBS is a life-threatening inflammatory/autoimmune condition, in which the immune system targets healthy nerve cells in the peripheral nervous system (PNS) (2). The common variants of GBS include acute inflammatory demyelinating polyradiculoneuropathy (AIDP) which is a motor sensory demyelinating disorder; and acute motor axonal neuropathy (AMAN), and acute motor and sensory axonal neuropathy (AMSAN), both of which are axonal disorders (3). The AMSAN variant of GBS has been associated with COVID-19 (4). The symptoms of AMSAN are severe and the prognosis is poor. To date, there are no reported cases of AMSAN involving the central neurovascular unit or discussions relating to the findings on cerebral magnetic resonance imaging (MRI). In this report, we described the first case of COVID-19-associated AMSAN, accompanied by a thalamic lesion detected on MRI. We also discussed the thalamic injury, in which the symptoms dynamic evolved and fluctuated (Figure 1).

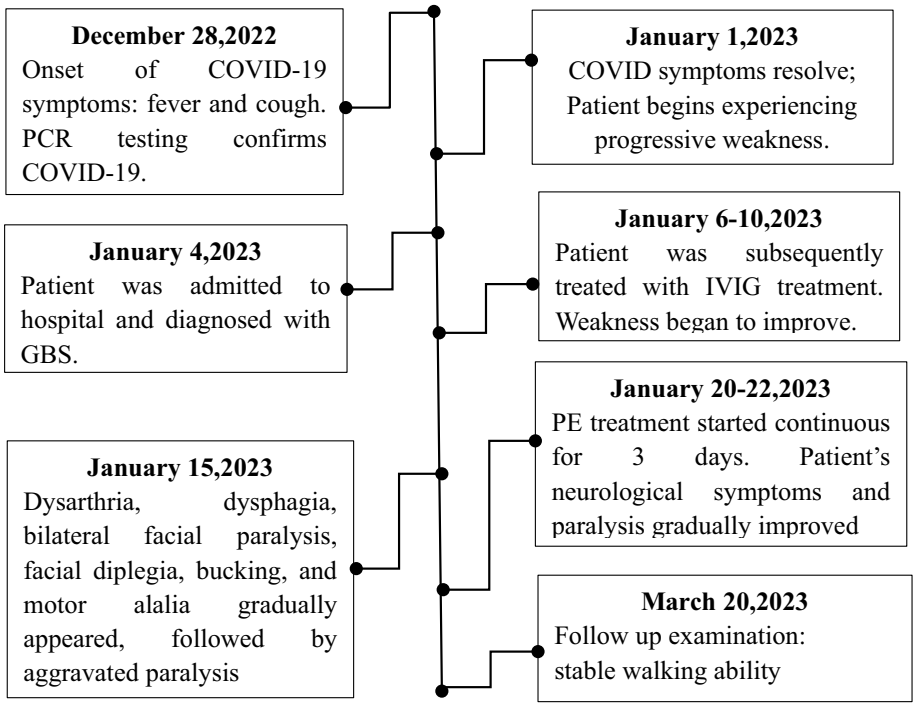

FIGURE 1
Patient timelines. Starting December 28, 2022, the timeline of the patient's diagnosis, treatment, recovery and other significant events are outlined until March 20, 2023, the symptoms of weakness recover.

Case presentation

On January 6, 2023, during the COVID-19 epidemic in this region of China, a 76-year-old woman, with known co-morbid type 2 diabetes mellitus, presented to the emergency room of our hospital, the Third Grade First Class Hospital, with complaints of weakness and paraesthesia in both her legs and arms for four days, and fever and dry cough for the past 5 days. A nasopharyngeal swab for SARS-CoV-2 returned positive. The patient had received the inactivated COVID-19 virus vaccine one year ago, and had not been administered any other specific antiviral therapy for a COVID-19 infection.

On admission, baseline laboratory investigations were performed (Table 1). A nasopharyngeal swab was repeated for COVID-19 PCR testing. The result of which was negative. However, the serologic test result was positive. A brain MR was performed prior to the patient's onset (2022.11), and no abnormal signals were detected (Figures 2A–D). Following admission, the patient underwent a subsequent cerebral MRI re-examination, which revealed slightly elevated signals (T2) and low signals in the right thalamus (SWI) (Figures 2F,G). However, no hyperintensity was observed in T1 or DWI (Figures 2E,H). The patient was treated with intravenous immunoglobulin (IVIG 0.4 g/kg·d) for 5 days.

On further investigation, the neuro-electrophysiology (Table 2) examination on January 8, 2023 showed a decreased compound muscle action potential (CMAP) amplitude and sensory nerve action potential (SNAP) amplitude in the left median and ulnar nerves. Based on these results, AMSAN was suggested. Cerebrospinal fluid (CSF) analysis was performed and the results demonstrated elevated protein levels (1871.9 mg/dL, normal 150–450 mg/dL) while the leukocyte level was normal (2/mm3), Based on the clinical findings, neurophysiological studies, CSF analysis, and cervical MRI, the patient was diagnosed with AMSAN, a GBS variant associated with COVID-19. The MRI of the patient's cervical spine revealed no abnormal signals in the cervical spinal cord, ruling out the possibility of limb numbness and weakness caused by lesions in the cervical spinal cord. Although we considered COVID-19-related AMSAN based on patients' history of COVID-19 infection, acute limb movement, sensory disturbance, protein cell isolation, and EMG results, there are limitations due to the lack of proximal CMAPs and the timing of the EMG study. Furthermore, despite the patient's history of diabetes, there were no neuropathic symptoms (sensory or motor) related to diabetes. Therefore, considering the distal axonal sensory and motor changes caused by AMSAN.

After some improvement of the limb weakness following treatment with IVIG, the patient experienced aggravated symptoms including choking on water, slurred speech, weakness during chewing, reduced muscle strength, and urinary retention. The neurological examination on day 11 reported the patient as conscious, with dysarthria, bilateral eyelid closure weakness, a left eye fissure of 6 mm and a right eye fissure of 4 mm, a flattened left nasolabial fissure, tongue deviation towards the right side on attempted protrusion, grade 3 upper limb muscle strength, grade 1 lower limb muscle strength, negative patellar reflex (−), and negative Babinski sign (−). The above symptoms continued to aggravate. On January 19, 2022, a re-examination with cerebral MRI revealed that the right thalamus had T1 hypointensity and a more pronounced T2 hyperintensity than before. Moreover, hypointensity was detected on the susceptibility-weighted imaging (SWI), while no hyperintensity was noted on the diffusion-weighted imaging (DWI) (Figures 2I–L). After 16 days of hospitalization, the patient underwent a continuous plasma exchange (PE) treatment for a duration of 3 days. On February 3, 2022, the patient had grade 4 muscle strength in the upper limbs and grade 2 muscle strength in the lower limbs. Another re-examination with cerebral MRI revealed a loss of both T1 hypointensity and T2 hyperintensity in the right thalamus. Only the hypointense lesion on SWI was visible (Figures 2M–P). Two weeks after the follow-up, the lower limb muscle strength of the patient improved to grade 4. The patient continued rehabilitation by OT/PT cotreatment sessions (Table 3). One month after the follow-up, the patient demonstrated stable walking ability and overall improvement of her condition.

TABLE 1 Baseline investigations of the patient on admission.

Parameter	Result	Normal range
Complete blood count		
Hb (g/dl)	143	115–150
MCV (fl)	88	82–100
MCH (pg)	30.8	27–34
MCHC (Gm/dL)	350	316–354
Total leukocyte count (*10^9/L)	1.75	1.1–3.2
Lymphocytes (%)	29.9	20–50
Neutrophils (%)	63.8	40–75
Platelets count (counts/uL)	262,000	125,000–350,000
Inflammatory markers		
CRP (mg/dL)	1.98	0–3
ESR (mm/h)	31	0–20
Biochemical profile		
Sodium (mEq/L)	135	135–145
Potassium (mEq/L)	3.91	3.5–5.5
Chloride (mEq/L)	97.2	96–108
Calcium (mEq/L)	2.27	2.12–2.52
Magnesium (mg/dl)	0.66	0.66–1.07
Phosphorous (mg/dl)	0.79	0.81–1.58
BUN (mg/dL)	3.94	3.2–7.1
Cr (mg/dl)	54.6	36–100
COVID-19 antigen		
IgG (500copy/ml)	149.02	0–1
IgM (500copy/ml)	3.45	0–1
CSF protein (mg/dL)	1871.9	150–450
CSF cell (*10^6/L)	2	0–1

Hb, Hemoglobin; MCV, Mean Corpuscular Volume; MCH, Mean Corpuscular Hemoglobin; MCHC, Mean Corpuscular Hemoglobin Concentration; CRP, C-Reactive Protein; ESR, Erythrocyte Sedimentation Rate; BUN, Blood Urea Nitrogen; Cr, creatinine; CSF, Cerebrospinal fluid.

Discussion

Several variants of GBS exist. It is an immune-mediated polyneuropathy that is most often preceded by an infection. In this report, we described a patient with AMSAN, a variant of GBS, that presented with a thalamic lesion, and was associated with COVID-19.

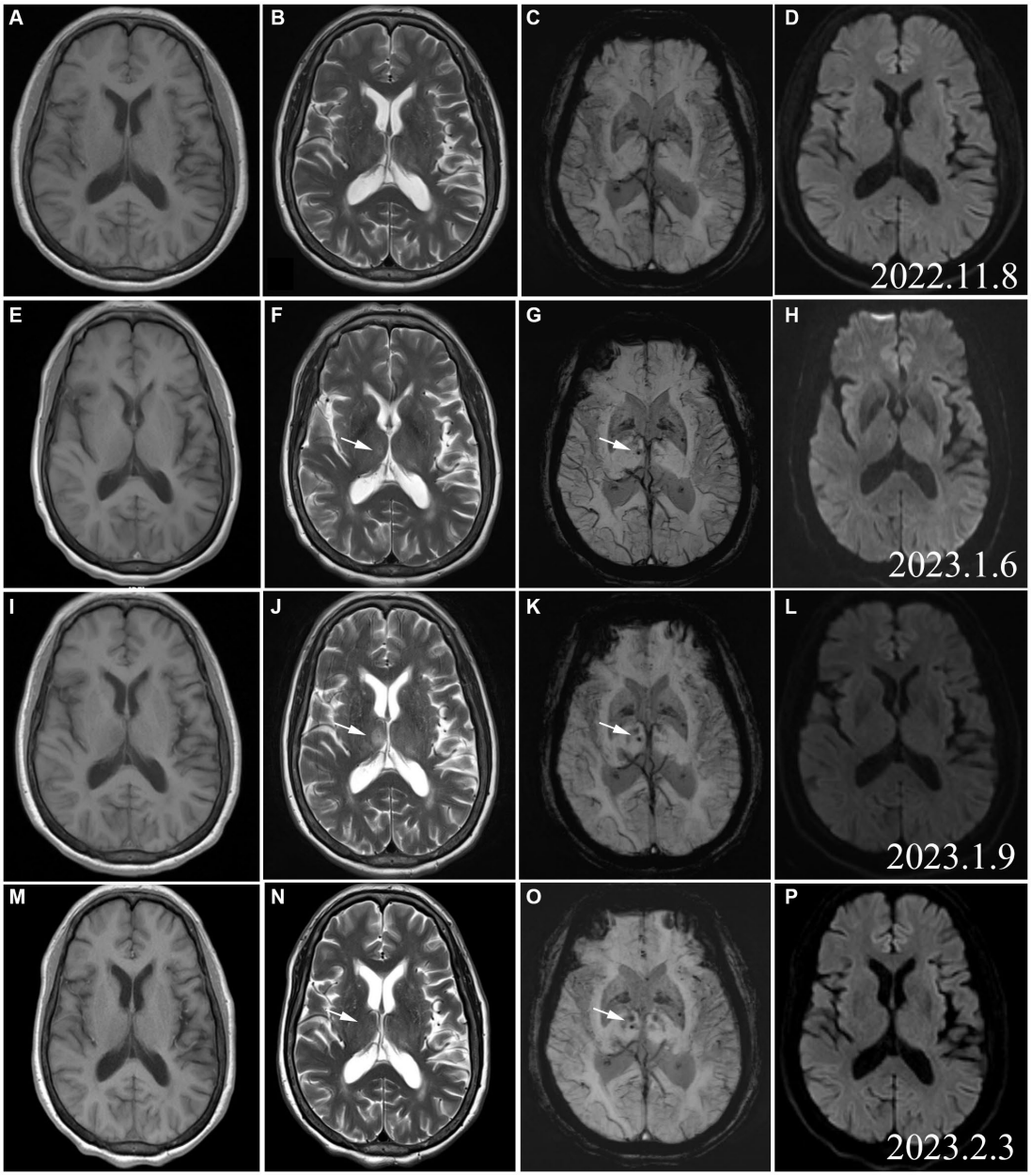

FIGURE 2
Cerebral MRI (2022.11): **(A)** T1WI; **(B)** T2WI; **(C)** SWI; **(D)** DWI. No signals in the right thalamus on the images acquired with these imaging sequences. MRI **(A–D)** conducted before the onset of the patient, and no abnormal signals were found. As a group of normal controls, we found subsequent changes in thalamic lesions. Cerebral MRI (2023.1.6): E: T1WI; **(F)** T2WI; **(G)** SWI hypointense punctate foci. **(H)** No DWI hyperintensity. Cerebral MRI (2023.1.19): **(I)** T1WI hypointensity in the right thalamus. **(J)** T2WI hyperintensity in the right thalamus; **(K)** SWI hypointense punctate foci in the right thalamus; **(L)** No DWI hyperintensity,represented the signal contrast of the rest of the MR Sequence; **(N)** T2WI hyperintensity in the right thalamus disappeared; **(O)** SWI hypointense punctate foci in the right thalamus; **(P)** No DWI hyperintensity.

AMSAN is more commonly associated with COVID-19 in Asia (4). In our patient with AMSAN, we observed fluctuations in symptom progression despite IVIG treatment. The patient's condition stabilized and improved only after receiving PE treatment. At the follow-up, significant improvements in muscle strength were observed. The pathophysiological mechanism of GBS caused by COVID-19 is still unclear. For GBS triggered by SARS-COV-2, it has been hypothesized to be the result of cross-reactivity between the viral protein–associated gangliosides and peripheral nerve gangliosides leading to molecular mimicry (5). In contrast, others have suggested that GBS was not associated with COVID-19, as autoantibodies were not detected (6). In our patient with AMSAN, anti-ganglioside antibodies and GD1b IgG antibodies were not detected in the serum and CSF samples. The patient's symptoms worsened once again after a brief period of improvement following immunoglobulin treatment, possibly indicating treatment-related fluctuations. It has been reported that one patient developed Guillain-Barré syndrome (GBS) after being infected with COVID-19, and treatment-related fluctuations (TRF) after receiving intravenous immunoglobulin (immunoglobulin) treatment. However, complete recovery was achieved after multiple rounds of

TABLE 2 Neuro-electrophysiology report results.

Motor nerve conduction study								
Nerve recording site	CMAPS amplitude (mV)		Distal latency (ms)		Proximal latency (m/s)		Conduction velocity (m/s)	
	Lt.	Normal value	Lt.	Normal value	Lt.	Normal value	Lt.	Normal value
Median APB	2.7	>4	8.78	<4.5	14.4		39.1	45–55
Ulnar ADM	5.0	>6*	4.31	<4.2	3.27		58.6	45–55
Peroneal EDB	0.044	>2	9.46	<6.5	17.4		33.3	40
Tibial AHB	0.74	>3	5.19	<6.5	16		30.7	40
Peroneal TA	0.080	>2	7.6	<3	28.4		36.5	40

Sensory nerve conduction study				
Nerve	Latency		Snaps Amplitude UV	
	Recording value	Normal range	Recording value	Normal range
Left Median	3.72	2.9–3.5	0.45	>15
Left Ulnar	2.97	2.9–3.5	7.7	>15
Left Sural	4.15	<4.2	3.8	>5

APB, Abductor pollicis brevis; ADM, abductor digiti minimi; EIP, extensor indicis proprius; EDB, extensor digitorum brevis; AHB, abductor halluces brevis; TA, tibialis anterior; *<70 years old, the baseline reference value for CAMP is > 4, >70 years old, the baseline diagnostic data for CMAP is > 6 (Stetson DS, JW. Albers. Effect of age, sex, and anthropometric factors on nerve conduction measures. Muscle Nerve, 1992,15:1096–1,104).

IV-IG treatment. The mechanism behind this improvement following repeated treatment may be attributed to a rebound in the immune response (7).

Another hypothesis has suggested the direct invasion of peripheral nerves by SARS-COV-2. The olfactory nerve is the most common cranial nerve that is directly affected in this way (2). Recently, a different mechanism for the nerve damage presented in COVID-19-associated GBS has been proposed, suggesting primary facilitation through T-cell activation, release of inflammatory factors, and activation of macrophages, resulting in a hyperinflammatory response. Furthermore, a novel para infectious mechanism for GBS mediated by the generalized, hyperinflammatory response that occurs with COVID-19 has also been suggested, because the acute symptoms overlap with the onset of GBS, and autoantibodies were not detected (8). Our case supports this hypothesis. We have included this suggestion in the article. However, we did not carry out additional CD4/8 T lymphocyte tests. Further research is required to confirm and evaluate the common T-cell biomarkers using specialized blood panels. For our patient, serum and CSF ganglioside antibodies and GD1b IgG antibodies were negative. Moreover, weakness and paraesthesia in both the legs and arms were accompanied by a dry cough on admission. The peripheral nerve damage was severe and extensive including the spinal nerves, cranial nerves, and autonomic nerves. Importantly, the patient improved after immunomodulation therapy. It was emphasized that follow-up rehabilitation was also very important for returning to the community (9).

After admission, we performed a series of cerebral MRI examinations on this patient. When we compared and analyzed the images obtained during hospitalization and those obtained before disease onset, we were surprised that cerebral MRI showed an emerging SWI signal from microhaemorrhage in the right thalamus with a slightly enhanced T2 signal at the early stage of the disease. As the disease aggravated, the T2 hyperintensity in the right thalamus was significantly more intense and the coverage was larger. However, the T2 hyperintensity and T1 hypointensity of the right thalamus resolved when clinical symptoms improved. The abnormal T2 signal

TABLE 3 Upper and lower extremity assessments (MRC scores).

Assessment	Admission	Progression	Discharge
RUE strength			
Shoulder	4−/5	3/5	4−/5
Elbow	4−/5	3/5	4−/5
Wrist	4/5	3+/5	4/5
Grip	4/5	3+/5	4/5
LUE strength			
Shoulder	4−/5	3/5	4−/5
Elbow	4−/5	3/5	4−/5
Wrist	4/5	3+/5	4/5
Grip	4/5	3+/5	4/5
RLE strength			
Hip flexion	2/5	1+/5	4−/5
Hip	2/5	1+/5	4−/5
Knee	2/5	1+/5	4−/5
Ankle dorsiflexion	2/5	1+/5	4−/5
RLE strength			
Hip flexion	2/5	1+/5	4−/5
Hip	2/5	1+/5	4−/5
Knee	2/5	1+/5	4−/5
Ankle dorsiflexion	2/5	1+/5	4−/5

RUE, right upper extremity; LUE, left upper extremity; RLE, right lower extremity; LLE, left lower extremity.

in the right thalamus evolved synchronously and dynamically with the changes in clinical symptoms. At the same time, in Figure 2O (SWI sequence from March 3, 2023), we observed changes in bilateral thalamic SWI, not only in the right thalamus, but also in support of the excessive immune response secondary to COVID-19. The presence of unilateral thalamus does not account for the patient's initial presentation or the deterioration of symptoms. Thalamic lesions may not be directly linked to COVID-19 infection, but could potentially be a result of secondary immune reactions. To our knowledge, this is the first reported case of AMSAN with observable damage to intracranial neurons and blood vessels.

Bickerstaff brainstem encephalitis, a variant of GBS, is known to cause damage to the brainstem. However, it mainly affects the cranial nerves and the reticular activating system. Moreover, the condition does not have any indications on medical imaging, such as cerebral MRI (10). In our patient, the lesion was located in the right thalamus with microhaemorrhages and abnormal changes in neuronal signals. The etiological analysis suggested that an exaggerated immune response to the SARS-CoV-2 infection may have affected the cerebral small vessels and thalamic neurons, thereby resulting in microhaemorrhages as well as damage and changes in the neurons.

Conclusion

AMSAN variants of GBS secondary to COVID-19 can cause severe peripheral nerve damage. The deterioration of symptoms in the patient after early immunotherapy may indicate treatment-related fluctuation (TRF) and could be attributed to immune rebound. Moreover, an excessive immune response post-COVID-19 infection may trigger concurrent damage to the central nervous system, indicating secondary harm to brain small blood vessels and nerve units. For suspected cases of GBS complicated by COVID-19, it is essential to conduct early brain MRI examinations in addition to routine peripheral nervous system evaluations to promptly detect any intracranial lesions. This facilitates appropriate immunotherapy and improves patient prognosis. Our study demonstrates that immunomodulatory therapy, such as the use of immunomodulatory drugs, can significantly alleviate both peripheral and central nervous system damage in patients with AMSAN variant GBS associated with COVID-19. This suggests that immunomodulatory drugs hold promising therapeutic value in addressing neurological symptoms related to COVID-19.

Data availability statement

The original contributions presented in the study are included in the article/supplementary material, further inquiries can be directed to the corresponding author.

Ethics statement

Ethical review and approval was not required for the study on human participants in accordance with the local legislation and institutional requirements. Written informed consent from the patients/ participants was not required to participate in this study in accordance with the national legislation and the institutional requirements. Written informed consent was obtained from the participant/patient(s) for the publication of this case report.

Author contributions

All authors listed have made a substantial, direct, and intellectual contribution to the work and approved it for publication.

Conflict of interest

The authors declare that the research was conducted in the absence of any commercial or financial relationships that could be construed as a potential conflict of interest.

Publisher's note

References

1. Fragiel M, Miró Ò, Llorens P, Jiménez S, Piñera P, Burillo G, et al. Incidence, clinical, risk factors and outcomes of Guillain-Barré in Covid-19. *Ann Neurol*. (2021) 89:598–3. doi: 10.1002/ana.25987

2. Ellul MA, Benjamin L, Singh B, Lant S, Michael BD, Easton A, et al. Neurological associations of COVID-19. *Lancet Neurol*. (2020) 19:767–3. doi: 10.1016/S1474-4422(20)30221-0

3. van den Berg B, Walgaard C, Drenthen J, Fokke C, Jacobs BC, van Doorn PA. Guillain-Barré syndrome: pathogenesis, diagnosis, treatment and prognosis. *Nat Rev Neurol*. (2014) 10:469–2. doi: 10.1038/nrneurol.2014.121

4. Ali S, Karam A, Lalani A, Jawed S, Moin M, Douba Z, et al. A remarkable case of acute motor-sensory axonal polyneuropathy (AMSAN) variant of Guillain Barré syndrome, in a diabetic patient infected with COVID-19: a case report and review of the literature. *Front Neurol*. (2022) 13:937989. doi: 10.3389/fneur.2022.937989

5. Sriwastava S, Kataria S, Tandon M, Patel J, Patel R, Jowkar A, et al. Guillain Barré syndrome and its variants as a manifestation of COVID-19: a systematic review of case reports and case series. *J Neurol Sci*. (2021) 420:117263. doi: 10.1016/j.jns.2020.117263

6. Toscano G, Palmerini F, Ravaglia S, Ruiz L, Invernizzi P, Cuzzoni MG, et al. Guillain-Barré syndrome associated with SARS-CoV-2. *N Engl J Med*. (2020) 382:2574–6. doi: 10.1056/NEJMc2009191

7. Gupta S, Chandra A, Ray BK, Pandit A. Treatment related fluctuation and response to intravenous immunoglobulin therapy in post COVID-19 Guillain-Barre syndrome. *Diab Metab Synd*. (2021) 15:102246. doi: 10.1016/j.dsx.2021.102246

8. Zhao H, Shen D, Zhou H, Liu J, Chen S. Guillain-Barré syndrome associated with SARS-CoV-2 infection: causality or coincidence? *Lancet Neurol*. (2020) 19:383–4. doi: 10.1016/S1474-4422(20)30109-5

9. Connors C, McNeill S, Hrdlicka HC. Occupational and physical therapy strategies for the rehabilitation of COVID-19-related Guillain-Barré syndrome in the long-term acute care hospital setting: case report. *JMIR Rehab Assist Technol*. (2022) 9:e30794. doi: 10.2196/30794

10. Shahrizaila N, Yuki N. Bickerstaff brainstem encephalitis and fisher syndrome: anti-GQ1b antibody syndrome. *J Neurol Neurosurg Psychiatry*. (2013) 84:576–3. doi: 10.1136/jnnp-2012-302824

frontiers | Frontiers in Neurology

TYPE Case Report
PUBLISHED 27 September 2023
DOI 10.3389/fneur.2023.1213090

OPEN ACCESS

EDITED BY
Giovanni Meola,
University of Milan, Italy

REVIEWED BY
Jinzhou Feng,
First Affiliated Hospital of Chongqing Medical University, China
Bei Cao,
Sichuan University, China
Zunbo Li,
Xi'an Gaoxin Hospital, China

*CORRESPONDENCE
Zegang Yin
✉ yinzegang@hotmail.com
Mingjie Zhang
✉ zhangmingjie1989@hotmail.com

†These authors have contributed equally to this work and share first authorship

RECEIVED 27 April 2023
ACCEPTED 15 June 2023
PUBLISHED 27 September 2023

CITATION
Cao X, Zeng L, Lu Z, Fan J, Tan S, Zhang M and Yin Z (2023) A female case report of LGMD2B with compound heterozygous mutations of the *DYSF* gene and asymptomatic mutation of the X-linked *DMD* gene. *Front. Neurol.* 14:1213090. doi: 10.3389/fneur.2023.1213090

A female case report of LGMD2B with compound heterozygous mutations of the *DYSF* gene and asymptomatic mutation of the X-linked *DMD* gene

Xiaojie Cao[1†], Li Zeng[2†], Zhijie Lu[1], Jin Fan[1], Song Tan[2], Mingjie Zhang[1*] and Zegang Yin[1*]

[1]Department of Neurology, The General Hospital of Western Theater Command, Chengdu, Sichuan Province, China, [2]Department of Neurology, Sichuan Academy of Medical Science and Sichuan Provincial People's Hospital, University of Electronic Science and Technology of China, Chengdu, Sichuan Province, China

We report the case of a 31-year-old Chinese woman with a chief complaint of weakness in the lower limbs, which was diagnosed as limb-girdle muscular dystrophy 2B (LGMD2B) with compound heterozygous mutations of the *DYSF* gene. Meanwhile, this woman is an asymptomatic carrier with the mutation of the X-linked *DMD* gene. The electromyography, muscle MRI, and muscle biopsy indicated a chronic myogenic injury with dysferlin deletion. As a result of genetic testing, compound heterozygous G-to-T base substitution at position 5,497 in exon 49 of the *DYSF* gene, leading to a codon change from glutamic acid to termination codon at position 1,833, and a heterozygous C-to-G base change at position 4,638 + 8 in intron 42 of the *DYSF* gene with a consequence of splice, which has never been reported, were identified as candidate causative mutations. Unfortunately, *DMD* gene mutation c.3921+12A>G of the *DMD* gene on the X chromosome was also found in this patient. Finally, the patient was diagnosed as LGMD2B clinically and genetically. In the previous 2 years, the patient's lower limb weakness became slightly worse, resulting in even the total distance walked than before. Fortunately, during the follow-up, her son had not shown slowness or limitation of movement. Genetic testing by next-generation sequencing confirmed the final diagnosis of LGMD2B, and we identified the novel compound heterozygous variants in the *DYSF* gene, which is of great significance to the accurate diagnosis of genetically coded diseases. Much attention needs to be paid in clinics toward hereditary neuromuscular diseases with multiple pathogenic gene mutations. Genetic counseling and clinical follow-up should be the priorities in future, and promising treatments are also worth exploring.

KEYWORDS

LGMD, DMD/BMD, dysferlin, dysferlinopathy, *DYSF* gene, case report

Introduction

Limb-girdle muscular dystrophy (LGMD) is a group of rare, genetically determined degenerative muscle disorders with high genetic heterogeneity and phenotypic diversity. The main clinical manifestations are weakness and atrophy of predominant pelvic and shoulder muscles, with the typical symptom of difficulty climbing stairs. Among 11 studies included in a meta-analysis including all age groups in 2016, the pooled prevalence of LGMD

was 1.63 per 100,000 (1). According to a genetic pattern, LGMD can be divided into the autosomal dominant inheritance (LGMD1) and autosomal recessive inheritance (LGMD2) forms. The LGMD2 form currently accounts for 90% of total LGMD patients and has an earlier onset and faster progression (2). LGMD2B and LGMD2A accounted for 75% of the total LGMDs, as the most common LGMD subtypes in a previous China-based cohort (3). LGMD2B, the more frequently diagnosed subtype of the two, is caused by homozygous or complex heterozygous mutations of the *Dysferlin* gene (*DYSF*), resulting in dysferlin protein deficiency or dysfunction (4).

Duchenne muscular dystrophy (DMD) is a rare X-linked recessive muscle degenerative disorder found predominantly in male children. The frequent clinical manifestations of DMD are proximal muscle weakness and wasting, gastrocnemius muscle hypertrophy, and gait abnormality, seriously affecting daily motor abilities. DMD is caused by mutations of the *Dystrophin* gene (*DMD*) in the Xp21.2 region that cause the absence of dystrophin protein or structural defects of the cytoskeleton (5). As reported in an updated meta-analysis, the pooled global DMD prevalence was 7.1 per 100,000 men, while the birth prevalence was 19.8 per 100,000 live male births (6). Usually, patients with DMD lose independent ambulation within the age of 12 or 13 years and die mainly due to cardiorespiratory failure before the age of 30 years. In comparison, Becker muscular dystrophy (BMD) is the allelic form characterized by a more benign clinical course (5).

LGMD and DMD/BMD are different types of progressive muscular dystrophies in consideration of age at onset, atrophic muscle distribution, disease progression, and prognosis. In this current report, we describe the case of a woman with a chief complaint of weakness in her lower limbs, which was finally diagnosed as LGMD2B with compound heterozygous mutations of the *DYSF* gene in combination with other means of inspection. Furthermore, this woman is an asymptomatic carrier with a mutation of the X-linked *DMD* gene, which is relatively uncommon in clinical practice. This report focuses on the diagnostic process of the female case and her family and attracts increasing attention to hereditary neuromuscular diseases with multiple pathogenic gene mutations.

Case presentation

A 31-year-old Chinese woman was admitted to the Department of Neurology of our hospital on 2 April 2021, with a chief complaint of lower limb weakness. More than 1 year before admission, the patient found that she had to pull the handrail to get on the bus because of the weakness of her lower limbs. Before 1 year, she began suffering from low back pain and experiencing difficulty in standing after squatting and weakness in her lower limbs when climbing uphill or stairs. The abovementioned symptoms were getting worse in the past 6 months. Unfortunately, she was unable to stand up after squatting, and she had to bend over and put her hands on her thighs when climbing uphill or stairs at the time of admission. The patient was gradually unable to perform coordinated running and jumping movements. There was no obvious abnormality when walking on a flat road. This patient was previously healthy. Her parents, her younger brother, her daughter, and her son had no similar symptoms.

On the day of admission, the patient's vital signs were normal. The neurological examination of the cranial nerves was negative. The patient had difficulty climbing the stairs or standing up after squatting during the physical examination. Movements of the hips and knees were slightly limited, while the feet were not. The proximal muscle strength of both lower limbs (mainly including the pelvic girdle and quadriceps muscles) was level 4 (0–5), and the distal muscle strength was level 5. The muscle strength of both upper limbs was normal. There were no sensory deficits in the four limbs. The tendon reflexes of both lower limbs were weakened, and the upper limbs were normal. The bilateral Babinski signs were negative. Gowers' sign was positive.

Laboratory data showed increased levels of glutamic-pyruvic transaminase (126.3 IU/L), glutamic-oxalacetic transaminase (122.8 IU/L), creatine kinase (CK, 8950.4 IU/L), myohemoglobin (846.140 ug/L), creatine kinase isoenzyme (94.960 ug/L) but decreased counts of white blood cell (3.62*10^9/L), red blood cell (3.95*10^12/L), hemoglobin concentration (97 g/L), red blood cell-specific volume (31.2%), neutrophil (1.74*10^9/L), mean red blood cell volume (78.9 fL), mean red blood cell hemoglobin content (24.6 pg), and mean corpuscular-hemoglobin concentration (312 g/L). Blood routine examination indicated iron deficiency anemia, thus ferritin (3.40 ng/ml), serum iron (4.58 umol/L), iron saturation (7.5%), unsaturated iron (56.79 umol/L), and total iron binding (61.37 umol/L) were further measured. In addition, autoantibody test results showed that the anti-nuclear antibody (1:100) and anti-mitochondrial antibody (M2) were positive. Anti-Ha/Tyr antibody IgG was also positive in the idiopathic inflammatory myopathy (IIM) spectrum test from the serum. Comprehensive infectious, paraneoplastic, and inflammatory examinations of the patient were negative.

Electrophysiological tests showed that the motor and sensory nerves of the limbs were normal. On needle electromyography (EMG), the spontaneous potentials of the muscles were not observed in the resting state. During light contraction, the mean amplitudes of the bilateral gastrocnemius and iliopsoas muscles and the left gluteus maximus decreased, and the mean time limit was narrow. These results indicated myogenic injury. There were no abnormal signs on cranial, cervical, and lumbar spine magnetic resonance imaging (MRI). To confirm the type of myopathy, we selectively performed the right limb muscle MRI, which showed that the muscle groups (anterior and posterior thigh and also posterior calf) were amyotrophic and spotted fatty degeneration, accompanied by partial muscle edema (Figure 1). Meanwhile, a muscle MRI of the right upper arm showed slight edema.

While combing through the current information analysis, we suspected that the patient suffered from muscular dystrophy. To confirm the hypothesis, muscle biopsy (Figure 2) and genetic testing were furtherly performed after getting approval. Hematoxylin-eosin (HE)-stained images of left gastrocnemius muscle biopsy showed muscle cells of slightly variable size and irregular shape and scattered necrotic fibers without the increased endomysial connective tissue and lymphocytic infiltration. Modified Gomori trichrome (MGT)-stained images showed sporadic ragged-red fibers (RRFs), while no small rod-like particles or rimmed vacuoles were observed. In addition, no

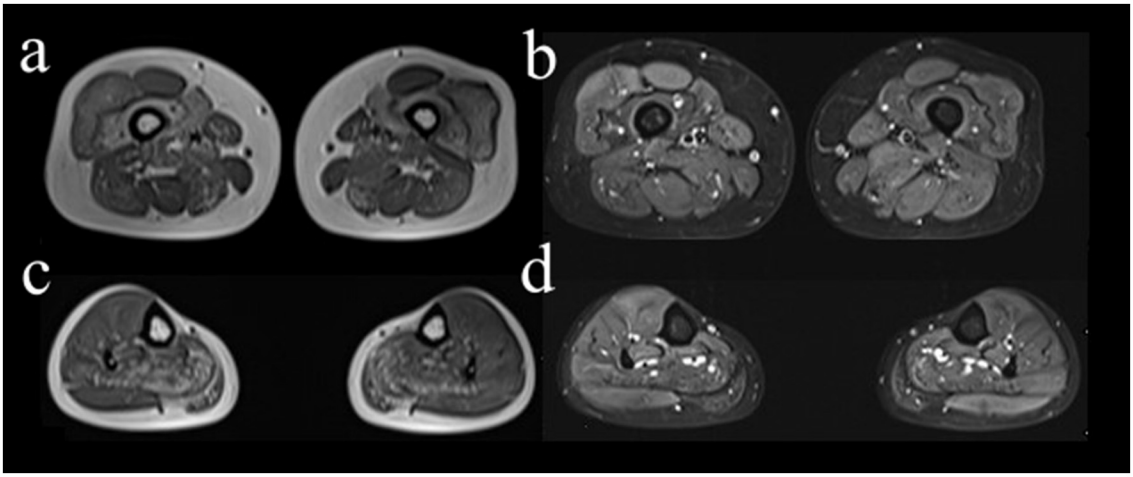

FIGURE 1
Axial MRI images of right lower limb muscles. The right vastus intermedius muscle **(a, b)**, medial head of gastrocnemius muscle, and soleus muscle **(c, d)** showed spotted fatty degeneration. The MRI sequences were T1-weighted imaging **(a, c)** and fat-suppressed T2-weighted imaging **(b, d)**, respectively.

evident abnormality was shown in the other histochemical staining techniques involving a reduced form of nicotinamide adenine dinucleotide (NADH), cytochrome C oxidase (COX), succinate dehydrogenase (SDH), periodic acid Schiff (PAS), oil red O (ORO), Sudan black B (SBB), and ATPase. Finally, immunohistochemical data demonstrated the absence of major histocompatibility complex class I (MHC I), myxovirus resistance protein A (MxA), membrane attack complex (MAC), and dysferlin. These results were consistent with the chronic myogenic injury with dysferlin deletion. In consideration of RRFs observed usually in mitochondrial damage, an additional complementary blood test was conducted. However, none of the mutations in the mitochondrial genome was detected in the genetic screening of the pathogenic mutations in the MITOMAP database.

As a genetic testing result (Figure 3A), compound heterozygous G-to-T base substitution at position 5,497 in exon 49 of the *DYSF* gene, leading to a codon change from glutamic acid to termination codon at position 1,833 (NM_003494.3: c.5497G>T, p.Glu1833Ter), and a heterozygous C-to-G base change at position 4,638 + 8 in intron 42 of the *DYSF* gene with a consequence of splice, which has never been reported, were identified as candidate causative mutations. According to related guides of the American College of Medical Genetics and Genomics (ACMG), the former mutation is pathogenic and the latter mutation is a variation of unknown clinical significance (VUS). The variant naming rules refer to Human Genome Variation Society (HGVS) recommendations. Unfortunately, *DMD* gene mutation c.3921+12A>G of the *DMD* gene on the X chromosome was also found in this patient. Further genealogical verification confirmed that c.5497G>T in the *DYSF* gene was derived from her mother and c.4638+8C>G was derived from her father, while there was no mutation in the *DMD* gene of her parents. Only c.5497G>T in the *DYSF* gene was identified in her younger brother without muscular atrophy symptoms. To further investigate the possibility of muscular dystrophy in the offspring, the son of the patient completed genetic verification and carried the same *DMD* gene mutation on the X chromosome. A pedigree chart was shown in Figure 3B to illustrate the genetic inheritance among the patient and her family members.

Finally, the patient was diagnosed as LGMD2B clinically and genetically. We offered symptomatic treatment during hospitalization, but the muscle weakness did not improve remarkably. We recommended regular medical follow-up for this patient after discharge. To date, the patient's lower limb weakness has become slightly worse, resulting in the walking distance becoming even shorter than before.

Discussion

Progressive muscular dystrophies comprise a group of inherited and degenerative diseases characterized by progressive muscle weakness and atrophy that induces dyskinesia. According to age at onset, atrophic muscle distribution, disease progression, and prognosis, progressive muscular dystrophies include DMD/BMD, LGMD, facioscapulohumeral muscular dystrophy (FSHD), Emery–Dreifuss muscular dystrophy (EDMD), congenital muscular dystrophy (CMD), oculopharyngeal muscular dystrophy (OPMD), distal muscular dystrophy, and other rare types (7–11).

LGMD mainly manifests as weakness and atrophy of predominantly pelvic and shoulder muscles with different genetic patterns and gene mutations. The current diagnosis of LGMD is based on clinical manifestations and genetic inheritance, besides laboratory criteria, such as elevated serum CK, muscle biopsy, histopathological features, and muscle imaging changes (2). The female patient discussed above suffered from proximal muscle weakness of both lower limbs with insidious onset, which aggravated gradually from the age of 30 years of the patient. Laboratory data showed elevated serum CK detected in the blood. In addition, EMG results indicated that muscular damage and right

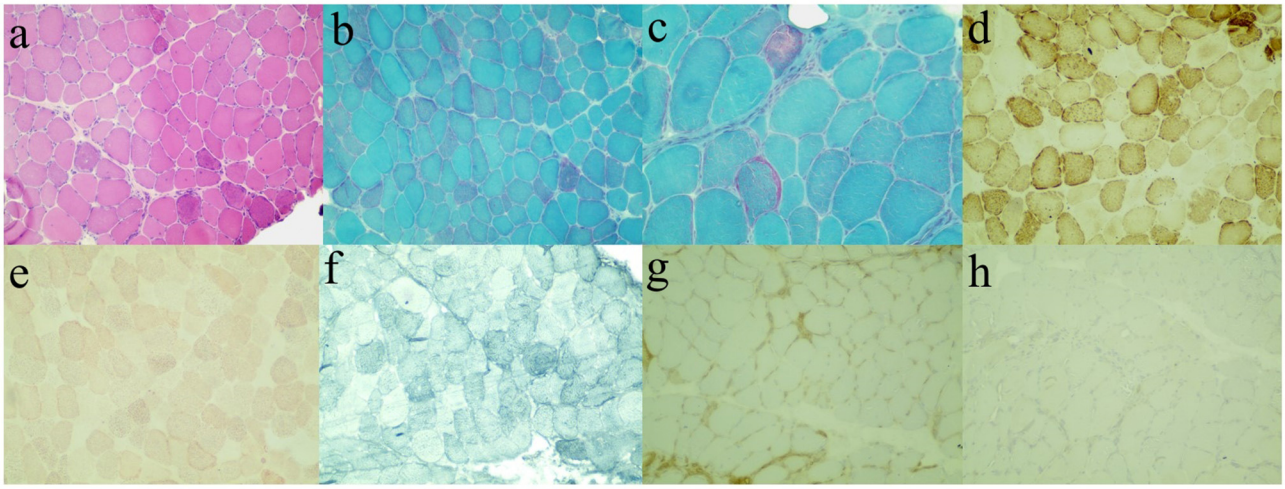

FIGURE 2
Immunohistochemical staining images of left gastrocnemius muscle biopsy. Hematoxylin-eosin (HE, **a**), modified Gomori trichrome (MGT, **b, c**), cytochrome C oxidase (COX, **d**), oil red O (ORO, **e**), Sudan black B (SBB, **f**), major histocompatibility complex class I (MHC I, **g**), and dysferlin **(h)**.

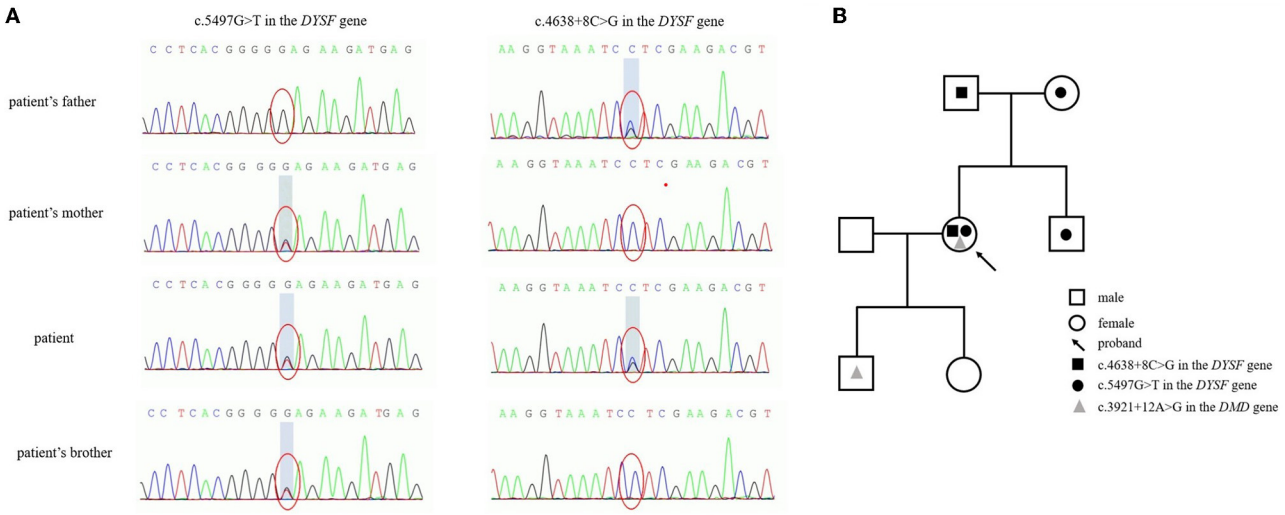

FIGURE 3
Genetic mutations in the *DYSF* gene **(A)** and a pedigree chart **(B)** to illustrate the genetic inheritance among the patient and her family members.

limb MRI showed widely spread muscular dystrophy. Furthermore, muscle biopsy indicated chronic myogenic injury with dysferlin deletion in accordance with dystrophic changes. This patient was therefore diagnosed as suffering from dysferlinopathy.

Dysferlinopathies are a group of autosomal recessive disorders characterized by the involvement of proximal and/or distal limb-girdle muscles caused by dysferlin deficiency/mutations (2, 4). Dysferlinopathy phenotypes at onset include LGMD2B, distal Miyoshi Myopathy (MM), proximal-distal limb-girdle phenotype, distal anterior compartment myopathy (DACM), and other less frequent phenotypes. In general, patients with LGMD2B present with weakness that is first evident in the proximal muscles of the pelvic girdle, leading to difficulties in walking upstairs or running (12). The age of LGMD2B onset is in the late teens or early adulthood. Moreover, the shoulder girdle and upper limb muscles are frequently involved later, while facial, neck, and hand muscles are usually unaffected during the course of the disease (4). Based on the clinical characteristics and the results mentioned above, the patient was diagnosed with LGMD2B.

Before the muscle biopsy and genetic testing, however, polymyositis (PM) should be considered in the differential diagnosis. PM is a CD8 (+) T cell-mediated autoimmune disease clinically manifested by symmetrical and proximal muscle weakness (13). LGMD2B and PM have some common clinical features, including weakness of proximal limbs, increased CK level, EMG changes indicating muscle-derived injury, and

MRI changes in the affected muscles (14). Furthermore, the positive myositis-specific autoantibody such as anti-Ha/Tyr antibody makes PM highly suspicious. However, there were still many points of disapproval. This patient did not suffer from neck flexor weakness, muscle tenderness, and other systemic symptoms along with elevated inflammatory or infectious indicators. Finally, the critical methods for distinguishing these two diseases are muscle biopsy and genetic testing of dysferlin deficiency/mutations.

Dysferlin, a protein encoded by the skeletal muscle gene *DYSF* in the 2p13 region, is mutated in dysferlinopathies (15). It has been identified as a crucial member of membrane repair, vesicle trafficking, and membrane remodeling in the skeletal muscle (16, 17). Moreover, dysferlin deficiency causes the activation of the muscle inflammasome to generate a proinflammatory environment and exacerbate muscle damage (18). As expected, immunohistochemical staining images of the left gastrocnemius muscle biopsy showed chronic myogenic injury with dysferlin deletion and no lymphocytic infiltration or MHC I expression, which could complement the evidence to discard the PM diagnosis.

A growing number of studies are being devoted to mitochondrial diseases (MIDs), especially those involving the neuromuscular system (19). MIDs are a group of genetically defective disorders that result from structural and functional alterations of the mitochondria, which then lead to respiratory chain and energy metabolism dysfunctions. In addition to molecular genetic tests as the gold standard, pathological examinations following a muscle biopsy can complement the diagnosis of mitochondrial myopathies, including (1) RRFs, (2) mitochondria proliferation observed in SDH staining often described as ragged-blue fibers, (3) COX deficient or negative, and (4) ultrastructurally abnormal mitochondria often with paracrystalline inclusions (20). The extent of mitochondrial abnormalities in dysferlinopathy is presently unclear but attracts sufficient interest (21). A previous LGMD case report has shown a mitochondrial deficit in histomorphology characterized by the presence of RRFs, deficiency of COX, and abnormal ultrastructure of mitochondria (22). Moreover, RRFs in the skeletal muscle of dysferlinopathy have been reported (23). Similarly, more cases with dysferlinopathy reported in a Chinese-based study displayed a higher proportion of RRFs and COX-deficient fibers in muscle pathologies (24). In consideration of sporadic RRFs observed in MGT-stained images of the present patient, additional gene sequencing was conducted, and no mitochondrial DNA mutations were found. Primary mitochondrial myopathy was not supported based on the molecular genetic test, but secondary muscle mitochondrial dysfunction could not be completely excluded.

In the last decades, Asian and European countries have conducted nationwide multicenter genetic studies regarding the mutations of the *DYSF* gene involving dozens to hundreds of patients. In world patients with dysferlinopathy, the exons with the most *DYSF* gene variants were exon 29, exon 39, exon 45, and exon 6, and the most common consequences were missense, splice, and frameshift variants (25). Reported in a Japanese cohort, the c.2997G > T (p.Trp999Cys), c.1566C > G (p.Tyr522Ter), and c.3373del (p.Glu1125Lys) variants were common in the MM subtype, while the c.2997G > T variant was definitely the most common in the LGMD2B subtype (26). However, c.1375dup was identified as the hotspot in the Chinese dysferlinopathy cohort, differing from the hotspot c.2997G>T in world patients (25). Hence, we reported the compound heterozygous mutations, c.5497G>T and c.4638+8C>G, in the *DYSF* gene of this patient. Additionally, c.5497G>T was a known nonsense mutation (15), while c.4638+8C>G was a splice mutation that has not been reported in any public databases. The parents and a brother of this patient were screened for further genealogical verification. The results showed that the mutations of this patient were derived from her parents, and her younger brother was a pathogenic mutation carrier without muscular atrophy symptoms, which confirmed that this disease accorded with the autosomal recessive inheritance rule. Therefore, gene sequencing confirmed her final diagnosis of LGMD2B and identified the novel compound heterozygous variants in the *DYSF* gene.

According to the autosomal recessive inheritance rules, the offspring of the patient will not suffer from the disease if her husband is not a pathogenic gene mutation carrier. However, unfortunately, the patient carried a *DMD* gene mutation c.3921+12A>G on the X chromosome, which has been reported earlier (27). It is reasonable to presume that this mutation can only come from her mother. Variants in the *DMD* gene caused X-linked recessive DMD/BMD characterized by progressive muscle degeneration and weakness. DMD/BMD generally affects men only, but there are still some female carriers experiencing muscle weakness (28). As a heterozygous carrier, this patient passed the genetic disease on to her son with a 50% chance, and her daughter has a 50% chance of being a carrier. To conduct appropriate genetic counseling, further genealogical verification was conducted and identified that the son of the patient has carried the same *DMD* gene mutation regrettably. To date, her 5-year-old son has not shown slowness or limitation of movement.

Hereditary neuromuscular disorders are a wide-ranging group of diseases influencing the life quality of patients severely. With the development of detection technology, hundreds of related genes and many more pathogenic variants are discovered. Genetic testing by the next-generation sequencing method to identify the pathogenic mutations is of great significance to the accurate diagnosis of genetically coded diseases. LGMD2B and DMD are different types of progressive muscular dystrophies and are caused by mutations to the *dysferlin* and *dystrophin* genes, respectively. In this current report, we reported a Chinese woman who was finally diagnosed as LGMD2B with the compound heterozygous mutations, c.5497G>T and c.4638+8C>G, in the *DYSF* gene. Additionally, c.4638+8C>G is a novel mutation and broadens the genetic spectrum of LGMD2B. Furthermore, this woman is an asymptomatic carrier with a mutation of the X-linked *DMD* gene and has passed the pathogenic mutation on to her son. A case of neuromuscular disease suffering multiple genetic pathogenic risks is relatively uncommon in clinical practice. Much attention must be paid in clinics toward hereditary neuromuscular diseases with multiple pathogenic gene mutations. Genetic counseling and clinical follow-up are the priorities in future, and promising treatments are also worth exploring.

Data availability statement

The raw sequence data reported in this paper have been deposited in the Genome Sequence Archive (Genomics, Proteomics & Bioinformatics 2021) in National Genomics Data Center (Nucleic Acids Res 2021), China National Center for Bioinformation/Beijing Institute of Genomics, Chinese Academy of Sciences (GSA: HRA005262) that are controlled accessible at (NGDC: https://ngdc.cncb.ac.cn/). Meanwhile, the raw sequence data can also be accessed after an approval application to the China National GeneBank DataBase (CNGBdb, https://db.cngb.org/). Please refer to https://db.cngb.org/, or email: CNGBdb@cngb.org for detailed application guidance. The accession number CNP0004583 should be included in the application.

Ethics statement

The studies involving human participants were reviewed and approved by the General Hospital of Western Theater Command. The patients/participants provided their written informed consent to participate in this study. Written informed consent was obtained from the individual(s) for the publication of any potentially identifiable images or data included in this article.

Author contributions

XC, ZL, and JF were responsible for the patient's management during hospitalization. LZ and ST performed muscle biopsy and further interpreted the results. XC and MZ prepared the manuscript. XC, LZ, MZ, and ZY reviewed and made significant contributions to the final version. All authors approved the final version of the manuscript.

Funding

This study was supported by the Southwest Medical University teaching reform project (ZYTS-157).

Acknowledgments

The authors gratefully acknowledge the patient for permitting us to disclose details relating to this case.

Conflict of interest

The authors declare that the research was conducted in the absence of any commercial or financial relationships that could be construed as a potential conflict of interest.

Publisher's note

References

1. Mah JK, Korngut L, Fiest KM, Dykeman J, Day LJ, Pringsheim T, et al. A systematic review and meta-analysis on the epidemiology of the muscular dystrophies. *Can J Neurol Sci.* (2016) 43:163–77. doi: 10.1017/cjn.2015.311

2. Angelini C, Giaretta L, Marozzo R. An update on diagnostic options and considerations in limb-girdle dystrophies. *Expert Rev Neurother.* (2018) 18:693–703. doi: 10.1080/14737175.2018.1508997

3. Yu M, Zheng Y, Jin S, Gang Q, Wang Q, Yu P, et al. Mutational spectrum of chinese lgmd patients by targeted next-generation sequencing. *PLoS ONE.* (2017) 12:e0175343 doi: 10.1371/journal.pone.0175343

4. Fanin M, Angelini C. Progress and challenges in diagnosis of dysferlinopathy. *Muscle Nerve.* (2016) 54:821–35. doi: 10.1002/mus.25367

5. Fortunato F, Farne M, Ferlini A. The DMD gene and therapeutic approaches to restore dystrophin. *Neuromuscul Disord.* (2021) 31:1013–20. doi: 10.1016/j.nmd.2021.08.004

6. Crisafulli S, Sultana J, Fontana A, Salvo F, Messina S, Trifiro G. Global epidemiology of duchenne muscular dystrophy: an updated systematic review and meta-analysis. *Orphanet J Rare Dis.* (2020) 15:141. doi: 10.1186/s13023-020-01430-8

7. Statland JM, Tawil R. Facioscapulohumeral muscular dystrophy. *Continuum.* (2016) 22:1916–31. doi: 10.1212/CON.0000000000000399

8. Heller SA, Shih R, Kalra R, Kang PB. Emery-dreifuss muscular dystrophy. *Muscle Nerve.* (2020) 61:436–48. doi: 10.1002/mus.26782

9. Butterfield RJ. Congenital muscular dystrophy and congenital myopathy. *Continuum.* (2019) 25:1640–61. doi: 10.1212/CON.0000000000000792

10. Yamashita S. Recent progress in oculopharyngeal muscular dystrophy. *J Clin Med.* (2021) 10:1375. doi: 10.3390/jcm10071375

11. Felice KJ. Distal myopathies. *Neurol Clin.* (2020) 38:637–59. doi: 10.1016/j.ncl.2020.03.007

12. Barthelemy F, Wein N, Krahn M, Levy N, Bartoli M. Translational research and therapeutic perspectives in dysferlinopathies. *Mol Med.* (2011) 17:875–82. doi: 10.2119/molmed.2011.00084

13. Findlay AR, Goyal NA, Mozaffar T. An overview of polymyositis and dermatomyositis. *Muscle Nerve.* (2015) 51:638–56. doi: 10.1002/mus.24566

14. Xu C, Chen J, Zhang Y, Li J. Limb-girdle muscular dystrophy type 2b misdiagnosed as polymyositis at the early stage: case report and literature review. *Medicine.* (2018) 97:e10539. doi: 10.1097/MD.0000000000010539

15. Liu J, Aoki M, Illa I, Wu C, Fardeau M, Angelini C, et al. Dysferlin, a novel skeletal muscle gene, is mutated in miyoshi myopathy and limb girdle muscular dystrophy. *Nat Genet.* (1998) 20:31–6. doi: 10.1038/1682

16. Bansal D, Miyake K, Vogel SS, Groh S, Chen C-C, Williamson R, et al. Defective membrane repair in dysferlin-deficient muscular dystrophy. *Nature.* (2003) 423:168–72. doi: 10.1038/nature01573

17. Cardenas AM, Gonzalez-Jamett AM, Cea LA, Bevilacqua JA, Caviedes P. Dysferlin function in skeletal muscle: possible pathological mechanisms and therapeutical targets in dysferlinopathies. *Exp Neurol.* (2016) 283:246–54. doi: 10.1016/j.expneurol.2016.06.026

18. Rawat R, Cohen TV, Ampong B, Francia D, Henriques-Pons A, Hoffman EP, et al. Inflammasome up-regulation and activation in dysferlin-deficient skeletal muscle. *Am J Pathol.* (2010) 176:2891–900. doi: 10.2353/ajpath.2010.090058

19. Lu J-Q, Tarnopolsky MA. Mitochondrial neuropathy and neurogenic features in mitochondrial myopathy. *Mitochondrion.* (2021) 56:52–61. doi: 10.1016/j.mito.2020.11.005

20. de Barcelos IP, Emmanuele V, Hirano M. Advances in primary mitochondrial myopathies. *Current Opinion in Neurology.* (2019) 32:715–21. doi: 10.1097/WCO.0000000000000743

21. Katsetos CD, Koutzaki S, Melvin JJ. Mitochondrial dysfunction in neuromuscular disorders. *Semin Pediatr Neurol.* (2013) 20:202–15. doi: 10.1016/j.spen.2013.10.010

22. Calore EE, Cavaliere MJ, Wakamatsu A, Perez NM, Maeda MY, Russo DH. An unusual case of muscular limb-girdle dystrophy and mitochondrial myopathy. *Pathologica.* (1994) 86:649–51.

23. Gayathri N, Alefia R, Nalini A, Yasha T, Anita M, Santosh V, et al. Dysferlinopathy: spectrum of pathological changes in skeletal muscle tissue. *Indian J Pathol Microbiol.* (2011) 54:350–4. doi: 10.4103/0377-4929.81636

24. Liu F, Lou J, Zhao D, Li W, Zhao Y, Sun X, et al. Dysferlinopathy: mitochondrial abnormalities in human skeletal muscle. *International Journal of Neuroscience.* (2016) 126:499–509. doi: 10.3109/00207454.2015.1034801

25. Zhong H, Yu M, Lin P, Zhao Z, Zheng X, Xi J, et al. Molecular landscape of DYSF mutations in dysferlinopathy: from a chinese multicenter analysis to a worldwide perspective. *Hum Mutat.* (2021) 42:1615–23. doi: 10.1002/humu.24284

26. Izumi R, Takahashi T, Suzuki N, Niihori T, Ono H, Nakamura N, et al. The genetic profile of dysferlinopathy in a cohort of 209 cases: genotype–phenotype relationship and a hotspot on the inner DYSF domain. *Hum Mutat.* (2020) 41:1540–54. doi: 10.1002/humu.24036

27. Kong X, Zhong X, Liu L, Cui S, Yang Y, Kong L. Genetic analysis of 1051 chinese families with duchenne/becker muscular dystrophy. *BMC Med Genet.* (2019) 20:139. doi: 10.1186/s12881-019-0873-0

28. Hoogerwaard EM, Bakker E, Ippel PF, Oosterwijk JC, Majoor-Krakauer DF, Leschot NJ, et al. Signs and symptoms of duchenne muscular dystrophy and becker muscular dystrophy among carriers in the netherlands: a cohort study. *Lancet.* (1999) 353:2116–9. doi: 10.1016/S0140-6736(98)10028-4

frontiers | Frontiers in Neurology

TYPE Case Report
PUBLISHED 29 September 2023
DOI 10.3389/fneur.2023.1267426

OPEN ACCESS

EDITED BY
Giovanni Meola,
University of Milan, Italy

REVIEWED BY
Roope Mannikko,
University College London, United Kingdom
Alessandro Capuano,
Azienda Sanitaria Locale di Viterbo, Italy

*CORRESPONDENCE
Alina S. Arestova
✉ rizvanova.alina@gmail.com

RECEIVED 26 July 2023
ACCEPTED 14 September 2023
PUBLISHED 29 September 2023

CITATION
Nuzhnyi EP, Arestova AS, Rossokhin AV, Protopopova AO, Abramycheva NY, Suponeva NA and Illarioshkin SN (2023) Case report: A novel *CACNA1S* mutation associated with hypokalemic periodic paralysis. *Front. Neurol.* 14:1267426. doi: 10.3389/fneur.2023.1267426

Case report: A novel *CACNA1S* mutation associated with hypokalemic periodic paralysis

Evgenii P. Nuzhnyi, Alina S. Arestova*, Alexey V. Rossokhin, Anna O. Protopopova, Nataliya Yu Abramycheva, Natalia A. Suponeva and Sergey N. Illarioshkin

Research Center of Neurology, Moscow, Russia

Background: Hypokalemic periodic paralysis (HypoKPP) is a rare neuromuscular genetic disorder causing recurrent episodes of flaccid paralysis. Most cases are associated with *CACNA1S* mutation, causing defect of calcium channel and subsequent impairment of muscle functions. Due to defined management approaches early diagnosis is crucial for promptly treatment and prevention new attacks.

Materials and methods: We report a case of HypoKPP associated with previously unreported mutation in *CACNA1S* gene (p.R900M). Molecular modeling of $Ca_V1.1$ was applied to evaluate its pathogenicity.

Results: As a patient referred between attacks neurological status, laboratory and neurophysiological examination were unremarkable. Molecular modeling predicted that the p.R900M mutation affects the process of calcium channels activation.

Conclusion: Novel *CACNA1S* mutation, associated with HypoKPP was identified. Monte-Carlo energy minimization of the $Ca_V1.1$ model supported the association of this mutation with this disease.

KEYWORDS

hypokalemic periodic paralysis, HypoKPP, *CACNA1S*, mutation, molecular modeling, case report

Introduction

Hypokalemic periodic paralysis (HypoKPP) is a rare neuromuscular disorder (channelopathy), characterized by the recurrent episodic attacks of muscle weakness lasting from minutes to several days accompanied by low serum potassium (1). The majority of HypoKPP cases are inherited and caused by mutations in skeletal muscle calcium (*CACNA1S*, up to 70%) and sodium (*SCN4A*, up to 20%) channels genes, while a small proportion remains genetically undefined (2). Acquired cases of HypoKPP are associated with thyrotoxicosis and other endocrine disorders, some may result from gastrointestinal and renal potassium loss (3).

Pathological variants in many ion channel diseases are widely distributed throughout the channel proteins, whereas those in HypoKPP are almost exclusively concentrated in the voltage sensor. Most such mutations affect arginine residues in S4 segments that contribute to voltage sensing, leading to abnormal channel functioning. However, the full spectrum of HypoPP mutations has not been defined (4).

We report a case of HypoKPP with a novel *de novo* pathogenic variant in the *CACNA1S* gene, supported by using molecular modeling approach. Currently, the generally accepted mechanism for the development of HypoKPP is the occurrence of a leak current through the voltage sensor domain (VSD) of $Ca_V1.1$ and $Na_V1.4$ channels with mutated arginines in the S4 helix (4–6). In this work, based on the structural analysis of the $Ca_V1.1$ channels, we predicted that the newly discovered p.R900M mutation affects the mobility of the IIIS4 helix, which leads to disruption of the channel activation process. We hypothesize that this mechanism also contributes to the development of HypoKPP.

Case description

A 19-years old man, originated from Tajikistan, presented with severe reversible episodes of muscle weakness for 3 years. The episode starts abruptly with progressive weakness in extremities and paraspinal muscles up to complete immobility by the third day with further spontaneous recovery. The episodes reoccur 3 times a year without any noticeable triggers. Breathing, swallowing, speech, urination is always intact. Between attacks the patient feels absolutely normal and has no complaints. The medical history was unremarkable for chronic conditions, constant medication use, substance abuse. There was no family history on similar symptoms or any neurological disorders (parents, two sibs are clinically unaffected) (Figure 1A).

During interictal period on neurological examination deep tendon reflexes were diminished and slight muscle hypotonia was observed in the extremities with no signs of muscle hypotrophy, paresis or percussion myotonia.

The laboratory testing revealed normal complete blood count and comprehensive metabolic panel, including sodium and potassium levels. It should be mentioned that during the attack the potassium level has never been investigated.

Brain MRI revealed *pituitary* microadenoma 0.5 × 0.5 × 0.8 cm and blood test showed normal levels of pituitary hormones. The patient was consulted by an endocrinologist, so an underlying endocrine pathology was excluded.

Neurophysiological examination included repetitive nerve stimulation test, short exercise test according to standardized protocol and needle EMG (7). No decrement was observed on repetitive nerve stimulation test, short exercise test was also unremarkable. Prolonged exercise test was not performed. Needle EMG of m. extensor digitorum communis and m. vastus lateralis did not demonstrated any myopathic changes.

Diagnosis of primary periodic paralysis was suspected. Next-generation sequencing with a related commercial gene panel ("Neuromuscular disorders," Illumina MiSeq) was performed. A c.2699G > T (p.Arg900Met, p.R900M, NM_000069.3, exon 21) variant in the *CACNA1S* gene was identified, satisfying the ACMG criteria of "likely pathogenic" (PS2, PM6, PM1), however according to InterVar the variant is interpreted as "uncertain significance" (8). Despite pathological variants in R900 substituting for another amino acid, like R900G and R900S, associated with HypoKPP, have already been reported (4, 9, 10), the identified variant was absent in the ExAc, gnomAD, GENOMED Databases.

The substitution was further confirmed by Sanger sequencing (Figure 1B). The mutation was not found in parents and two sibs, suggesting that it had arisen *de novo*.

In order to confirm either the novel identified variant is pathogenic and to evaluate its effect on calcium channel functioning, the molecular modeling was applied.

To build a homology model of the α1S subunit of the human calcium voltage-gated channel, a cryo-EM (EM - electron microscopic) structure of the inactivated $Ca_V1.1$ channel (5GJW, code in the Protein Data Bank) of the rabbit, in which the voltage sensors are in the activated position, was used as a template (11). A schematic representation and structural model of the α1S subunit of $Ca_V1.1$ are shown in Figures 2A,C. Model building was preceded by alignment of the amino acid sequences (UniProt entries Q13698 CAC1S_HUMAN and P07293 CAC1S_RABIT). Aligned sequences of S4 segments are shown in Figure 2B.

We used the Monte-Carlo energy minimization (MCM) method (12) to optimize the model geometry. Non-bonded interactions were calculated using the AMBER force field (13). Electrostatic interactions were calculated using the solvent exposure- and distance-dependent dielectric function (14). Energy was minimized in the space of internal

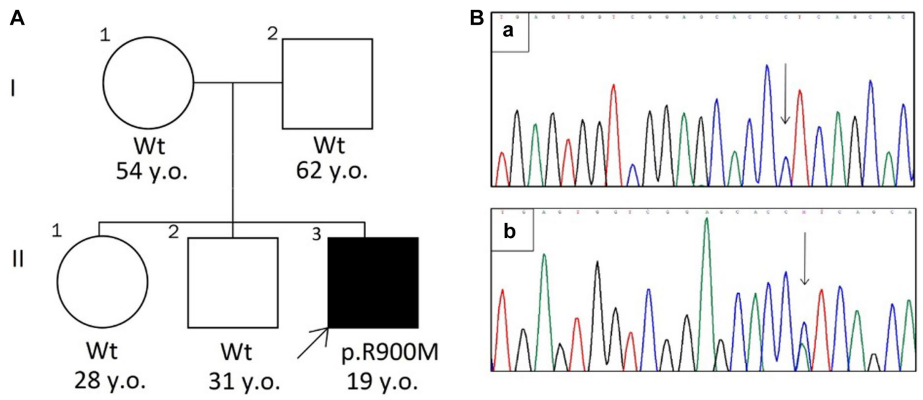

FIGURE 1
(A) The pedigree chart. The arrow indicates the proband with HypoKPP (Wt—wild type allele). **(B)** Sanger sequencing chromatograms (revers variant) shows wild type allele (a) and c.2699G > T mutation (b).

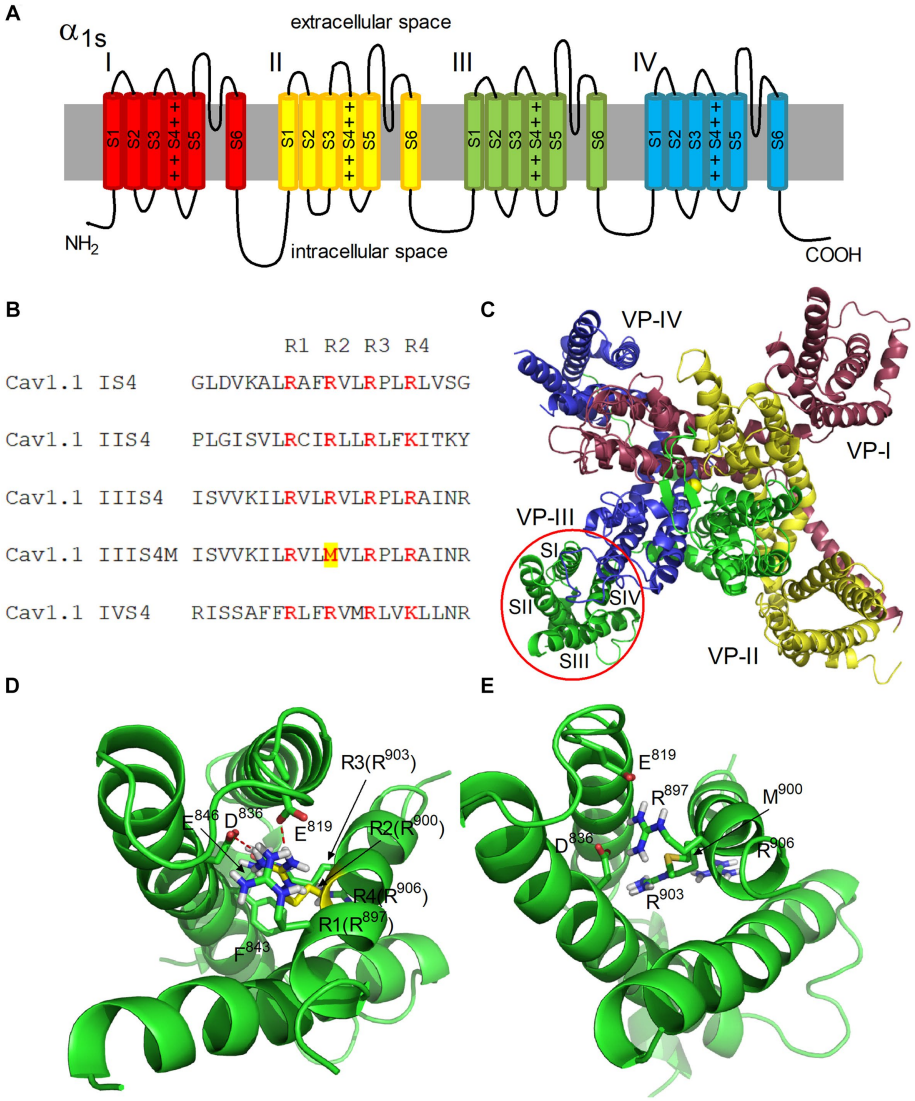

FIGURE 2
Architecture of the hetero-tetrameric voltage-gated human calcium channel $Ca_V1.1$. **(A)** Schematic representation of four domains (I–IV) of the α1S subunit. S1–S6 transmembrane helices and four positive charges of S4 helix are shown in each domain. **(B)** Alignment of S4 segments of domains I-IV of $Ca_V1.1$. Positively charged Arg residues (R1-R4) are highlighted in color. The Arg900Met mutation is highlighted in the IIIS4M (mutated) segment. **(C)** Structural model of the α1S subunit of $Ca_V1.1$. View from the extracellular space is presented. The color coding of domains corresponds to **(A)**. Transmembrane helices S1–S4 forming a voltage sensor (*VS*) are denoted in domain III. Yellow sphere in the center represents Ca^{2+} ion in the selective filter of the channel. **(D,E)** Structural models of *VS*-III in the activated state in the native and mutated forms, respectively. Residues R1-R4 of the S4 helix are shown, as well as residues E819, D836, E846, and F843 of the S2 helix interacting with them. The side chain of R900 is highlighted in yellow **(D)**. Ionic contacts formed by R900 with residues E819 and D836 are shown as red dashed lines.

model coordinates, which are the lengths of valence bonds, valence and torsion angles, Cartesian coordinates and Euler angles that determine the position of individual molecules, using the ZMM program (14).

The MC minimization was carried out in two stages. At the first stage, the energy was minimized with constraints imposed on Cα atoms. Minimizing the energy of the model with a system of constraints allows to avoid the deformation of the structure given by the template due to steric conflicts, which are inevitable in the starting geometry of the model. After a constrained MCM trajectory converged, all constraints were removed and the model was finally refined. Each MCM trajectory was terminated if 5,000 successive changes in the model coordinates did not lead to a decrease in the model energy. A detailed description of the MCM method is given in our previously published papers (15, 16).

The α1 subunit of Ca_V includes four domains I-IV, each of which contains six transmembrane helices S1-S6 (Figure 2A). The S5, S6 helices form a pore with a selective filter and an activation gate (17). The S1–S4 helices form the VSD of the channel (Figure 2C). Each S4 helix contains positively charged Arg and Lys residues (Figure 2B).

At the resting state, a negative membrane potential pulls the positively charged S4 helices toward the cytoplasmic side of the membrane, keeping the channel gate closed. Membrane depolarization is accompanied by a change in the electric field, which leads to a shift of S4 across the membrane plane, which initiates a conformational

transition of the channel from the resting (closed) state to the open state (18, 19).

According to this mechanism, the R1–R4 charges of the S4 helix of domain III (Arg897, Arg900, Arg903, and Arg906) alternately form ion pairs with countercharges of the S2 helix (Asp836 and Glu846) when the helix moves in an electric field (20). In our $Ca_V1.1$ model, *VS* is in an activated state, and Arg900 (R2) forms salt bridges with Asp836 and Glu819 residues (Figure 2D). MC minimization showed that these contacts are lost when positively charged Arg900 is replaced by nonpolar Met (Figure 2E). Thus, salt bridges between Met900 (S4) and Asp836/Glu819 (S2) in domain III cannot be formed in the mutated channel, which obviously leads to a decrease in the probability of domain III transition to an activated state. Therefore, disruption of domain III activation should decrease the probability of the entire channel transition to the open state.

Thus, our calculations predict the association of the p.R900M mutation in *CACNA1S* gene with the disease.

Since hypokalemia has not been identified in the patient, there is a chance of normokalemic periodic paralysis (NormoKPP). However, the type of mutation increases our suspicion in favor of HypoKPP and the patient was prescribed with potassium supplementation and spironolactone (25 mg per day) ex juvantibus and educated to notice and avoid possible triggers. For 10-months follow-up the patient has not experienced new attacks and the potassium level has remained normal.

Discussion

Primary hypokalemic periodic paralysis is a rare condition, yet with established approaches to management for prevention severe attacks and life-threatening consequences (1). The majority of primary HypoKPP cases is associated with mutations in *CACNA1S* gene, which encodes the α1S subunit of the calcium voltage-gated channel $Ca_V1.1$ (4). The first identified mutation in the *CACNA1S* gene was reported in 1994 (21). Up to date it has been shown that most mutations occur at positively charged arginine in the VSD (S4 helix) of the α1S subunit (4).

Activation of nicotinic acetylcholine receptors at the neuromuscular junctions leads to the entry of sodium ions and depolarization of muscle cells. Depolarization causes an influx of calcium ions through the voltage-gated $Ca_V1.1$ channels and through $Ca_V1.1$-bound ryanodine receptors (RYR1) in the sarcoplasmic reticulum (SR), which triggers muscle contraction. Mutation in *CACNA1S* gene (p.R900M) identified in this study impairs the functioning of the voltage sensor in domain III of the $Ca_V1.1$ channels. Therefore, this mutation affects the channel opening process and results in the loss of function of these channels.

RYR1 are intracellular receptors and have no voltage-sensing structures. The $Ca_V1.1$ channels associated with RYR1 act as a voltage sensor of calcium release from SR (22). Savalli et al. (23) showed that VSD III in the $Ca_V1.1$ channels bound to RyR1 exhibits fast activation compatible with Ca^{2+}-release kinetics form SR. Therefore, the R900M mutation may also impair calcium release from the SR through RyR1.

It was previously shown that mutations of S4 Arg residues are also accompanied by a leak current carried by protons or other monovalent cations through a gating pore (5, 6). The gating pore is a tunnel formed between S1 and S4 helices in which the S4 helix moves across the membrane in response to changes in membrane potential (24). Sokolov et al. (6) showed that mutations of the two outermost Arg669 and Arg672 to Gly in domain II of Nav1.4 result in generation of a cation leak through the gating pore at hyperpolarized potentials. In the Shaker potassium channel, mutations of the more intracellular S4 Arg to His resides resulted in a leak current carried by protons already at depolarized potentials (25). It has been suggested that such leak currents mainly contribute to the pathophysiology of HypoKPP (5, 26), supported by the fact that the muscles of HypoKPP patients are usually depolarized (27).

Here we demonstrate a HypoKPP case associated with *CACNA1S* gene mutation p.R900M, previously unreported. Matthews et al. (4) have reported a HypoKPP patient with p.R900S mutation; however, clinical characteristics were not described. Pathological variants in R900 substituting for another amino acid, p.Arg900Ser and p.Arg900Gly, have also been reported in two Chinese and Japanese families (9, 10). The clinical features of these cases and our patient are presented in Table 1.

TABLE 1 Clinical features of the cases due to R900 mutations in the *CACNA1S* gene.

Cases (references)	Family 1 (9)			Family 2 (10)			Present study
Nationality	Chinese			Japanese			Tajik
Age/Sex	25/M (sib)	27/M (sib)	46/M (father)	41/M (sib)	35/M (sib)	69/M (father)	19/M
Onset age	16	17	17	21	13	13	16
Frequency of attacks (times per year)	12–100	10–12	10–40	5	10	5	3
Duration of attack (hours)	24–48	12–24	<24	12–48	No data	No data	72–84
Attack triggers	High carbohydrate meal, exhaustion, staying up late, prolonged immobility	High carbohydrate meal, exhaustion	Exhaustion, high carbohydrate meal, alcohol, coldness	Hard physical exercises	Hard physical exercises, overeating		Not identified
Mutation	c.2700G > C (p.R900S)			c.2698A > G (p.R900G)			c.2699G > T (p.R900M)

All patients had a typical HypoPP phenotype with attacks onset in the second decade. Also all patients were male, which may confirm the hypothesis of different gender penetrance and disease severity in males and females (28). In our patient, the frequency of attacks was less, but the attacks were more severe (up to 84 h). We did not identify any attack triggers; however, this fact does not contradict the diagnosis. It can be assumed that the R900 mutations in the *CACNA1S* gene are associated with the classical phenotype of HypoKPP with varying severity.

In rare cases, mutations in the *CACNA1S* gene can cause $Ca_V1.1$-related myopathy (congenital and late-onset limb-girdle forms) with both autosomal dominant and recessive inheritance with at least one nonsense mutation (29). The clinical features of congenital $Ca_V1.1$-related myopathy includes severe generalized muscle weakness and atrophy; in case with a late disease onset – proximal leg weakness with signs of vacuolar myopathy on the muscle biopsy (29, 30). Our patient had not any clinical signs of myopathy, also creatine kinase level was normal and needle EMG did not show myogenic changes.

Another disease caused by *CACNA1S* gene mutations is NormoKPP. We were unable to exclude the diagnosis of NormoKPP because the blood potassium level was never examined during the attack; however, in all previously published cases with mutations in the R900 position the diagnosis of HypoKPP was laboratory confirmed (9, 10). Also the positive effect of the potassium supplementation and spironolactone indirectly confirms the diagnosis of HypoKPP.

The amplitude of the gating pore current contributing to the development of HypoKPP depends on the number of mutated Arg residues and the size of the side chains of the newly included residues (4, 26). Thor et al. (31) showed the appearance of such current through the $Na_V1.4$ channels when R2 in S4 VSD I is mutated to Trp. However, the amplitude of this current was approximately two times less compared to the mutation of the same residue on Gly. In our case, only one of the two outermost arginine residues in S4 VSD III is mutated to Met, which has a rather bulky side chain. Obviously, this mutation will contribute less to the flow of gating pore current compared to the R900G and R900S mutations (see Table 1).

We suppose that multiple pathophysiological mechanisms are involved in the development of HypoKPP in our patient, including depolarization of muscle cells due to leak current through the VSD III, disruption the gating of the main pore of the $Ca_V1.1$ channels, and, possibly impaired calcium release from the SR through RYR1. We hypothesize that these pathophysiological mechanisms may be involved to varying degrees in the development of the disease in different patients (see Table 1). In patients with more gentle attacks, depolarization of muscle cells due to leak current may predominate, and in our patient (severe attacks), the latter two causes may contribute more significantly to the development of HypoKPP. Further studies, including molecular dynamics simulations, are needed to provide a better understanding of the extent to which different pathophysiological mechanisms are involved in HypoKPP caused by the IIIS4 R900M mutation.

Data availability statement

The data presented in the study are deposited in the https://www.ncbi.nlm.nih.gov/clinvar/ repository, accession number VCV002575080.1.

Ethics statement

The studies involving humans were approved by the Research Center of Neurology Ethical Committee. The studies were conducted in accordance with the local legislation and institutional requirements. The participants provided their written informed consent to participate in this study. Written informed consent was obtained from the individual(s) for the publication of any potentially identifiable images or data included in this article.

Author contributions

EN: Conceptualization, Data curation, Investigation, Methodology, Writing – original draft, Writing – review & editing, Visualization. AA: Conceptualization, Data curation, Investigation, Methodology, Writing – original draft, Writing – review & editing. AR: Investigation, Methodology, Software, Visualization, Writing – original draft. AP: Investigation, Methodology, Writing – review & editing. NA: Investigation, Methodology, Writing – review & editing. NS: Supervision, Writing – review & editing. SI: Supervision, Writing – review & editing, Project administration.

Funding

The author(s) declare that no financial support was received for the research, authorship, and/or publication of this article.

Acknowledgments

The computations were carried out using the equipment of the shared research facilities of HPC computing resources at the Lomonosov Moscow State University.

Conflict of interest

The authors declare that the research was conducted in the absence of any commercial or financial relationships that could be construed as a potential conflict of interest.

Publisher's note

References

1. Statland JM, Fontaine B, Hanna MG, Johnson NE, Kissel JT, Sansone VA, et al. Review of the diagnosis and treatment of periodic paralysis. *Muscle Nerve*. (2018) 57:522–30. doi: 10.1002/mus.26009

2. Venance SL, Cannon SC, Fialho D, Fontaine B, Hanna MG, Ptacek LJ, et al. The primary periodic paralyses: diagnosis, pathogenesis and treatment. *Brain*. (2006) 129:8–17. doi: 10.1093/brain/awh639

3. Jandhyala SN, Madireddi J, Belle J, Rau NR, Shetty R. Hypokalaemic periodic paralysis- a prospective study of the underlying etiologies. *J Clin Diagn Res*. (2015) 9:OC17–9. doi: 10.7860/JCDR/2015/13237.6529

4. Matthews E, Labrum R, Sweeney MG, Sud R, Haworth A, Chinnery PF, et al. Voltage sensor charge loss accounts for most cases of hypokalemic periodic paralysis. *Neurology*. (2009) 72:1544–7. doi: 10.1212/01.wnl.0000342387.65477.46

5. Wu F, Quinonez M, Cannon SC. Gating pore currents occur in Cav1.1 domain iii mutants associated with HypoPP. *J Gen Physiol*. (2021) 153:e202112946. doi: 10.1085/jgp.202112946

6. Sokolov S, Scheuer T, Catterall WA. Gating pore current in an inherited ion Channelopathy. *Nature*. (2007) 446:76–8. doi: 10.1038/nature05598

7. Preston DC, Shapiro BE. *Electromyography and neuromuscular disorders: clinical-electrophysiologic correlations*. London, United Kingdom: Elsevier Saunders (2012).

8. Richards S, Aziz N, Bale S, Bick D, Das S, Gastier-Foster J, et al. Standards and guidelines for the interpretation of sequence variants: a joint consensus recommendation of the American College of Medical Genetics and Genomics and the Association for Molecular Pathology. *Genet Med*. (2015) 17:405–24. doi: 10.1038/gim.2015.30

9. Ke Q, He F, Lu L, Yu P, Jiang Y, Weng C, et al. The R900S mutation in CACNA1S associated with hypokalemic periodic paralysis. *Neuromusc Disorde*. (2015) 25:955–8. doi: 10.1016/j.nmd.2015.09.006

10. Hirano M, Kokunai Y, Nagai A, Nakamura Y, Saigoh K, Kusunoki S, et al. A novel mutation in the calcium channel gene in a family with hypokalemic periodic paralysis. *J Neurol Sci*. (2011) 309:9–11. doi: 10.1016/j.jns.2011.07.046

11. Wu J, Yan Z, Li Z, Qian X, Lu S, Dong M, et al. Structure of the voltage-gated calcium channel ca(V)1.1 at 3.6 a resolution. *Nature*. (2016) 537:191–6. doi: 10.1038/nature19321

12. Li Z, Scheraga HA. Monte Carlo-minimization approach to the multiple-minima problem in protein folding. *Proc Natl Acad Sci U S A*. (1987) 84:6611–5. doi: 10.1073/pnas.84.19.6611

13. Weiner J, Kollman PA, Case DA, Singh UC, Chio C, Alagona G, et al. A new force field for molecular mechanical simulation of nucleic acids and proteins. *J Am Chem Soc*. (1984) 106:765–84. doi: 10.1021/ja00315a051

14. Garden DP, Zhorov BS. Docking flexible ligands in proteins with a solvent exposure- and distance-dependent dielectric function. *J Comput Aided Mol Des*. (2010) 24:91–105. doi: 10.1007/s10822-009-9317-9

15. Rossokhin A, Dreker T, Grissmer S, Zhorov BS. Why does the inner-helix mutation A413C double the stoichiometry of Kv1.3 channel block by emopamil but not by verapamil? *Mol Pharmacol*. (2011) 79:681–91. doi: 10.1124/mol.110.068031

16. Rossokhin AV, Sharonova IN, Dvorzhak A, Bukanova JV, Skrebitsky VG. The mechanisms of potentiation and inhibition of Gabaa receptors by non-steroidal anti-inflammatory drugs, mefenamic and niflumic acids. *Neuropharmacology*. (2019) 160:107795. doi: 10.1016/j.neuropharm.2019.107795

17. Catterall WA, Wisedchaisri G, Zheng N. The chemical basis for electrical signaling. *Nat Chem Biol*. (2017) 13:455–63. doi: 10.1038/nchembio.2353

18. Catterall WA, Lenaeus MJ, Gamal El-Din TM. Structure and pharmacology of voltage-gated sodium and calcium channels. *Annu Rev Pharmacol Toxicol*. (2020) 60:133–54. doi: 10.1146/annurev-pharmtox-010818-021757

19. Yarov-Yarovoy V, DeCaen PG, Westenbroek RE, Pan CY, Scheuer T, Baker D, et al. Structural basis for gating charge movement in the voltage sensor of a sodium channel. *Proc Natl Acad Sci U S A*. (2012) 109:E93–E102. doi: 10.1073/pnas.1118434109

20. Fernandez-Quintero ML, El Ghaleb Y, Tuluc P, Campiglio M, Liedl KR, Flucher BE. Structural determinants of voltage-gating properties in calcium channels. *eLife*. (2021) 10:10. doi: 10.7554/eLife.64087

21. Jurkat-Rott K, Lehmann-Horn F, Elbaz A, Heine R, Gregg RG, Hogan K, et al. A calcium channel mutation causing hypokalemic periodic paralysis. *Hum Mol Genet*. (1994) 3:1415–9. doi: 10.1093/hmg/3.8.1415

22. Rios E, Pizarro G, Stefani E. Charge movement and the nature of signal transduction in skeletal muscle excitation-contraction coupling. *Annu Rev Physiol*. (1992) 54:109–33. doi: 10.1146/annurev.ph.54.030192.000545

23. Savalli N, Angelini M, Steccanella F, Wier J, Wu F, Quinonez M, et al. The distinct role of the four voltage sensors of the skeletal Cav1.1 channel in voltage-dependent activation. *J Gen Physiol*. (2021) 153:e202112915. doi: 10.1085/jgp.202112915

24. Sokolov S, Scheuer T, Catterall WA. Ion permeation through a voltage- sensitive gating pore in brain sodium channels having voltage sensor mutations. *Neuron*. (2005) 47:183–9. doi: 10.1016/j.neuron.2005.06.012

25. Starace DM, Bezanilla F. Histidine scanning mutagenesis of basic residues of the S4 segment of the shaker K^+ channel. *J Gen Physiol*. (2001) 117:469–90. doi: 10.1085/jgp.117.5.469

26. Struyk AF, Cannon SC. A Na^+ channel mutation linked to hypokalemic periodic paralysis exposes a proton-selective gating pore. *J Gen Physiol*. (2007) 130:11–20. doi: 10.1085/jgp.200709755

27. Tan SV, Suetterlin K, Mannikko R, Matthews E, Hanna MG, Bostock H. *In vivo* assessment of interictal sarcolemmal membrane properties in hypokalaemic and hyperkalaemic periodic paralysis. *Clin Neurophysiol*. (2020) 131:816–27. doi: 10.1016/j.clinph.2019.12.414

28. Li FF, Li QQ, Tan ZX, Zhang SY, Liu J, Zhao EY, et al. A novel mutation in CACNA1S gene associated with hypokalemic periodic paralysis which has a gender difference in the penetrance. *J Mol Neurosci*. (2012) 46:378–83. doi: 10.1007/s12031-011-9596-1

29. Flucher BE. Skeletal muscle $Ca_V1.1$ channelopathies. *Pflugers Arch*. (2020) 472:739–54. doi: 10.1007/s00424-020-02368-3

30. López-Hernández JC, Galnares-Olalde JA, Benitez-Alonso E, Alcalá RE, Vargas-Cañas ES. Vacuolar myopathy associated to CACNA1S mutation as a rare cause of late-onset limb-girdle myopathy: a Case report. *Cureus*. (2021) 13:e18873. doi: 10.7759/cureus.18873

31. Thor MG, Vivekanandam V, Sampedro-Castaneda M, Tan SV, Suetterlin K, Sud R, et al. Myotonia in a patient with a mutation in an S4 arginine residue associated with hypokalaemic periodic paralysis and a concomitant synonymous *CLCN1* mutation. *Sci Rep*. (2019) 9:17560. doi: 10.1038/s41598-019-54041-0

frontiers | Frontiers in Neurology

TYPE Case Report
PUBLISHED 09 November 2023
DOI 10.3389/fneur.2023.1291702

OPEN ACCESS

EDITED BY
Giovanni Meola,
University of Milan, Italy

REVIEWED BY
Tomoo Mano,
Nara Medical University, Japan
Kevin Chen,
University of Michigan, United States

*CORRESPONDENCE
Hui Lu
huilu@zju.edu.cn

RECEIVED 10 September 2023
ACCEPTED 11 October 2023
PUBLISHED 09 November 2023

CITATION
Sun J, Zou X, Fu Q, Wu J, Yuan S, Alhaskawi A, Dong Y, Zhou H, Abdalbary SA and Lu H (2023) Case report: Ultrasound-guided needle knife technique for carpal ligament release in carpal tunnel syndrome treatment.
Front. Neurol. 14:1291702.
doi: 10.3389/fneur.2023.1291702

Case report: Ultrasound-guided needle knife technique for carpal ligament release in carpal tunnel syndrome treatment

Jianjun Sun[1], Xiaodi Zou[2], Qinyun Fu[1], Jianhua Wu[1], Shuaishuai Yuan[1], Ahmad Alhaskawi[3], Yanzhao Dong[3], Haiying Zhou[3], Sahar Ahmed Abdalbary[4] and Hui Lu[3]*

[1]Department of Anesthesiology, Pujiang County Hospital of Traditional Chinese Medicine, Jinhua, China, [2]Second Affiliated Hospital, Zhejiang Chinese Medical University, Hangzhou, Zhejiang, China, [3]First Affiliated Hospital, School of Medicine, Zhejiang University, Hangzhou, Zhejiang, China, [4]Nahda University, Beni Suef, Beni Suef, Egypt

Carpal tunnel syndrome (CTS) is a common peripheral neuropathy of the hand, mainly manifesting as sensory disturbances, motor dysfunctions, and pain in the fingers and hand. The pathogenesis of the disease is associated with fibrosis of the transverse carpal ligament in the carpal tunnel, which compresses median nerve. In our case, we demonstrate an ultrasound-guided needle knife technique to treat CTS. We guided the patient to a supine position on the examination table. The skin of the wrist area was sterilized for the procedure. After the skin was dry, we positioned sterile drapes, located the median nerve and compression, and marked the compression point. Local anesthesia was administered. An ultrasound-guided needle knife was inserted. The needle knife was advanced under ultrasound guidance. The carpal ligament was incised. A gradual release of pressure on the median nerve was observed on the ultrasound monitor. After treatment, the patient's finger sensation and motor function can significantly improve, and pain symptoms are markedly reduced, this case demonstrates that small needle-knife treatment can serve as a safe and effective minimally invasive therapeutic method.

KEYWORDS

minimally invasive surgery, ultrasound-guided, needle knife technique, carpal tunnel syndrome, carpal tunnel release

1. Introduction

Carpal tunnel syndrome (CTS) is a prevalent and debilitating condition characterized by the compression of the median nerve as it passes through the carpal tunnel at the wrist. CTS (Carpal Tunnel Syndrome) is one of the common peripheral nerve injury disorders (1). This compression results in symptoms such as hand numbness, tingling, and pain, often impairing a patient's ability to perform daily activities. Diagnosis of CTS typically involves a combination of clinical tests and electrodiagnostic studies, some common clinical tests include Phalen's test, carpal compression test, Tinel's test, and Durkan's compression test (2–6). These tests help assess the sensitivity, specificity, and predictive values for CTS diagnosis. However, relying on a single test may not be sufficient for definitive diagnosis, and a combination of clinical and paraclinical tests may be necessary (3). Nerve conduction studies (NCS) are often used to confirm CTS diagnosis based on the latency, amplitude, distance, and velocity of the median and ulnar nerves (7). Ultrasound has emerged as a noninvasive diagnostic alternative to NCS for CTS (8). It evaluates the median nerve's cross-sectional area, regional echogenicity, and coexisting pathologies that may increase pressure in the carpal tunnel.

Conservative methods for CTS include non-surgical treatments such as splinting, physiotherapy, corticosteroid, neurodynamic techniques, gabapentin, therapeutic ultrasound, and extracorporeal shockwave therapy (9). However, conservative treatment has been effective for mild and moderate idiopathic (10). Traditional surgical interventions for CTS involve a number of different methods for surgical release, including traditional open dissection, double incision cannula (11), single-small incision release (12), and endoscopic release (13). However, there remain several controversies regarding the advantages and disadvantages of various surgical methods, such as longer recovery times, scarring, and potential complications. (14). In recent years, there has been growing interest in the development of minimally invasive techniques for carpal ligament release, aimed at alleviating the compression on the median nerve. One such technique that has gained attention is the ultrasound-guided needle knife technique. This innovative approach combines the precision of ultrasound imaging with a minimally invasive needle knife to achieve carpal ligament release. By directly visualizing the anatomy and pathology of the carpal tunnel using ultrasound, clinicians can accurately guide the needle knife to the point of ligamentous compression, thus reducing the risk of injury to surrounding structures. Ultrasound guidance can also diagnose other causes of median nerve injury, such as tumors, gout, and more (15–17).

The ultrasound-guided needle knife technique offers several potential advantages over traditional open surgical approaches. First and foremost, it allows for a smaller incision and reduced tissue trauma, leading to quicker postoperative recovery and decreased scarring. Additionally, the real-time visualization provided by ultrasound ensures accurate targeting of the compressed median nerve, minimizing the risk of inadvertent nerve or vessel damage. This technique has the potential to provide patients with a more efficient and less painful treatment option, ultimately improving their quality of life. After the treatment of ultrasound-guided needle knife technique, we can judge the effectiveness and safety of the treatment by ultrasonography, which can assess median nerve and carpal tunnel dimensions, median nerve position within the tunnel, and flexor retinacular bowing and thickness (18).

In this protocol, we present a detailed description of the ultrasound-guided needle knife technique for carpal ligament release in the treatment of carpal tunnel syndrome. We outline the steps involved in the procedure, from preoperative preparation to postoperative care. Furthermore, we discuss the potential benefits and limitations of this technique and its significance in the context of existing treatment methods. By offering a less invasive alternative, we aim to contribute to the advancement of effective and patient-friendly approaches for managing carpal tunnel syndrome. And we provide a comprehensive guide to implementing this innovative technique and discuss its potential implications in the field of hand surgery.

2. Protocol

2.1. Reoperative preparation

2.1.1. Informed consent

Before initiating the procedure, ensure thorough communication with the patient regarding the ultrasound-guided needle knife technique. Explain the purpose of the procedure, the potential benefits, risks (puncture site infection, bleeding at the puncture site, median nerve injury et al.), and alternatives. Obtain written informed consent from the patient, addressing any concerns or questions they may have.

2.1.2. Patient positioning

In an operating room, gently guide the patient to a comfortable supine position on the examination table. Instruct the patient to extend the affected hand with the palm facing upward. Encourage relaxation to minimize muscle tension during the procedure.

2.1.3. Skin preparation and sterilization

Prepare the skin for the procedure by cleaning the wrist area using an antiseptic solution. Begin by cleaning the entire wrist and hand, including the palm and fingers. Use a circular motion while cleaning, moving from the center outward to create a sterile field.

2.1.4. Application of sterile drape

Once the skin is clean and dry, carefully position a sterile drape over the wrist area. Ensure that the drape covers the entire wrist and hand, leaving only the target area exposed for the procedure. Maintain the sterility of the draped area throughout the procedure.

2.1.5. Anesthesia discussion

Engage in a discussion with the patient about local anesthesia administration. Address the type of anesthesia to be used, the sensation they might experience, and its purpose in ensuring their comfort during the procedure. Reiterate their ability to communicate any discomfort or sensations during the procedure.

2.1.6. Verification of patient identity

Before proceeding, verify the patient's identity by confirming their name and date of birth. Cross-reference this information with their medical records and the consent form to ensure accurate patient identification.

2.1.7. Patient comfort and reassurance

Take a moment to ensure the patient's comfort and address any last-minute concerns they may have. Reiterate the steps of the procedure and emphasize your commitment to their well-being and safety throughout the process. An ECG monitor is connected to the patient.

2.2. Ultrasound-guided localization of median nerve

2.2.1. Application of sterile ultrasound gel

Dispense a sufficient amount of sterile ultrasound gel onto the wrist area where the median nerve is expected to be located. The gel enhances acoustic coupling between the skin and the ultrasound transducer, facilitating clear visualization of the underlying structures.

2.2.2. Ultrasound transducer placement

Hold the ultrasound transducer (WISONIC WA55-23020232022-03) with a sterile transducer cover in your dominant hand and gently position it over the wrist area covered with ultrasound gel. Orient the transducer to obtain a longitudinal view of the wrist, aligning it

parallel to the forearm. Gradually adjust the transducer's angle and orientation until you obtain a clear view of the median nerve.

2.2.3. Identification of median nerve and compression point

Slowly slide the ultrasound transducer along the wrist while observing the real-time ultrasound images on the monitor. Identify the median nerve as a hypoechoic structure with internal fascicular patterns. Differentiate the nerve from surrounding tendons and ligaments.

Using the ultrasound imaging, identify the specific point where the median nerve is compressed within the carpal tunnel. This point may exhibit hypoechoic changes or narrowing of the nerve diameter, indicating the site of compression. Measure the diameter of the compressed portion of the median nerve to quantify the degree of compression.

2.2.4. Marking the compression point

With the compression point identified and visualized on the ultrasound monitor, use a sterile marking pen to place a small dot on the patient's skin directly above the compressed region. This mark will serve as a reference point during the subsequent steps of the procedure.

2.2.5. Documentation and image capture

Capture representative ultrasound images of the median nerve in both its normal and compressed states. These images will serve as visual documentation for patient records and can be referred to during the procedure to ensure accurate needle placement.

2.3. Needle knife technique for carpal ligament release

2.3.1. Administration of local anesthesia

Prepare a syringe containing the predetermined volume of local anesthetic (2% lidocaine 5 mL) with a fine needle attached. Administer local anesthesia at the marked site over the compressed median nerve. Insert the needle gently, avoiding excessive pressure. Slowly inject the anesthetic while monitoring the patient's comfort and response. Wait for a few moments to allow the anesthetic to take effect.

2.3.2. Insertion of ultrasound-guided needle knife

Once adequate anesthesia is achieved, prepare the ultrasound-guided needle knife. Hold the needle knife (HUAYOU small needle-knife 0.6*0.8 mm) in your dominant hand, positioning it at the marked site (0.5 cm above transverse striation of palm wrist) over the compressed median nerve. Align the needle knife(at an insertion angle of 30°) with the orientation observed on the ultrasound monitor.

2.3.3. Needle knife advancement under ultrasound guidance

Begin advancing the needle knife slowly and steadily under continuous ultrasound guidance. As you progress, closely monitor the needle's trajectory on the ultrasound monitor to ensure accurate positioning in relation to the compressed median nerve. Adjust the angle and depth of insertion as necessary to maintain the needle's alignment with the target site.

2.3.4. Carpal ligament incision

With the needle knife accurately positioned near the compressed median nerve, initiate the incision of the carpal ligament. Employ controlled and deliberate movements, ensuring the needle knife's trajectory remains aligned with the nerve. As you incise the ligament, observe for any reduction in tension or pressure on the median nerve, which may be visualized on the ultrasound monitor.

2.3.5. Monitoring patient comfort and anesthesia adjustment

Throughout the procedure, maintain open communication with the patient. Inquire about their comfort level and any sensations they may experience. If the patient expresses discomfort or pain, administer additional local anesthesia as needed. It is essential to prioritize the patient's well-being and ensure they remain comfortable throughout the intervention.

2.3.6. Continuous ultrasound visualization

During the entire needle knife technique, maintain continuous visualization of the needle's position and its proximity to the median nerve using the ultrasound monitor. Adjust the needle's orientation and trajectory as necessary to optimize accuracy and avoid unintended structures.

2.3.7. Gradual release of pressure

As the carpal ligament is incised, you may observe a gradual release of pressure on the compressed median nerve on the ultrasound monitor. This reduction in compression should result in morphological changes of the previously compressed median nerve, which can be visually assessed during the procedure.

2.4. Postoperative care and follow-up

2.4.1. Application of sterile dressing

Following the completion of the needle knife technique, ensure hemostasis at the incision site. Gently clean the area with sterile saline solution to remove any residual blood or debris. Apply a sterile dressing over the incision site to protect it from external contaminants and to facilitate wound healing. Ensure that the dressing is secure but not too tight, allowing for adequate circulation.

2.4.2. Wrist elevation and activity restrictions

Instruct the patient to keep the treated wrist elevated for the first 24 to 48 h after the procedure. Elevating the wrist helps minimize swelling and promotes fluid drainage. Advise the patient to avoid engaging in strenuous activities or heavy lifting for several days postoperatively to prevent unnecessary strain on the healing tissues.

2.4.3. Pain medication and antibiotics

Prescribe pain medication as necessary to manage postoperative discomfort. Educate the patient on the proper dosage and administration schedule of the prescribed pain relievers. Additionally, if deemed appropriate, prescribe a short course of antibiotics to minimize the risk of infection at the incision site.

2.4.4. Scheduling a follow-up appointment

During the patient's discharge, schedule a follow-up appointment for a comprehensive assessment of their recovery progress. This appointment should occur within a suitable timeframe, typically 1 to 2 weeks postoperatively. During the follow-up visit, assess whether the puncture site is infected, pain levels, and overall comfort. Assess the effectiveness of the procedure in alleviating symptoms and improving median nerve function.

2.4.5. Patient education

Provide the patient with detailed postoperative instructions in written form. Include information on wound care, signs of infection, and guidelines for gradual resumption of normal activities. Emphasize the importance of adhering to the prescribed medication regimen and attending the scheduled follow-up appointment.

2.4.6. Monitoring and complications

Educate the patient about potential complications that may arise after the procedure, such as infection, bleeding, or persistent discomfort. Instruct them to promptly seek medical attention if they experience worsening pain, signs of infection (redness, swelling, warmth, pus), or any concerning symptoms.

2.4.7. Rehabilitation and physical therapy

Consider incorporating rehabilitation and physical therapy into the patient's recovery plan. Collaborate with rehabilitation specialists to design a tailored program that aims to restore wrist strength, mobility, and function. Rehabilitation can help accelerate the patient's return to regular activities while minimizing the risk of complications.

3. Representative results

The ultrasound-guided needle knife technique led to improved patient outcomes, reducing hand numbness and pain. Median nerve diameter increased after carpal ligament release, indicating successful decompression (see Figures 1, 2).

4. Discussion

Open release and medical management are two common approaches for treating CTS. Each approach has its advantages and disadvantages (19). Open release is a surgical procedure that involves cutting the transverse carpal ligament to relieve pressure on the median nerve. This technique has been shown to be effective in treating CTS, with high success rate and low complication rete (20). However, there are some disadvantages to open release, including a longer recovery time compared to minimally invasive techniques (21), potential scarring, and the risk of complications such as infection or nerve damage. Medical management for CTS typically involves conservative treatment such as wrist splinting, nonsteroidal anti-inflammatory drugs (NSAIDs), and corticosteroid injections. These treatments can provide temporary relief of symptoms and may be effective for mild cases for CTS. However, medical management may not provide long-term relief for more serve cases, and patients may eventually require surgery. Additionally, corticosteroid injections can have side effects, such as pain at the injection site and potential weaking of the tendons (22). The protocol introduces a novel and innovative approach—the ultrasound-guided needle knife technique—for the release of carpal ligament in the management of carpal tunnel

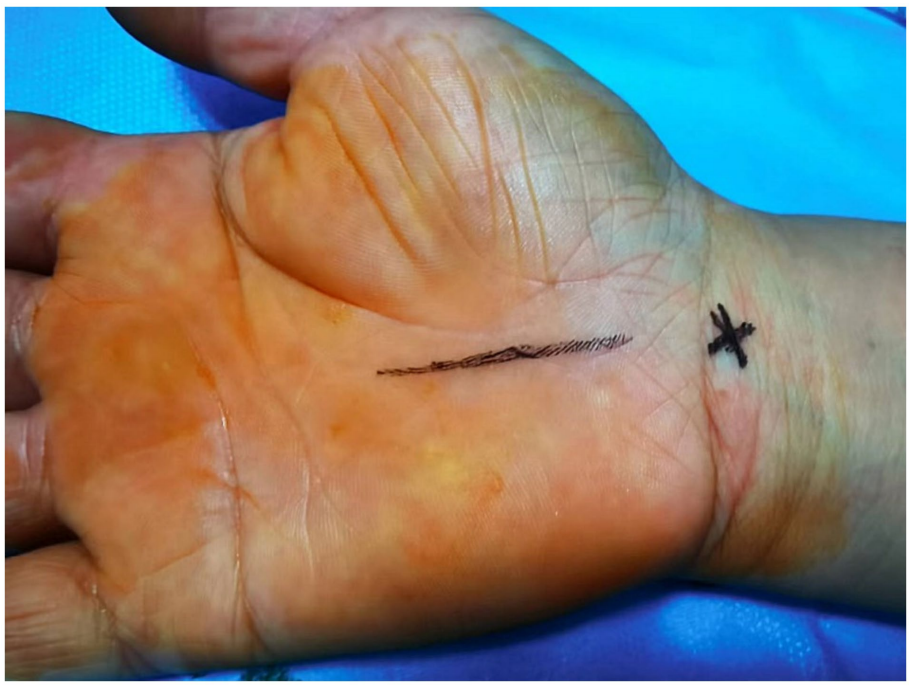

FIGURE 1
Puncture point located on the body surface. The x marks entry site. The vertical line marks the direction of advancing the needle knife.

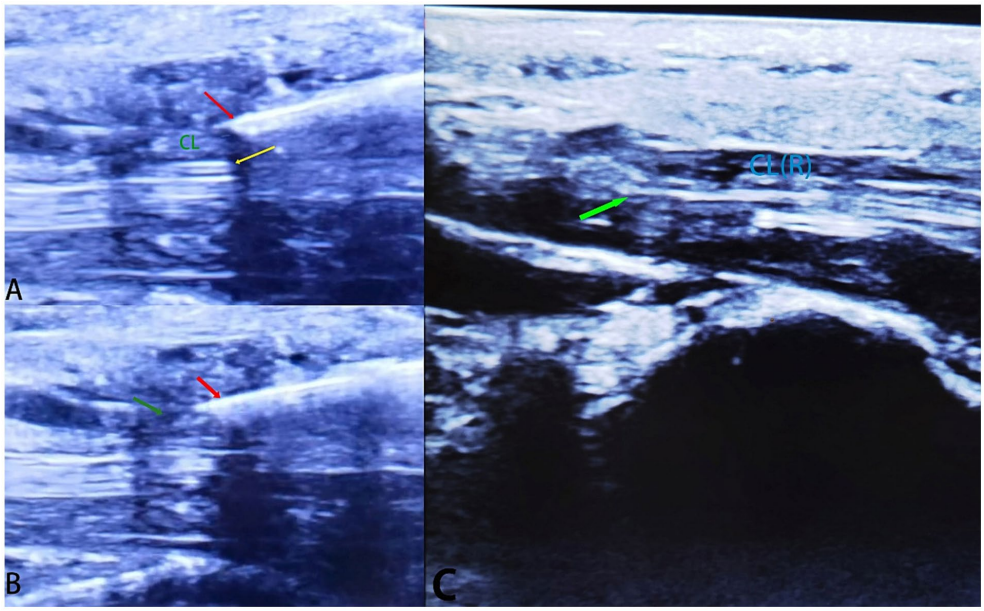

FIGURE 2
Ultrasound Images Demonstrating Median Nerve Compression and Carpal Ligament Release **(A)** Ultrasound image illustrating the location of median nerve compression before carpal ligament release. The compressed median nerve is indicated by the yellow arrow, and the carpal ligament is labeled as "CL." Red arrow marks the needle knife. **(B)** The needle knife is slowly and carefully advanced (red arrow) to incise the carpal ligament, relieving pressure on the median nerve (MN). Green arrow marks the partly sectioned carpal ligament. **(C)** Ultrasound image showing the same area after carpal ligament release. The relieved median nerve is highlighted by the green arrow, and the incised carpal ligament is denoted as "CL(R)." The reduction in compression and enhanced nerve space can be observed.

syndrome (CTS). This technique presents a paradigm shift from traditional open surgeries, offering a range of distinct advantages that significantly enhance patient outcomes (23). In a clinical study using ultrasound-guided percutaneous release to treat stenosing flexor tenosynovitis with a needle knife, The results suggest that this technique is both safe and effective for the treatment of stenosing flexor tenosynovitis. The length and percentage of released A1 pulley were found to be longer with ultrasound guidance compared to non-ultrasound-guided techniques. The full release rate was highest in the ultrasound-guided group. However, it is important to note that the full release rate was still relatively low (13.6 to 31.4%) in all groups (24).

One of the primary advantages of the ultrasound-guided needle knife technique is its potential to expedite patient recovery. Compared to open surgical procedures, this minimally invasive approach involves a smaller incision, reduced tissue disruption, and decreased postoperative pain (24). As a result, patients may experience a quicker return to daily activities and work, mitigating the economic burden associated with extended recovery periods observed in conventional surgeries. The reduced trauma to surrounding tissues also contributes to the overall comfort of the patient during the postoperative phase. Another compelling benefit of the technique lies in the minimal to even no scarring it produces. The smaller incision and precision-guided nature of the needle knife approach result in esthetically pleasing outcomes that are particularly important in visible areas like the wrist (25). This can have positive psychological effects on patients, enhancing their body image and self-confidence during the recovery process. Furthermore, the real-time ultrasound guidance ensures accurate localization of the median nerve and precise targeting of the compressed ligament. This reduces the risk of inadvertent damage to adjacent structures, such as vessels or nerves, which is a concern in open surgeries (26). The technique's accuracy contributes to a safer and more predictable procedure, further bolstering patient safety and positive outcomes. Several percutaneous ultrasound-guided approaches have been reported, including the "X" blade, needle release, hook knife, carpX, and thread carpal tunnel release (27). However, these methods still have certain limitations, such as the utilization of proprietary tools and a lack of larger clinical case studies. Among these techniques, the needle-knife technique has gained widespread usage and has been proven to be a cost-effective and efficient method (28).

The adoption of the ultrasound-guided needle knife technique not only offers immediate benefits to patients but also has wider implications for the field of hand surgery (29). The combination of ultrasound imaging and minimally invasive procedures is a promising avenue for advancing the treatment of various musculoskeletal and neurologic conditions. The technique's success in CTS management highlights its potential to be adapted for other pathologies with similar anatomical constraints. Despite its numerous advantages, it is essential to acknowledge the potential limitations of the technique. The learning curve associated with ultrasound guidance and precise needle manipulation could impact procedural efficiency. As with any procedure, patient selection and thorough preoperative assessment remain pivotal for successful outcomes. While the ultrasound-guided needle knife technique offers significant advantages over traditional

open surgeries, it is important to address potential challenges and consider its broader impact on clinical practice and research. One important aspect to consider is the role of operator expertise and training in the successful implementation of the technique. Ultrasound-guided procedures require a level of skill and familiarity with imaging technology. Ensuring that healthcare providers receive adequate training and hands-on experience is crucial to achieve consistent and optimal outcomes. As the technique gains popularity, specialized training programs and certification processes can contribute to its widespread adoption.

The long-term efficacy and durability of the results obtained from the ultrasound-guided needle knife technique warrant ongoing investigation. While short-term outcomes have shown improved patient comfort and function, longitudinal studies are necessary to assess the technique's impact over extended periods. Monitoring patient outcomes, recurrence rates, and long-term nerve function will provide a comprehensive understanding of its sustainability. In the context of evolving healthcare practices, the economic implications of the ultrasound-guided needle knife technique should also be considered. While the technique may lead to faster recovery and reduced healthcare costs in the short term, comprehensive cost-effectiveness analyses are needed to assess its economic benefits in the long run. These analyses can inform healthcare decision-makers and policymakers when evaluating the integration of the technique into clinical practice. The successful adoption of the ultrasound-guided needle knife technique also highlights the importance of interdisciplinary collaboration. Close collaboration between radiologists, surgeons, and rehabilitation specialists is essential to optimize patient outcomes. Additionally, continuous collaboration between researchers and clinicians can drive further refinements of the technique based on real-world feedback and clinical insights. Furthermore, the technique's successful application in carpal tunnel syndrome treatment raises intriguing possibilities for its adaptation in other clinical scenarios. Exploring its potential for other nerve compression syndromes, such as cubital tunnel syndrome or tarsal tunnel syndrome, could expand the scope of its clinical utility. This calls for multidisciplinary research efforts to explore its efficacy in various anatomical locations and patient populations.

Data availability statement

The original contributions presented in the study are included in the article/Supplementary material, further inquiries can be directed to the corresponding author.

Ethics statement

This study has been reviewed and approved by Ethical Review Board of Pujiang County Hospital of Traditional Chinese Medicine (2023C01). The written informed consent of all study participants has been obtained for this study. Written informed consent was obtained from the individual(s) for the publication of any potentially identifiable images or data included in this article.

Author contributions

JS: Writing – original draft. XZ: Writing – original draft. QF: Writing – original draft. JW: Writing – review & editing, Formal analysis. SY: Writing – review & editing. AA: Writing – review & editing. YD: Writing – review & editing. HZ: Writing – review & editing. SA: Writing – review & editing. HL: Writing – review & editing.

Funding

This research was supported by Zhejiang Provincial Natural Science Foundation Academic Exchange Program (grant number: LS21H0600010).

Conflict of interest

The authors declare that the research was conducted in the absence of any commercial or financial relationships that could be construed as a potential conflict of interest.

Publisher's note

Supplementary material

The Supplementary material for this article can be found online at: https://www.frontiersin.org/articles/10.3389/fneur.2023.1291702/full#supplementary-material

References

1. Fu J, Li X, Jin F, Dong Y, Zhou H, Alhaskawi A, et al. The potential roles of dental pulp stem cells in peripheral nerve regeneration. *Front Neurol.* (2022) 13:1098857. doi: 10.3389/fneur.2022.1098857

2. Babaei A, Froughi F, Sadeghian A. Comparative analysis of the predictive values of Phalen's and carpal compression tests in diagnosis and Management of the Carpal Tunnel Syndrome Patients based on Electrodiagnostic testing. *Quar J Nurs Manag.* (2020) 9:46–54.

3. Sang A-M, Phúc NT, Mừng PĐ, Binh N, Khoa T, Quyền VT, et al. Sensitivity and specificity of clinical tests in the diagnosis of carpal tunnel syndrome. *Can J Plast Surg.* (2021)

4. Maroufi P, Moharrami M. Clinical trials versus Electrodiagnostic tests (EDX) in the diagnosis of carpal tunnel syndrome. *Neuroscience.* (2021) 9:291–8.

5. Dong Y, Alhaskawi A, Zhou H, Zou X, Liu Z, Ezzi SHA, et al. Imaging diagnosis in peripheral nerve injury. *Front Neurol.* (2023) 14:14. doi: 10.3389/fneur.2023.1250808

6. Zhou H, Bai Q, Hu X, Alhaskawi A, Dong Y, Wang Z, et al. Deep CTS: a deep neural network for identification MRI of carpal tunnel syndrome. *J Digit Imaging.* (2022) 35:1433–44. doi: 10.1007/s10278-022-00661-4

7. Demino C, Fowler JR. The sensitivity and specificity of nerve conduction studies for diagnosis of carpal tunnel syndrome: a systematic review. *Hand (N Y).* (2021) 16:174–8. doi: 10.1177/1558944719855442

8. Drakopoulos D, Mitsiokapa E, Karamanis E, Kontogeorgakos V, Mavrogenis AF. Ultrasonography provides a diagnosis similar to that of nerve conduction studies for

carpal tunnel syndrome. *Orthopedics*. (2019) 42:e460–4. doi: 10.3928/01477447-20190604-02

9. Karjalanen T, Raatikainen S, Jaatinen K, Lusa V. Update on efficacy of conservative treatments for carpal tunnel syndrome. *J Clin Med*. (2022) 11:950. doi: 10.3390/jcm11040950

10. Hernández-Secorún M, Montaña-Cortés R, Hidalgo-García C, Rodríguez-Sanz J, Corral-de-Toro J, Monti-Ballano S, et al. Effectiveness of conservative treatment according to severity and systemic disease in carpal tunnel syndrome: a systematic review. *Int J Environ Res Public Health*. (2021) 18:2365. doi: 10.3390/ijerph18052365

11. Uchiyama S, Yasutomi T, Fukuzawa T, Nakagawa H, Kamimura M, Kato H. Reducing neurologic and vascular complications of endoscopic carpal tunnel release using a modified chow technique. *J Arthrosc Relat Surg*. (2007) 23:816–21. doi: 10.1016/j.arthro.2007.02.009

12. Pataradool K, Kitidumrongsook P, Patradul A. Carpal tunnel release by mini palmar incision. *Asian Biomed*. (2011) 5:139–42. doi: 10.5372/1905-7415.0501.017

13. Dj N. Endoscopic carpal tunnel release. *Hand Clin*. (2002) 18:xi. doi: 10.1016/S0749-0712(02)00022-7

14. Karl JW, Gancarczyk SM, Strauch RJ. Complications of carpal tunnel release. *Orthop Clin North Am*. (2016) 47:425–33. doi: 10.1016/j.ocl.2015.09.015

15. Lu H, Chen Q, Shen H. A repeated carpal tunnel syndrome due to tophaceous gout in flexor tendon: a case report. *Medicine*. (2017) 96:e6245. doi: 10.1097/MD.0000000000006245

16. Zhou H, Yao C, Dong Y, Alhaskawi A, Wang Z, Lai J, et al. Clinical characteristics and management experience of schwannoma in extremities: lessons learned from a 10-year retrospective study. *Front Neurol*. (2022) 13:1083896. doi: 10.3389/fneur.2022.1083896

17. Zhou H-Y, Jiang S, Ma F-X, Lu H. Peripheral nerve tumors of the hand: clinical features, diagnosis, and treatment. *World J Clin Cases*. (2020) 8:5086–98. doi: 10.12998/wjcc.v8.i21.5086

18. Erickson M, Lawrence M, Lucado A. The role of diagnostic ultrasound in the examination of carpal tunnel syndrome: an update and systematic review. *J Hand Ther*. (2022) 35:215–25. doi: 10.1016/j.jht.2021.04.014

19. Raymond C, David MR, Homer S. Ultrasound-guided percutaneous carpal tunnel release: a systematic review. *PM R*. (2023) 15:363–79. doi: 10.1002/pmrj.12801

20. Li Y, Luo W, Wu G, Cui S, Zhang Z, Gu X. Open versus endoscopic carpal tunnel release: a systematic review and meta-analysis of randomized controlled trials. *BMC Musculoskelet Disord*. (2020) 21:272. doi: 10.1186/s12891-020-03306-1

21. Wise A, Pourcho AM, Henning PT, Latzka EW. Evidence for ultrasound-guided carpal tunnel release. *Curr Phys Med Rehabil Rep*. (2021) 9:11–22. doi: 10.1007/s40141-020-00305-0

22. Susana Gabriela PL, Paulina M, José Carlos JG, Rubén T-E, Samantha Emily B-C, José María Z-T. Carpal tunnel syndrome: anatomo-clinical review. *Diagn Treat Int J Med Sci Clin Res Stud*. (2022) 46:2. doi: 10.47191/ijmscrs/v2-i6-08

23. Cromheecke M, Haignère V, Mares O, De Keyzer P-B, Louis P, Cognet J-M. An ultrasound-guided percutaneous surgical technique for trigger finger release using a minimally invasive surgical knife. *Tech Hand Up Extrem Surg*. (2022) 26:103–9. doi: 10.1097/BTH.0000000000000367

24. Qiu Z, Li H, Shen Y, Jia Y, Sun X, Zhou Q, et al. Safety and efficacy of ultrasound-guided percutaneous A1 pulley release using a needle knife: an anatomical study. *Front Surg*. (2022) 9:967400. doi: 10.3389/fsurg.2022.967400

25. Jiang L, Liu H, Li H, Jiang J, Liu X. Ultrasound-guided needle-knife for De Quervain's disease. *Medicine*. (2021) 100:e24877. doi: 10.1097/MD.0000000000024877

26. Thibodeau R, Simone BA, Tanny S, Hahn SS, Aridgides PD. Advantages of real-time transabdominal ultrasound guidance in combined interstitial/intracavitary cervical brachytherapy: a case-based review. *J Contemp Brachyther*. (2021) 13:211–20. doi: 10.5114/jcb.2021.105290

27. McCool L. A review of advances in carpal tunnel release. *J Neurol Neuromed*. (2017) 2:6–8. doi: 10.29245/2572.942X/2017/10.1157

28. Thaveepunsan S, Shields MN, O'Driscoll SW. The needle-and-knife technique: a safe technique for anterolateral portal placement in elbow arthroscopy. *Orthop J Sports Med*. (2019) 7:1723. doi: 10.1177/2325967118817232

29. Canena J, Lopes L, Fernandes J, Alexandrino G, Figueiredo L, Moreira M, et al. Efficacy and safety of primary, early and late needle-knife fistulotomy for biliary access. *Sci Rep*. (2021) 11:16658. doi: 10.1038/s41598-021-96142-9

frontiers | Frontiers in Neurology

TYPE Case Report
PUBLISHED 16 November 2023
DOI 10.3389/fneur.2023.1295374

OPEN ACCESS

EDITED BY
Giovanni Meola,
University of Milan, Italy

REVIEWED BY
Suresh Bokoliya,
UCONN Health, United States
Vincenzo Di Stefano,
University of Palermo, Italy

*CORRESPONDENCE
Jian-Quan Shi
myxiyi_0717@163.com

RECEIVED 16 September 2023
ACCEPTED 31 October 2023
PUBLISHED 16 November 2023

CITATION
Huang SQ, Wang B, Gao L, Wang M, Zhao HD and Shi JQ (2023) Case report: Coexistence of triple-seronegative myasthenia gravis and pathology-proven cryptogenic organizing pneumonia. *Front. Neurol.* 14:1295374. doi: 10.3389/fneur.2023.1295374

Case report: Coexistence of triple-seronegative myasthenia gravis and pathology-proven cryptogenic organizing pneumonia

Shi-Qi Huang[1], Bin Wang[2], Lin Gao[3], Meng Wang[1], Hong-Dong Zhao[1] and Jian-Quan Shi[1]*

[1]Department of Neurology, Nanjing First Hospital, Nanjing Medical University, Nanjing, Jiangsu, China, [2]Department of Pathology, Nanjing First Hospital, Nanjing Medical University, Nanjing, Jiangsu, China, [3]Department of Respiratory Medicine, Nanjing First Hospital, Nanjing Medical University, Nanjing, Jiangsu, China

Objective: Emerging evidence shows that patients with myasthenia gravis (MG) were at a higher risk for the co-occurrence of other autoimmune diseases, which reflects phenotypic heterogeneity in MG. The coexistence of MG and cryptogenic organizing pneumonia (COP) has rarely been reported. The present case is to report the coexistence of triple-seronegative MG and pathology-proven COP in a patient.

Methods: The clinical data of the patient were derived from medical records of Nanjing First Hospital, Nanjing Medical University, China. Written informed consent was obtained from the patient.

Results: We presented a 56-year-old man with acute respiratory syndrome, who was diagnosed with COP based on the intra-alveolar fibroinflammatory buds (Masson's bodies) in the pathology of bronchoscopy biopsy. Oral prednisone induced dramatic symptomatic improvement and complete resolution of previous lung lesions. After a stable course of no respiratory symptom for 2 months, he was referred to the neurology department with complaints of fluctuating generalized muscle weakness. He was diagnosed with triple-seronegative MG based on fluctuating weakness, neostigmine test-positivity and RNS-positivity. After three-month treatment with pyridostigmine in combination with tacrolimus, the symptoms gradually improved and he achieved minimal symptom expression.

Conclusions: This case highlights the rare coexistence of triple-seronegative MG and pathology-proven COP. However, a causal association between COP and MG cannot be explicitly ascertained. In future, more data are needed to clarify the relationship, taking into account the limited number of cases reported with this coexistence of the diseases.

KEYWORDS

myasthenia gravis, cryptogenic organizing pneumonia, coexistence, seronegative, antibody

Introduction

Myasthenia gravis (MG) is a rare autoimmune disease, which is characterized by fatigable muscle weakness. The disease is an organ-specific disease mediated by autoantibodies, including antibodies against acetylcholine receptor (AChR), muscle-specific tyrosine kinase (MuSK) and lipoprotein receptor-related protein 4 (LRP4) (1). However, about 10% of MG patients without detectable antibodies are classified as triple-seronegative MG, which represents a heterogeneous group (2). Patients with MG carried an elevated risk of developing other autoimmune diseases simultaneously or successively, which reflects phenotypic heterogeneity in MG (3, 4). As we previously reported, MG could coexsit with autoimmune thyroid disease, Sjögren's syndrome, rheumatoid arthritis, psoriasis, vitiligo, autoimmune hemolytic anemia, idiopathic thrombocytopenic purpura, polymyositis and autoimmune hepatitis (5).

Here, we reported the rare coexistence of triple-seronegative MG and pathology-proven cryptogenic organizing pneumonia (COP) in a patient. COP has no recognizable cause, which is classified as a subtype of idiopathic interstitial pneumonia. To the best of our knowledge, the coexistence of MG and COP in a single patient has not been reported in the literature.

Case presentation

A 56-year-old man presented to the department of respiratory medicine with cough, sputum and mild chest pain for 4 days. He also reported fever with the highest temperature of 38°C. He denied dyspnea, night sweat and weight loss. The patient's medical history include hypertension, which was well controlled. His family history was unremarkable. Lung auscultation revealed normal breath sounds. Routine blood tests and biochemical tests were within normal ranges. Tumor markers and autoantibodies of connective tissue diseases were normal. The elevated C-reactive protein level of 87.27 mg/L (normal range < 10 mg/L) was revealed. Subsequent arterial blood gas analysis was normal. The blood culture and sputum culture were negative. High-resolution computed tomography (HRCT) indicated irregular nodular opacitie in the upper lobe and lower lobe of the right lung and the middle lobe of left lung (Figures 1A–C). Initially, he was diagnosed with community-acquired pneumonia and treated with piperacillin/tazobactam. However, the symptoms were not alleviated after 1-week antibiotic therapy. The lesions on chest HRCT expanded gradually (Figures 1D–F). Bronchoalveolar lavage revealed a nonspecific inflammatory pattern with lack of eosinophil and tumor cell. The pathology of bronchoscopy biopsy showed preservation of the lung architecture with a patchy distribution of intra-alveolar fibroinflammatory buds, in the form of Masson's bodies (Figures 1J–L). Based on the findings, lung cancer, infection, connective tissue diseases or other diseases that can cause interstitial pneumonia were ruled out. Hence, he was diagnosed with COP. Oral prednisone (60 mg QD, 0.75 mg/kg of weight) as a monotherapy was initiated with dramatic symptomatic improvement after 1 week. This initial dose was given for 4 weeks and the symptom of COP was remitted completely during the period. Then, the dose of prednisone was reduced by 10 mg/d every 2 weeks. After a stable course of no symptom for 2 months (the dose of prednisone at that time was 40 mg QD), he was referred to the neurology department with complaints of fluctuating ptosis, diplopia, mild dysphagia to solid foods, and generalized muscular weakness for 2 weeks. On neurological examination, he presented bilateral ptosis. He had difficulty in crouching down or walking on his toes or heels. Stretch reflexes, muscle tone, tropism, and sensation were normal. There was bilaterally moderate weakness (Medical Research Council grade 3/5) in shoulder abduction, elbow flexion, wrist extension, hip flexion, knee extension, and foot dorsiflexion. The quantitative MG (QMG) score was 20. The MG activities of daily living (MG-ADL) score was 9. The neostigmine test was positive. Repetitive Nerve Stimulation (RNS) at the deltoid muscle showed a 26.5% decrement. The chest HRCT showed no evidence of thymoma and complete resolution of previous lung lesions (Figures 1G–I). Furthermore, anti-AChR, anti-MuSK and anti-LRP4 antibodies were negative by ELISA. He was diagnosed with triple-seronegative MG based on fluctuating weakness, neostigmine test-positivity and RNS-positivity. In order to decrease the dose of prednisone and to avoid the side effects, pyridostigmine 60 mg TID and tacrolimus 3 mg QD was added (the dose of prednisone at that time was 40 mg QD). After 3-month follow-up (time from the diagnosis of MG), his symptoms gradually improved. The QMG score was 1 (ptosis). The MG-ADL score was 1 (ptosis). Prednisone was tapered to 20 mg QD, while the dose of tacrolimus remained unchanged. Figure 2 summarizes the clinical course.

Discussion

This report presented the coexistence of triple-seronegative MG and pathology-proven COP in a patient. MG with no detectable AChR, MuSK, or LRP4 antibodies in serum represents a heterogeneous group, which is classified triple-seronegative MG. Different methods are available for the detection of anti-AChR, anti-MuSK or anti-LRP4 antibodies, but the current gold standard remains the radioimmunoprecipitation assay (RIPA) (1). Damato et al. (6) reported that cell-based assay (CBA) can detect the antibodies in a proportion of triple-seronegative MG patients by RIPA. Initially, ELISA was employed to detect serum antibodies, although its sensitivity was relatively low. Recently, we have detected the antibodies in stored serum sample (stored at first visit to the neurology department) by CBA. The anti-AChR, anti-MuSK and anti-LRP4 antibodies were still negative by CBA. Given that the patient was taking prednisone (40 mg QD, for the treatment of COP) when the onset of myasthenic symptom, it is plausible that the immunosuppressive therapy before antibody testing might complicate the identification of the patient's seropositivity. Similar cases have been reported in other antoimmune diseases, such as Celiac disease (7). In addition to detection methods and immunosuppressants in use, other factors might predispose to seronegativity in MG, including unknown autoantibodies, rapid autoantibody clearance and so on (8).

The diagnosis and treatment are more challenging in triple-seronegative MG. As no detectable specific antibodies, diagnosis of triple-seronegative MG should be supported by adequate clinical characteristics and electrophysiological support, especially when

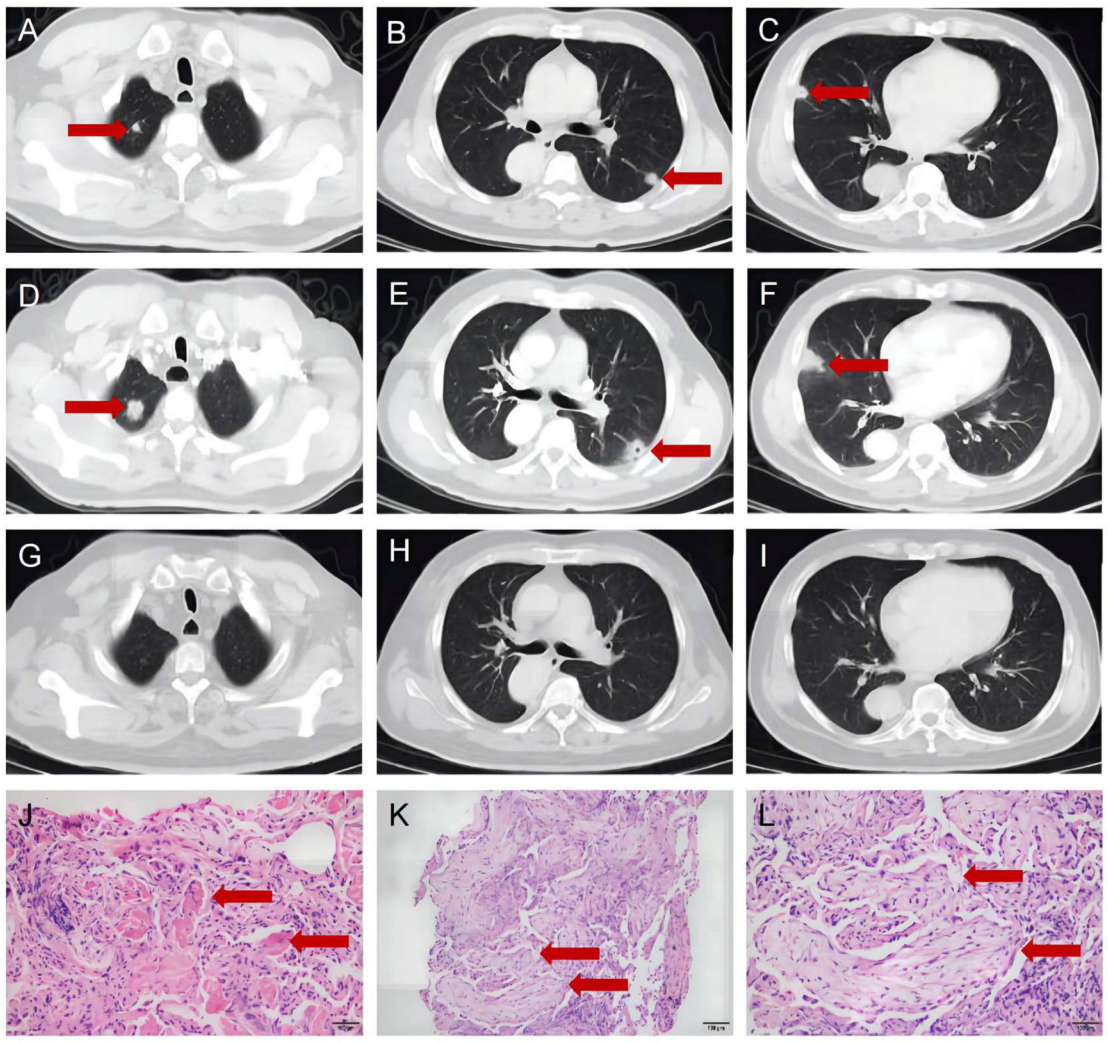

FIGURE 1
The chest high-resolution computed tomography and pathology of bronchoscopy biopsy. **(A–C)** The chest high-resolution computed tomography at onset indicated irregular nodular opacities in the upper and lower lobe of the right lung and the middle lobe of left lung (Red arrows). **(D–F)** The chest high-resolution computed tomography after 1-week antibiotic therapy indicated expanded lesions (Red arrows). **(G–I)** The chest high-resolution computed tomography at 2-month follow-up showed complete resolution of previous lung lesions (Red arrows). **(J–L)** The pathology of bronchoscopy biopsy showed intra-alveolar fibroinflammatory buds **(**Red arrows, **J)**, in the form of Masson's bodies **(**Red arrows, **K, L)**.

the effectiveness of standard treatment is dissatisfactory. From a clinical point of view, it is observed that the clinical characteristics of triple-seronegative MG patients varied among different age groups (9). The overall prognosis of triple-seronegative MG is relatively good, with a low occurrence of crisis. Pyridostigmine is the drug of choice for symptomatic treatment. To improve efficacy and minimize side effects of steroids, a combination of immunosuppressive drugs for the majority of MG patients is recommended, which is based on the sum of guidelines, clinical experience, and relevant research. Efgartigimod is a novel neonatal Fc receptor (FcRn)-inhibiting agent, which have shown significant efficacy in the treatment of anti-AChR generalized MG (10). Efgartigimod is believed to be a new treatment choice for anti-AChR generalized MG and can reduce the dosage of steroids or other immunosuppressants (11). Whether efgartigimod can improve the symptoms of triple-seronegative MG needs further study. Triple-seronegative MG has shown positive response to steroids and pyridostigmine, with approximately a third of patients achieving either complete stable remission or pharmacological remission (9). After 3-month treatment with pyridostigmine in combination with immunosuppressive therapy, the present patient achieved minimal symptom expression, which was defined as MG-ADL score of 0 or 1 and regarded as an practical tool for MG treatment goals (12).

Individuals with MG have an increased vulnerability to other autoimmune diseases, which may manifest before or after the onset of MG. Notably, the incidence of autoimmune thyroid disease appears to be higher in patients with MG (3). We reported a case of triple-seronegative MG with COP. Apart from COP, no other autoimmune diseases were observed during follow-up.

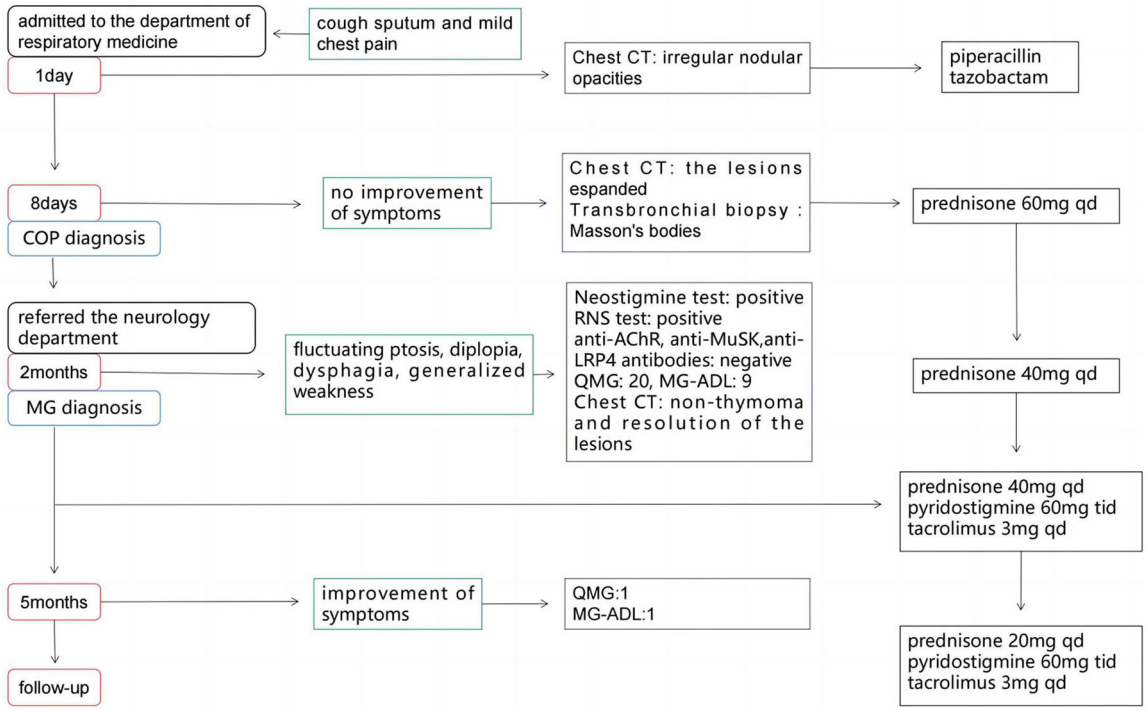

FIGURE 2
The timeline of the case.

As an idiopathic form of interstitial pneumonia, COP is pathologically characterized by intra-alveolar fibroinflammatory buds (Masson's bodies). The pathogenesis of COP still remains elusive. However, the abnormal immune process might play a pivotal role in the pathogenesis. The diagnosis of COP is an exclusive one to rule out infective pneumonia, eosinophilic pneumonia, other forms of interstitial pneumonia, alveolar hemorrhage, and malignancy and so on (13). The diagnosis of COP requires multidisciplinary approaches, including clinical, radiologic and pathologic expertise. This patient presented with flu-like symptoms prior to the diagnosis of MG, which was initially treated as community-acquired pneumonia. But he had a poor response to antibiotic treatment. Typical radiologic findings, bronchoalveolar lavage and transbronchial biopsy are valuable in the diagnosis of COP. Poletti et al. reported a series of 37 patients with suspected COP. The sensitivity and specificity of bronchoalveolar lavage was 63 and 57%, respectively. Meanwhile, the sensitivity and specificity of transbronchial biopsy was 64 and 86%, respectively (14).

In addition, COP is associated with a high recovery rate if managed appropriately (15). COP patients have a significant response to corticosteroids, which is considered to be one of the strong evidences for the diagnosis of COP. Furthermore, a small proportion of COP patients may recover spontaneously without medical intervention. Corticosteroid therapy is considered the preferred treatment for patients with nonresolving or progressive COP (13). Complete resolution of radiologic infiltrates can be observed after a 3-month period of treatment. However, a retrospective study showed that 31.5% (23/73) of patients relapsed after reduction or cessation of corticosteroids (16). Another study revealed that the recurrence rate after 1-year follow-up was 38.2% (13/30) (17). Clarithromycin has also been proposed for the treatment of COP, with fewer side effects and recurrences than corticosteroids (18). However, it is currently unclear whether macrolides play a specific role in the treatment of COP.

In a retrospective cohort with 91 patients initially diagnosed with COP, 4 patients were eventually identified as OP that was secondary to connective tissue diseases (16). Notably, no clinical or pathological evidence of connective tissue disease was present in the initial evaluation. In other words, secondary OP was the initial manifestation of connective tissue diseases. Hence, it should be acknowledged that OP may not always be cryptogenic. Furthermore, regular prospective monitoring of other clinical manifestation and dynamic assessment of serum biomarkers might be of great significance in identifying potential etiology. During the follow-up period, clinicians need to be aware of screening for other immune-mediated diseases.

More interestingly, OP can coexist with autoimmune neurological diseases. A Japanese retrospective cohort study suggested that 4 in 52 patients with neuromyelitis optica spectrum disease showed pulmonary involvement with a diagnosis of OP, which preceded or coincided with neuromyelitis optica spectrum disease (19, 20). Anti-AQP4 antibody induced complement-dependent cytotoxicity of lung epithelial cells is believed to be partially involved in the development of OP. To our knowledge, there are no reports of the coexistence of COP and triple-seronegative MG in a single patient. Herein, a rare case of triple-seronegative MG in pathologically-confirmed COP is

reported. We speculated that the rare co-occurrence might be ascribed to the common immune-mediated mechanisms.

Few reports focus on any association between these two distinct conditions. It could be argued that an immune response to pulmonary antigens might elicit an immune attack against neuromuscular junction. To explore this association is crucial for both diagnosis and management of patients presenting with these rare conditions. There is another possibility that the coexistence of triple-seronegative MG and COP in this case could just be a simple coincidence.

This case highlights the rare coexistence of pathology-proven COP and triple-seronegative MG. However, this descriptive study cannot definitively ascertained the causal association between COP and MG. In future, more data are needed to clarify the relationship, taking into account the limited number of cases reported with this coexistence of the diseases.

Data availability statement

The original contributions presented in the study are included in the article/supplementary material, further inquiries can be directed to the corresponding author.

Ethics statement

The studies involving humans were approved by Nanjing First Hospital, Nanjing Medical University. The studies were conducted in accordance with the local legislation and institutional requirements. The participants provided their written informed consent to participate in this study. Written informed consent was obtained from the individual(s) for the publication of any potentially identifiable images or data included in this article.

Author contributions

SQH: Conceptualization, Data curation, Writing—original draft. BW: Conceptualization, Data curation, Writing—review & editing. LG: Conceptualization, Writing—review & editing. MW: Conceptualization, Data curation, Writing—review & editing. HDZ: Writing—review & editing. JQS: Writing—review & editing.

Funding

The author(s) declare that no financial support was received for the research, authorship, and/or publication of this article.

Conflict of interest

The authors declare that the research was conducted in the absence of any commercial or financial relationships that could be construed as a potential conflict of interest.

Publisher's note

References

1. Gilhus NE, Verschuuren JJ. Myasthenia gravis: subgroup classification and therapeutic strategies. *Lancet Neurol.* (2015) 14:1023–36. doi: 10.1016/S1474-4422(15)00145-3

2. Vinciguerra C, Bevilacqua L, Lupica A, Ginanneschi F, Piscosquito G, Rini N, et al. Diagnosis and management of seronegative myasthenia gravis: lights and shadows. *Brain Sci.* (2023) 13:1286. doi: 10.3390/brainsci13091286

3. Mao Z-F, Yang L-X, Mo X-A, Qin C, Lai Y-R, He N-Y, et al. Frequency of autoimmune diseases in myasthenia gravis: a systematic review. *Int J Neurosci.* (2011) 121:121–9. doi: 10.3109/00207454.2010.539307

4. Gilhus NE, Nacu A, Andersen JB, Owe JF. Myasthenia gravis and risks for comorbidity. *Eur J Neurol.* (2015) 22:17–23. doi: 10.1111/ene.12599

5. Shi J, Huan X, Zhou L, Xi J, Song J, Wang Y, et al. Comorbid autoimmune diseases in patients with myasthenia gravis: a retrospective cross-sectional study of a Chinese cohort. *Front Neurol.* (2021) 12:790941. doi: 10.3389/fneur.2021.790941

6. Damato V, Spagni G, Monte G, Woodhall M, Jacobson L, Falso S, et al. Clinical value of cell-based assays in the characterisation of seronegative myasthenia gravis. *J Neurol Neurosurg Psychiatry.* (2022) 93:995–1000. doi: 10.1136/jnnp-2022-329284

7. Schiepatti A, Sanders DS, Biagi F. Seronegative coeliac disease: clearing the diagnostic dilemma. *Curr Opin Gastroenterol.* (2018) 34:154–8. doi: 10.1097/MOG.0000000000000436

8. Lenti MV, Rossi CM, Melazzini F, Gastaldi M, Bugatti S, Rotondi M, et al. Seronegative autoimmune diseases: a challenging diagnosis. *Autoimmun Rev.* (2022) 21:103143. doi: 10.1016/j.autrev.2022.103143

9. Li W, Liu P, Cui W, Wang S, Ji Y, Zhang L, et al. Clinical characteristics of anti-AChR-MuSK-LRP4 antibody-negative myasthenia gravis in China. *Muscle Nerve.* (2023) 67:481–8. doi: 10.1002/mus.27822

10. Howard JF Jr, Bril V, Vu T, Karam C, Peric S, Margania T, et al. Safety, efficacy, and tolerability of efgartigimod in patients with generalised myasthenia gravis (ADAPT): a multicentre, randomised, placebo-controlled, phase 3 trial. *Lancet Neurol.* (2021) 20:526–36. doi: 10.1016/S1474-4422(21)00159-9

11. Di Stefano V, Alonge P, Rini N, Militello M, Lupica A, Torrente A, et al. Efgartigimod beyond myasthenia gravis: the role of FcRn-targeting therapies in stiff-person syndrome. *J Neurol.* (2023). doi: 10.1007/s00415-023-11970-1. [Epub ahead of print].

12. Vissing J, Jacob S, Fujita KP, O'Brien F, Howard JF, REGAIN study group. 'Minimal symptom expression' in patients with acetylcholine receptor antibody-positive refractory generalized myasthenia gravis treated with eculizumab. *J Neurol.* (2020) 267:1991–2001. doi: 10.1007/s00415-020-09770-y

13. Raghu G, Meyer KC. Cryptogenic organising pneumonia: current understanding of an enigmatic lung disease. *Eur Respir Rev.* (2021) 30:210094. doi: 10.1183/16000617.0094-2021

14. Poletti V, Cazzato S, Minicuci N, Zompatori M, Burzi M, Schiattone ML. The diagnostic value of bronchoalveolar lavage and transbronchial lung biopsy in cryptogenic organizing pneumonia. *Eur Respir J.* (1996) 9:2513–6. doi: 10.1183/09031936.96.09122513

15. King TE Jr, Lee JS. Cryptogenic organizing pneumonia. *N Engl J Med.* (2022) 386:1058–69. doi: 10.1056/NEJMra2116777

16. Zhou Y, Wang L, Huang M, Ding J, Jiang H, Zhou K, et al. A long-term retrospective study of patients with biopsy-proven cryptogenic organizing pneumonia. *Chron Respir Dis.* (2019) 16:1479973119853829. doi: 10.1177/1479973119853829

17. Drakopanagiotakis F, Paschalaki K, Abu-Hijleh M, Aswad B, Karagianidis N, Kastanakis E, et al. Cryptogenic and secondary organizing pneumonia: clinical presentation, radiographic findings, treatment response, and prognosis. *Chest.* (2011) 139:893–900. doi: 10.1378/chest.10-0883

18. Radzikowska E, Wiatr E, Langfort R, Bestry I, Skoczylas A, Szczepulska-Wójcik E, et al. Cryptogenic organizing pneumonia-results of treatment with clarithromycin versus corticosteroids-observational study. *PLoS ONE.* (2017) 12:e0184739. doi: 10.1371/journal.pone.0184739

19. Rimpa T, Katsenos S, Akrivaki A, Fakas N, Psathakis K. Organizing pneumonia associated with optic neuromyelitis: coincidental occurrence or causal association? *Pulmonology.* (2021) 27:572–4. doi: 10.1016/j.pulmoe.2021.02.007

20. Furube A, Kadota T, Gochi M, Saito S, Shibata S, Inaki S, et al. Clinical features of organizing pneumonia in anti-aquaporin-4 antibody-positive neuromyelitis optica spectrum disorders. *Respir Investig.* (2022) 60:684–93. doi: 10.1016/j.resinv.2022.06.008

frontiers | Frontiers in Neurology

TYPE Case Report
PUBLISHED 21 November 2023
DOI 10.3389/fneur.2023.1283874

OPEN ACCESS

EDITED BY
Angelo Schenone,
University of Genoa, Italy

REVIEWED BY
Deepak Menon,
National Institute of Mental Health and Neurosciences (NIMHANS), India
Akira Machida,
Tsuchiura Kyodo General Hospital, Japan

*CORRESPONDENCE
Yuzhou Guan
✉ pumc_huangyy@student.pumc.edu.cn

RECEIVED 27 August 2023
ACCEPTED 30 October 2023
PUBLISHED 21 November 2023

CITATION
Shi J, Niu J, Wu D, Zhang L, Huang Y, Zhang H, Guan H, Liu M and Guan Y (2023) Case report: Mononeuropathy multiplex of extranodal natural killer/T-cell lymphoma misdiagnosed as systemic vasculitis. *Front. Neurol.* 14:1283874. doi: 10.3389/fneur.2023.1283874

Case report: Mononeuropathy multiplex of extranodal natural killer/T-cell lymphoma misdiagnosed as systemic vasculitis

Jiayu Shi[1], Jingwen Niu[1], Di Wu[2], Lei Zhang[1], Yangyu Huang[1], Hui Zhang[3], Hongzhi Guan[1], Mingsheng Liu[1] and Yuzhou Guan[1]*

[1]Neurology Department, Peking Union Medical College Hospital, Chinese Academy of Medical Sciences, Beijing, China, [2]Rheumatology and Immunology Department, Peking Union Medical College Hospital, Chinese Academy of Medical Sciences, Beijing, China, [3]Pathology Department, Peking Union Medical College Hospital, Chinese Academy of Medical Sciences, Beijing, China

Background: Extranodal NK/T-cell lymphoma (ENKTL) is an aggressive non-Hodgkin lymphoma that typically develops in the upper aerodigestive tract.

Case presentation: We encountered an ENKTL patient who presented with purpura-like rashes and foot drops as initial symptoms and later developed other peripheral nerve involvement. The nerve conduction study of both the motor nerve and the sensory nerve showed axonal damage resembling mononeuropathy multiplex. Although the initial response to steroids was encouraging, the patient's symptoms reappeared and aggravated. A biopsy of the abdominal subcutaneous fat tissue with additional immunohistochemistry revealed neoplastic NK/T lymphocytes.

Conclusion: We reported the first case presented as mononeuropathy multiplex as the initial clinical manifestation in ENKTL patients. Lymphoma should be considered in the diagnosis of atypical mononeuropathy in multiplex patients.

KEYWORDS

mononeuropathy multiplex, extranodal NK/T-cell lymphoma, axonal neuropathy, immunohistochemistry, biopsy

Background

Extranodal NK/T-cell lymphoma (ENKTL) is an aggressive non-Hodgkin lymphoma (NHL) that most frequently occurs in East Asia and Latin America (1, 2). ENKTL usually arises in the nasal cavity, but extra-nasal sites are sometimes involved, including the skin, soft tissue, and gastrointestinal tract (3). Extra-nasal site involvement might cause infrequent manifestations. The morphology and immunohistochemical characteristics of neoplastic cells are various. Since the clinical and pathological variability of ENKTL can sometimes be misleading, the correct diagnosis of patients might be delayed. ENKTL is scarcely relevant to PNS manifestations. We here report a case of ENKTL, which first manifested as mononeuropathy multiplex mimicking systemic vasculitis and gradually developed polyneuropathy.

Case presentation

An 18-year-old previously healthy female experienced bilateral purpura-like rashes on both calves 9 months before admission. The details of the subsequent clinical course are outlined in timeline form in Figure 1. After 1 month, she developed a sudden right-foot drop and steppage gait. On month 4, she noticed numbness on the ulnar side of her right hand with an intermittent fever of 39°C. She was admitted to a local hospital, and an abnormal full blood count was found (WBC 1.30–2.9×10^9/L, Hgb 91–95 g/L, PLT 175–238×10^9/L). ESR was elevated to 64–94 mm/h. Serum immunoglobulin G (IgG) was 37.62 g/L. Autoimmune antibodies provided a positive result for PR3-anti-neutrophil cytoplasmic antibody (ANCA). Urine routine, liver and kidney function, serum Epstein–Barr virus (EBV), and cytomegalovirus (CMV) DNA, high-sensitive C-reactive protein (hsCRP), serum immunofixation electrophoresis, bone marrow biopsy, bone marrow pathology, and bone marrow flow cytometry analysis showed no abnormality. Nerve conduction studies were conducted, and the results are shown in Supplementary Table 1. Cranial, cervical, and thoracic vertebrae magnetic resonance imaging (MRI) showed no obvious abnormality. She was then treated with antibiotics, and her fever was relieved, but in month 5, she gradually developed symptoms of bilateral pain in both hands and feet, which disturbed her daily life. She was diagnosed with systemic vasculitis and was referred to the Department of Rheumatology and Immunology for further diagnosis. Serum tests showed PR3-ANCA at 60 RU/ml titer and anti-nuclear antibody (ANA) S1:160(+). She was diagnosed with connective tissue disease and was treated with methylprednisolone (MP) 1 g intravenously for 3 days, followed by 48 mg prednisone orally. She was also treated with cytoxan (CTX) 1 g intravenously. After treatment, her symptoms of hand and foot pain were relieved dramatically, but limb weakness and numbness did not change. On month 7, hand and foot pain re-appeared to a severe extent, and she developed a sudden left-foot drop. She gradually lost the strength of her left hand, and on month 9, she was unable to hold a spoon or lift her both wrists. She was treated with MP 1 g×3 days, CTX 1 g once, and intravenous immunoglobulins (IVIg) at 0.4 g/kg×10 days, but her symptoms did not relieve. On month 9, muscle atrophy could be observed on both of her hands, forearms, and calves. Before 1 week of admission, she developed signs of left peripheral facial palsy. She was admitted to our hospital 9 months after the disease onset.

Physical examinations at admission showed a few old eruption stains on both calves, but no fresh rashes could be observed. Nervous system physical examinations showed signs of left peripheral facial palsy. Tendon reflexes were absent. The muscle atrophy of the thenar and interosseous muscles of both hands could be observed. The proximal muscle strength of the right upper limb is grade IV, while the left upper limb is grade III. The strength of the distal muscles of the upper limbs was grades I–II. The proximal muscle strength of both lower limbs is grade V, and the muscle strength of the dorsum of the foot is grades I–II. The muscle tension was normal. The Romberg sign was positive. The sensation of acupuncture and vibration decreased in a sock-like and glove-like fashion in both upper and lower limbs.

The work-up, including serum tests, cerebral-spinal fluid (CSF) examinations, positron emission tomography-computer tomography (PET-CT), and electrodiagnostic tests, was conducted after admission. Serum tests for EBV DNA showed a positive result with a copy number varying from 500 to 2,400/ml. Serum tests for IgG and IgM of HBV, HCV, HIV, RPR, TPPA, CMV, Lyme, and brucellosis were all negative. Serum tests of ANA, ANCA, and anti-C1q were negative. Serum and CSF anti-GM1, anti-GQ1b, anti-Hu, anti-Yo, anti-Ri, anti-α-amino-3-hydroxy-5-methyl-4-isoxazole-propionicacid (AMPA), anti-CV2, anti-γ-aminobutyric acid (GABA), anti-Amphiphysin, anti-contactin-associated protein 2 (CASPR2), and anti-leucine-rich glioma-inactivated 1 (LGI1) were all negative. The serum levels of interleukin (IL) 10 and tumor necrosis factor (TNF) α were elevated at 16.4 and 28.5 pg/ml. The CSF results showed a slightly elevated protein level of 52–54 mg/dL, and the cell count was 32–34 cells/μl. Oligoclonal bands were negative in CSF. Cells in CSF were mostly lymphocytes, and no atypical cell was observed. Next-generation sequencing (NGS) for pathogens in CSF proved to be positive for EBV with a copy number of 2,564. The CSF levels of IL6, IL8, and IL10 were all elevated at 18.3, 222, and 15.4 pg/ml, respectively. CSF flow cytometry was negative. PET-CT gave a very interesting finding of hypermetabolism in the subcutaneous fat tissue all over the body with a slightly elevated standard uptake value (SUV) maximum of 1.6 (Figure 2). PET-CT also showed a soft tissue signal with a SUVmax of 3.3 in the bilateral nasal meatus. Nerve conduction study results are shown in Supplementary Table 1. Electromyogram (EMG) results showed an enormous amount of positive sharp waves and fibrillation discharges in the left deltoideus muscle and left tibialis anterior muscle. Nerve ultrasound was conducted and revealed an unremarkable cross-sectional area (CSA) enlargement in bilateral median, posterior tibial, and peroneal nerves.

Pathological tests of both abdominal subcutaneous fat tissue and left nasal meatus soft tissue were conducted subsequently. The histologic study of abdominal subcutaneous fat tissue revealed many distended vessels filled with atypically large lymphoid cells, causing vessel occlusion. The tumor cells had large, irregular hyperchromatic nuclei and ample eosinophilic cytoplasm that was not only confined to the vessels but also disseminated in the fat tissue. Immunohistochemical staining showed the cluster of differentiation (CD)21(–), CD138(–), CD34(around vessels+),

Abbreviations: ENKTL, extranodal NK/T-cell lymphoma, NHL, non-Hodgkin's lymphoma, Ig, immunoglobulin, ANCA, anti-neutrophil cytoplasmic antibody, EBV, Epstein–Barr virus, CMV, cytomegalovirus, hsCRP, high-sensitive C-reactive-protein, MRI, magnetic resonance imaging, ANA, anti-nuclear antibody, MP, methylprednisolone, CTX, cytoxan, IVIg, intravenous immunoglobulins, CSF, cerebro-spinal fluid, PET-CT, positron emission tomography-computer tomography, AMPA, α-amino-3-hydroxy-5-methyl-4-isoxazole-propionicacid, GABA, γ-aminobutyric acid, CASPR2, contactin-associated protein 2, LGI1, leucine-rich glioma-inactivated 1, NGS, next-generation sequencing, SUV, standard uptake value, EMG, electromyogram, CSA, cross-sectional area, CD, cluster of differentiation, TIA, cytotoxic granule associated protein, EBER, EBV-encoded RNA, DXM, dexamethasone, MTX, methotrexate, VP16, vepeside, Iv, intravenously, HL Hodgkin's lymphoma.

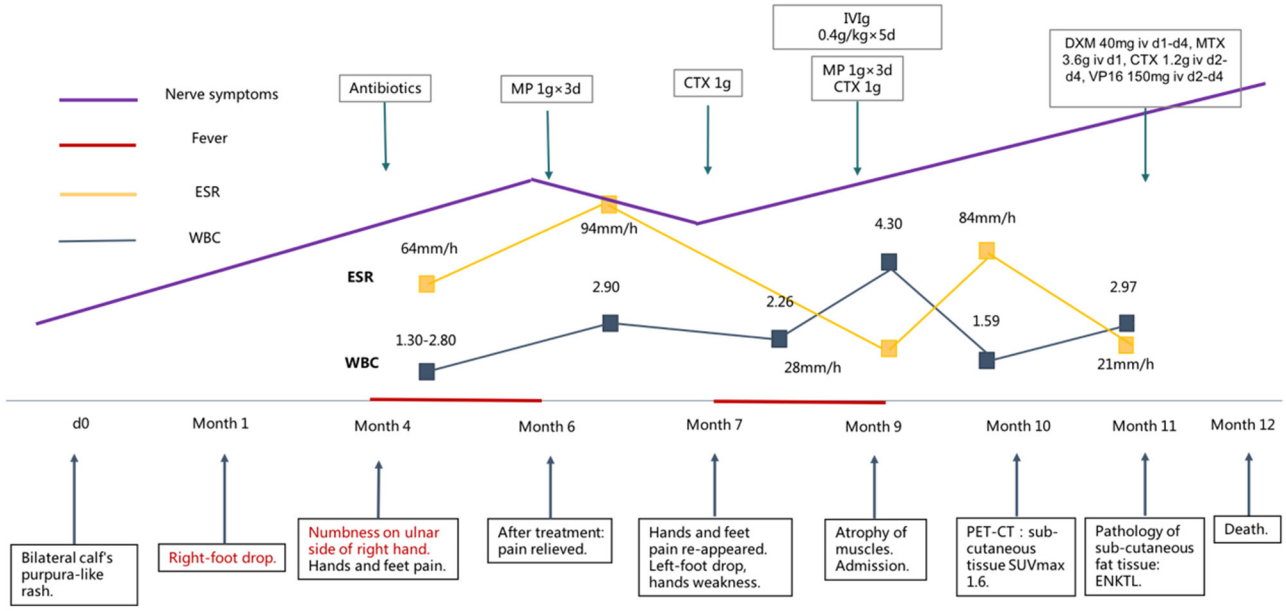

FIGURE 1
Clinical and therapeutic course of the patient. ENKTL, extranodal NK/T-cell lymphoma, MP, methylprednisolone, CTX, cytoxan, IVIg, intravenous immunoglobulins, DXM, dexamethasone, MTX, methotrexate, VP16, vepeside, PET-CT, positron emission tomography/computed tomography.

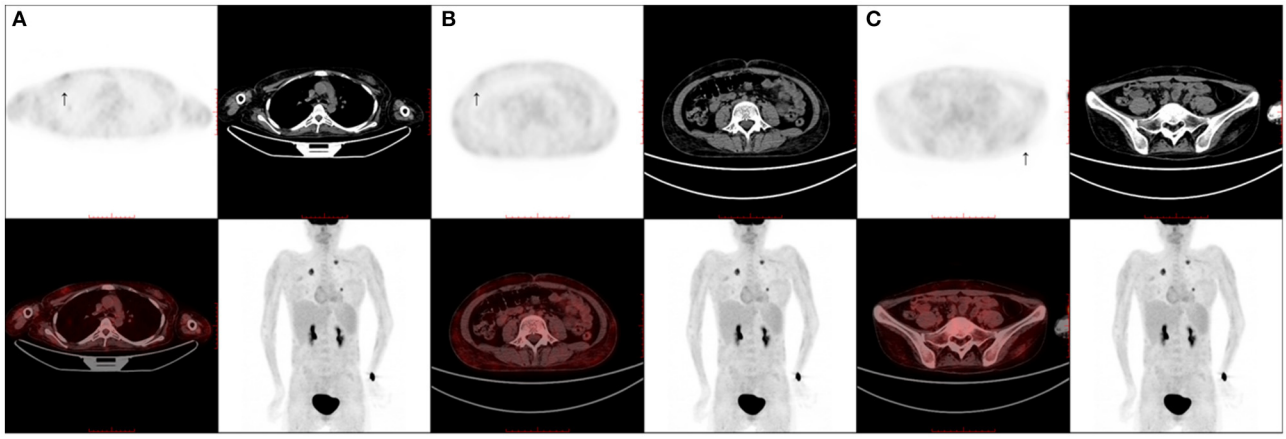

FIGURE 2
Positron emission tomography/computed tomography scans. A positron emission tomography/computed tomography scan shows multiple slightly fluorodeoxyglucose-avid subcutaneous fat tissue lesions scattered throughout the body (SUVmax of 1.6). **(A)** Thoracic wall (arrow); **(B)** abdominal wall (arrow); **(C)** pelvic wall (arrow).

CD20(+), CD3(+), Ki-67(index 80%), CD56(−), CD5(+), CD7(-), CD2(+), CD4(+), CD38(+), granzyme B(+), TIA-1(+), and EBER (+), which consisted of the diagnosis of ENKTL (Figure 3). The left nasal meatus soft tissue showed a microscopic finding of pseudostratified ciliated columnar epithelium infiltrated by lymphocytes and plasma cells, which was regarded as an EBV-related T-cell proliferative disease. The patient was diagnosed as ENKTL, staging IVb.

The patient was then treated with a classic scheme for ENKTL, including dexamethasone (DXM) 40 mg iv d1-d4, methotrexate (MTX) 3.6 g iv d1, cytoxan (CTX) 1.2 g iv d2-d4, vepeside (VP16) 150 mg iv d2-d4, after which her nervous system symptoms showed no improvement. The patient developed septic shock and digestive tract hemorrhage and succumbed to the disease 12 months after its disease onset.

Discussion and conclusion

Lymphomas are hematopoietic neoplasms originating from immunocompetent cells. They are divided into the NHL and HL (1). HL and NHL both infrequently cause peripheral nervous system complications, with NHL a much more common cause. In a case series, 98% of lymphoma patients with peripheral nerve system

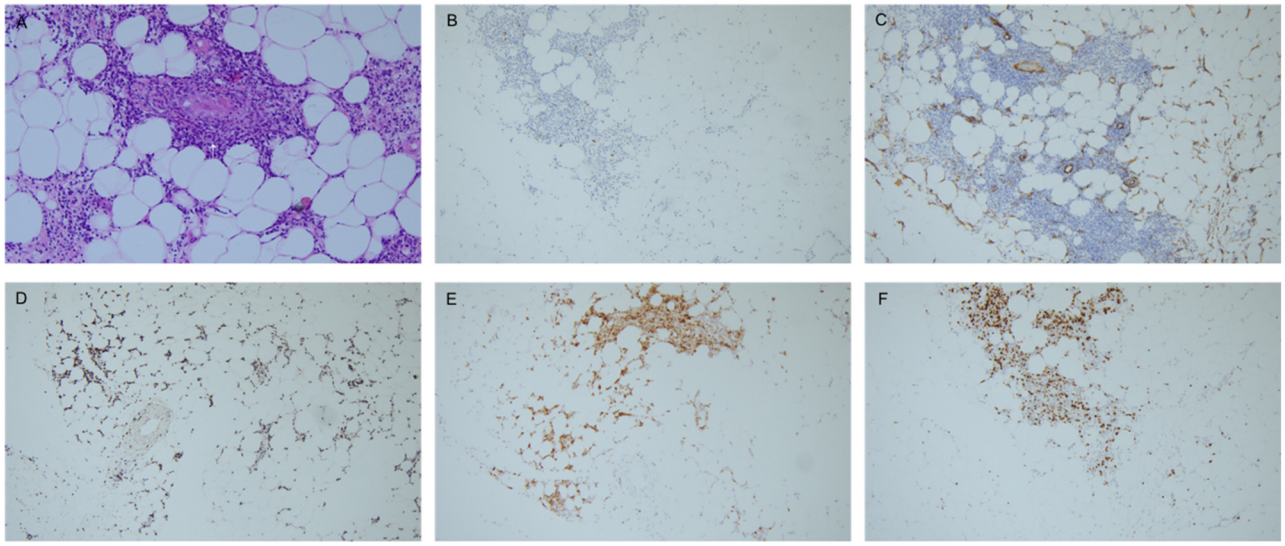

FIGURE 3
Immunohistochemical staining. **(A)** Histological findings of the subcutaneous fat tissue (hematoxylin-eosin: **A**, × 200), showing distended vessels filled with atypically large lymphoid cells, causing vessel occlusion (arrow). Infiltration of atypical lymphoid cells could also be observed in the subcutaneous fat tissue. **(B–E)** Immunohistochemical staining was positive for CD20 (**B**, × 100), CD34 (**C**, ×100), EBER (**D**, ×100), granzyme B (**E**, ×100). F: Ki-67 index 80% (**F**, ×100). Pathological figures are provided by the Pathology Department, Peking Union Medical College Hospital.

complications had NHL (2, 3). Most are B-cell NHL, with T-cell NHL accounting for only approximately 10% (2). The mechanisms of nerve damage caused by lymphoma are usually not clear, but several hypotheses have been proposed. First, direct invasion of lymphoma cells into the PNS, known as neurolymphomatosis is the most common cause of PNS system involvement (1, 4). Malignant lymphocytes that react with the antibody of a neural cell adhesion molecule, including CD56, may adhere to neural cell adhesion molecules, which allow the passage of certain classes of lymphocytes across the blood–nerve barrier, causing neurolymphomatosis (5). Most infiltrative neuropathies in humans are due to B-cell lymphoma, but peripheral T-cell lymphoma has also been reported to cause infiltrative neuropathies (1, 6). This phenomenon may cause unusual sites of involvement in lymphoma. Second, inflammatory, dys-immune neuropathies such as GBS, CIDP, or vasculitic neuropathy can occur in lymphoma due to the accompanying or preexisting immune perturbation, also known as paraneoplastic neuropathy (4, 7). These disorders are more commonly reported with HL than NHL. Third, hematogenous metastases can occlude vessels by local intravascular proliferation or direct pressure (8). Angiotrophic lymphoma, characterized by neoplastic lymphoid cells and immune-complex deposition within the walls of the vasa nervorum, could lead to vessel occlusion and cause nerve infarction (9).

ENKTL is most common in Asia and Central and South America and affects adults with a male predominance. It classically arises in the nasal cavity, the paranasal sinuses, or the palate and is associated with EBV infection but can also be observed in 15–20% of other sites such as the skin (60%), sub-cutaneous tissue, gastro-intestinal tract, testis, and even pancreas, without nasal localization (10). ENKTL is scarcely related to peripheral nervous system complications, based on our review of the English literature (Table 1), and only six cases of ENKTL invasion of peripheral nerves have been reported. All cases reported are women, and the age range is from 17 to 70 years. Most cases' clinical presentation is mononeuropathy, presented as tumor infiltration of a single nerve, including the median nerve, ulnar nerve, and tibial nerve (5, 11, 12). In addition to our case, two other cases presented as polyneuropathy (13, 14). One case, reported by Tian et al., (13) also presented with rashes before nervous system involvement. In another case, because of nerve root enlargement, AIDP was diagnosed in the first place (14).

Back to our case, it is a pity that the patients' parents refused a nerve biopsy, worrying about the deterioration of nerve function caused by the procedure. As a nerve biopsy was not obtainable, the mechanism of patient PNS involvement could only be hypothesized. We conducted nerve ultrasonography to directly observe the CSA of involved nerves, showing no obvious CSA enlargement that does not support neurolymphomatosis (15). From the abdominal subcutaneous fat tissue biopsy, we could observe vessel occlusions and vessel wall thickening (Figure 3A, arrow), which pathologically support the hypothesis of nerve infarction caused by vessel occlusions. Additionally, the patient's tumor cells expressed the antibody CD34 (Figure 3C), which is reactive to the vascular endothelial cell marker, leading to tumor cells propensity to attach to vessel walls (16). In contrast with typical ENKTL, the immunohistochemical result of our case is relatively rare since CD56 was negative while CD20 was positive. Although CD56 is an important clue to diagnose NK/T cell lymphoma and is believed to be a marker for ENKTL, it has been infrequently reported to be negative in some cases, especially in cases with uncommon clinical manifestations (17). ENKTL with aberrant CD20 expression is extremely rare. To the best of our knowledge, there have only been 11 CD20-positive ENKTLs

TABLE 1 Clinical characteristics of patients with ENKTCL-NT combined with peripheral neuropathy.

References	Year	Age/sex	Neuropathy manifestation	Primary site of ENKTL	Primary diagnosis	Prognosis
Kim et al. (5)	1998	70/F	Mononeuropathy, median nerve	NR	NR	Survival
Wills et al. (14)	2008	29/F	Lumbar nerve roots	Lumbar nerve roots	AIDP	Survival
Agrawal et al. (11)	2013	57/F	Mononeuropathy, ulnar nerve	Nasal cavity	ENKTL	Survival
Aynardi et al. (12)	2018	59/F	Mononeuropathy, tibial nerve	Nasal cavity	ENKTL	Survival
Tian et al. (13)	2023	17/F	Polyneuropathy	Skin	Granuloma annulare	Survival
Our case	2023	18/F	Mononeuropathy multiplex	Skin	Vasculitis	Death

NR, not recorded.

reported. ENKTL with aberrant CD20 expression primarily occurred at extra-nasal sites rather than in the nasal cavity, including the testis, skin, and soft tissue, with a relatively aggressive clinical course, which is in accordance with our case (18). The rare immunohistochemistry of our case could help to explain infrequent clinical symptoms and the site of tumor origin. The patient's original diagnosis was systematic vasculitis, which was based on the result of a positive PR3 ANCA in the former hospital. The false-positive result of auto-antibody is not uncommon in lymphoma patients due to cross-immune reactions (13) and could be misleading in these patients' diagnoses.

In conclusion, we reported that the first case manifested as mononeuropathy multiplex and was diagnosed as ENKTL. Patients with lymphoma can manifest various neuropathic patterns. Although an infrequent clinical manifestation, lymphoma should never be overlooked in patients with neuropathy of various forms, especially those with mononeuropathy multiplex. It is possible that mononeuropathy multiplex is misdiagnosed as systematic angiitis since the clinical course could be similar and show the presence of signs of an axonal neuropathy pattern. ENKTL is extremely rare to show PNS symptoms, and its mechanism of neuropathy is still not established, requiring further research.

Data availability statement

The raw data supporting the conclusions of this article will be made available by the authors, without undue reservation.

Ethics statement

The studies involving humans were approved by Peking Union Medical College Hospital. The studies were conducted in accordance with the local legislation and institutional requirements. The human samples used in this study were acquired from a by-product of routine care or industry. Written informed consent for participation was not required from the participants or the participants' legal guardians/next of kin in accordance with the national legislation and institutional requirements. Written informed consent was obtained from the individual(s) for the publication of any potentially identifiable images or data included in this article.

Author contributions

JS: Writing—original draft, Writing—review & editing, Conceptualization, Methodology, Supervision. JN: Conceptualization, Methodology, Writing—review & editing. DW: Conceptualization, Investigation, Supervision, Writing—review & editing. LZ: Methodology, Writing—review & editing. YH: Data curation, Methodology, Writing—review & editing. HZ: Methodology, Writing—review & editing. HG: Conceptualization, Supervision, Writing—review & editing. ML: Methodology, Supervision, Writing—review & editing. YG: Conceptualization, Methodology, Supervision, Writing—review & editing.

Funding

The author(s) declare that financial support was received for the research, authorship, and/or publication of this article. The research was supported by National High Level Hospital Clinical Research Funding (2022-PUMCH-B-017).

Conflict of interest

The authors declare that the research was conducted in the absence of any commercial or financial relationships that could be construed as a potential conflict of interest.

Publisher's note

Supplementary material

The Supplementary Material for this article can be found online at: https://www.frontiersin.org/articles/10.3389/fneur.2023.1283874/full#supplementary-material

References

1. Kelly JJ, Karcher DS. Lymphoma and peripheral neuropathy: a clinical review. *Muscle Nerve*. (2005) 31:301–13. doi: 10.1002/mus.20163

2. Giglio P, Gilbert MR. Neurologic complications of non-Hodgkin's lymphoma. *Curr Oncol Rep*. (2005) 7:61–5. doi: 10.1007/s11912-005-0027-8

3. Diaz-Arrastia R, Younger DS, Hair L, Inghirami G, Hays AP, Knowles DM, et al. Neurolymphomatosis: a clinicopathologic syndrome re-emerges. *Neurology*. (1992) 42:1136–41. doi: 10.1212/wnl.42.6.1136

4. Tomita M, Koike H, Kawagashira Y, Iijima M, Adachi H, Taguchi J, et al. Clinicopathological features of neuropathy associated with lymphoma. *Brain*. (2013) 136(Pt 8):2563–78. doi: 10.1093/brain/awt193

5. Kim J, Kim YS, Lee EJ, Kang CS, Shim SI. Primary CD56-positive NK/T-cell lymphoma of median nerve: a case report. *J Korean Med Sci*. (1998) 13:331–3. doi: 10.3346/jkms.1998.13.3.331

6. Kern WF, Spier CM, Hanneman EH, Miller TP, Matzner M, Grogan TM. Neural cell adhesion molecule-positive peripheral T-cell lymphoma: a rare variant with a propensity for unusual sites of involvement. *Blood*. (1992) 79:2432–7.

7. Kuchukhidze G, Helbok R, Unterberger I, Koppelstaetter F, Bodner T, Trinka E. Bilateral mesial temporal polymicrogyria: a case report. *J Neurol Neurosurg Psychiatry*. (2008) 79:483–4. doi: 10.1136/jnnp.2007.138792

8. Vital C, Vital A, Julien J, Rivel J, deMascarel A, Vergier B, et al. Peripheral neuropathies and lymphoma without monoclonal gammopathy: a new classification. *J Neurol*. (1990) 237:177–85. doi: 10.1007/bf00314591

9. Lynch KM, Katz JD, Weinberg DH, Lin DI, Folkerth RD. Isolated mononeuropathy multiplex–a rare manifestation of intravascular large B-cell lymphoma. *J Clin Neuromuscul Dis*. (2012) 14:17–20. doi: 10.1097/CND.0b013e318262ab5c

10. Dotlic S, Ponzoni M, King RL, Oschlies I, Ferry J, Calaminici M, et al. The broad and challenging landscape of extranodal lymphoproliferations. *Virchows Arch*. (2020) 476:633–46. doi: 10.1007/s00428-019-02702-w

11. Agrawal S, Gi MT, Ng SB, Puhaindran ME, Singhania P. MRI and PET-CT in the diagnosis and follow-up of a lymphoma case with multifocal peripheral nerve involvement. *Diagn Interv Radiol*. (2013) 19:25–8. doi: 10.4261/1305-3825.DIR.5876-12.1

12. Aynardi M, Raikin SM. Recurrence of extranodal natural killer/T-cell lymphoma presenting as tarsal tunnel syndrome. *Am J Orthop*. (2018) 47. doi: 10.12788/ajo.2018.0025

13. Tian Z, Tian J, Liao J. NK/T-cell lymphoma with rash and peripheral neuropathy as the first manifestation: a case report and literature review. *Diagn Pathol*. (2023) 18:2. doi: 10.1186/s13000-023-01286-z

14. Wills AJ, O'Connor S, McMillan A. Sub-acute demyelinating neuropathy associated with an NK/T cell lymphoma. *J Neurol Neurosurg Psychiatry*. (2008) 790:484–5. doi: 10.1136/jnnp.2007.133694

15. Kerasnoudis A, Tsivgoulis G. Nerve ultrasound in peripheral neuropathies: a review. *J Neuroimaging*. (2015) 25:528–38. doi: 10.1111/jon.12261

16. Liu Y, Zhang W, An J, Li H, Liu S. Cutaneous intravascular natural killer-cell lymphoma: a case report and review of the literature. *Am J Clin Pathol*. (2014) 142:243–7. doi: 10.1309/AJCP1JLYXLGDNOCH

17. Liu LH, Huang Q, Liu YH, Yang J, Fu H, Jin L. Muscular involvement of extranodal natural killer/T cell lymphoma misdiagnosed as polymyositis: a case report and review of literature. *World J Clin Cases*. (2020) 8:963–70. doi: 10.12998/wjcc.v8.i5.963

18. Huang Y, Chen S, Wei R, Guo X, Yang X, Cao Q, et al. CD20-positive extranodal NK/T cell lymphoma: clinicopathologic and prognostic features. *Virchows Arch*. (2020) 477:873–83. doi: 10.1007/s00428-020-02776-x

frontiers | Frontiers in Neurology

TYPE Case Report
PUBLISHED 11 December 2023
DOI 10.3389/fneur.2023.1290960

OPEN ACCESS

EDITED BY
Giovanni Meola,
University of Milan, Italy

REVIEWED BY
Wladimir Bocca Vieira De Rezende Pinto,
Federal University of São Paulo, Brazil
Danielius Serapinas,
Lithuanian University of Health Sciences,
Lithuania

*CORRESPONDENCE
Greta Asadauskaitė
✉ greta.asadauskaite@mf.stud.vu.lt

RECEIVED 08 September 2023
ACCEPTED 17 November 2023
PUBLISHED 11 December 2023

CITATION
Asadauskaitė G, Vilimienė R, Augustinavičius V and Burnytė B (2023) Case report of a family with hereditary inclusion body myopathy with *VCP* gene variant and literature review.
Front. Neurol. 14:1290960.
doi: 10.3389/fneur.2023.1290960

Case report of a family with hereditary inclusion body myopathy with *VCP* gene variant and literature review

Greta Asadauskaitė[1]*, Ramunė Vilimienė[2], Vytautas Augustinavičius[3] and Birutė Burnytė[4]

[1]Faculty of Medicine, Vilnius University, Vilnius, Lithuania, [2]Faculty of Medicine, Institute of Clinical Medicine, Vilnius University, Vilnius, Lithuania, [3]Center of Radiology and Nuclear Medicine, Vilnius University Hospital Santaros Klinikos, Vilnius, Lithuania, [4]Faculty of Medicine, Institute of Biomedical Sciences, Vilnius University, Vilnius, Lithuania

Background: Missense *VCP* gene variants lead to a disruption in protein homeostasis causing a spectrum of progressive degenerative diseases. Myopathy is the most frequent manifestation characterized by slowly progressing weakness of proximal and distal limb muscles. We present a family with myopathy due to c.277C > T variant in *VCP* gene.

Case presentation: The patient's phenotype includes symmetrical muscle wasting and weakness in the proximal parts of the limbs and axial muscles, a wide based gait, lordotic posture, positive Gowers' sign, mild calf enlargement, impaired mobility, elevated CK, and myopathy in proximal limb muscles. Whole body MRI revealed fatty replacement, predominantly affecting right vastus intermedius and medialis, gastrocnemius and soleus in calf, abdomen wall and lumbar muscles. Next-generation sequencing analysis revealed a pathogenic heterozygous variant c.277C > T (p.(Arg93Cys)) in exon 3 of the *VCP* gene. Segregation analysis showed that the detected variant is inherited from the affected father who developed symptoms at 60.

Conclusion: The patients described experienced muscle wasting and weakness in the proximal and distal parts of the limbs which is a common finding in VCP related disease. Nevertheless, the patient has distinguishing features, such as high CK levels, early onset of the disease, and rapid mobility decline.

KEYWORDS

VCP gene, VCP related disease, inclusion body myopathy, multisystem proteinopathy, degenerative disease

1 Introduction

Valosin-containing protein (VCP) related disease is a rare, autosomal dominant, multisystem proteinopathy characterized by inclusion body myopathy (IBM), Paget disease of bone (PDB) and frontotemporal dementia (FTD), affecting around 90%, 28–42%, and 14–30% of patients accordingly (1, 2). Other manifestations include amyotrophic lateral sclerosis (ALS), Alzheimer's disease, Parkinson's disease, Charcot–Marie-Tooth type 2 disease and complex hereditary spastic paraplegia (3–6).

VCP related disease has been associated with heterozygous missense variants in *VCP* gene. VCP belongs to the ATPases associated with diverse cellular Activities (AAA+) family, which uses ATP for protein remodeling. Each subunit contains N-terminal binding domain and two ATPase domains, D1 and D2 (7, 8). VCP is involved in a variety of cellular activities such as cell cycle control, organelle biogenesis and elimination, cellular signaling, membrane fusion, transcription, regulation of autophagy and protein degradation (8, 9). Missense variants at the NTD-D1 interface of the VCP are thought to cause a disruption in protein homeostasis causing a spectrum of progressive degenerative diseases (7, 10, 11).

In this paper we report patient and his father with c.277C > T [p.(Arg93Cys)] variant in *VCP* gene, presenting with IBM. Patient's and his father's phenotype is compared with phenotypes reported in literature.

2 Case description

Proband is a 49-year-old male. At the age of 38, the patient reported difficulties in standing-up from a sitting position. Symptoms showed a slow but progressive worsening. He noticed upper and lower limb weakness and difficulty in daily activities such as carrying a child and stumbling. At the age of 49, the patient had difficulties in walking unaided, climbing up the stairs, and standing up from sitting and lying positions (Table 1).

Neurological examination at the age of 46 revealed symmetric atrophy and weakness of limb proximal muscle. Shoulder abduction and adduction were 4/5 grades (MRC-scale) on both sides. Elbow flexion and extension 4/5 bilaterally. Wrist and fingers flexion and extension were normal. Hip flexion was 3/5, hip extension - 4/5 bilaterally. Knee flexion and extension were 3/5 grades bilaterally. Ankle plantar flexion was 4/5 and dorsiflexion - 4/5 on both sides. We observed weakness of axial muscles predominantly affecting the paraspinal and abdominal muscles. The patient showed a wide based gait with a lordotic posture. Positive Gowers' sign and mild enlargement of the calves was also noted. Tendon reflexes, sensory examination, and cranial nerve examination were normal. Cognitive testing did not reveal any frontal lobe and other cognitive abnormalities. During 4 years of follow up the muscle weakness slowly progressed. We noticed the muscle strength deterioration in the distal parts of the upper limbs. A slight asymmetry of muscle strength appeared with the right limbs being more affected. The patient can walk unaided a few meters and uses walking sticks most of the time. We did not find any cognitive deterioration. A nerve conduction study at the age of 46 did not show any abnormalities. Needle electromyography revealed myopathic changes without spontaneous activity. The myopathic pattern was more prominent in the proximal parts of the limbs. His creatine kinase (CK) level at the age of 46 was 1,237 U/L (reference range: 25–195 U/L), it increased to 1,309 U/L after a year. Whole body bone scintigraphy showed no abnormalities characteristic of Paget's disease.

Whole body MRI showed fatty replacement, predominantly affecting right vastus intermedius and medialis, gastrocnemius and soleus in calf, abdomen wall and lumbar muscles (Figure 1).

Family history revealed a similar phenotype of the patient's father and paternal uncle. The uncle had difficulty walking and experienced muscle weakness from the age of 40, however he died at 59.

The patient's father is a 73-year-old male. At the age of 60, he started to struggle climbing stairs, and he suffered from frequent falls. At the age of 68, he had difficulty walking and started using crutches. He also has difficulty standing up from sitting and lying positions. ENMG examination revealed signs of partial axonal degeneration of the motor nerves in the lower limbs. Myopathic patterns were recorded in all muscles of the lower limbs (especially the quadriceps femoris) and the proximal muscles of the upper limbs. His CK level was 119 U/L.

Next-generation sequencing analysis of the proband revealed a previously reported pathogenic heterozygous variant NM_007126.5:c.277C > T (NP_009057.1:p.(Arg93Cys)) in exon 3 of the *VCP* gene. Based on the guidelines of ACMG/AMP for interpretation of sequence variants, it is classified as pathogenic (categories: PP5, PP3, PM1, PM5, and PM2) (12). Segregation analysis showed that the detected variant is inherited from the affected father. The detailed sequencing and analysis methods have previously been described (13).

TABLE 1 Patients' timelines.

Proband					
Onset of symptoms	Neurological examination: symmetrical muscle wasting of proximal parts of the limbs	CK 1237 U/L	Whole body bone scintigraphy showed no abnormalities	CK 1309 U/L	Progression of muscle weakness, impaired mobility
38 y.o	46 y.o			47 y.o	49 y.o
Proband's paternal uncle					
Onset of symptoms			Died (suddenly)		
40 y.o			59 y.o		
Proband's father					
Onset of symptoms	Started using crutches		CK 119 U/L	Whole body bone scintigraphy showed no abnormalities	
60 y.o	68 y.o		69 y.o	70 y.o	

CK, creatine kinase.

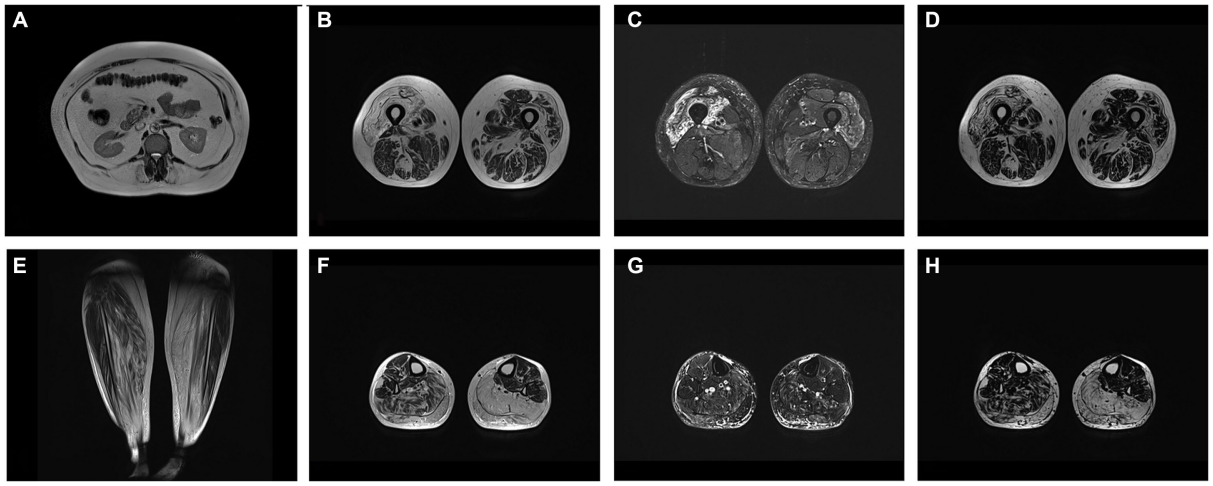

FIGURE 1
(A) T2W axial image at level of L1 showing fatty replacement of abdominal wall and lumbar muscles. Axial at level of middle third of femur T2W **(B)**, T2 DIXON WATER **(C)** and FAT **(D)** images showing mm. vastus intermedius and medialis edema with fatty replacement. Coronal T2W **(E)**, axial at level of proximal third of calf T2W **(F)**, T2 DIXON WATER **(G)** and FAT **(H)** images showing fatty replacement of muscle in mm. soleus and gastrocnemius (more prominent on left side).

3 Discussion

Myopathy is the most frequent manifestation of VCP related disease affecting around 90% of patients with pathogenic variants in *VCP* gene (1, 2). It is characterized by slowly progressing weakness and atrophy of proximal and distal upper and lower limb muscles, initially involving shoulder and pelvic muscles (1, 2, 14). Some of the other symptoms include axial muscle weakness, scapular winging, respiratory impairment, lower motor neuron sings, dysautonomia, dysphagia (1). Patients often have abnormal gait, lordotic stance, experience difficulty climbing stairs, raising arms (14, 15). Our patient presented with typical symptoms: weakness of proximal and distal limbs, atrophied shoulder and pelvic girdle muscles, wide based gait, lordotic posture. Both the patient and his father experienced difficulties in daily activities such as climbing up the stairs, standing up from a sitting position. However, the patient's father is unable to move around without the crutches showing the progression of the disease.

An electromyographic (EMG) examination showed a myopathic pattern mainly in patient's proximal limb muscles and in all leg muscles and proximal arm muscles in patient's father. Myopathic pattern in EMG is characteristic of IBM. Purely myopathic pattern is observed in 31–47% of patients in literature. 11–21% of patients have neurogenic and 14–20% mixed myopathic and neurogenic pattern (1, 3). The patient's father showed signs of partial axonal degeneration of the motor nerves in the legs. Motor neuron involvement was reported in 25% of patients in Schiava et al. cohort. Of those, almost a half showed exclusively lower motor neuron signs (1).

It is worth mentioning that while patients with VCP related myopathy usually exhibit normal or slightly increased CK levels (2–4), the CK levels of our proband are higher than what is typically observed. However, there have been some reported cases of elevated CK levels in individuals with certain *VCP* gene variants, such as homozygous p.Arg159His variant with early disease onset at 29 years (16), or the newly described case of a heterozygous variant of c.760A > T with CK levels >2,378 (17). The patient's relatively early age of disease onset and the aggressive progression of their symptoms are also noteworthy. While the mean age of symptoms onset for VCP related disease is around 43 years (2, 3), there can be a significant variation depending on the specific variant and other factors. Patients with heterozygous c.277C > T variant experience first symptoms later than our patient (1). Similarly, patient's uncle had difficulty walking at the age of 40. In comparison, patient's father experienced the onset of symptoms at the age of 60, which has been observed in several cases with c.277C > T variant (18, 19). As a result, the combination of early onset and high CK levels might suggest a more severe form of the disease in this patient.

Human Gene Mutation Database (HGMD) reports 71 variants of *VCP* gene, 66 of those are missense/nonsense (20). In Varsome database 89 of the reported *VCP* gene variants were identified as pathogenic or likely pathogenic (21). Although genotype–phenotype correlations are not yet well defined a few studies have identified some correlations between phenotype and specific variants (2, 3). In Schiava et al. study variant c.277C > T was associated with older age of disease onset compared to c.464G > A. Median age for c.277C > T variant was 52.3 ± 5.6 years (1). Table 2 summarizes clinical findings of reported patients with c.277C > T. Of the reported cases in literature with c.277C > T variant, the lowest age of symptom manifestation was 42 years (23). In the reported cases with c.277C > T variant, most patients have myopathy together with FTD or PDB. In comparison, only one case was reported with all 3 manifestations of the disease and only one case where FTD was the only manifestation of the disease (19). CK in most of the reported cases was slightly above normal. Most reported patients did not lose ambulation, but some have difficulty moving (25, 26). Both proximal and distal muscles were affected in reported cases with c.277C > T variant (1).

As muscle weakness progresses, especially in the lower limbs, patients eventually lose ambulation. In Schiava et al. study after 8.5 years 23% of the patients were no longer ambulant (1). In Figueroa-Bonaparte et al. study mean time to lose ambulation was 13.37 ± 6.6 years (23). Over time muscle weakness involves respiratory

TABLE 2 Clinical findings of patients with c.277C > T variant of *VCP* gene found in literature.

Reference	*N*	Type	Age of onset	Age at follow up	CK (U/L)	ALP (IU/L)	Wheelchair use	Muscle weakness (onset)
Schiava et al. (1)	17	Muscle weakness – 94% FTD – 24% PDB – 44%	52.3 ± 5.6	64.2 ± 5.3	NA	NA	20%	Proximal UL 80%; Proximal LL 90%; Distal UL and LL 73%
Mengel et al. (22)	1	IBM + cognitive impairment	50	74	288	NA	NA	Distal > proximal
Figueroa-Bonaparte et al. (23)	1	IBM + cognitive impairment	42	56	400	high	No	Distal LL
	1	IBM + cognitive impairment	48	67	normal	normal	No	Distal LL > UL
Mehta et al. (3)	2	IBM + PDB IBM + FTD	60	NA	370	NA	NA	NA
Shi et al. (24)	1	IBM	58	70	286	NA	NA	Proximal>distal
Fanganiello et al. (25)	1	IBM + PDB	55	62	285–572	NA	No, has difficulties moving	Proximal>distal
Krause et al. (26)	1	IBM + FTD	55	74	115	154	No, requires assistance	Distal>proximal
Guyant- Maréchal et al. (19)	1	FTD	60	61	NA	NA	NA	Proximal and distal muscles, absent in muscles of face, tongue, and scapular fixators
	1	PBD + FTD	55	60	NA	NA	NA	
	1	IBM + PDB + FTD	48	68	NA	NA	NA	
	1	IBM + FTD	44	49	NA	NA	NA	
Present study proband	1	IBM	38	49	1,237–1,309	56	No, uses crutches	Proximal UL, proximal and distal LL
Present study affected father	1	IBM	60	69	92–119	87	No, uses crutches	Proximal UL, proximal and distal LL

N, number of patients; NA, not available; FTD, frontotemporal dementia; IBM, inclusion body myopathy; PDB, Paget disease of bone; CK, creatine kinase; ALP, alkaline phosphatase; UL, upper limb; LL, lower limb.

and cardiac muscles leading to death from respiratory or cardiac failure (1, 3). Schiava et al. identified forced vital capacity (FCV) below 50% as the major risk factor associated with loss of ambulation and FCV below 70% with higher risk of death (1). Patients usually die in their 60s 15–20 years after the onset of the disease (1, 3).

This study adds to previous evidence demonstrating a summary of clinical findings of reported patients with c.277C > T variant in *VCP* gene.

Data availability statement

The original contributions presented in the study are included in the article/supplementary material, further inquiries can be directed to the corresponding author.

Ethics statement

Written informed consent to participate in this study was not required from the participants or the participants' legal guardians/next of kin in accordance with the national legislation and the institutional requirements. Written informed consent was obtained from the individual(s) for the publication of any potentially identifiable images or data included in this article.

Author contributions

GA: Conceptualization, Writing – original draft. RV: Data curation, Writing – review & editing. VA: Data curation, Writing – review & editing. BB: Conceptualization, Data curation, Supervision, Writing – review & editing.

Funding

The author(s) declare that no financial support was received for the research, authorship, and/or publication of this article.

Acknowledgments

The authors would like to thank the patients for their collaboration.

Conflict of interest

The authors declare that the research was conducted in the absence of any commercial or financial relationships that could be construed as a potential conflict of interest.

Publisher's note

References

1. Schiava M, Ikenaga C, Villar-Quiles RN, Caballero-Ávila M, Topf A, Nishino I, et al. Genotype–phenotype correlations in valosin-containing protein disease: a retrospective multicenter study. *Neurol Neurosurg Psychiatry*. (2022) 93:1099–111. doi: 10.1136/jnnp-2022-328921

2. Al-Obeidi E, Al-Tahan S, Surampalli A, Goyal N, Wang AK, Hermann A, et al. Genotype-phenotype study in patients with valosin-containing protein mutations associated with multisystem proteinopathy. *Clin Genet*. (2018) 93:119–25. doi: 10.1111/cge.13095

3. Mehta SG, Khare M, Ramani R, Watts GDJ, Simon M, Osann KE, et al. Genotype-phenotype studies of VCP-associated inclusion body myopathy with paget disease of bone and/or frontotemporal dementia. *Clin Genet*. (2013) 83:422–31. doi: 10.1111/cge.12000

4. Wang SC, Smith CD, Lombardo DM, Kimonis V. Characteristics of VCP mutation-associated cardiomyopathy. *Neuromuscul Disord*. (2021) 31:701–5. doi: 10.1016/j.nmd.2021.06.005

5. Gonzalez MA, Feely SM, Speziani F, Strickland AV, Danzi M, Bacon C, et al. A novel mutation in VCP causes Charcot-Marie-tooth type 2 disease. *Brain*. (2014) 137:2897–902. doi: 10.1093/brain/awu224

6. Souza PVS, Bortholin T, Dias RB, Chieia MAT, Burlin S, Naylor FGM, et al. New genetic causes for complex hereditary spastic paraplegia. *J Neurol Sci*. (2017) 379:283–92. doi: 10.1016/j.jns.2017.06.019

7. Meyer H, Weihl CC. The VCP/p97 system at a glance: connecting cellular function to disease pathogenesis. *J Cell Sci*. (2014) 127:3877–83. doi: 10.1242/jcs.093831

8. van den Boom J, Meyer H. VCP/p97-mediated unfolding as a principle in protein homeostasis and signaling. *Mol Cell*. (2018) 69:182–94. doi: 10.1016/j.molcel.2017.10.028

9. Ferrari V, Cristofani R, Tedesco B, Crippa V, Chierichetti M, Casarotto E, et al. Valosin containing protein (VCP): a multistep regulator of autophagy. *Int J Mol Sci*. (2022) 23:1939. doi: 10.3390/ijms23041939

10. Poksay KS, Madden DT, Peter AK, Niazi K, Banwait S, Crippen D, et al. Valosin-containing protein gene mutations: cellular phenotypes relevant to neurodegeneration. *J Mol Neurosci*. (2011) 44:91–102. doi: 10.1007/s12031-010-9489-8

11. Watts GDJ, Wymer J, Kovach MJ, Mehta SG, Mumm S, Darvish D, et al. Inclusion body myopathy associated with Paget disease of bone and frontotemporal dementia is caused by mutant valosin-containing protein. *Nat Genet*. (2004) 36:377–81. doi: 10.1038/ng1332

12. Richards S, Aziz N, Bale S, Bick D, Das S, Gastier-Foster J, et al. Standards and guidelines for the interpretation of sequence variants: a joint consensus recommendation of the American College of Medical Genetics and Genomics and the Association for Molecular Pathology. *Genet Med*. (2015) 17:405–24. doi: 10.1038/gim.2015.30

13. Siavrienė E, Petraitytė G, Burnytė B, Morkūnienė A, Mikštienė V, Rančelis T, et al. Compound heterozygous c.598_612del and c.1746-20C > G CAPN3 genotype cause autosomal recessive limb-girdle muscular dystrophy-1: a case report. *BMC Musculoskelet Disord*. (2021) 22:1020. doi: 10.1186/s12891-021-04920-3

14. Kimonis V. Inclusion body myopathy with Paget disease of bone and/or frontotemporal dementia In: MP Adam, GM Mirzaa and RA Pagon, editors. *GeneReviews®*. Seattle: University of Washington (1993)

15. Kimonis VE, Fulchiero E, Vesa J, Watts G. VCP disease associated with myopathy, Paget disease of bone and frontotemporal dementia: review of a unique disorder. *Biochim Biophys Acta Mol basis Dis*. (2008) 1782:744–8. doi: 10.1016/j.bbadis.2008.09.003

16. De Ridder W, Azmi A, Clemen CS, Eichinger L, Hofmann A, Schröder R, et al. Multisystem proteinopathy due to a homozygous p.Arg159His VCP mutation: a tale of the unexpected. *Neurology*. (2020) 94:e785–96. doi: 10.1212/WNL.0000000000008763

17. Columbres RCA, Chin Y, Pratti S, Quinn C, Gonzalez-Cuyar LF, Weiss M, et al. Novel variants in the VCP gene causing multisystem Proteinopathy 1. *Genes*. (2023) 14:676. doi: 10.3390/genes14030676

18. Al-Tahan S, Al-Obeidi E, Yoshioka H, Lakatos A, Weiss L, Grafe M, et al. Novel valosin-containing protein mutations associated with multisystem proteinopathy. *Neuromuscul Disord*. (2018) 28:491–501. doi: 10.1016/j.nmd.2018.04.007

19. Guyant-Maréchal L, Laquerrière A, Duyckaerts C, Dumanchin C, Bou J, Dugny F, et al. Valosin-containing protein gene mutations. *Neurology*. (2006) 67:644–51. doi: 10.1212/01.wnl.0000225184.14578.d3

20. Stenson PD, Mort M, Ball EV, Chapman M, Evans K, Azevedo L, et al. The human gene mutation database (HGMD®): optimizing its use in a clinical diagnostic or research setting. *Hum Genet*. (2020) 139:1197–207. doi: 10.1007/s00439-020-02199-3

21. Kopanos C, Tsiolkas V, Kouris A, Chapple CE, Albarca Aguilera M, Meyer R, et al. VarSome: the human genomic variant search engine. *Bioinformatics*. (2019) 35:1978–80. doi: 10.1093/bioinformatics/bty897

22. Mengel D, Librizzi D, Schoser B, Gläser D, Clemen CS, Dodel R, et al. Inclusion body myopathy, paget's disease, and Fronto-temporal dementia: a VCP-related multisystemic proteinopathy. *Fortschr Neurol Psychiatr*. (2018) 86:434–8. doi: 10.1055/s-0044-101033

23. Figueroa-Bonaparte S, Hudson J, Barresi R, Polvikoski T, Williams T, Töpf A, et al. Letter: mutational spectrum and phenotypic variability of VCP-related neurological disease in the UK. *J Neurol Neurosurg Psychiatry*. (2016) 87:680–1. doi: 10.1136/jnnp-2015-310362

24. Shi Z, Hayashi YK, Mitsuhashi S, Goto K, Kaneda D, Choi YC, et al. Characterization of the Asian myopathy patients with VCP mutations. *Eur J Neurol*. (2012) 19:501–9. doi: 10.1111/j.1468-1331.2011.03575.x

25. Fanganiello RD, Kimonis VE, Côrte CC, Nitrini R, Passos-Bueno MR. A Brazilian family with hereditary inclusion body myopathy associated with paget disease of bone and frontotemporal dementia. *Braz J Med Biol Res*. (2011) 44:374–80. doi: 10.1590/S0100-879X2011007500028

26. Krause S, Göhringer T, Walter MC, Schoser BGH, Reilich P, Linn J, et al. Brain imaging and neuropsychology in late-onset dementia due to a novel mutation (R93C) of valosin-containing protein. *Clin Neuropathol*. (2007) 26:232–40. doi: 10.5414/npp26232

frontiers | Frontiers in Neurology

TYPE Case Report
PUBLISHED 05 January 2024
DOI 10.3389/fneur.2023.1320757

OPEN ACCESS

EDITED BY
Giovanni Meola,
University of Milan, Italy

REVIEWED BY
Murat Mert Atmaca,
University of Health Sciences, Türkiye
Georgios E. Manousakis,
University of Minnesota, United States

*CORRESPONDENCE
Alina Zorina Stuparu
✉ zorina.stroe@yahoo.com

RECEIVED 12 October 2023
ACCEPTED 22 November 2023
PUBLISHED 05 January 2024

CITATION
Gogu AE, Jianu DC, Parv F, Motoc AGM, Axelerad A, Stuparu AZ and Gogu AA (2024) Case report: Clinical profile, molecular genetics, and neuroimaging findings presenting in a patient with Kearns-Sayre syndrome associated with inherited thrombophilia. *Front. Neurol.* 14:1320757. doi: 10.3389/fneur.2023.1320757

Case report: Clinical profile, molecular genetics, and neuroimaging findings presenting in a patient with Kearns-Sayre syndrome associated with inherited thrombophilia

Anca Elena Gogu[1,2], Dragos Catalin Jianu[1,2], Florina Parv[3], Andrei Gheorghe Marius Motoc[4], Any Axelerad[5], Alina Zorina Stuparu[5]* and Andreea Alexandra Gogu[6]

[1]Department of Neurology, "Victor Babeş" University of Medicine and Pharmacy, Timişoara, Romania, [2]Centre for Cognitive Research in Neuropsychiatric Pathology (Neuropsy-Cog), Faculty of Medicine, "Victor Babeş" University of Medicine and Pharmacy, Timişoara, Romania, [3]Department of Cardiology, "Victor Babeş" University of Medicine and Pharmacy, Timişoara, Romania, [4]Department of Anatomy and Embryology, "Victor Babeş" University of Medicine and Pharmacy, Timişoara, Romania, [5]Department of Neurology, General Medicine Faculty, "Ovidius" University, Constanța, Romania, [6]Medicine Faculty, "Victor Babeş" University of Medicine and Pharmacy, Timişoara, Romania

Background: Kearns-Sayre syndrome (KSS) is classified as one of the mitochondrial DNA (mtDNA) deletion syndromes with multisystemic involvement. Additionally, the negative prognosis is associated with inherited thrombophilia, which includes the presence of homozygous Factor V G1691A Leiden mutation, MTHFR gene polymorphisms C677T and A1298C, and PAI-1 675 homozygous genotype 5G/5G.

Case presentation: This case report presents a 48-year-old man with chronic progressive external ophthalmoplegia, bilateral ptosis, cerebellar ataxia, cardiovascular signs (syncope, dilated cardiomyopathy, and cardiac arrest) with electrocardiographic abnormalities (first-degree atrioventricular block and major right bundle branch block), endocrine dysfunction (short stature, growth hormone insufficiency, primary gonadal insufficiency, hypothyroidism, and secondary hyperparathyroidism), molecular genetic tests (MT-TL2 gene), and abnormal MRI brain images, thus leading to the diagnosis of KSS. The patient came back 4 weeks after the diagnosis to the emergency department with massive bilateral pulmonary embolism with syncope at onset, acute cardiorespiratory failure, deep left femoral-popliteal vein thrombophlebitis, and altered neurological status. In the intensive care unit, he received mechanical ventilation through intubation. Significant improvement was seen after 2 weeks. The patient tested positive for inherited thrombophilia and was discharged in stable conditions on a new treatment with Rivaroxaban 20 mg/day. At 6 months of follow-up, ECG-Holter monitoring and MRI brain images remained unchanged. However, after 3 months, the patient died suddenly while sleeping at home.

Conclusion: The genetic tests performed on KSS patients should also include those for inherited thrombophilia. By detecting these mutations, we can prevent major complications such as cerebral venous sinus thrombosis, coronary accidents, or sudden death.

KEYWORDS

Kearns-Sayre syndrome (KSS), inherited thrombophilia, heart conduction block, brain magnetic resonance imaging, genetic tests

1 Introduction

Kearns-Sayre syndrome (KSS), initially reported in 1958 at the Mayo Clinic (1, 2), is an uncommon mitochondrial myopathy. It is characterized by a greater severity compared to chronic progressive external ophthalmoplegia (CPEO), encompassing multiple systems in its manifestation. There are three cardinal clinical features of KSS: onset prior to 20 years of age, pigmentary retinopathy, and progressive external ophthalmoplegia (3, 4). Furthermore, the diagnosis of KSS requires the presence of at least one of the features, including cardiac conduction abnormalities, cerebellar ataxia, cerebrospinal fluid (CSF) protein level above 100 mg/dl, short stature, endocrine abnormalities, and cognitive decline (5).

Inherited thrombophilia genetic risk factors include factor V G1691A-Leiden mutation, prothrombin G20210A mutation, methylenetetrahydrofolate reductase (MTHFR) gene C677T and A1298C mutation, and plasminogen-activator inhibitor PAI-1 675 5G/5G mutation, correlated with cardiovascular risk factors, which represents an aggravating status for patients with KSS due to the risk of pulmonary embolism, deep venous thrombosis, or cerebral venous sinus thrombosis (CVST) (6, 7).

This article describes a case of Kearns-Sayre syndrome without a family history of KSS or other mitochondrial disorders in which inherited thrombophilia was detected, complicated with pulmonary embolism and deep venous thrombosis, leading to the patient's death. The patient was assessed by a multidisciplinary team (neurologist, cardiologist, endocrinologist, neuro-ophthalmologist, and neuro-radiologist) to establish a clinical diagnosis of KSS.

2 Case presentation

A 48-year-old male patient presented to the emergency department with headache, dizziness, unstable gait, limb weakness, accentuation of eyelid ptosis, external ophthalmoplegia, and sinus tachycardia. The disease manifested in the patient at the age of 16, initially presenting with a small stature and symptoms related to the extraocular muscles. As the disease progressed, the patient experienced a gradual onset of additional clinical characteristics such as heart conduction issues, endocrine dysfunction, and a slight cognitive decline.

The diagnosis of KSS was supported by identifying relevant clinical characteristics that indicated an abnormality in the patient's ophthalmologic system: bilateral ptosis, diplopia, chronic progressive external ophthalmoplegia, and a moderate decrease in visual acuity (Figure 1A). Considering that the patient's ophthalmoplegia did not match a specific group of cranial nerve palsies (oculomotor nerve palsy, fourth nerve palsy, and sixth nerve palsy), the likelihood for myopathies was even higher. Paralysis of the vertical movements of the eyeballs was observed (Figure 1B). No retinitis pigmentosa was discovered during the fundus examination performed by the ophthalmologist, but retinal angiosclerosis has been described.

Following ophthalmologic observations, the neurological examination highlights mild generalized muscle weakness, cerebellar ataxia, cerebellar tremor, and a slight cognitive impairment (Mini-Mental State Examination score of 22 points).

The patient had endocrinological symptoms and signs that preceded the neurological manifestations, including short stature (154 cm) caused by growth hormone insufficiency, delayed puberty, primary hypogonadism, hypothyroidism, secondary hyperparathyroidism, gynecomastia, frontal baldness, and brachydactily. The patient had no children.

Cardiac involvement is common in disorders characterized by mitochondrial dysfunction due to their impact on organs that rely heavily on energy (8). Following the confirmation of the diagnosis, the patient underwent a series of medical tests, including 12-lead surface electrocardiography (ECG), transthoracic echocardiography, and 24-h Holter monitoring. Conduction abnormalities were seen, including first-degree atrioventricular block (AVB), significant right bundle branch block (RBBB), and sinus tachycardia (Figure 2). The echocardiogram revealed mild anterior mitral valve prolapses (MVP) and type I diastolic and systolic LV dysfunction (LVEF = 40%).

Given the presence of many clinical features suggesting KSS in this patient, we conducted a comprehensive analysis of biochemical and genetic tests related to cardiovascular risk factors. The lab testing demonstrated WBC of 12,460/μl (NV 4,000–9,500/μl), hemoglobin of 17.9 g/dl (NV 13.6–17.2 g/dl), hematocrit of 53.6% (NV 39–51%), blood glucose of 101 mg/dl (NV 74–106 mg/dl), aspartate aminotransferase of 58 U/L (NV 15–37 U/L), alanine aminotransferase of 71 U/L (NV 30–65 U/L), lactic dehydrogenase of 356 U/L (NV 85–227 U/L), creatinine kinase of 308 U/L (NV 39–308 U/L), and creatinine kinase-MB of 42 U/L (NV 7–25 U/L). The serum ionogram revealed ionic calcium of 3.95 mg/dl (NV 4.2–5.2 mg/dl), magnesium of 2.2 mg/dl (NV 1.8–2.4 mg/dl), potassium of 5.5 mmol/L (NV 3.5–5.1 mmol/L), and sodium of 149 mmol/L (NV 136–145 mmol/L).

Endocrinological analyses showed the following values: growth hormone (hGH) <0.050 ng/ml (NV 0.4–10 ng/ml) and the thyroid hormone levels were FT3 of 3.35 pmol/L (NV 3.54–6.47 pmol/L), FT4 of 15.19 pmol/L (NV 11.48–22.70 pmol/L), TSH of 0, 150 mIU/ml (NV 0.55–4.78 mIU/ml), anti-TG of 24.6 U/ml (NV 0–60 U/ml), and anti-TPO of 31.9 U/ml (NV 0–60 U/ml). Intact PTH

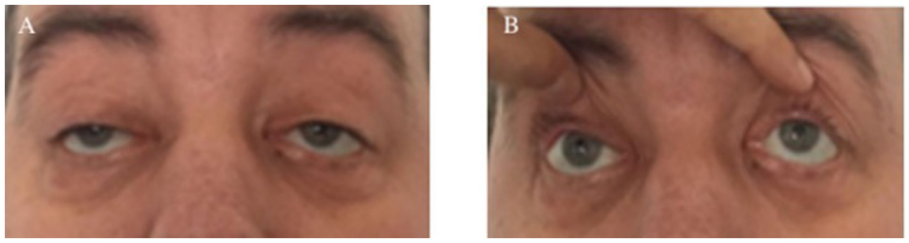

FIGURE 1
Clinical ophthalmologic symptoms. Bilateral ptosis **(A)** and external ophthalmoplegia with paralysis of vertical movements **(B)**.

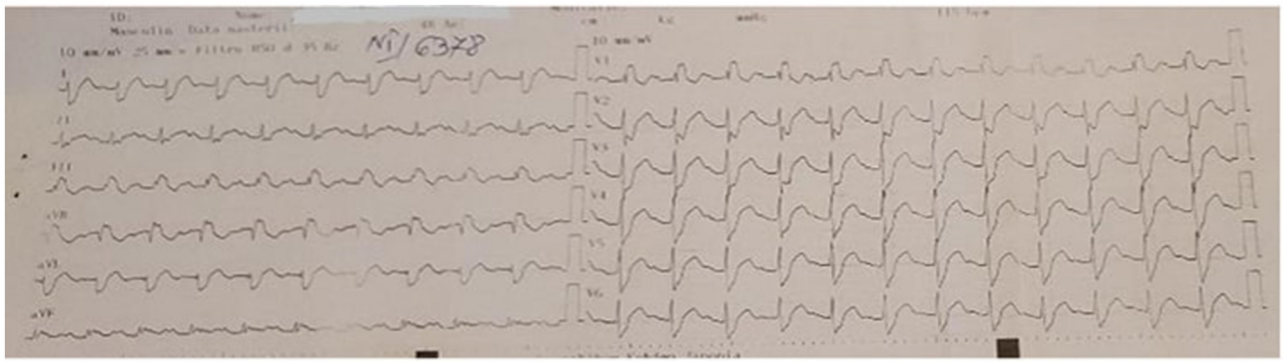

FIGURE 2
ECG–first-degree atrioventricular block, major right bundle branch block, and sinus tachycardia.

was 61.8 pg/ml (NV 7.5–53.5 pg/ml) with a low level of ionic calcium (3.95 mg/dl). Gonadotropic hormones were testosterone of 182.76 ng/dl (NV 241–827 ng/dl), FSH of 22.56 mIU/mL (NV 1.4–18.1 mIU/mL), and LH of 24.39 mIU/mL (NV 1.5–9.3 mIU/mL). Serum cortisol was normal (15.16 μg/dl). CSF indicated a high protein level of 91 mg/dl (NV 0.12–0.60 mg/dl) and a high glucose level of 131 mg/dl (NV 40–70 mg/dl) in the absence of white blood cells during a lumbar puncture procedure. For the differential diagnosis of myasthenia gravis, we tested anti-acetylcholine receptor antibodies, which were normal (AChR < 0.2 nmol/L).

Performing next-generation sequencing (NGS) on mitochondrial DNA extracted from peripheral blood leukocyte samples is the primary diagnostic method for identifying deletions in situations where KSS is clinically suspected (5, 9). We requested the testing for sequence analysis of the MT-TL2 gene; this test was developed and its performance was validated by CENTOGENE AG (Rostock, Germany) for clinical purposes. The blood sample was processed by enriching targeted sequences, and sequencing was done using NGS Technologies.

We did not detect any clear pathogenic variant in the MT-TL2 gene sequencing, including the variant m.12315G>A, which has been reported to be associated with KSS. However, it should be noted that the variants encoded in the mitochondrial genome may not be detected in blood if the percentage of heteroplasmy is low (typically <15% heteroplasmy) (10). In this situation, it is recommended to test a sample from an affected tissue, but the patient did not agree to the muscle biopsy.

Electromyography (EMG) showed a myogenic pathway with small amplitude and short-duration motor unit potentials with an early recruitment pattern (bilateral frontal and deltoid muscles). Electroencephalography (EEG) revealed a generalized theta background pattern; the lesion-type route was maintained even when activated by hyperventilation or intermittent light stimulation (6–12 Hz).

Upon admission to our clinic, brain magnetic resonance imaging (MRI) was performed with and without contrast. The results revealed symmetrical high-T2 and Flair signals in the cerebral white matter of both temporal lobes and in the bilateral insula of the Reil lobes (Figure 3).

The appearance of brain lesions did not change; the patient underwent several brain MRIs in the year in which he was supervised. Unusual high-T2 signals were identified in the white matter of the cerebellum. Figure 4 shows the presence of cerebellar atrophy.

The patient was discharged in stable condition with the recommendation of cardiological monitoring. There is now no known remedy for this uncommon condition, and all available therapies only provide support. It was advised to undergo hormone replacement therapy and take Coenzyme Q10 (CoQ10). The patient presented at the emergency department 1 month later with a severe case of bilateral pulmonary embolism, accompanied by syncope at the onset, acute cardiorespiratory

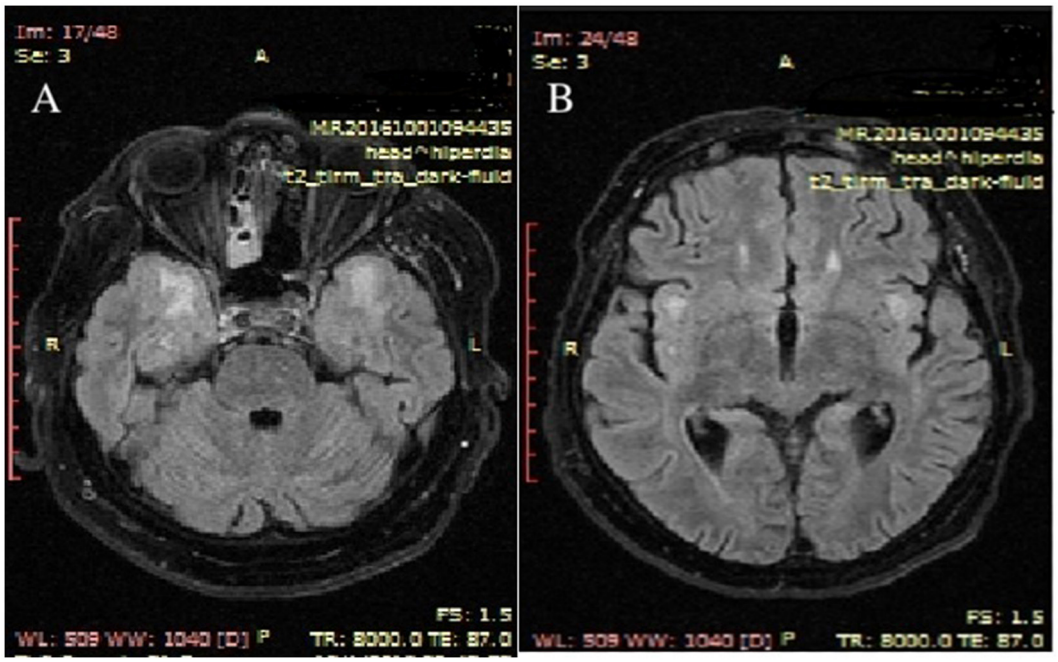

FIGURE 3
Upon admission to the hospital, MRI brain scans with contrast revealed T2 axial hypersignal in the subcortical white matter of both temporal lobes **(A)** and in the bilateral insula of the Reil lobes **(B)**. MRI stands for magnetic resonance imaging.

failure, proximal deep vein thrombosis in the left limb (the femoral-popliteal veins), and altered neurological status characterized by a depressed level of consciousness and extreme agitation. He received intubation and mechanical ventilation in the critical care unit.

The patient's laboratory results showed WBC of 10,800/μl, hemoglobin of 16.1 g/dl, hematocrit of 48.6%, platelets of 263,000/μl, blood glucose of 128 mg/dl, aspartate aminotransferase of 6,570 U/L, alanine aminotransferase of 5,735 U/L, lactic dehydrogenase of 4,736 U/L, creatinine kinase of 535 U/L, creatinine kinase-MB of 48 U/L, cholinesterase of 14,428 U/L (NV 5,320–12,920 U/L), and lactic acid of 3.2 mmol/L (NV 0.5–2.2 mmol/L). Serum inflammatory workup showed elevated hsCRP of 71.98 mg/L (NV 0–10 mg/L) and fibrinogen of 599 mg/L (NV 200–393 mg/L). The hepatitis panel (AcHBs, aHCV, and HAV Ig M) was negative. The hormone levels were FT3 of 2.55 pmol/L, FT4 of 15.08 pmol/L, TSH of 1,003 mIU/ml, and anti-TPO of 45.3 U/L; FSH of 2.76 mIU/ml, LH of 3.70 mIU/ml, and testosterone of 66.80 ng/dl. Coagulation tests were prothrombin time of 16.0 s (NV 9.4–12.5 s), APTT of 74.1 s (NV 25.1–36.5 s), and INR of 1.43 (NV 0.80–1.07).

Chest-computed tomography (chest-CT) revealed massive bilateral pulmonary embolism with multifocal infiltrates. The echocardiogram showed dilation of the right cardiac chambers and moderate secondary pulmonary hypertension. The venous Doppler ultrasonography of the lower extremities detected recent total thrombosis in the left femoral and popliteal veins. The patient was tested for inherited thrombophilia, obtaining the following genetic mutations: homozygous Factor V G1691A Leiden, MTHFR gene polymorphism C677T and A1298C, and PAI-1 675 homozygous genotype 5G/5G. The patient did not present a prothrombin G20210A mutation or protein C, protein S, or antithrombin deficiencies. In individuals with Kearns-Sayre syndrome, the presence of inherited thrombophilia, together with pre-existing cardiovascular disease, is indicative of a poor prognosis.

Significant improvement was seen after 2 weeks, and the patient returned home in stable conditions on a novel treatment with an oral anticoagulant drug (Rivaroxaban 20 mg/day). At 6 months of follow-up, ECG-Holter monitoring and MRI brain images remain unchanged. After 3 months, the patient died suddenly while sleeping at home.

3 Discussion

This is an exceptional instance where a patient has Kearns-Sayre syndrome (KSS) together with inherited thrombophilia, namely, the homozygous Factor V G1691A Leiden mutation, MTHFR gene polymorphisms C677T and A1298C, and PAI-1 homozygous genotype 5G/5G. Unfortunately, this combination of conditions leads to a catastrophic prognosis.

KSS is an uncommon mitochondrial disorder characterized by both systemic and ocular symptoms. These symptoms include chronic progressive external ophthalmoplegia (CPEO), pigmentary retinopathy, and a beginning of symptoms before the age of 20. Patients who have chronic progressive external ophthalmoplegia (CPEO) who satisfy some, but not all the criteria for KSS are referred to as having "KSS minus" or "CPEO plus" (1, 11).

The patient in our case report did not have a familial predisposition to KSS or any other mitochondrial illnesses. Our findings indicate that the patient had symptoms related to ophthalmology, neurology, cardiology, and endocrinology. This result aligns with the diagnosis of KSS.

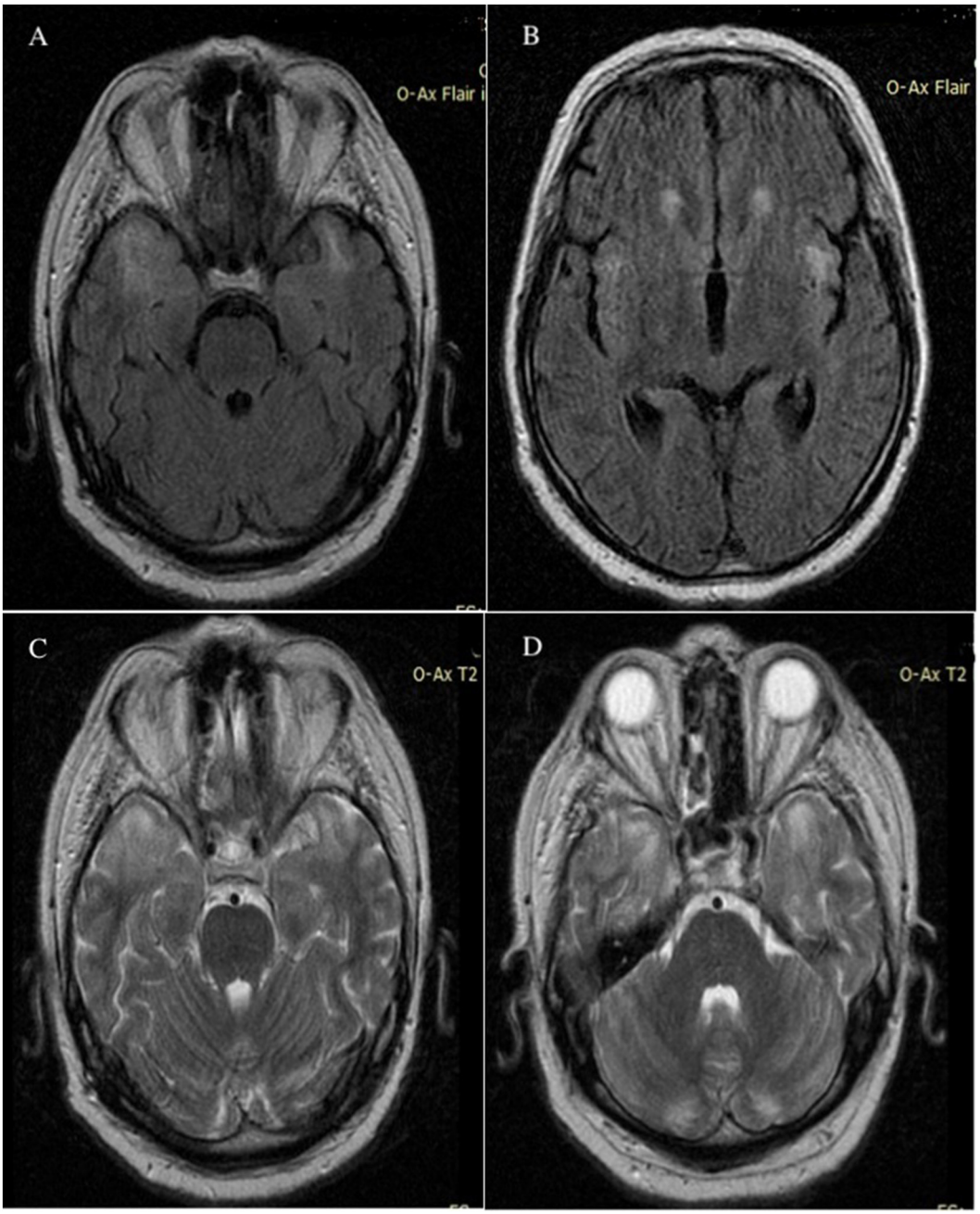

FIGURE 4
MRI axial Flair FSE images without contrast demonstrated abnormally high signals in the bilateral temporal lobes **(A)** and in the bilateral insula of the Reil lobes **(B)** MRI T2 axial images without contrast showed hypersignal in bilateral temporal lobes **(C)** and cerebellar white matter **(D)**; imaging appearance was unchanged after 6 months. MRI, magnetic resonance imaging; Flair, fluid attenuated inversion recovery; FSE, fast spin echo.

The condition manifested in the second decade of life, with the first symptom being unilateral ptosis, which subsequently developed into bilateral ptosis and external ophthalmoplegia. We used a serial examination of old photos to establish the chronic, progressive nature of this disorder. As a particularity of this case, we did not find pigmentary retinopathy, and a dilated fundus examination revealed retinal angiosclerosis. The patient had considerably diminished visual acuity and was presenting with retinopathy.

Additionally, our investigation highlighted the presence of cardiovascular involvement. Yu et al. reported a study including 19 patients with KSS diagnosed with conduction defects that were aggravating but not constant, gradually deteriorating from bundle branch blockage to complete atrio-ventricular block (14). Other reports also demonstrated that the primary cause of sudden death in KSS patients was a complete atrio-ventricular block, and the incidence of sudden cardiac death was 20% as reported. The most common type of ventricular arrhythmia reported in KSS

patients by others was bradycardia-related polymorphic ventricular tachycardia (14, 15). We identified conduction abnormalities characterized by first-degree atrioventricular block (AVB), major right bundle branch block (RBBB), and sinus tachycardia. The criteria for permanent pacemaker/implanted cardioverter defibrillator (PPM/ICD) insertion include high-grade heart block, bradycardia, a combination of heart block and bradycardia, and broadening of the QRS complex (1). Given the circumstances, the patient did not meet the criteria for PPM/ICD devices. Throughout a span of 1 year, the patient had ECG-Holter monitoring, which revealed no more abnormal heart rhythms. Prior research on progressive heart block and sudden cardiac death in individuals with KSS recommends considering regular preventive installation of a pacemaker (PPM) or implantable cardioverter-defibrillator (ICD). It also suggests having a low threshold to perform electrophysiological testing rather than doing formal electrophysiological testing in these patients, with a preference for a lower threshold (1, 12–14).

KSS has been associated with several endocrine disorders. Khambatta et al. reported a case series of 35 adults and children with KSS. They identified patients with short stature, delayed puberty, diabetes mellitus, and hypothyroidism. However, hyperaldosteronism and hypoparathyroidism, which have been reported in previous studies, were not observed in their study (1). Endocrine disturbances are frequently reported in KSS, similar to those in our patient, including short stature and brachydactyly from low growth hormone, delayed puberty, primary hypogonadism, frontal baldness, and gynecomastia caused by gonadotropic insufficiency and hypothyroidism. Usually, a patient with KSS has primary hypoparathyroidism, but in our case, the patient had been reported to have secondary hyperparathyroidism with an increased level of PTH and a low level of ionic calcium. Hypocalcemia associated with elevated PTH values in a patient with normal renal function suggests resistance to PTH actions.

Throughout the progression of the illness, the individual had a progressive onset of other neurological symptoms, including cerebellar ataxia, cerebellar tremor, muscular weakness in the limbs and shoulders, and a decline in cognitive abilities. The results of the brain magnetic resonance imaging (MRI), both with and without contrast, showed abnormalities. In a previous study conducted by other scholars, it was shown that the subcortical white matter had a 90.9% involvement rate, the basal ganglia and brainstem had a 63.6% involvement rate each, the thalamus had a 54.5% involvement rate, and the cerebellum had a 25.0% involvement rate (15, 16). The patient exhibited cerebral involvement, namely in the bilateral temporal lobes and bilateral insula of the Reil lobes, as well as cerebellar white matter involvement. However, there was no involvement of the brainstem. There was evidence of cerebellar atrophy. Subsequent investigations should include extended clinical and MRI monitoring to more accurately monitor the progression of brain MRI abnormalities and their correlation with clinical characteristics (15).

Prior published case series have included individuals diagnosed with KSS. Yamashita et al. reported on a group of 136 individuals who had mtDNA deletions. However, after using the diagnostic criteria established by Roland et al., they discovered that 24% of these patients fulfilled the criteria for Kearns-Sayre syndrome (KSS) (4, 17). Khambatta et al. conducted a study on 35 individuals with KSS. They relied on the diagnosis made by the treating physician instead of retrospectively applying criteria based on positive genetic test results (1). The patients exhibited more heterogeneity, including cases with onset occurring beyond the age of 20 years and lacking both progressive external ophthalmoplegia (PEO) and pigmentary retinopathy. Our investigation has constraints. No pathogenic variant was identified in the MT-TL2 gene sequencing. Additionally, due to logistical constraints, additional genetic testing could not be performed since it is only available in another country. If patients with a high likelihood of having KSS based on their physical characteristics have negative blood tests for KSS, it is recommended to sequence their muscle mtDNA. This is because tissue-specific mutations can sometimes be overlooked, and low levels of heteroplasmy in the blood can result in false-negative outcomes (5). Regrettably, the patient declined to have the muscle biopsy.

Since the patient returned to the emergency department with massive bilateral pulmonary embolism with syncope at onset, cardiorespiratory acute failure, proximal deep vein thrombosis, and altered neurological status without atrial fibrillation, we did tests for inherited thrombophilia, obtaining the following genetic mutations: homozygous Factor V G1691A Leiden, MTHFR gene polymorphisms C677T and A1298C, and PAI-1 675 homozygous genotype 5G/5G. A differential diagnosis was made with cerebral venous sinus thrombosis. The diagnostic assessment using magnetic resonance imaging (MRI) and magnetic resonance venography (MRV-2D TOF) disproved the diagnosis of cerebral venous sinus thrombosis (CVST).

A study conducted by Tripathi et al. (18) examined a population in North India and found a correlation between the MTHFR C677T gene polymorphism, elevated plasma homocysteine levels, and coronary artery diseases. Previous literature studies have shown the significance of the MTHFR C677T polymorphism in the development of ischemic stroke and cerebral venous sinus thrombosis (6, 7, 19, 20). MTHFR deficiency is an inherited disorder that affects the way the brain processes folate. In 2004, Ramaekers et al. coined the term cerebral folate deficiency (CFD) to include any neuropsychiatric or neurodevelopmental diseases that are linked to low MTHFR concentration in cerebrospinal fluid (CSF), despite normal levels of folate, vitamin B12, and homocysteine outside the nervous system (21, 22). Mitochondrial abnormalities related to mutations in nuclear- or mitochondrial-encoded DNA are a significant cause of CFD syndrome. These mutations are responsible for mitochondrial encephalopathies, KSS, and Alper's illness. MTHFR deficiency is a genetic condition that causes elevated levels of homocysteine, leading to many symptoms, including developmental delay, eye issues, thrombosis, and osteoporosis (23). The presence of either homozygous (C677T) mutations or compound heterozygous (C677T and A1298C) mutations is anticipated to result in reduced MTHFR enzyme activity, which may present a variety of clinical neurological symptoms similar to those seen in infantile CFD (24, 25). In our patient diagnosed with KSS, it would have been necessary to dose folate in the CSF. MTHFR gene polymorphisms C677T and A1298C did not mean that the patient had cerebral folate deficiency, but determination of the folate level in the CSF

would have been important to institute treatment with folic acid. In our patient diagnosed with KSS and having both heterozygous C677T and A1298C mutations, the presence of a cerebral folate deficit may play a role in the development of leukoencephalopathy and cognitive symptoms. Additionally, this deficiency significantly increases the likelihood of experiencing venous and arterial thrombosis. In addition to quantifying the proteins in the cerebrospinal fluid by lumbar puncture, we firmly believe that it is essential to determine the concentration of folic acid as early as possible in the evolution of the disease.

4 Conclusion

Patients with high suspicion of KSS must be examined by clinicians from a neurological, cardiological, endocrinological, and ophthalmological point of view. Specific medical tests may assist in the diagnosis, including genetic tests for mitochondrial DNA deletions, muscle biopsy, spinal tap (to assess the protein and folic acid in the cerebrospinal fluid), blood tests, EKG and echocardiogram, MRI of the brain, and screening for endocrinological disorders (dosing of hormones, especially thyroid, gonadotropins, and growth hormone).

This presentation in the patient with KSS associated with inherited thrombophilia is a coincidence discovered following thromboembolic complications that appeared with a reserved prognosis. We consider that genetic testing for inherited thrombophilia in KSS patients with pulmonary thromboembolism, deep vein thrombosis, or cerebral venous sinus thrombosis is necessary, including the following mutations: MTHFR gene polymorphism C677T and A1298C, PAI-1 675 homozygous genotype, Factor V G1691A Leiden, prothrombin G20210A mutation, protein C, protein S, and antithrombin deficiencies. The mutations in the MTHFR and PAI-1 genes were not clinically important alone, but when found with Factor V Leiden, they could contribute to the risk of thromboembolism. By detecting these mutations, we can prevent major complications that can have a fatal prognosis, such as cerebral venous sinus thrombosis, ischemic stroke, coronary accidents, or sudden death. Therefore, certain treatments should include oral anticoagulant drugs, folic acid, hormone replacement, and a pacemaker for heart rhythm problems.

Data availability statement

The raw data supporting the conclusions of this article will be made available by the authors, without undue reservation.

Ethics statement

The studies involving humans were approved by Ethics Committee for Clinical Studies of the Timisoara County Emergency Clinical Hospital (registration number 400/29.06.2023). The studies were conducted in accordance with the local legislation and institutional requirements. The participants provided their written informed consent to participate in this study. Written informed consent was obtained from the individual(s) for the publication of any potentially identifiable images or data included in this article.

Author contributions

AEG: Conceptualization, Data curation, Formal analysis, Funding acquisition, Investigation, Methodology, Project administration, Resources, Software, Supervision, Validation, Visualization, Writing—original draft, Writing—review & editing. DCJ: Conceptualization, Data curation, Formal analysis, Investigation, Methodology, Resources, Software, Validation, Visualization, Writing—original draft. FP: Conceptualization, Writing—original draft. AGM: Conceptualization, Writing—original draft, Writing—review & editing. AA: Conceptualization, Writing—original draft. AZS: Conceptualization, Writing—original draft. AAG: Conceptualization, Writing—original draft.

Funding

The author(s) declare that no financial support was received for the research, authorship, and/or publication of this article.

Conflict of interest

The authors declare that the research was conducted in the absence of any commercial or financial relationships that could be construed as a potential conflict of interest.

Publisher's note

All claims expressed in this article are solely those of the authors and do not necessarily represent those of their affiliated organizations, or those of the publisher, the editors and the reviewers. Any product that may be evaluated in this article, or claim that may be made by its manufacturer, is not guaranteed or endorsed by the publisher.

References

1. Khambatta S, Nguyen DL, Beckman TJ, Wittich CM. Kearns-Sayre syndrome: a case series of 35 adults and children. *Int J Gen Med.* (2014) 7:325–32. doi: 10.2147/IJGM.S65560

2. Kearns TP, Sayre GP. Retinitis pigmentosa, external ophthalmoplegia and complete heart block: unusual syndrome with histologic study in one of two cases. *AMA Arch Ophthalmol.* (1958) 60:280–289. doi: 10.1001/archopht.1958.00940080296016

3. Berardo A, DiMauro S, Hirano M. A diagnosis algorithm for metabolic myopathies. *Curr Neurol Neurosci Rep.* (2010) 10:118–26. doi: 10.1007/s11910-010-0096-4

4. Rowland LP, Hays AP, DiMauro S, DeVivo DC, Behrens M. Diverse clinical disorders associated with morphological abnormalities in mitochondria. In: Scarlato, G., Cerri, C. editors. *Mitochondrial Pathology in Muscle Diseases: Proceedings of the Satellite Symposium of the 5th International Congress on Neuromuscular Diseases*. Padua: Piccin Medical Books. (1983). p. 141–158.

5. Shemesh A, Margolin E. *Kearns- Sayre Syndrome*. Stat Pearls Publishing- NCBI Bookshelf. (2023). https://www.ncbi.nlm.nih.gov/books/NBK482341 (accessed July 17, 2023).

6. Gogu AE, Jianu DC, Dumitrascu V, Ples H, Stroe AZ, Axelerad Docu D, et al. MTHFR gene polymorphisms and cardiovascular risk factors, clinical- imagistic features and outcome in cerebral venous sinus thrombosis. *Brain Sci.* (2021) 11:23. doi: 10.3390/brainsci11010023

7. Gogu AE, Motoc AG, Stroe AZ, Axelerad Docu A, Axelerad Docu D, Petrica L, et al. Plasminogen activator inhibitor-1 (PAI-1) gene polymorphism associated with cardiovascular risk factors involved in cerebral venous sinus thrombosis. *Metabolites*. (2021) 22:266. doi: 10.3390/metabo11050266

8. Barrera- Ramirez CF, Barragan-Campos HM, Ilarraza H, Iturralde P, Ávila-Casado MC, Oseguera J. Cardiac involvement in Kearns- Sayre syndrome. *Rev Esp Cardiol*. (2005) 58:443–446. doi: 10.1016/S1885-5857(06)60673-7

9. Clamp M, Yen M, Lee NG, Burkat CN. *Kearns- Sayre Ptosis*. (2003). Available online at: https://eyewiki.org/w/index.php?title=Kearns-Sayre_Ptosis$\updelta$oldid=93756 (accessed October 1, 2023).

10. DiMauro S, Schon EA, Hirano M, Rowland LP. Mitochondrial Encephalomyopathies: Diseases of Mitochondrial DNA. In: Goetz, C.G. editor *Textbook of clinical neurology*. London: Saunders (2007).

11. DiMauro S, Hirano M. Mitochondrial DNA deletion syndromes. In: Pagon RA, Adam MP, Ardinger HH editors *Gene Reviews Seattle*, WA: University of Washington, Seattle. (2011).

12. Limongelli G, Tome-Esteban M, Dejthevaporn C, Rahman S, Hanna MG, Elliott PM. Prevalence and natural history of heart disease in adults with primary mitochondrial respiratory chain disease. *Eur J Heart Fail.* (2010) 12:114–21. doi: 10.1093/eurjhf/hfp186

13. Charles R, Holt S, Kay JM, Epstein EJ, Rees JR. Myocardial ultrastructure and the development of atrioventricular block in Kearns- Sayre syndrome. *Circulation*. (1981) 63:214–219. doi: 10.1161/01.CIR.63.1.214

14. Hirano M, Davidson M, DiMauro S. Mitochondria and heart disease. *Curr Opin Cardiol.* (2001) 16:201–210. doi: 10.1097/00001573-200105000-00008

15. Yu M, Zhang Z, Wang QQ, Liu J, Zuo YH, Yu L, et al. Clinical and brain magnetic resonance imaging features in a cohort of Chinese patients with Kearns- Sayre syndrome. *Chin Med J.* (2016) 129:1419–24. doi: 10.4103/0366-6999.183417

16. Serrano M, García-Silva MT, Martin-Hernandez E, O'Callaghan Mdel M, Quijada P, Martinez-Aragón A, et al. Kearns-Sayre syndrome: cerebral folate deficiency, MRI findings and new cerebrospinal fluid biochemical features. *Mitochondrion.* (2010) 10:429–32. doi: 10.1016/j.mito.2010.04.001

17. Yamashita S, Nishino I, Nonaka I, Goto YI. Genotype and phenotype analyses in 136 patients with single large- scale mitochondrial DNA deletion. *J Hum Genet.* (2008) 53:598–606. doi: 10.1007/s10038-008-0289-8

18. Tripathi R, Tewari S, Singh PK, Agarwal S. Association of homocysteine and methylenetetrahydrofolate reductase (MTHFR C677T) gene polymorphism with coronary artery disease (CAD) in the population of North India. *Genet Mol Biol.* (2010) 33:224–228. doi: 10.1590/S1415-47572010005000026

19. Alluri RV, Mohan V, Komandur S, Chawda K, Chaudhuri JR, Hasan Q. MTHFR C677T gene mutation as a risk factor for arterial stroke: a hospital based study. *Eur J Neurol.* (2005) 12:40–4. doi: 10.1111/j.1468-1331.2004.00938.x

20. Jianu DC, Jianu SN, Dan TF, Munteanu G, Copil A, Birdac CD, et al. An integrated approach on the diagnosis of cerebral veins and dural sinuses thrombosis. *Life.* (2022) 12:717. doi: 10.3390/life12050717

21. Ramaekers VT, Blau N. Cerebral folate deficiency. *Dev Med Child Neurol.* (2004) 46:843–51. doi: 10.1111/j.1469-8749.2004.tb00451.x

22. Ramaekers VT, Quadros EV. Cerebral folate deficiency syndrome: early diagnosis, intervention and treatment strategies. *Nutrients*. (2022) 14:3096. doi: 10.3390/nu14153096

23. Fattal-Valevski A, Bassan H, Korman SH, Lerman-Sagie T, Gutman A, Harel S. Methylenetetrahydrofolate reductase deficiency: Importance of early diagnosis. *J Child Neurol.* (2000) 15:539–43. doi: 10.1177/088307380001500808

24. Banka S, Blom HJ, Walter J, Aziz M, Urquhart J, Clouthier CM, et al. Identification and characterization of an inborn error of metabolism caused by dihydrofolate reductase deficiency. *Am J Hum Genet.* (2011) 88:216–25. doi: 10.1016/j.ajhg.2011.01.004

25. Ramaekers VT, Weis J, Sequeira JM, Quadros EV, Blau N. Mitochondrial complex I encephalomyopathy and cerebral 5- methyltetrahydrofolate deficiency. *Neuropediatrics.* (2007) 38:184–7. doi: 10.1055/s-2007-991150

frontiers | Frontiers in Neurology

TYPE Case Report
PUBLISHED 05 January 2024
DOI 10.3389/fneur.2023.1268053

OPEN ACCESS

EDITED BY
Giovanni Meola,
University of Milan, Italy

REVIEWED BY
Essam Mohamed Elmatbouly Saber,
Benha University, Egypt
Zhaoxia Wang,
Peking University, China
Haibing Xiao,
The University of Hong Kong, China
Weian Chen,
First Affiliated Hospital of Wenzhou Medical University, China

*CORRESPONDENCE
Xiude Qin
✉ qinxiude@foxmail.com
Fanxin Kong
✉ kfx1662@gzucm.edu.cn

†These authors have contributed equally to this work and share first authorship

RECEIVED 27 July 2023
ACCEPTED 05 December 2023
PUBLISHED 05 January 2024

CITATION
Feng Z, Lai R, Wei J, Liu X, Chen X, Liu Y, Qin W, Qin X and Kong F (2024) Have one's view of the important overshadowed by the trivial: chronic progressive external ophthalmoplegia combined with unilateral facial nerve injury: a case report and literature review. *Front. Neurol.* 14:1268053. doi: 10.3389/fneur.2023.1268053

Have one's view of the important overshadowed by the trivial: chronic progressive external ophthalmoplegia combined with unilateral facial nerve injury: a case report and literature review

Ziyang Feng [1†], Rui Lai [2†], Jia Wei [1,3], Xuan Liu[1,3], Xueqin Chen [1,3], Yangsicheng Liu [1], Wenxin Qin [1], Xiude Qin [1,3*] and Fanxin Kong [1,3*]

[1]The Fourth Clinical Medical College, Guangzhou University of Chinese Medicine, Shenzhen, China, [2]School of Acupuncture and Tuina, Chengdu University of Traditional Chinese Medicine, Chengdu, China, [3]Department of Encephalopathy and Psychology, Shenzhen Traditional Chinese Medicine Hospital, Shenzhen, China

Chronic progressive external ophthalmoplegia (CPEO) is a mitochondrial encephalomyopathy that is characterized by progressive ptosis and impaired ocular motility. Owing to its nonspecific clinical manifestations, CPEO is often misdiagnosed as other conditions. Herein, we present the case of a 34-year-old woman who primarily presented with incomplete left eyelid closure and limited bilateral eye movements. During the 6-year disease course, she was diagnosed with myasthenia gravis and cranial polyneuritis. Finally, skeletal muscle tissue biopsy confirmed the diagnosis. Biopsy revealed pathological changes in mitochondrial myopathy. Furthermore, mitochondrial gene testing of the skeletal muscle revealed a single chrmM:8469-13447 deletion. In addition, we summarized the findings of 26 patients with CPEO/Kearns–Sayre syndrome who were misdiagnosed with other diseases owing to ocular symptoms. In conclusion, we reported a rare clinical case and emphasized the symptomatic diversity of CPEO. Furthermore, we provided a brief review of the diagnosis and differential diagnosis of the disease.

KEYWORDS

chronic progressive external ophthalmoplegia, case report, misdiagnosis, muscle biopsy, genetic testing

Introduction

In clinical settings, some atypical symptoms often misdirect doctors' attention during the diagnosis of some difficult diseases, thereby rubbing shoulders with the truth. For example, when chronic progressive external ophthalmoplegia (CPEO) is combined with other eye or facial symptoms, the diagnosis may be delayed for several years. CPEO is a subtype of mitochondrial encephalomyopathy that is characterized by a mutation in mitochondrial DNA (mtDNA) or nuclear DNA; this impairs adenosine triphosphate synthesis and subsequently leads to energy deficiency. Chronic progressive ptosis and impaired eye movement are the hallmark clinical symptoms of CPEO. In general, this disease occurs sporadically, with onset ranging from early childhood to ~50 years of age;

nevertheless, it most often occurs before 30 years of age and affects both men and women at a similar ratio of ∼1:1.8–2.5 (1, 2). Bilateral ptosis is often the initial symptom of CPEO; however, some patients may also experience diplopia and fatigue intolerance as initial symptoms. Progressive ptosis, ocular motility disorders, fatigue, and proximal limb weakness are the primary clinical manifestations of CPEO (3). However, the clinical presentation of CPEO overlaps with other conditions, including oculomotor myasthenia gravis, resulting in potential misdiagnosis. Herein, we present the case of a patient who was diagnosed after 6 years of seeking medical attention for her rare clinical presentation. Simultaneously, we briefly summarized the findings of previous patients with CPEO who were misdiagnosed with other diseases owing to their ocular symptoms.

Case report

A 34-year-old woman presented with a history of incomplete left eyelid closure and limited eye mobility for 8 years; she had no relevant family history. In addition, she reported mild physical activity limitation; however, she did not promptly seek medical attention. Her parents are healthy non-blood relatives. In 2017, she visited an ophthalmology hospital for these symptoms; fundoscopy and optical coherence tomography revealed the absence of any anomalies. Subsequently, she was diagnosed with myasthenia gravis and prescribed oral pyridostigmine (60 mg tid) and prednisone (30 mg qd); however, her symptoms did not significantly improve. Prednisone dosage was gradually decreased to 15 mg QD. In 2018, she experienced fatigue and weakness 6 months after giving birth. In September 2019, she discontinued pyridostigmine and prednisone because she did not notice any substantial changes in her symptoms while on this medication. In late 2020, she developed left-sided facial hypoesthesia. In 2021, her limited eye movement worsened, with emotional stress during the 8th month of pregnancy, resulting in retesting and strabismus. She sought medical attention at another hospital, where she tested negative for anti-AchR, anti-MuSK, anti-Titin, and anti-VGCC antibodies. Routine biochemical tests and cerebrospinal fluid pressure were unremarkable. However, oligoclonal bands were observed in both blood and cerebrospinal fluid samples. Moreover, in both blood and cerebrospinal fluid samples, she tested negative for anti-AQP4, anti-MOG, anti-GFAP, and anti-MBP antibodies. Enhanced chest computed tomography (CT) did not reveal any thymoma. Furthermore, cranial magnetic resonance imaging showedrevealed no significant anomalies. Electromyography (EMG) results revealed the following: (1) mixed damage to the motor fibers of the temporal branch of the left facial nerve; (2) neurogenic injury of the left orbicularis oculi muscle; and (3) bilateral neurogenic injury of the quadriceps and tibialis anterior muscles. Finally, she was diagnosed with polyneuritis cranialis. Treatment with methylprednisolone pulse therapy and B vitamins was initiated; as a result, her strabismus and diplopia improved. She was discharged on oral prednisone (60 mg qd) and B vitamins; however, the symptoms of incomplete left eyelid closure and limited eye movement did not resolve.

When she was admitted to our department in September 2021, neurological examination revealed incomplete left eyelid closure and decreased sensation on the left side of her face. Furthermore, she exhibited limited eye movement in both eyes: there was significant upward, downward, outward, and inward movement in the left eye and significant upward, downward, and outward movement in the right eye. However, bilateral ptosis and nystagmus were not observed. The bilateral upper extremity muscle strength grade was 5, whereas the bilateral lower extremity muscle strength grade was 5-, with no muscle bundle tremor.

She gave birth to one son and one daughter. The eldest daughter seems to displaying signs of fatigue intolerance.

Laboratory examination

At rest, the blood lactic acid levels were 1.8 mmol/L. After 15 min of exercise, lactic acid levels increased to 11.9 mmol/L; however, after 10 min of rest, they decreased to 8.1 mmol/L. The levels of serum lactate dehydrogenase (LDH), creatine kinase (CK), and creatine kinase isoenzyme (CK-MB) were in the normal range. Other blood routine and biochemical tests were unremarkable. Electrocardiography revealed mild changes in the T wave without any conduction block. EMG revealed the following: (1) electrophysiological signs of left facial nerve damage, characterized by lower wave amplitudes of action potentials in the orbicularis oculi, orbicularis oris, and nasal muscles compared with the contralateral side, with normal latency; and (2) negative electrophysiological findings in the repetitive electrical stimulation test. Brain magnetic resonance imaging revealed no anomalies. Finally, peripheral blood samples were collected for whole-exome and full-length mitochondrial gene sequencing. Genetic testing did not reveal any mutations in the relevant genes.

In December 2021, after obtaining consent from the patient, biopsy of the biceps muscle was performed for tissue analysis and genetic testing. Tissue biopsy revealed changes in mitochondrial myopathy. Furthermore, hematoxylin and eosin staining revealed muscle fibers of different sizes and scattered atrophic muscle fibers (Figure 1A). Modified Gömöri trichrome staining revealed a few ragged-red fibers (RRF) (Figure 1B). Moreover, succinate dehydrogenase (SDH) staining revealed scattered ragged-blue fibers (RBF) (Figure 1C). Cytochrome c oxidase (COX) staining revealed several scattered negative muscle fibers (Figure 1D). Although blood genetic testing did not reveal any relevant mutations, muscle genetic testing revealed the deletion of a meaningfully large fragment in the mitochondrial gene. Finally, mitochondrial gene analysis revealed the deletion of a large gene segment, with a single deletion region in chrmM:8469-13447. Based on these findings, the patient was finally diagnosed with CPEO (Figure 2).

Discussion

CPEO is a rare disease that was first reported by Von Grafe in 1868. Studies have reported that the prevalence of CPEO differs in different populations. For example, a study published in *Neurology* in 2005 reported that the prevalence of large-fragment mtDNA deletions is 1.6/100,000 in adults in northern Finland (4). Another study reported that the minimum estimated prevalence of CPEO

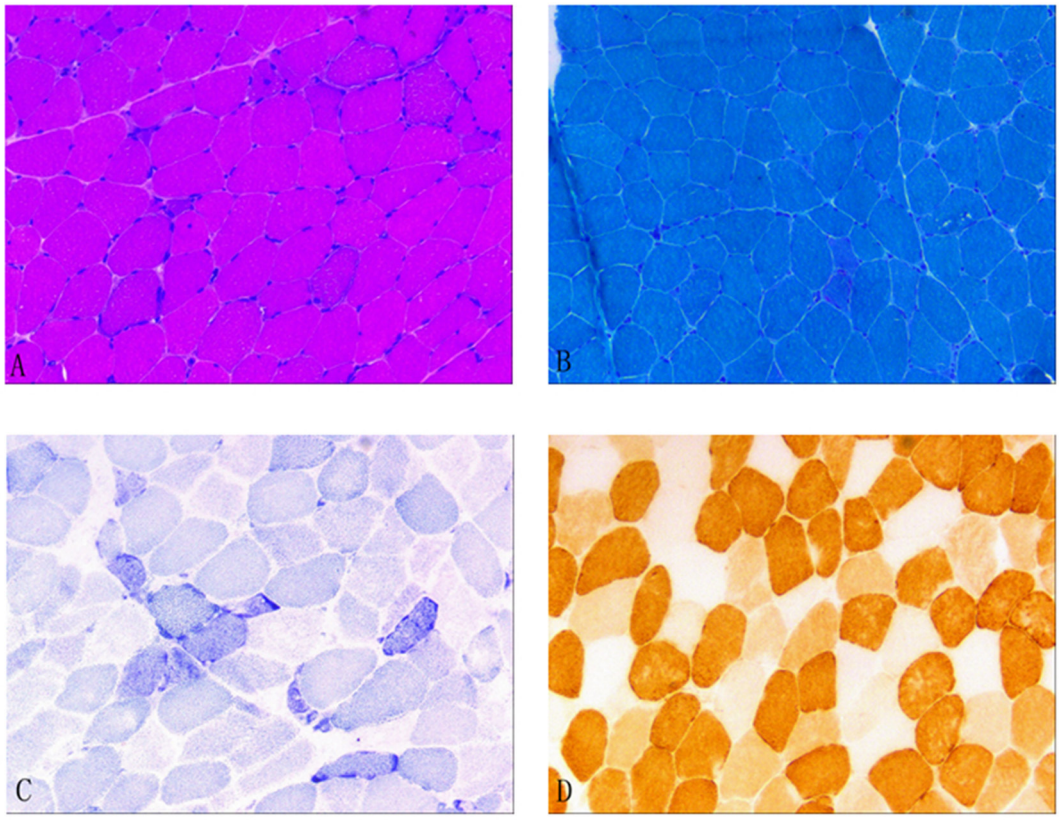

FIGURE 1
(A) Hematoxylin and eosin (HE) staining; **(B)** Modified Gömöri trichrome (MGT) staining; **(C)** Succinate dehydrogenase (SDH) staining; and **(D)** Cytochrome c oxidase (COX) staining. **(A)** HE staining revealed different muscle fiber sizes and scattered atrophic muscle fibers. **(B)** MGT staining revealed a few ragged-red fibers. **(C)** SDH staining revealed scattered ragged-blue fibers. **(D)** COX staining revealed several scattered negative muscle fibers.

is 3.39/100,000 in the UK (5). CPEO can manifest at any age; however, it is often observed during childhood and adolescence, with a higher prevalence before 30 years of age. This condition can sporadically occur or run in families, indicating that it has both sporadic and familial forms. In general, CPEO initially presents with ptosis, with patients possibly experiencing diplopia and fatigue as their initial symptoms. Because no universally accepted diagnostic criteria for CPEO are available, a comprehensive approach involving clinical evaluation, laboratory tests, muscle tissue biopsies, and mitochondrial genetic testing is warranted to establish a diagnosis. Owing to symmetrical paralysis of the bilateral extraocular muscles and slow disease progression over months or years, compensatory mechanisms in the extraocular muscles frequently maintain a balanced ocular movement, resulting in infrequent complaints of diplopia or visits to the clinics for diplopia symptoms specifically (6, 7). In biochemical tests, the levels of CK, CK-MB, and LDH are frequently measured; these markers are generally normal or only mildly increased in patients with CPEO and serve as the initial screening indicators during diagnosis. Furthermore, blood lactic acid and pyruvate tests are vital for evaluating mitochondrial function. In some cases, blood lactic acid and pyruvate levels fail to return to normal within 10 min after exercise. However, in our case, only blood lactic acid was measured, without measuring pyruvate. Nevertheless, lactic acid test results aligned with the characteristic metabolic changes associated with CPEO.

Muscle tissue biopsy of the extremities is a valuable tool for diagnosing CPEO; it generally focuses on examining the proximal skeletal muscle. Necrotic and degenerated muscle fibers can be observed under a light microscope. Gömöri staining, which stains abnormal mitochondria, reveals the presence of RRF, which is a characteristic pathological feature of mitochondrial diseases. Furthermore, SDH staining, also called RBF staining, stains the muscle fibers blue; in general, it is a more sensitive method for detecting anomalies (8). COX staining can reveal COX(−) muscle fibers because respiratory chain enzymes are inhibited in mitochondrial diseases. In the present case, muscle tissue biopsy revealed the presence of RRF, RBF, and COX(−) muscle fibers; these findings were consistent with the characteristic histological changes associated with CPEO. Figure 1 provides a visual representation of the study findings.

In patients with CPEO, the primary mutation type is a single large-fragment deletion of mtDNA (9). A study conducted at Peking University First Hospital has revealed that the size of the deletion fragment of mtDNA is inversely correlated with the disease onset age, with larger deletions associated with earlier disease onset (10). Furthermore, point mutations in mtDNA or nuclear DNA can result in CPEO development (11, 12).

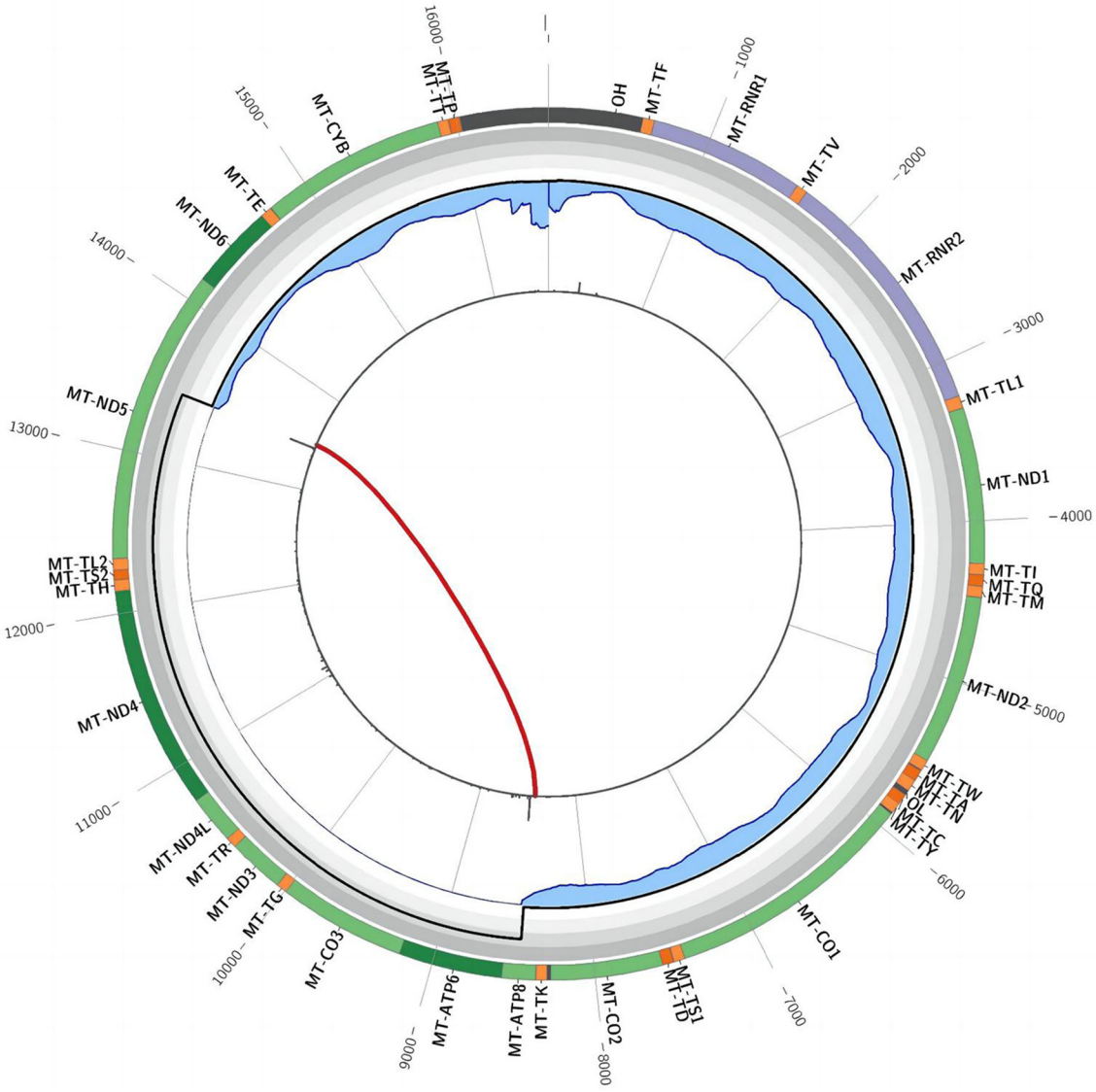

FIGURE 2
Triangular muscle mitochondrial gene testing. A single deletion (chrmM:8469-13447, arrow) was observed in the mitochondrial gene.

Mitochondrial genetic testing is the gold standard for CPEO diagnosis. Biological samples such as blood, urine, saliva, hair follicles, and muscle tissues can be used to perform genetic testing for mitochondrial encephalomyopathy. The first four samples can be collected non-invasively; however, muscle tissues achieve the highest positive rate, whereas blood samples achieve the lowest rate (13–16). Because mutant mtDNA is abundant in skeletal muscle tissues, they are generally preferred for testing purposes. A single major fragment deletion of mtDNA is commonly observed in patients with sporadic CPEO. Schon (17) identified a deletion fragment of 1.3 kb—7.6 kb, spanning from base 8483 to base 13459. In the present case, whole-exome sequencing of peripheral blood samples and full-length sequencing of mitochondrial genes only revealed mutations with no clinical significance. However, these findings did not align with muscle biopsy results; therefore, the patient underwent muscle tissue genetic testing. Fortunately, genetic testing confirmed the presence of CPEO (Figure 2).

Interestingly, in the present case, unilateral eyelid closure opacification and facial hypoesthesia were observed during the definitive diagnosis. EMG revealed facial nerve damage and neurogenic orbicularis oculi damage; therefore, the hospital diagnosed the patient with polyneuritis cranialis. This diagnosis was supported by improvements in the patient's symptoms after treatment with corticosteroids and B vitamins. Although CPEO is associated with peripheral neuropathy, it generally manifests as symmetric sensory and motor deficits in the limbs, rarely affecting the unilateral cranial nerves (2, 18, 19). Previous studies (20–22) have reported that the orbicularis oculi is involved in CPEO, resulting in incomplete closure of the eyelid. However, electromyography generally indicates myopathic weakness, with involvement of both sides. Furthermore, some studies (23, 24) have identified RRF in the muscle tissues of patients with CPEO and weakness of the orbicularis oculi via muscle biopsies, suggesting a myogenic lesion. Therefore, in the present case, the patient

presented with a combination of unilateral facial nerve injury, which was supported by neurophysiological findings, and a possible trigeminal nerve injury, which remains unreported. Considering that incomplete eyelid closure did not worsen with the progression of oculomotor limitation in 2021, we suggest that the facial nerve injury in the present case was independent of CPEO. Subsequently, we believe that our patient experienced an independent left facial nerve injury during CPEO progression.

Owing to its rare clinical symptoms, CPEO can be easily overlooked or misdiagnosed. Therefore, differentiating it from other conditions that may present with similar extraocular muscle paralysis, including oculopharyngeal myasthenia gravis (OMG), oculopharyngeal muscular dystrophy (OPMD), and ocular pharyngeal distal myopathy (OPDM), is vital. Therefore, we reviewed the relevant literature on cases of CPEO/ Kearns–Sayre syndrome (KSS) that were previously misdiagnosed as other diseases owing to ocular symptoms (Table 1).

In total, 26 patients were misdiagnosed. Of these, 14 were females (53.8%). In 7 of 26 patients, the disease started when they were minors (≤18 years old); furthermore, 17 of 26 patients presented with symptoms in adulthood. For 2 patients, the age of disease onset was not mentioned.

The onset age was recorded in 20 patients, with a mean age of 31.55 ± 16.72 years. The age at first diagnosis was recorded in 10 patients, with a mean age of 33.5 ± 16.88 years. The age at final diagnosis was recorded in 12 patients, with a mean age of 38 ± 16.78 years. Considering the differences in the onset age between patients with KSS and CPEO, the mean onset age was 34.20 ± 15.47 years for 18 of 24 patients with CPEO, the mean age at first diagnosis was 36.33 ± 15.37 years for 9 of 24 patients, and the mean age at final diagnosis was 43.10 ± 13.42 years for 10 of 24 patients.

Oculomotor palsy was observed in 23 of 26 patients and ptosis was observed in 23 of 26 patients. Fatigue or malaise was observed in 15 of 26 patients. Strabismus was observed in 2 of 26 patients (case 2 and our patient). Diplopia was also observed in 2 of 26 patients (case 24 and our patient). Moreover, dysarthria or dysphagia was observed in 6 of 26 patients. Vision and hearing loss were observed in 1 of 26 patients, and arthralgia was also observed in 1 of 26 patients (case 19). Finally, 1 of 26 patients experienced unsteady gait and bradykinesia (case 3).

Of the 16 documented patients, 1 (case 18) tested positive for serum AchR antibodies via ELISA, resulting in the diagnosis of myasthenia gravis. However, clinical symptoms did not improve after 2 months of oral brompheniramine. After subjecting the initial serum samples to radioimmunoassay, the results were negative. This emphasizes the interference of test results in the presence of false positives in disease diagnosis.

Serum lactate was higher than normal in 4 of 8 patients. Furthermore, LDH was increased in 2 of 4 patients and CK was increased in 5 of 15 patients.

The muscle biopsy findings of 22 patients were reported, of which 20 exhibited RRF or/and COX(−) muscle fibers, whereas the remaining 2 patients had possible mitochondrial lesions (cases 1 and 22).

Furthermore, the genetic testing results of 19 patients were reported. Four patients had a single large-fragment deletion, whereas 15 patients had a point mutation.

Twenty patients were previously diagnosed with myasthenia gravis: 18 patients were diagnosed with ocular myasthenia and administered brompheniramine. On the other hand, five patients were previously diagnosed with OPMD, and two patients were previously diagnosed with myositis owing to increased LDH and CK levels (cases 19 and 21). Progressive supranuclear palsy owing to ataxia was suspected in one patient (case 3).

In general, OMG manifests as ptosis and diplopia, with milder symptoms in the morning, which worsen as the day progresses. OMG is commonly characterized by positive muscle fatigue and Tensilon test findings, the presence of serum anti-AChR antibodies, and positive repeated nerve stimulation test results. Furthermore, chest CT may confirm the presence of thymoma, and corticosteroid therapy is often effective. In our case, relevant antibodies and repeated nerve stimulation test results were negative, and chest CT revealed thymoma; therefore, OMG was excluded as a diagnosis.

OPMD frequently starts in middle age. Paralysis of the extraocular and pharyngeal muscles is an early clinical manifestation, with symptoms progressively exacerbating. Muscle pathology reveals rimmed vacuoles and fenestrated intranuclear inclusion bodies in the muscle fibers. Furthermore, genetic testing reveals mutations in *PABPN1*.

In general, the initial symptom of OPDM is droopy eyelids; however, it later progresses to dysphagia and limb weakness. Studies (38–41) have linked this condition to mutations in genes such as *LRP12*, *GIPC1*, *NOTCH2NLC*, and *RILPL1*. In the present case, we did not observe pharyngeal muscle weakness, and the genetic testing results were inconsistent with those of OPDM. Therefore, oculopharyngeal distal myopathy was excluded from the diagnosis.

KSS, a severe subtype of CPEO, is characterized by the risk of sudden death owing to heart block. It is defined using specific criteria (3, 42), including (1) onset before 20 years of age; (2) clinical features of CPEO accompanied by retinopathy pigmentosa; and (3) presence of one of the following: cardiac conduction anomalies, cerebrospinal fluid protein level > 1 g/L, or cerebellar dysfunction. In the present case, symptoms presented after 20 years of age, with no evidence of retinopathy pigmentosa. The protein levels in the cerebrospinal fluid were in the normal range, with no signs of ataxia or other types of cerebellar dysfunctions. Furthermore, electrocardiography did not reveal any conduction blocks. Therefore, our patient did not fulfill the diagnostic criteria for KSS at that time.

During the follow-up period until April 2023, incomplete left eyelid closure persisted, with limited movement of both eyes. Fortunately, there was no significant disease progression, and electrocardiography did not reveal any conduction block.

At present, no specific treatment modalities are available for CPEO, and medication primarily involves administering vitamins and coenzyme factors (43). Corticosteroids may help decrease lactic acid accumulation and provide therapeutic benefits for the disease. However, gene therapy holds promise as a potential treatment strategy for CPEO. Ongoing advances in gene therapy may lead to significant breakthroughs in the treatment of this disease in the future.

In the present study, we demonstrated the challenges faced by physicians in diagnosing CPEO, a rare presentation. The patient's clinical symptoms can mislead the physician's direction of

TABLE 1 Literature review of patients with CPEO/KSS who were misdiagnosed with other diseases owing to ocular symptoms.

#	Sex	Onset age	Age at initial diagnosis	Age at final diagnosis	Clinical features	AchR	Serum lactate	LDH	CK	Muscle biopsy findings	Nucleotide changes	Previous treatment	Previous diagnosis	Final diagnosis	References
1	F	NM	35	56	Ophthalmoplegia and subjective muscle fatigue	Negative	NM	NM	NM	Possible mitochondrial cytopathy	NM	IVIG, AZA, pyridostigmine, and prednisone	MG	CPEO	(25)
2	M	7	8	15	Ptosis, exotropia, ophthalmoplegia, and weakness	Negative	NM	NM	NM	NM	m.6578-14460	Pyridostigmine	MG	KSS	(26)
3	M	57	58	61	Ptosis, diplopia, ophthalmoplegia, bradykinesia, and unsteady gait	Negative	NM	NM	NM	COX-negative fibers	POLG (c.2209G > A and c.3287G > A)	Pyridostigmine and levodopa	MG and possible progressive supranuclear palsy	CPEO	(27)
4	F	8	NM	10	Ptosis, weakness, decreased vision, and impaired hearing	Negative	NM	NM	NM	RRF	NM	NM	MG	KSS	(28)
5	M	30	NM	NM	Ophthalmoplegia, ptosis, weakness, dysarthria, and dysphagia	NM	NM	NM	Increase	NM	TWNK c.1361T > G	No treatment	OPMD	CPEO	(29)
6	F	adult	NM	NM	Ophthalmoplegia and ptosis	Negative	NM	NM	NM	RRF and COX-negative fibers	TWNK c.1070G > C	No treatment	MG	CPEO	
7	M	40	NM	NM	Ophthalmoplegia, ptosis, and weakness	Negative	Increase	NM	Normal	NM	TWNK c.1070G > C	Pyridostigmine	MG	CPEO	
8	F	60	NM	NM	Ophthalmoplegia, ptosis, weakness, and dysphagia	Negative	NM	NM	Normal	RBF and COX-negative fibers	TWNK c.1070G > C	Pyridostigmine and glucocorticoids	MG	CPEO	
9	M	17	NM	NM	Ophthalmoplegia and ptosis	Negative	Normal	NM	Normal	COX-negative fibers	TWNK c.1121G > A	No treatment	MG	CPEO	

(Continued)

10.3389/fneur.2023.1268053

TABLE 1 (Continued)

#	Sex	Onset age	Age at initial diagnosis	Age at final diagnosis	Clinical features	AchR	Serum lactate	LDH	CK	Muscle biopsy findings	Nucleotide changes	Previous treatment	Previous diagnosis	Final diagnosis	References
10	F	60	NM	NM	Ophthalmoplegia and ptosis	Negative	Normal	NM	Normal	RRF and COX-negative fibers	TWNK c.1361T > G	Pyridost igmine, acute episodes: IVIg, plasma exchange, and immunosu ppression	MG	CPEO	
11	M	25	NM	NM	Ophthalmoplegia and ptosis	Negative	Normal	NM	Increase	RBF and COX-negative fibers	TWNK c.1070G > C	No treatment	MG and OPMD	CPEO	
12	M	adult	NM	NM	Ophthalmoplegia and ptosis	NM	NM	NM	NM	RBF and COX-negative fibers	TWNK c.908G > A	No treatment	OPMD	CPEO	
13	F	40	NM	NM	Ptosis, weakness, and dysphagia	NM	NM	NM	NM	RRF and COX-negative fibers	TWNK c.1106C > T	No treatment	OPMD	CPEO	
14	M	40	NM	NM	Ptosis	Negative	NM	NM	Normal	RRF and COX-negative fibers	TWNK c.1070G > C	No treatment	MG	CPEO	
15	F	NM	NM	NM	Ophthalmoplegia	Negative	NM	NM	Normal	RRF and COX-negative fibers	TWNK c.1361T > G	No treatment	MG	CPEO	
16	F	adult	NM	NM	Ophthalmoplegia, ptosis, and weakness	NM	NM	NM	Normal	RRF	TWNK c.1361T > G	No treatment	OPMD	CPEO	
17	M	child-hood	NM	NM	Ophthalmoplegia and ptosis	Negative	NM	NM	Increase	COX-negative fibers	TWNK c.1084G > C	No treatment	MG	CPEO	

(Continued)

10.3389/fneur.2023.1268053

TABLE 1 (Continued)

#	Sex	Onset age	Age at initial diagnosis	Age at final diagnosis	Clinical features	AchR	Serum lactate	LDH	CK	Muscle biopsy findings	Nucleotide changes	Previous treatment	Previous diagnosis	Final diagnosis	References
18	F	29	34	34	Ophthalmoplegia and ptosis	Positive (ELISA) and negative (RIA)	NM	NM	NM	RRF	a single, large-fragment mitochondrial DNA deletion	Pyridost igmine	Possible ocular myasthenia	CPEO	(30)
19	F	40	41	43	Ophthalmoplegia, ptosis, arthralgias, proximal muscular weakness, and dysphonia	Negative	NM	Increase	Increase	RRF and COX-negative fibers	NM	Corticosteroids	Polymyositis	CPEO	(31)
20	M	40	64	64	Ophthalmoplegia, ptosis, neck weakness, quadriparesis, and dyspnea	Negative	Normal	NM	NM	RRF and COX-negative fibers	C10orf2 c.1433 G > T	Plasmapheresis, neostigmine, prednisone, and mechanical ventilation	Myasthenic crisis	CPEO	(32)
21	F	33	34	35	Ophthalmoplegia, ptosis, and weakness	NM	NM	Increase	Increase	RRF and COX-negative fibers	m.a deletion of 16.6 kilobases significant	Corticosteroid and cyclosporin A	Polymyositis	KSS	(33)
22	F	6	NM	25	Ophthalmoplegia, ptosis, weakness, and dysarthria	NM	Normal	Normal	Normal	Abnormal mitochondria	NM	NM	MG	CPEO	(34)
23	F	46	NM	52	Ophthalmoplegia, ptosis, and weakness	NM	NM	NM	NM	RRF and COX-negative fibers	NM	Anticholinesterases	MG	CPEO	(35)
24	M	14	16	29	Ophthalmoplegia, ptosis, diplopia, and weakness	NM	Increase	NM	Normal	RRF	NM	Anticholinesterases	Ocular myasthenia	CPEO	(36)
25	M	13	17	NM	Ophthalmoplegia and ptosis	NM	NM	NM	NM	NM	NM	NM	MG	CPEO	(37)
26	F	26	28	32	Ophthalmoplegia, incomplete left eyelid closure, exotropia, diplopia, and weakness	Negative	Increase	Normal	Normal	RRF, RBF, and COX-negative fibers	m.8469-13447	Pyridost igmine and glucocorticoids	MG and polyneuritis	CPEO	Our case

M, male; F, female; NM, not mentioned.

10.3389/fneur.2023.1268053

diagnosis. Therefore, to diagnose such patients, physicians should master the diagnostic process as well as be familiar with the differential diagnosis of related diseases.

Our study has some limitations that should be acknowledged. Initially, the results of peripheral blood gene sequencing were not positive. We performed skeletal muscle biopsy only after a 3-month interval. Therefore, we suggest that patients with a clinical suspicion of mitochondrial encephalomyopathy, who can tolerate the pain associated with biopsy, should undergo skeletal muscle biopsy after directly consulting with them.

Data availability statement

The original contributions presented in the study are included in the article/Supplementary material, further inquiries can be directed to the corresponding authors.

Ethics statement

The studies involving humans were approved by the Shenzhen Traditional Chinese Medicine Hospital Ethics Committee. The studies were conducted in accordance with the local legislation and institutional requirements. The participants provided their written informed consent to participate in this study. Written informed consent was obtained from the individual(s) for the publication of any potentially identifiable images or data included in this article.

Author contributions

ZF: Writing – original draft, Writing – review & editing, Supervision. RL: Writing – review & editing, Software. JW: Resources, Writing – review & editing, Investigation. XL: Resources, Writing – review & editing, Investigation. XC: Writing – review & editing, Investigation. YL: Writing – review & editing, Software. WQ: Investigation, Writing – review & editing. XQ: Writing – review & editing, Resources, Funding acquisition. FK: Writing – review & editing, Funding acquisition, Supervision, Writing – original draft.

Funding

The author(s) declare financial support was received for the research, authorship, and/or publication of this article. This work was supported by the Sanming Project of Medicine in Shenzhen (grant number SZZYSM202111011), Traditional Chinese Medicine Bureau of Guangdong Province (grant number 20221357), and 3030 project of Clinical Research Program in Shenzhen Traditional Chinese Medicine Hospital in 2021 (grant number G3030202132).

Acknowledgments

We thank Nanfang Hospital Precision Medicine Center for excellent Gene Technical Assistance. The authors would like to thank Associate Professor Hai-Shan Jiang from Neurology Department Nanfang Hospital for the case consolation. We thank Bullet Edits Limited for the linguistic editing and proofreading of the manuscript.

Conflict of interest

The authors declare that the research was conducted in the absence of any commercial or financial relationships that could be construed as a potential conflict of interest.

Publisher's note

All claims expressed in this article are solely those of the authors and do not necessarily represent those of their affiliated organizations, or those of the publisher, the editors and the reviewers. Any product that may be evaluated in this article, or claim that may be made by its manufacturer, is not guaranteed or endorsed by the publisher.

Supplementary material

The Supplementary Material for this article can be found online at: https://www.frontiersin.org/articles/10.3389/fneur.2023.1268053/full#supplementary-material

References

1. Heighton JN, Brady LI, Newman MC, Tarnopolsky MA. Clinical and demographic features of chronic progressive external ophthalmoplegia in a large adult-onset cohort. *Mitochondrion.* (2019) 44:15–9. doi: 10.1016/j.mito.2017.12.006

2. Pfeffer G, Sirrs S, Wade NK, Mezei MM. Multisystem disorder in late-onset chronic progressive external ophthalmoplegia. *Can J Neurol Sci.* (2011) 38:119–23. doi: 10.1017/S031716710001115X

3. Fraser JA, Biousse V, Newman NJ. The neuro-ophthalmology of mitochondrial disease. *Surv Ophthalmol.* (2010) 55:299–334. doi: 10.1016/j.survophthal.2009.10.002

4. Remes AM, Majamaa-Voltti K, Kärppä M, Moilanen JS, Uimonen S, Helander H, et al. Prevalence of large-scale mitochondrial DNA deletions in an adult Finnish population. *Neurology.* (2005) 64:976–81. doi: 10.1212/01.WNL.0000154518.31302.ED

5. Yu-Wai-Man P, Clements A, Nesbitt V, Griffiths PG, Gorman GS, Schaefer AM, McFarland R. A national epidemiological study of chronic progressive external ophthalmoplegia in the United Kingdom-molecular genetic features and neurological burden. *Inv Ophthalmol Visual Sci.* (2014) 55:5109.

6. McClelland C, Manousakis G, Lee MS. Progressive external ophthalmoplegia. *Curr Neurol Neurosci Rep.* (2016) 16:1–10. doi: 10.1007/s11910-016-0652-7

7. Bau V, Zierz S. Update on chronic progressive external ophthalmoplegia. *Strabismus.* (2005) 13:133–42. doi: 10.1080/09273970500216432

8. Hammans SR, Sweeney MG, Holt IJ, Cooper JM, Toscano A, Clark JB, et al. Evidence for intramitochondrial complementation between deleted and normal mitochondrial DNA in some patients with mitochondrial myopathy. *J Neurol Sci.* (1992) 107:87–92. doi: 10.1016/0022-510X(92)90213-5

9. Moraes CT, DiMauro S, Zeviani M, Lombes A, Shanske S, Miranda AF, et al. Mitochondrial DNA deletions in progressive external ophthalmoplegia and Kearns-Sayre syndrome. *New England J Med.* (1989) 320:1293–9. doi: 10.1056/NEJM198905183202001

10. Qi L. Clinical phenotype and genotype analysis in 61 patients with large scale single deletion in mitochondrial DNA. *Chin J Neurol.* (2015) 48: 382–9. doi: 10.3760/cma.j.issn.1006-7876.2015.05.007

11. Bacalhau M, Simões M, Rocha MC, Hardy SA, Vincent AE, Durães J, et al. Disclosing the functional changes of two genetic alterations in a patient with chronic progressive external ophthalmoplegia: report of the novel mtDNA m. 7486G> A variant. *Neuromuscular Disorders.* (2018) 28:350–60. doi: 10.1016/j.nmd.2017.11.006

12. Grady JP, Campbell G, Ratnaike T, Blakely EL, Falkous G, Nesbitt V, et al. Disease progression in patients with single, large-scale mitochondrial DNA deletions. *Brain.* (2014) 137:323–34. doi: 10.1093/brain/awt321

13. O'Callaghan MM, Emperador S, Pineda M, López-Gallardo E, Montero R, Yubero D, et al. Mutation loads in different tissues from six pathogenic mtDNA point mutations. *Mitochondrion.* (2015) 22:17–22. doi: 10.1016/j.mito.2015.03.001

14. Ma Y, Fang F, Yang Y, Zou L, Zhang Y, Wang S, et al. The study of mitochondrial A3243G mutation in different samples. *Mitochondrion.* (2009) 9:139–43. doi: 10.1016/j.mito.2009.01.004

15. Sue CM, Quigley A, Katsabanis S, Kapsa R, Crimmins DS, Byrne E, et al. Detection of MELAS A3243G point mutation in muscle, blood and hair follicles. *J Neurol Sci.* (1998) 161:36–9. doi: 10.1016/S0022-510X(98)00179-8

16. Kotsimbos N, Jean-Francois MB, Huizing M, Kapsa RM, Lertrit P, Siregar NC, et al. Rapid and noninvasive screening of patients with mitochondrial myopathy. *Hum Mutat.* (1994) 4:132–5. doi: 10.1002/humu.1380040207

17. Schon EA, Rizzuto R, Moraes CT, Nakase H, Zeviani M, DiMauro S. A direct repeat is a hotspot for large-scale deletion of human mitochondrial DNA. *Science.* (1989) 244:346–9. doi: 10.1126/science.2711184

18. Amati-Bonneau P, Valentino ML, Reynier P, Gallardo ME, Bornstein B, Boissière A, et al. OPA1 mutations induce mitochondrial DNA instability and optic atrophy 'plus' phenotypes. *Brain.* (2008) 131:338–51. doi: 10.1093/brain/awm298

19. Milone M, Brunetti-Pierri N, Tang LY, Kumar N, Mezei MM, Josephs K, et al. Sensory ataxic neuropathy with ophthalmoparesis caused by POLG mutations. *Neuromuscular Disorders.* (2008) 18:626–32. doi: 10.1016/j.nmd.2008.05.009

20. Melberg A, Lundberg PO, Henriksson KG, Olsson Y, Stålberg E. Muscle-nerve involvement in autosomal dominant progressive external ophthalmoplegia with hypogonadism. *Muscle and Nerve Off J Am Assoc Electrodiag Med.* (1996) 19:751–7. doi: 10.1002/(SICI)1097-4598(199606)19:6<751::AID-MUS10>3.0.CO;2-O

21. Croft PB, Cutting JC, Jewesbury ECO, Blackwood W, Mair WGP. Ocular myopathy (progressive external ophthalmoplegia) with neuropathic complications. *Acta Neurol Scand.* (1977) 55:169–97. doi: 10.1111/j.1600-0404.1977.tb05638.x

22. Magora A, Zauberman H. Ocular myopathy. *Arch Neurol.* (1969) 20:1–8. doi: 10.1001/archneur.1969.00480070011001

23. Almousa R, Charlton A, Rajesh ST, Sundar G, Amrith S. Optimizing muscle biopsy for the diagnosis of mitochondrial myopathy. *Ophthal Plast Reconstr Surg.* (2009) 25:366–70. doi: 10.1097/IOP.0b013e3181b2fd06

24. Eshaghian J, Anderson RL, Weingeist TA, Hart MN, Cancilla PA. Orbicularis oculi muscle in chronic progressive external ophthalmoplegia. *Arch Ophthalmol.* (1980) 98:1070–3. doi: 10.1001/archopht.1980.01020031060010

25. Harrison P, Barton J, Winkel A. Chronic mimics of myasthenia gravis: a retrospective case series. *Neuromuscular Disorders.* (2023) 33:250–6. doi: 10.1016/j.nmd.2023.01.006

26. Sokol JT, Hoyek S, Fulton AB, Patel NA. Kearns-sayre syndrome masquerading as myasthenia gravis. *Retinal Cases Brief Rep.* (2022) 10–1097. doi: 10.1097/ICB.0000000000001397

27. Elwan M, Schaefer AM, Craig K, Hopton S, Falkous G, Blakely EL, et al. Changing faces of mitochondrial disease: autosomal recessive POLG disease mimicking myasthenia gravis and progressive supranuclear palsy. *BMJ Neurology Open.* (2022) 4:e000352. doi: 10.1136/bmjno-2022-000352

28. Pawar N, Manayath GJ, Verghese S, Chandrakanth P, Shah V, Raut A, et al. Potpourri of retinopathies in rare eye disease–A case series. *Ind J Ophthalmol.* (2022) 70:2605. doi: 10.4103/ijo.IJO_3002_21

29. Bermejo-Guerrero L, Serrano-Lorenzo P, Blázquez-Encinar A, Gutiérrez-Gutiérrez G, Martínez-Vicente L, Galán-Dávila L, et al. Clinical, histological, and genetic features of 25 patients with autosomal dominant progressive external ophthalmoplegia (Ad-PEO)/PEO-plus due to TWNK mutations. *J Clin Med.* (2022) 11:22. doi: 10.3390/jcm11010022

30. Rajput R, Sachdev A, Din N, Damato EM, Murray A. False positive acetylcholine receptor antibodies in a case of unilateral chronic progressive external ophthalmoplegia: case report and review of literature. *Orbit.* (2018) 37:385–8. doi: 10.1080/01676830.2017.1423350

31. Bisceglia M, Crociani P, Fogli D, Centola A, Galliani CA, Pasquinelli G. Selected case from the Arkadi M. Rywlin international pathology slide series: mitochondrial myopathy presenting with chronic progressive external ophthalmoplegia (CPEO): a case report. *Adv Anatomic Pathol.* (2014) 21:461–8. doi: 10.1097/PAP.0000000000000045

32. Gonzalez-Moron D, Bueri J, Kauffman MA. Progressive external ophthalmoplegia (PEO) due to a mutation in the C10orf2 (PEO1) gene mimicking a myasthenic crisis. *Case Rep.* (2013) 2013:bcr2013010181. doi: 10.1136/bcr-2013-010181

33. Corrado A, Cantatore FP, Serlenga L, Amati A, Petruzzella V, Lapadula G. Mitochondrial disease mimicking polymyositis: a case report. *Clin Rheumatol.* (2002) 21:411–4. doi: 10.1007/s100670200110

34. Calderón-Garcidueñas AL, Pérez-Loria O, Alberto-Sagástegui J, Farías-García R. External progressive ophthalmoplegia secondary to mitochondrial myopathy. *Rep Case Rev Liter Gaceta Medica de Mexico.* (2000) 136:267–71.

35. Johnson MA, Turnbull DM, Dick DJ, Sherratt HSA. A partial deficiency of cytochrome c oxidase in chronic progressive external ophthalmoplegia. *J Neurol Sci.* (1983) 60:31–53. doi: 10.1016/0022-510X(83)90125-9

36. Byrne E. Clinical features of mitochondrial myopathy. *Aust N Z J Med.* (1983) 13:353–8. doi: 10.1111/j.1445-5994.1983.tb04480.x

37. Beckerman BL, Henkind P. Progressive external ophthalmoplegia and benign retinal pigmentation. *Am J Ophthalmol.* (1976) 81:89–92. doi: 10.1016/0002-9394(76)90197-5

38. Deng J, Yu J, Li P, Luan X, Cao L, Zhao J, et al. Expansion of GGC repeat in GIPC1 is associated with oculopharyngodistal myopathy. *The Am J Hum Genetics.* (2020) 106:793–804. doi: 10.1016/j.ajhg.2020.04.011

39. Ishiura H, Shibata S, Yoshimura J, Suzuki Y, Qu W, Doi K, et al. Noncoding CGG repeat expansions in neuronal intranuclear inclusion disease, oculopharyngodistal myopathy and an overlapping disease. *Nat Genet.* (2019) 51:1222–32. doi: 10.1038/s41588-019-0458-z

40. Zeng YH, Yang K, Du GQ, Chen YK, Cao CY, Qiu YS, et al. GGC repeat expansion of RILPL1 is associated with oculopharyngodistal myopathy. *Ann Neurol.* (2022) 92:512–26. doi: 10.1002/ana.26436

41. Yu J, Deng J, Guo X, Shan J, Luan X, Cao L, et al. The GGC repeat expansion in NOTCH2NLC is associated with oculopharyngodistal myopathy type 3. *Brain.* (2021) 144:1819–32. doi: 10.1093/brain/awab077

42. Finsterer J. Central nervous system manifestations of mitochondrial disorders. *Acta Neurol Scand.* (2006) 114:217–38. doi: 10.1111/j.1600-0404.2006.00671.x

43. DiMauro S, Mancuso M. Mitochondrial diseases: therapeutic approaches. *Biosci Rep.* (2007) 27:125–37. doi: 10.1007/s10540-007-9041-4

frontiers | Frontiers in Neurology

TYPE Case Report
PUBLISHED 11 January 2024
DOI 10.3389/fneur.2023.1334743

OPEN ACCESS

EDITED BY
Giovanni Meola,
University of Milan, Italy

REVIEWED BY
Paulo Victor Sgobbi Souza,
Federal University of São Paulo, Brazil
Wladimir Bocca Vieira De Rezende Pinto,
Federal University of São Paulo, Brazil
Elena Di Pierro,
IRCCS Ca 'Granda Foundation Maggiore Policlinico Hospital, Italy

*CORRESPONDENCE
Zhihua Si
✉ sizhihua35@126.com

RECEIVED 07 November 2023
ACCEPTED 19 December 2023
PUBLISHED 11 January 2024

CITATION
Lin J, Liu J, Wang A and Si Z (2024) A case report of acute intermittent porphyria leading to severe disability. *Front. Neurol.* 14:1334743. doi: 10.3389/fneur.2023.1334743

A case report of acute intermittent porphyria leading to severe disability

Jie Lin[1], Jinzhi Liu[2], Aihua Wang[2] and Zhihua Si[2]*

[1]Department of Neurology, Shandong Provincial Qianfoshan Hospital, Shandong University, Shandong Institute of Neuroimmunology, Shandong Key Laboratory of Rheumatic Disease and Translational Medicine, Shandong, China, [2]Department of Neurology, The First Affiliated Hospital of Shandong First Medical University & Shandong Provincial Qianfoshan Hospital, Shandong Institute of Neuroimmunology, Shandong Key Laboratory of Rheumatic Disease and Translational Medicine, Shandong, China

Acute intermittent porphyria (AIP) is a rare inherited metabolic disorder resulting from increased production of porphyrins and their precursors, δ-aminolevulinic acid (ALA) and porphobilinogen (PBG), due to deficiencies in the enzymatic activity of the heme synthesis pathway. The disease is typically characterized by a triad of abdominal pain, neurologic impairment symptoms, and psychiatric abnormalities. However, only a small percentage of patients present with this classic triad of symptoms. Our female patient, aged 23, was admitted to the hospital with a 4-year history of abnormal mood episodes and weakness in the limbs for over 1 week. She had a previous medical history of intestinal obstruction. After admission, a cranial MRI revealed reversible posterior leukoencephalopathy imaging manifestations, and the patient exhibited weakness of the extremities, respiratory failure, seizures, and severely reduced serum sodium concentration. The diagnosis of AIP was ultimately confirmed by a positive urine PBG-sunlight test and analysis of HMBS gene variants. The absence of typical triadic signs in acute attacks of AIP can make early recognition of the disease challenging. We present a case with multiple typical clinical manifestations of AIP in the hope of aiding clinicians in fully recognizing acute intermittent porphyria.

KEYWORDS

acute intermittent porphyria, abdominal pain, limb weakness, epilepsy, psychiatric abnormalities

Introduction

Porphyrias are a group of metabolic disorders resulting from impaired heme biosynthesis, leading to abnormally high concentrations of porphyrins or their precursors that accumulate in tissues and cause cellular damage. These diseases are primarily caused by enzyme defects and are inherited in an autosomal dominant manner with low epistasis (1). They can be categorized into two groups based on the site of porphyrin production: erythropoietic porphyrias, characterized by skin damage and minimal neurological involvement, and hepatic porphyrias, characterized by neurological and visceral signs and symptoms (2). Hepatic porphyrias is subdivided into acute hepatic porphyria and chronic hepatic porphyria. Acute hepatic porphyrias (AHPs) is a complex group of inborn errors of metabolism that result in acute episodic neurovisceral attacks, encompassing four life-threatening disorders—acute intermittent porphyria (AIP), hereditary coproporphyria (HCP), variegate porphyria (VP), and delta- or 5-aminolevulinic acid (ALA) dehydratase deficiency (or Doss porphyria) (ALADP). The mode of inheritance of acute hepatic

porphyria is autosomal dominant with low penetrance, except for ALAD-deficiency hematoporphyria (ALADP), which is autosomal recessive. AIP is classified as a subtype of acute hepatic porphyria and is the most frequently encountered type of this disorder (3, 4). AIP is a hereditary disease resulting from defects in the HMBS gene encoding porphobilinogen deaminase (PBG deaminase), the third key enzyme in the heme synthesis pathway. Deficiency of this enzyme leads to the accumulation of toxic porphyrin precursors, primarily δ-aminolevulinic acid (ALA) and porphobilinogen (PBG). Due to its toxic impact on nerve fibers, AIP can manifest clinically as abdominal pain, neuropathy, and psychiatric abnormalities (5). AIP is a rare disease often overlooked by clinicians. As patients may not exhibit multiple typical symptoms simultaneously, there can be a considerable delay between the first symptom and the diagnosis of porphyria, resulting in decreased quality of life, permanent neuropathy, severe and long-lasting sequelae, and even death. Here, we present a case of acute intermittent porphyria with an acute onset of severe limb weakness progressing to respiratory muscle weakness and respiratory failure. This case report aims to raise awareness among clinicians and facilitate early recognition and accurate diagnosis of this rare disease.

Case

On April 9, 2023, a 23-year-old woman was admitted to the hospital with a history of abnormal mood episodes for 4 years and weakness in the extremities for over 1 week. The patient had experienced intestinal obstruction in 2018, which was conservatively treated with satisfactory results, without any significant personal or family medical history. The patient began to exhibit mood abnormalities 4 years ago, manifesting as signs of depression and irritability. Over the years, the patient has frequently experienced abdominal and lumbar pain, leading her to engage in habitual jumping to alleviate these discomforts. These physical symptoms were accompanied by panic attacks, chest tightness, and difficulty sleeping. These symptoms often preceded menstruation and resolved spontaneously post-menstruation. Despite being treated with citalopram, olanzapine, and quetiapine at a hospital, the symptoms persisted. One month ago, the patient again became irritable and experienced insomnia, accompanied by unresponsiveness. Consequently, she was admitted to an external hospital, though the details of the consultation and treatment remain unknown. The symptoms did not improve significantly. One week prior to admission, the patient developed weakness in all four limbs, particularly the upper limbs, and progressively became bedridden. She also experienced dysphagia, shortness of breath, urination difficulties, and mental depression. Physical examination revealed moderate growth, malnutrition, a passive position, emaciation, and cyanosis. The patient had a urinary catheter and gastric tube in place. The remaining examination findings were unremarkable. The neurological examination showed that the patient was unconscious, non-verbal, and could only open her eyes in response to stabbing pain. The bilateral pupils were equal in size and round, with a diameter of approximately 4.0 mm, and the direct and indirect light reflexes were sensitive. The muscle strength of the limbs was weak, and there was a slight avoidance response to stabbing pain. Additionally, the patient exhibited decreased muscle tone in the extremities, absent tendon reflexes in the extremities, absent bilateral baroreflexes, neck tenderness, and kyphosis. Blood gas analysis indicated an oxygen partial pressure of 27 mmHg and carbon dioxide partial pressure of 68 mmHg, suggestive of type II respiratory failure. Despite being admitted to the hospital and receiving cardiac monitoring, high-concentration oxygen therapy, and sputum suction, the patient's SpO2 remained below 70%. As a result, she was intubated and ventilated with ventilator-assisted ventilation. Laboratory test results revealed a significant elevation in the white blood cell count at 24.52*109/L, a significantly reduced sodium ion concentration at 115.5 mmol/L, and an elevated calcitoninogen level at 0.530↑ng/mL. BNP, troponin I, coagulation routine, hepatic function, renal function, thyroid function, ANCA, and rheumatoid immune series did not exhibit any significant abnormalities. The results of infection markers, aspergillus serology test, and fungal D-glucan were within normal limits. On April 11, 2023, cranial magnetic resonance imaging (MRI) revealed high signal intensity in the bilateral parieto-occipital lobe and right temporal lobe in T2-FLAIR, local high signal intensity in the diffusion-weighted imaging (DWI) sequence, and a slightly low signal intensity in the corresponding ADC. No obvious abnormality of low signal intensity was observed in the brain parenchyma on the susceptibility-weighted imaging (SWI). Based on these imaging findings, reversible posterior white matter encephalopathy was considered (see Figure 1). Electromyography showed peripheral nerve damage in the upper and lower extremities involving both motor and sensory fibers, as well as axonal damage. The cell count in the cerebrospinal fluid was normal, while the protein concentration was elevated; ganglioside antibodies were negative in both blood and cerebrospinal fluid. Guillain-Barré syndrome (GBS) was suspected due to the acute onset and rapid progression of spinal and cranial nerve damage in the extremities, along with the presence of albuminocytological dissociation in the cerebrospinal fluid. Therefore, we administered human immunoglobulin (0.4 g/kg.d) for 5 days, methylcobalamin and lipoic acid to nourish the nerves, antibiotics to combat infection, and 3% hypertonic saline to correct hyponatremia, among other treatments. However, the patient's limb weakness did not show any significant improvement, and she still had difficulty with extrication and quadriplegia. Nine days after admission, the patient in the ICU experienced repeated loss of consciousness, failure to call out, and limb twitching. These symptoms could be terminated after administering sedative diazepam. Seizures were considered, so levetiracetam and sodium phenobarbital were added for antiepileptic purposes. Electroencephalogram showed a slowing of the background rhythm. At that time, we carefully considered the possibility of a misdiagnosis and further summarized the patient's condition. The patient had a history of intestinal obstruction and subsequently developed intermittent psychiatric abnormalities and abdominal pain related to the menstrual cycle. Recently, the patient had experienced acutely worsening peripheral neurological symptoms, which were consistent with the classic triad of acute intermittent porphyria. We observed that the patient's urine darkened to a dark brown color when exposed to sunlight (see Figure 2). Additionally, we

collected urine samples from the patient's parents and found that the father's urine did not significantly change color after exposure to sunlight, while the mother's urine exhibited a mild darkening. Further genetic analysis of the patient's family line revealed that the patient carried a heterozygous missense variant in the *HMBS* gene (c.518G>A:p.R173Q), which was inherited from the patient's mother and was not present in the patient's father or younger brother. Ultimately, a definitive diagnosis of acute intermittent porphyria was made. Subsequently, we adjusted the patient's treatment regimen to include progesterone injections of 20 mg once daily (QD) intramuscularly to delay menstruation, dextrose injections of 150 g twice daily (BID) intranasally, and discontinued the use of aggravating medications such as sodium phenobarbital. On April 28, 2023, the patient's repeat cranial brain MRI revealed a significant decrease in the extent of the abnormal signal in the bilateral parietal-occipital lobes and right temporal lobe compared to the previous scan (see Figure 3). Despite being hospitalized for 32 days, the patient was still unable to be discharged, and her family requested an automatic discharge. At the time of discharge, she was coherent but mentally impaired, with normal comprehension and attention span. Her bilateral pupils were equal in size and round, measuring approximately 3 mm in diameter, and light reflexes were present. Both eyes were incompletely closed, and her bilateral frontal lines and nasolabial folds were symmetrical. The muscle strength of both upper limbs was grade 0, the distal muscle strength of both lower limbs was grade 1, and the muscle tone of all limbs was reduced. Tendon reflexes of the extremities were not elicited, and Babinski's sign was not present on both sides. The patient exhibited no signs of meningeal irritation, and the remaining portions of the examination could not be coordinated. On follow-up 10 days after discharge, the patient tolerated being weaned off the ventilator but still had weakness in all four limbs. Three months after discharge, the patient was on an intermittent high-sugar diet, and her limbs had significantly improved in strength, allowing her to stand on her own. Although she could breathe on her own, she still exhibited emotional irritability.

Discussion

Porphyrias are a group of diseases resulting from enzyme deficiencies in the heme synthesis pathway, which leads to increased production of porphyrins and their precursors, δ-aminolevulinic acid (ALA) and porphobilinogen (PBG) (1). Heme, an iron porphyrin compound, serves as the cofactor for numerous crucial proteins in the blood, including hemoglobin, myoglobin, cytochromes, and peroxidase (6). Hemoglobin biosynthesis involves eight steps, and enzyme impairments at any of these steps can cause porphyrin dysregulation, resulting in the development of distinct porphyria subtypes. Based on the site of porphyrin production, they are classified as either hepatic or erythrocytic porphyrins (2). Acute intermittent porphyria (AIP) is the most prevalent form of acute hepatic porphyria (AHP) and is characterized by the accumulation of toxic neurological substances, such as porphyrins and their precursors, due to the absence of the third crucial enzyme in heme synthesis. Acute attacks manifest as the classic triad of abdominal pain, neurological symptoms, and psychiatric abnormalities (5). An analysis of the REBRAPPO study, which examines Brazilian patients suffering from porphyria, reveals that among 148 individuals diagnosed with AHP, the most common initial clinical manifestations were abdominal pain in 77 patients (52.0%) and acute muscle weakness in 23 patients (15.5%) (7). Similarly, a prospective, multinational observational study of patients with recurrent AHP found that 92% of patients experienced abdominal pain, while 91% presented with a change in urine color. The most common psychiatric symptoms were fatigue, anxiety, and sleep disturbances (8). However, a recent statistical analysis of AHP cases between 2012 and 2018 showed that only 32% of patients presented with the "classic triad" of symptoms during an attack. Additionally, 42% of patients exhibited two of these symptoms, while 55% reported dark-colored urine. Therefore, timely diagnosis of AIP remains a challenge for clinicians. Early diagnosis and effective treatment of AIP can significantly reduce the medical burden on both the patient's family and society, and improve prognosis (9). This case involves a young woman who was severely disabled by AIP for about 5 years, from the initial intestinal obstruction to the appearance of neurologic symptoms such as limb weakness and respiratory muscle weakness. During this time, she visited several hospitals. This patient presented with "classic triad" of AIP symptoms, including abdominal pain resulting from intestinal obstruction, neurological deficits manifesting as muscular weakness, and psychological anomalies in the form of sleep disturbances and alterations in mood. Due to the rarity of AIP and its non-specific symptoms, it is crucial that physicians across various specialties, including gastroenterology, neurology, psychiatry, and endocrinology, are aware of this disease to prevent potentially serious consequences of delayed diagnosis.

AIP is an autosomal dominant disorder caused by mutations in the *HMBS* gene, which encodes porphobilinogen deaminase (PBG deaminase). DNA sequencing of genes involved in heme biosynthesis has made it possible to pinpoint disease-causing mutations in an almost comprehensive manner for patients suffering from porphyria. However, it is noteworthy that significant genetic variations still remain elusive in a minority of patients exhibiting clinical and biochemical manifestations. The rapid development of next-generation sequencing (NGS) technologies could lead to an increase in the detection of missing genetic variants (10). DNA sequencing and analysis of *HMBS* genes to detect these mutations represent the gold standard for diagnosing AIP. Genetic diagnosis not only confirms the presence of AIP in individuals but also predicts disease severity and treatment responsiveness. The severity of clinical symptoms and disease progression in AIP appears to be mutation-specific. For instance, patients harboring p.W198X, c.1073delA, and p.R26C variants tend to exhibit more severe symptoms, while those with p.R167W, p.R225G, and c.G33T variants typically have a more indolent disease course with milder manifestations (11). In the present case report, we describe a patient with an *HMBS* gene mutation located at p.R173Q. Although the relationship between this specific mutation and disease severity remains unclear, our patient developed severe neurological damage and rapidly worsening symptoms of myasthenia gravis, suggesting a poor prognosis. This case underscores the importance of early genetic diagnosis in AIP to facilitate timely intervention and potentially alter disease outcomes.

10.3389/fneur.2023.1334743

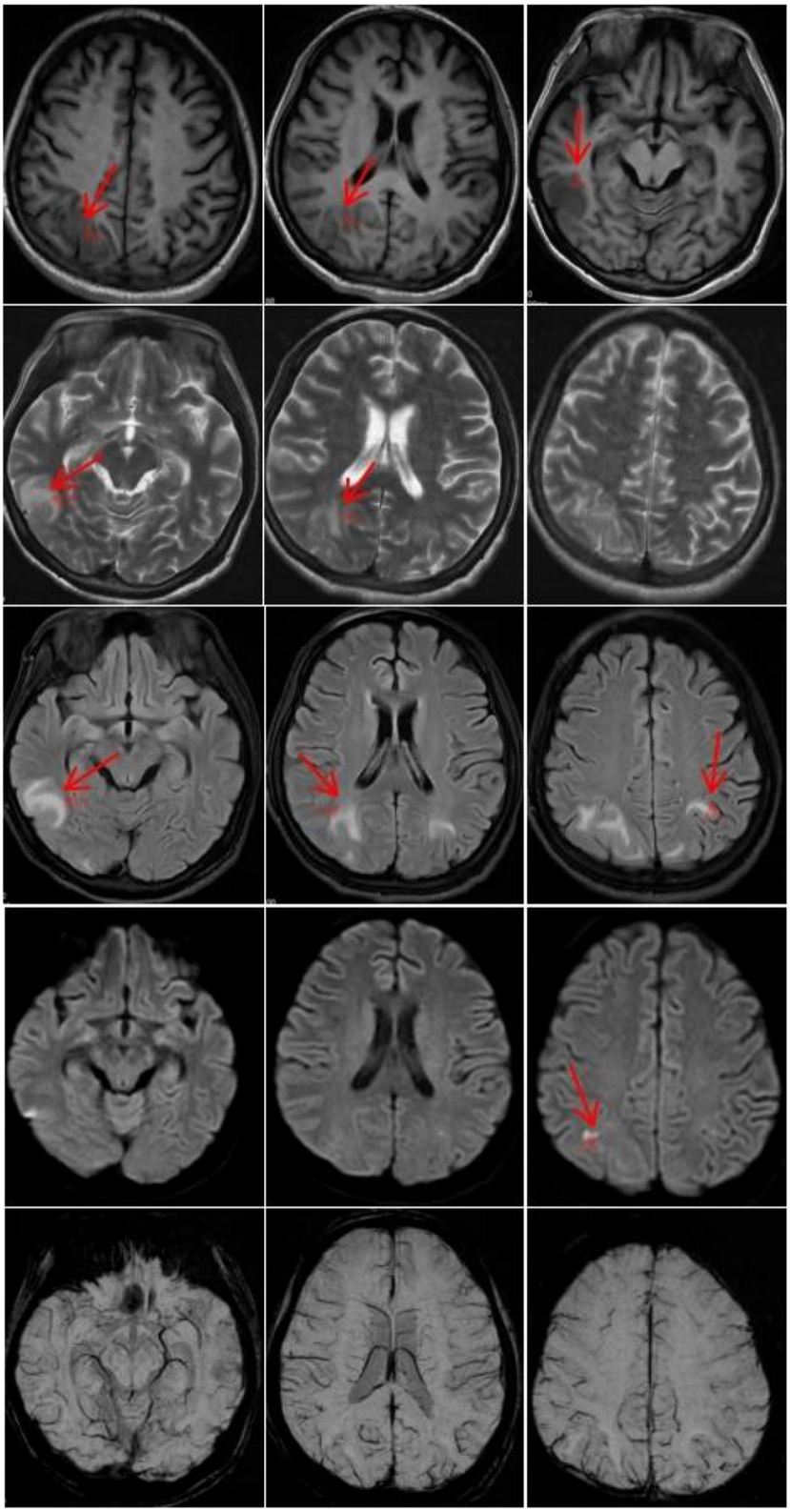

FIGURE 1
On April 11, 2022, cranial magnetic resonance imaging (MRI) revealed high-signal intensities in the bilateral parieto-occipital lobes and the right temporal lobe on T2-FLAIR sequences. Additionally, diffusion-weighted imaging (DWI) demonstrated localized areas of high signal. Susceptibility-weighted imaging (SWI) within the brain parenchyma did not detect any noticeable abnormal low-signal intensities. The neuroimaging features are highly suggestive of PRES syndrome diagnosis. The red arrows indicate lesion locations.

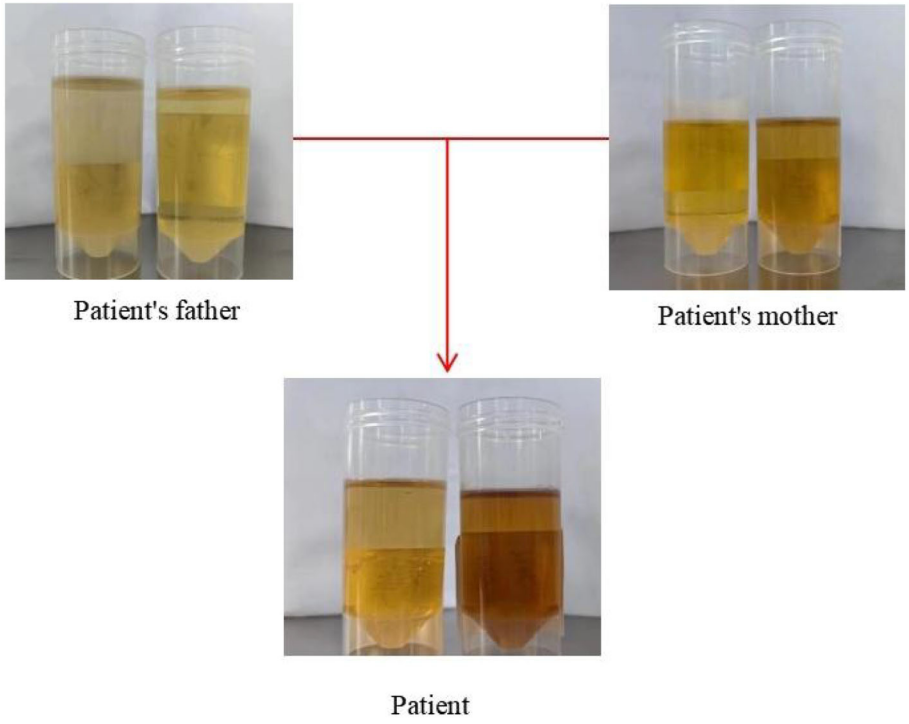

FIGURE 2
This figure displays the outcomes of urinary PBG solarization tests conducted on patient and her parents.

AIP is not only an autosomal dominant disorder but also a monogenic one. Patients with AIP can retain up to 50% of enzyme activity when the mutated *HMBS* gene is inherited from one of their parents, a level sufficient for normal hemoglobin synthesis. As a result, most patients are asymptomatic carriers (12). AIP has been reported worldwide, with its distribution varying across regions and populations. *HMBS* gene variants have a low frequency in the general population but are more common in AIP families. Analysis of genome/exome sequencing data from 45,955 Caucasians revealed a prevalence of AIP of <1%, suggesting that acquired factors such as drugs, alcohol, hormones, starvation, and stress play a crucial role in the acute onset of the disease. The disease occurs in all races, with Europeans having a rate of *HMBS* gene mutations of approximately 1 in 1700. In contrast, the frequency of mutations in Caucasians may be as high as 6 in 1000. Studies conducted in 11 European countries found an annual incidence of symptomatic AIP of 0.13 per million. Due to the founder effect, the prevalence is significantly higher in the Nordic region, with rates of 0.51 and 0.22 per million reported in Sweden and Switzerland, respectively (13, 14). The *HMBS* variant rate in the Chinese general population is estimated to be 1 in 1765. Although the outlier rate is low, the large population size in China results in a considerable number of patients with symptomatic AIP. A retrospective study conducted on the general population of Hebei Province, China, between 2011 and 2020 showed an annual incidence of symptomatic AIP of approximately 0.03-0.08 per million. Given that the population of Hebei Province exceeds 70 million, it is estimated that there are around 400 patients with symptomatic AIP (15). Upon comparing and analyzing the data from the aforementioned studies, it becomes apparent that the incidence of symptomatic AIP in China is significantly lower than that in Europe. This difference can be attributed to the early recognition of porphyria in Europe and the establishment of a robust diagnostic and management system for AIP patients, along with enhanced family screening and preventive counseling (16). Furthermore, while there is no gender difference in carriers of the *HMBS* gene variant, the majority of studies indicate a higher proportion of acute exacerbations in female patients with AIP compared to males, suggesting a close association between female hormones and the development of AIP (17).

Most patients experience symptom onset between the ages of 20 and 40, with a smaller proportion experiencing symptoms during the prepubertal and postmenopausal periods. AIP typically manifests as acute, intermittent episodes, and its clinical presentations are complex and varied, making it challenging to differentiate from other common disorders solely through clinical assessment. AIP can affect the autonomic nervous system, the peripheral nervous system, and the central nervous system. Abdominal pain is the most common and earliest autonomic symptom of an attack, occurring in over 90% of patients (18). This pain is typically intermittent colic without significant pressure and is often accompanied by nausea, vomiting, and constipation. Patients' episodes of abdominal pain are acute and severe, and are frequently misdiagnosed as acute abdominal diseases such as intestinal obstruction, appendicitis, pancreatitis, among others. Some patients undergo unnecessary surgical treatments due to recurrent episodes that do not allow for a clear etiology. Additionally, these gastrointestinal symptoms lead to decreased

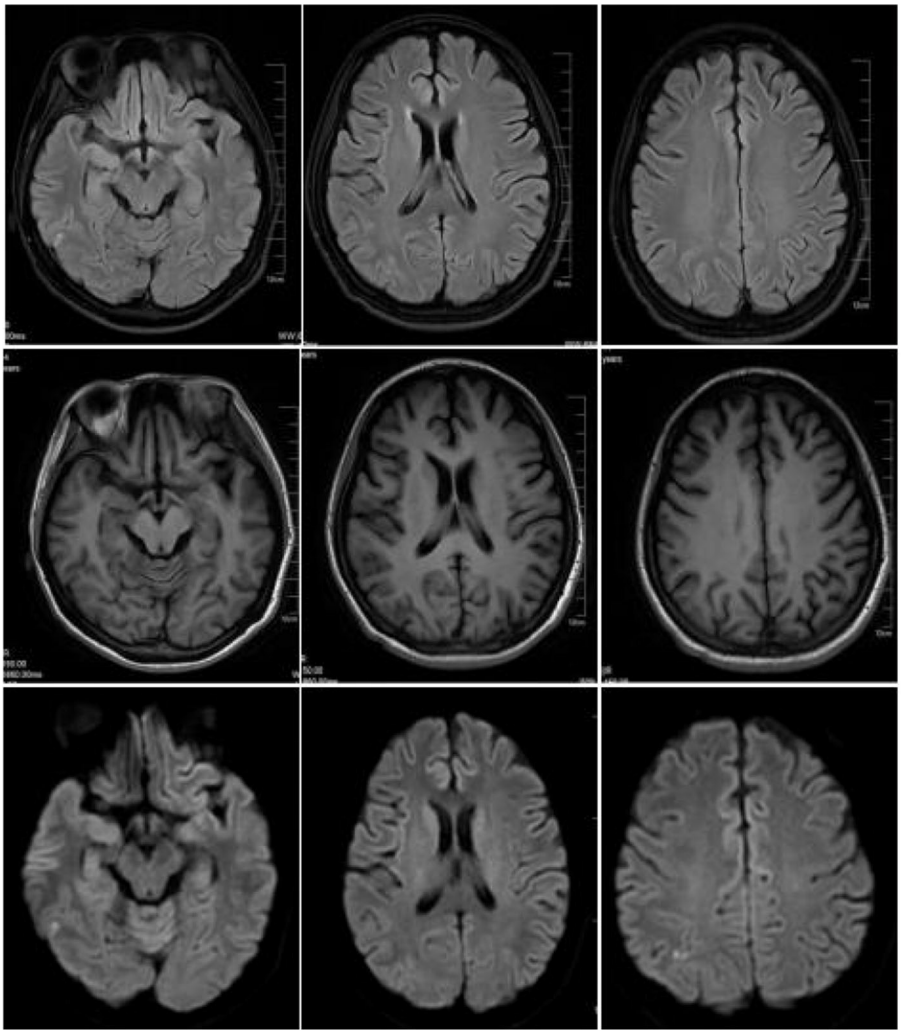

FIGURE 3
On April 28, 2023, cranial magnetic resonance imaging (MRI) revealed high-signal intensities in the bilateral parieto-occipital lobes and the right temporal lobe on T2-FLAIR sequences, while DWI sequences demonstrated localized areas of high signal. The extent of these signals has significantly decreased compared to the previous examination conducted on April 11, 2023.

appetite and reduced energy intake, resulting in negative energy balance in patients, which further exacerbates attacks (19). A large-scale, population-based survey study conducted in the United States in 2020 revealed that approximately one-fourth of patients with a history of abdominal pain experienced symptoms similar to those of acute hepatic porphyria (20). Although the incidence of AIP is low, it remains a crucial differential diagnosis in patients presenting with recurrent episodes of severe abdominal pain. Autonomic neuropathy can also induce other symptoms, such as hypertension, tachycardia, diarrhea, postural hypotension, and abnormal sweating (21). Neuropsychiatric symptoms in AIP patients manifest in various forms, lacking specificity and occurring at any given time. The typical manifestation of peripheral neuropathy is acute motor nerve axonal damage, initially affecting proximal muscles and upper limbs, gradually progressing to lower limbs and distal extremities, primarily manifesting as muscle weakness. In severe cases, motor polyneuropathy can result in quadriplegia and respiratory failure (22, 23). In some patients, sensory nerves are involved, resulting in a "glove-and-stocking" distribution of sensory deficits, which may manifest as neuralgia, hyperalgesia, or numbness, with loss of nociceptive sensation being less common (24). Epilepsy occurs in up to 20% of AIP patients, typically manifesting as complex partial seizures, myoclonic jerks, and tonic-clonic seizures (25). Additionally, other symptoms of acute AIP onset may induce seizures, such as hyponatremia and post-reversible encephalopathy syndrome (PRES) (26). PRES is a reversible subcortical vasogenic cerebral edema, characterized by symptoms such as headache, seizures, encephalopathy, and visual disturbances. AIP is a rare cause of this condition (27). Recent studies examining the clinical features of AIP patients with PRES have revealed that the mean age of onset for PRES is between 24–44 years, with a significant predominance of women over men. Seizures were present in 85%-95% of PRES patients (28, 29). Hyponatremia is the most commonly observed laboratory abnormality during acute seizures of AIP, which may be associated with the syndrome of inappropriate antidiuretic

hormone secretion (SIADH) (30). During an acute seizure of AIP, damage to the hypothalamus resulting from a large accumulation of porphyrin precursors and abnormal hemoglobin activity leads to increased vasopressor secretion and substantial fluid retention, ultimately causing dilutional hyponatremia (31). Frequent and debilitating chronic symptoms affect over 65% of patients with AHP, with a substantial proportion of these symptoms being linked to neurological and psychiatric conditions. Such manifestations include severe chronic pain (whether abdominal, neuropathic, or diffuse myalgia), anxiety and mood disorders, fatigue, sleep disturbances (notably insomnia), and muscle weakness that impede daily routines. These symptoms, in turn, can serve as precipitants for acute episodes of AIP, leading to exacerbation of the condition (32, 33). In addition to affecting the nervous system, abnormalities in porphyrin metabolism can also cause disorders of the endocrine and metabolic systems. The prevalence of insulin resistance and impaired glucose metabolism is higher among AIP patients compared to the general population (34). However, there is a scarcity of literature on the impact of porphyrin metabolism on the endocrine system, and further investigation is warranted to elucidate its pathogenesis. This case involved abdominal pain presenting 5 years ago. At that time, due to atypical clinical symptoms, the clinician treated it as the most common abdominal disease, intestinal obstruction, which had a fair effect. However, later on, intermittent mood abnormalities accompanied by abdominal pain emerged. Upon presentation to our hospital, the patient exhibited weakness in the extremities, respiratory failure, reversible posterior leukoencephalopathy imaging findings, hyponatremia, and seizures. The patient had a history of acute intermittent seizures for ∼5 years, ultimately leading to quadriplegia and a poor prognosis. This case highlights that AIP is prone to misdiagnosis and delayed diagnosis, which can significantly impact the patient's prognosis.

The exact mechanism behind the pathogenesis of AIP remains elusive, with studies revealing significant elevations in plasma levels of cytokines, chemokines, growth factors, and other inflammatory markers among AIP patients. This suggests a potential association between AIP and low-grade inflammation. Perforin 3 (PTX3), an inflammatory mediator produced by immune cells, emerges as a key player in this low-grade inflammation and serves as a marker of AIP disease activity (35). The dissemination of ALA from the liver to other body parts contributes significantly to the neurological manifestations observed in AIP. High concentrations of ALA exhibit neurotoxicity and bear structural similarities to γ-aminobutyric acid (GABA). Consequently, ALA acts as a partial agonist or antagonist of GABA at GABA receptors, leading to neuronal cell damage and apoptosis. Additionally, high levels of ALA impair glutamate uptake by augmenting oxidative stress. The occurrence of confusion, epilepsy, and psychiatric abnormalities during acute seizures in AIP may be linked to these underlying mechanisms (36). Another perspective suggests that prolonged heme deficiency in AIP patients impairs neuronal axonal transport. During acute seizures of AIP, severe hepatic heme deficiency disrupts tryptophan metabolism, and excessive tryptophan hinders neurotransmission, resulting in neurological dysfunction. To replenish the heme pool, the liver exerts negative regulation on the first rate-limiting enzyme in the heme synthesis pathway, 5-aminolevulinic acid synthetase-1 (ALAS1), which generates substantial amounts of ALA and partially converts it to PBG. Patients with AIP lack the enzyme PBG deaminase, ultimately leading to the accumulation of porphyrin precursors, ALA, and PBG (18).

Cranial MR imaging plays a crucial role in the diagnosis of AIP. Hematoporphyrinopathies involve lesions located in the cortex or subcortical white matter of each lobe of the brain, primarily affecting white matter and often presenting symmetrically. In MRI, these lesions are characterized by long T1 and long T2 signals, with some lesions fused, exhibiting low signals in DWI, high signals in ADC, and high signals in FLAIR. Reversibility was observed in some lesions, resembling the distribution and characteristics of lesions seen in PRES (37). The pathogenic basis of AIP-associated PRES remains elusive. Previous studies have posited that hypertension triggers a loss of control in autoregulatory mechanisms, leading to secondary hyperperfusion during an acute episode of AIP. This results in the rupture of the blood-brain barrier and leakage of fluid from the vascular lumen into the brain interstitium, ultimately causing vasogenic edema. Additionally, it has been suggested that the heme deficiency in the body during an acute attack of AIP decreases nitric oxide (NO) production, leading to an increase in blood pressure and cerebral vasoconstriction (38). During an acute attack of AIP, ischemic changes may occur, which can be reversible or irreversible. In the former case, reversible vasospasm is present without any organic lesions visible on cranial MRI. However, in the latter case, foci of softening can be observed on MRI imaging. Severe stenosis of cerebral vessels may even manifest as stroke-like symptoms (39). Moreover, AIP presents with some nonspecific electrophysiologic manifestations, including increased slow waves or epileptic discharges on electroencephalogram, and neurogenic damage and motor neuron axonal injury rather than demyelinating neuropathy on electromyography (40). Cerebrospinal fluid examination does not reveal typical protein separation. Biochemical tests, such as the urine PBG sunlight test, are crucial in diagnosing AIP. In patients with AIP, the test results are positive, as fresh urine exposed to sunlight for several hours turns reddish-brown or burgundy due to the conversion of colorless PGB in urine to colored porphyrin compounds. Collecting random urine samples during an acute attack and qualitatively testing for urinary PBG allows for rapid screening of porphyrias (41). The analysis of urinary PBG, ALA, and porphyrin levels in fecal and blood samples obtained from patients experiencing an acute attack of AIP serves as a valuable diagnostic tool. However, solely relying on this approach may not be sufficient. Genetic testing can properly identify pathogenic or suspected variants in PPOX, CPOX, ALAD or HMBS genes associated with Acute Hepatic Porphyria (42).

AIP is a complex multisystem disease with diverse clinical manifestations, making prompt diagnosis a challenging task. When AIP presents as acute abdominal pain, it is crucial to differentiate it from various acute abdominal conditions to exclude organic abdominal disease, such as intestinal obstruction and inflammatory diseases. Testing urine PBG levels can aid in the differential diagnosis. Guillain-Barré syndrome typically does not manifest with psychiatric symptoms, and porphyrins and their metabolites are typically within normal limits. Lead poisoning can result

in elevated porphyrin or ALA levels, which can mimic the clinical presentation of AIP. Therefore, clinicians must focus on differentiating lead poisoning when diagnosing acute porphyrias. The clinical manifestations of lead poisoning depend on blood lead levels, with high levels leading to anemia, constipation, abdominal pain, peripheral neuropathy, and even impaired consciousness. Patients with lead poisoning typically have a clear history of lead exposure and significantly elevated blood and urine lead levels (43). An elderly woman with chronic, long-term gastrointestinal symptoms including abdominal pain and weight loss, as well as chronic neurologic symptoms of memory impairment, has recently been reported. This patient exhibited elevated urinary porphyrins and was initially diagnosed with acute porphyria; however, given the patient's age, it was imperative to consider alternative diagnoses. Subsequently, the patient was found to have significantly elevated blood lead levels, ultimately leading to a final diagnosis of lead poisoning (suspected ayurvedic use) (44). This case underscores the complexity of diagnosing porphyria and emphasizes the need for clinicians to enhance their understanding of AIP to prevent delayed misdiagnosis.

The principles of treatment for AIP encompass the elimination of the causative agent, management of the acute exacerbation phase, treatment of recurrent episodes, and prevention and treatment of complications. AIP is caused by a variant of the HMBS gene, but the manifestation of the disease phenotype requires additional genetic or acquired factors. Acute attacks of AIP can be precipitated by menstruation, pregnancy, infection, stress, inadequate caloric intake, and certain medications such as barbiturates, antiepileptic drugs, sulfonamide antibiotics, and steroid hormones like progesterone (5). Prevention of acute AIP attacks involves identifying triggers and avoiding exposure to them, including reducing or avoiding smoking and alcohol consumption, maintaining a healthy diet with adequate intake of carbohydrates, proteins, and fats to minimize porphyrin precursor excretion, and avoiding dieting in patients with porphyria (45). Additionally, patients should avoid oral porphyrin-derived medications that induce cytochrome P450. Those with AIP associated with epilepsy should exercise caution in selecting antiepileptic drugs; for instance, phenytoin sodium and carbamazepine induce CYP450, whereas gabapentin and levetiracetam are more suitable alternatives (46). Patients with AIP related to the menstrual cycle may consider taking oral contraceptives to prevent acute attacks. The preferred treatment for acute-phase episodes of AIP is intravenous hemin, which effectively inhibits ALAS1, reducing the accumulation of heme precursors and their byproducts, and rapidly decreasing plasma and urinary levels of PBG and ALA. Due to the instability of heme in water, it should be reconstituted with 25% human albumin. The optimal route of administration is via a central venous catheter, with a standard dosing regimen of 3–4 mg/kg/day for 4 days. If complete remission is not achieved within this period, the duration of treatment may be extended. Hemin is a safe option to use during pregnancy and should be administered as soon as possible following an acute episode of AIP. If hemin is unavailable, carbohydrate-loading therapy can be administered orally or intravenously with glucose. Good therapeutic outcomes can also be achieved effectively with glucose alone in patients with AHP (47). Glucose stimulates insulin release by reducing peroxisome proliferator receptor gamma coactivator 1-α (PGC1-α), which mediates hepatic ALAS1 downregulation and impairs ALA synthesis. In the early stages of AIP episodes, when mild pain is present without severe clinical manifestations, glycogen loading therapy (300 g/day) can be utilized. It is crucial to note that large amounts of intravenous glucose may result in hemodilution, potentially exacerbating the risk of hyponatremia (48). Symptomatic supportive therapy is provided when other complications are present: opioid analgesics such as morphine and pethidine are relatively safe in acute episodes of abdominal pain; gabapentin and levetiracetam are recommended for patients with epileptic seizures; and for patients with severe hyponatremia, 3% hypertonic saline is administered via intravenous infusion (49). Emerging Therapies—Givosiran is a highly specific, double-stranded small interfering ribonucleic acid (siRNA) designed to bind and silence ALAS1 mRNA within hepatocytes. This action inhibits the synthesis of ALAS1, leading to a decrease in circulating δ-ALA and PBG levels among patients experiencing AHP and severe relapses. In the ENVISION Phase 3 trial, which was conducted in a randomized, double-blind, and multinational setting, givosiran demonstrated a significant reduction in the annual incidence of acute attacks, including those necessitating hospitalization, emergency medical interventions, or at-home intravenous hemoglobin administrations. Furthermore, patients with relapsing AIP who received Givosiran showed decreased reliance on hemoglobin infusions and pain medications compared to those given a placebo. The available evidence strongly indicates that Givosiran represents a pivotal new treatment modality for individuals with AHP and severe relapses (50). Liver transplantation remains the last effective resort for managing all symptoms in critically ill patients who have exhausted other treatment options. However, challenges such as donor shortage and long-term oral immunosuppression post-transplantation must be faced by patients (51). AIP is associated with a high incidence of chronic complications like hypertension, chronic kidney disease, and hepatocellular carcinoma. Therefore, patients with AIP require continual monitoring of liver and kidney function, along with regular screening for hepatocellular carcinoma (9). As hemoglobin preparations are unavailable in our hospital, we administered progesterone injections to delay menstruation and prevent acute attacks, supplemented by glucose-loading therapy. Eventually, the patient and her family opted for automatic discharge, and the patient was discharged from the hospital on an intermittent high-glucose diet, with significant improvement in limb muscle strength and spontaneous respiration.

Conclusion

Acute intermittent porphyria is a rare and clinically demanding disease. Only a small fraction of patients manifest the "classic triad," and there often exists a considerable lag between the advent of symptoms and the establishment of a diagnosis. Given its multi-systemic nature, it is imperative for clinicians across neurology, psychiatry, gastroenterology, and other fields to recognize this ailment, thus averting any delays in diagnosis and treatment. The presence of unexplained abdominal pain, accompanied by neurologic and psychiatric signs, should serve as a red flag for porphyria. If the urine darkens to a deep red or wine-colored hue

upon exposure to sunlight and the urine PBG test returns positive, further genetic testing can be conducted to affirm the diagnosis and typing, thereby expediting the confirmation of hematoporphyria and the prompt initiation of appropriate treatment. We present a case exhibiting a myriad of typical clinical manifestations of AIP, in the hope of aiding clinicians in gaining a comprehensive understanding of the disease and facilitating timely and accurate diagnosis in patients presenting with analogous symptoms.

Data availability statement

The original contributions presented in the study are included in the article/supplementary material, further inquiries can be directed to the corresponding author.

Ethics statement

The studies involving humans were approved by Ethics Committee of the Shandong Provincial Qianfoshan Hospital. The studies were conducted in accordance with the local legislation and institutional requirements. The participants provided their written informed consent to participate in this study. Written informed consent was obtained from the individual(s) for the publication of any potentially identifiable images or data included in this article.

Author contributions

JLin: Writing – original draft. JLiu: Writing – review & editing. AW: Writing – review & editing. ZS: Writing – review & editing.

Funding

The author(s) declare financial support was received for the research, authorship, and/or publication of this article. This study was supported by grants from Traditional Chinese Medicine Science and Technology Development Program of Shandong Province, China (2019-0369), Key Research and Development Plan of Shandong Province, China (Public Welfare) (2019GSF108008 and 2019GSF108033), Cultivation Fund of the National Natural Science Foundation of China (QYPY2019NSFC0616), and Medical and Health Science and Technology Development Plan of Shandong Province, China (Health Care Project) (2021BJ000005).

Conflict of interest

The authors declare that the research was conducted in the absence of any commercial or financial relationships that could be construed as a potential conflict of interest.

Publisher's note

All claims expressed in this article are solely those of the authors and do not necessarily represent those of their affiliated organizations, or those of the publisher, the editors and the reviewers. Any product that may be evaluated in this article, or claim that may be made by its manufacturer, is not guaranteed or endorsed by the publisher.

References

1. Dickey AK, Leaf RK, Balwani M. Update on the porphyrias. *Annu Rev Med.* (2023). doi: 10.1146/annurev-med-042921-123602

2. Ramanujam VS, Anderson KE. Porphyria diagnostics-part 1: a brief overview of the porphyrias. *Curr Protoc Hum Genet.* (2015) 86:17.20.1–26. doi: 10.1002/0471142905.hg1720s86

3. Souza PVS, Badia BML, Farias IB, Gonçalves EA, Pinto WBVR, Oliveira ASB. Acute hepatic porphyrias for the neurologist: current concepts and perspectives. *Arq Neuropsiquiatr.* (2021) 79:68–80. doi: 10.1590/0004-282x20200096

4. Gerischer LM, Scheibe F, Nümann A, Köhnlein M, Stölzel U, Meisel A. Acute porphyrias - a neurological perspective. *Brain Behav.* (2021) 11:e2389. doi: 10.1002/brb3.2389

5. Wang B, Rudnick S, Cengia B, Bonkovsky HL. Acute hepatic porphyrias: review and recent progress. *Hepatol Commun.* (2018) 3:193–206. doi: 10.1002/hep4.1297

6. Phillips JD. Heme biosynthesis and the porphyrias. *Mol Genet Metab.* (2019) 128:164–77. doi: 10.1016/j.ymgme.2019.04.008

7. Souza PVS, Afonso G, Pinto WBVd, Serrano Pd, Badia BdL, Farias IB, et al. Brazilian registry of patients with porphyria: REBRAPPO study. *Orphanet J Rare Dis.* (2023) 18:49. doi: 10.1186/s13023-023-02653-1

8. Gouya L, Ventura P, Balwani M, Bissell DM, Rees DC, Stölzel U, et al. EXPLORE: a prospective, multinational, natural history study of patients with acute hepatic porphyria with recurrent attacks. *Hepatology.* (2020) 71:1546–58. doi: 10.1002/hep.30936

9. Neeleman RA, Wagenmakers MAEM, Koole-Lesuis RH, Mijnhout GS, Wilson JHP, Friesema ECH, et al. Medical and financial burden of acute intermittent porphyria. *J Inherit Metab Dis.* (2018) 41:809–17. doi: 10.1007/s10545-018-0178-z

10. Di Pierro E, De Canio M, Mercadante R, Savino M, Granata F, Tavazzi D, et al. Laboratory diagnosis of porphyria. *Diagnostics.* (2021) 11:1343. doi: 10.3390/diagnostics11081343

11. Ma L, Tian Y, Peng C, Zhang Y, Zhang S. Recent advances in the epidemiology and genetics of acute intermittent porphyria. *Intractable Rare Dis Res.* (2020) 9:196–204. doi: 10.5582/irdr.2020.03082

12. Edel Y, Mamet R. Porphyria: what is it and who should be evaluated? *Rambam Maimonides Med J.* (2018) 9:e0013. doi: 10.5041/RMMJ.10333

13. Chen B, Solis-Villa C, Hakenberg J, Qiao W, Srinivasan RR, Yasuda M, et al. Acute intermittent porphyria: predicted pathogenicity of HMBS variants indicates extremely low penetrance of the autosomal dominant disease. *Hum Mutat.* (2016) 37:1215–22. doi: 10.1002/humu.23067

14. Elder G, Harper P, Badminton M, Sandberg S, Deybach JC. The incidence of inherited porphyrias in Europe. *J Inherit Metab Dis.* (2013) 36:849–57. doi: 10.1007/s10545-012-9544-4

15. Ma L, Tian Y, Qi X, Li P, Li J, Teng Q, et al. Acute intermittent porphyria: prevalence of pathogenic HMBS variants in China, and epidemiological survey in Hebei Province, China. *Ann Transl Med.* (2022) 10:560. doi: 10.21037/atm-22-1600

16. Fraunberg MVUZ, Pischik E, Udd L, Kauppinen R. Clinical and biochemical characteristics and genotype-phenotype correlation in 143 Finnish and Russian patients with acute intermittent porphyria. *Medicine.* (2005) 84:35–47. doi: 10.1097/01.md.0000152455.38510.af

17. Anderson KE, Desnick RJ, Stewart MF, Ventura P, Bonkovsky HL. Acute hepatic porphyrias: "purple flags"-clinical features that should prompt specific diagnostic testing. *Am J Med Sci.* (2022) 363:1–10. doi: 10.1016/j.amjms.2021.09.009

18. Ma Y, Teng Q, Zhang Y, Zhang S. Acute intermittent porphyria: focus on possible mechanisms of acute and chronic manifestations. *Intractable Rare Dis Res.* (2020) 9:187–95. doi: 10.5582/irdr.2020.03054

19. Heymans B, Meersseman W. Porphyria: awareness is the key to diagnosis! *Acta Clin Belg.* (2022) 77:703–9. doi: 10.1080/17843286.2021.1918876

20. Lakhoo K, Almario CV, Khalil C, Spiegel BMR. Prevalence and characteristics of abdominal pain in the United States. *Clin Gastroenterol Hepatol.* (2021) 19:1864–72.e5. doi: 10.1016/j.cgh.2020.06.065

21. Nabin A, Thapa LJ, Paudel R, Rana PV. Acute intermittent porphyria with SIADH and fluctuating dysautonomia. *Kathmandu Univ Med J.* (2012) 10:96–9. doi: 10.3126/kumj.v10i2.7354

22. O'Malley R, Rao G, Stein P, Bandmann O. Porphyria: often discussed but too often missed. *Pract Neurol.* (2018) 18:352–8. doi: 10.1136/practneurol-2017-001878

23. Ramzan A, Cao JJL, Frazer JS, Stein P, Ahmad S. A case of acute intermittent porphyria leading to severe disability in a young 21-year-old female. *Cureus.* (2023) 15:e34757. doi: 10.7759/cureus.34757

24. Solinas C, Vajda FJ. Neurological complications of porphyria. *J Clin Neurosci.* (2008) 15:263–8. doi: 10.1016/j.jocn.2006.11.015

25. Bylesjö I, Forsgren L, Lithner F, Boman K. Epidemiology and clinical characteristics of seizures in patients with acute intermittent porphyria. *Epilepsia.* (1996) 37:230–5. doi: 10.1111/j.1528-1157.1996.tb00018.x

26. Redmond J, Fazio T, Buzzard K. Acute intermittent porphyria presenting with first episode seizure and rhabdomyolysis. *Acta Neurol Belg.* (2023) 123:1611–4. doi: 10.1007/s13760-022-02134-5

27. Swart G, Lim SS, Jude M. Acute intermittent porphyria presenting with posterior reversible encephalopathy syndrome (PRES) and abdominal pain. *Pract Neurol.* (2020) 20:486–8. doi: 10.1136/practneurol-2020-002599

28. Zheng X, Liu X, Wang Y, Zhao R, Qu L, Pei H, et al. Acute intermittent porphyria presenting with seizures and posterior reversible encephalopathy syndrome: Two case reports and a literature review. *Medicine.* (2018) 97:e11665. doi: 10.1097/MD.0000000000011665

29. Jaramillo-Calle DA, Solano JM, Rabinstein AA, Bonkovsky HL. Porphyria-induced posterior reversible encephalopathy syndrome and central nervous system dysfunction. *Mol Genet Metab.* (2019) 128:242–53. doi: 10.1016/j.ymgme.2019.10.011

30. Solares I, Tejedor M, Jericó D, Morales-Conejo M, de Salamanca RE, Fontanellas A, et al. Management of hyponatremia associated with acute porphyria-proposal for the use of tolvaptan. *Ann Transl Med.* (2020) 8:1098. doi: 10.21037/atm-20-1529

31. Li Y, Qu H, Wang H, Deng H, Liu Z. Novel A219P mutation of hydroxymethylbilane synthase identified in a Chinese woman with acute intermittent porphyria and syndrome of inappropriate antidiuretic hormone. *Ann Hum Genet.* (2015) 79:310–2. doi: 10.1111/ahg.12107

32. Duque-Serrano L, Patarroyo-Rodriguez L, Gotlib D, Molano-Eslava JC. Psychiatric aspects of acute porphyria: a comprehensive review. *Curr Psychiatry Rep.* (2018) 20:5. doi: 10.1007/s11920-018-0867-1

33. de Souza PVS, Badia BML, Farias IB, Pinto WBVR, Oliveira ASB. Acute hepatic porphyria: pathophysiological basis of neuromuscular manifestations. *Front Neurosci.* (2021) 15:715523. doi: 10.3389/fnins.2021.715523

34. Solares I, Jericó D, Córdoba KM, Morales-Conejo M, Ena J, de Salamanca RE, et al. Understanding carbohydrate metabolism and insulin resistance in acute intermittent porphyria. *Int J Mol Sci.* (2022) 24:51. doi: 10.3390/ijms24010051

35. Storjord E, Dahl JA, Landsem A, Fure H, Ludviksen JK, Goldbeck-Wood S, et al. Systemic inflammation in acute intermittent porphyria: a case-control study. *Clin Exp Immunol.* (2017) 187:466–79. doi: 10.1111/cei.12899

36. Bonkovsky HL, Dixon N, Rudnick S. Pathogenesis and clinical features of the acute hepatic porphyrias (AHPs). *Mol Genet Metab.* (2019) 128:213–8. doi: 10.1016/j.ymgme.2019.03.002

37. Jing Yuan, Bin Yuan, Hui You. Clinical and neuroimaging features of central nervous system impairments in acute intermittent porphyria. *Nat Med J China.* (2011) 91:2776–8. doi: 10.3760/cma.j.issn.0376-2491.2011.39.012

38. Abdulla MC. Acute intermittent porphyria and posterior reversible encephalopathy syndrome. *Ann Indian Acad Neurol.* (2020) 23:711–2. doi: 10.4103/aian.AIAN_233_19

39. Attout H, Guez S. Reversible cerebral vasospasm in acute intermittent porphyria: a case report and review of the literature. *Eur J Case Rep Intern Med.* (2022) 9:003543.

40. Wu C-L, Ro L-S, Jung S-M, Tsai T-C, Chu C-C, Lyu R-K, et al. Clinical presentation and electrophysiological findings of porphyric neuropathies: a follow-up study. *Muscle Nerve.* (2015) 51:363–9. doi: 10.1002/mus.24327

41. Lefever S, Peersman N, Meersseman W, Cassiman D, Vermeersch P. Development and validation of diagnostic algorithms for the laboratory diagnosis of porphyrias. *J Inherit Metab Dis.* (2022) 45:1151–62. doi: 10.1002/jimd.12545

42. Stölzel U, Doss MO, Schuppan D. Clinical guide and update on porphyrias. *Gastroenterology.* (2019) 157:365–81.e4. doi: 10.1053/j.gastro.2019.04.050

43. Gitelman J, An H, Spilchuk V, Kim J. Lead toxicity from Ayurvedic medicines. *CMAJ.* (2023) 195:E1010–2. doi: 10.1503/cmaj.230592

44. Willett LL, Bromberg GK, Chung R, Leaf RK, Goldman RH, Dickey AK. Case 38-2021: a 76-year-old woman with abdominal pain, weight loss, and memory impairment. *N Engl J Med.* (2021) 385:2378–88. doi: 10.1056/NEJMcpc2107354

45. Petrides PE. Therapy follows diagnosis: old and new approaches for the treatment of acute porphyrias, what we know and what we should know. *Diagnostics.* (2022) 12:1618. doi: 10.3390/diagnostics12071618

46. Wang B, Bonkovsky HL, Lim JK, Balwani M. AGA clinical practice update on diagnosis and management of acute hepatic porphyrias: expert review. *Gastroenterology.* (2023) 164:484–91. doi: 10.1053/j.gastro.2022.11.034

47. Di Pierro E, Granata F. Nutrients and porphyria: an intriguing crosstalk. *Int J Mol Sci.* (2020) 21:3462. doi: 10.3390/ijms21103462

48. Longo M, Paolini E, Meroni M, Dongiovanni P. Cutting-edge therapies and novel strategies for acute intermittent porphyria: step-by-step towards the solution. *Biomedicines.* (2022) 10:648. doi: 10.3390/biomedicines10030648

49. Pischik E, Kauppinen R. An update of clinical management of acute intermittent porphyria. *Appl Clin Genet.* (2015) 8:201–14. doi: 10.2147/TACG.S48605

50. Syed YY. Givosiran: a review in acute hepatic porphyria. *Drugs.* (2021) 81:841–8. doi: 10.1007/s40265-021-01511-3

51. Singal AK, Parker C, Bowden C, Thapar M, Liu L, McGuire BM. Liver transplantation in the management of porphyria. *Hepatology.* (2014) 60:1082–9. doi: 10.1002/hep.27086

frontiers | Frontiers in Neurology

TYPE Case Report
PUBLISHED 16 January 2024
DOI 10.3389/fneur.2023.1336273

OPEN ACCESS

EDITED BY
Ghazala Hayat,
Saint Louis University, United States

REVIEWED BY
Liuxi Chu,
Southeast University, China
Zhu Yufu,
The Affiliated Hospital of Xuzhou Medical University, China
Ping Allen Wu,
Wenzhou Medical University, China

*CORRESPONDENCE
Yong Liu
✉ yl198188@126.com
Yuanjie Zou
✉ zouyuanjie0115@126.com

RECEIVED 10 November 2023
ACCEPTED 28 December 2023
PUBLISHED 16 January 2024

CITATION
Ding F, Li P, Zuo X, Song W, Xiao Y, Wang D, Geng L, Hu X, Yang K, Liu Y and Zou Y (2024) Case report: Significance of the large rhomboid lip in microvascular decompression: insights from two clinical cases. *Front. Neurol.* 14:1336273. doi: 10.3389/fneur.2023.1336273

Case report: Significance of the large rhomboid lip in microvascular decompression: insights from two clinical cases

Feiyu Ding[1], Pan Li[1], Xiaozhou Zuo[1], Wenxiong Song[2,3], Yong Xiao[1], Dong Wang[1], Liangyuan Geng[1], Xinhua Hu[1], Kun Yang[1], Yong Liu[1]* and Yuanjie Zou[1]*

[1]Department of Neurosurgery, Affiliated Nanjing Brain Hospital, Nanjing Medical University, Nanjing, China, [2]Department of Neurosurgery, Beijing Tiantan Hospital, Capital Medical University, Beijing, China, [3]China National Clinical Research Center for Neurological Diseases, Beijing, China

The rhomboid lip (RL) is a layer of neural tissue that extends outside the fourth ventricle and is connected to the lateral recess of the fourth ventricle. Although this anatomical structure has been rigorously studied, it is often overlooked in microvascular decompression (MVD) surgery. In this report, we present two cases, one of hemifacial spasm (HFS) and one of glossopharyngeal neuralgia (GPN), in which a large RL was observed during surgery. We found that a large RL is easily confused with arachnoid cysts, and accurate identification and dissection are important to protect the lower cranial nerves.

KEYWORDS

rhomboid lip, microvascular decompression, hemifacial spasm, glossopharyngeal neuralgia, flocculus

Introduction

Microvascular decompression surgery is an effective treatment for hemifacial spasm (HFS) and glossopharyngeal neuralgia (GPN). Using the lateral suboccipital infraflocculus approach, the culprit vessels can be identified and isolated, which results in satisfactory outcomes. In this approach, the choroid plexus protruding from the foramen of Luschka serves as a significant anatomical landmark to locate the root exit zone (REZ) (1). The choroid plexus and the lower cranial nerves can be adequately visualized by gently retracting the flocculus posterosuperiorly. The rhomboid lip (RL) is sometimes encountered during dissection; however, it is sometimes discovered under normal circumstances (2–5). In this study, we report two microvascular decompression (MVD) cases with a large RL.

Case presentation

Case 1

A 68-year-old female was admitted to the hospital due to involuntary contraction at the corners of the right eye and mouth for over 3 years. Magnetic resonance imaging (MRI) revealed that the right anterior inferior cerebellar artery (AICA) formed a vascular loop and compressed the REZ of the facial nerve

(Figure 1A). Additionally, a cystic structure was observed adjacent to the choroid plexus and connected medially to the foramen of Luschka (Figure 1B).

Once contraindications to surgery were excluded, the patient underwent MVD surgery under general anesthesia. Intraoperative electrophysiological monitoring was employed. The patient was positioned in the lateral park bench position. The dura was incised in a "C" shape and then suspended. Intraoperatively, a white translucent membranous cystic RL structure with tight adhesions to the lower cranial nerves was observed (Figures 1C, D). After excision and release of the RL, the lateral suboccipital infrafloccular approach was used to explore the REZ of the facial nerve. It was observed that the right AICA was ascending and compressing the REZ of CN VII (Figure 1E). Following the dissection of the arachnoid, a Teflon felt pledget was inserted (Figures 1F, G), resulting in the immediate disappearance of the LSR waveform during electrophysiological monitoring.

After the surgery, the patient's symptoms on the right side of the face disappeared. There were no observed cases of hearing impairment, facial paralysis, or recurrence during the 1-year follow-up period.

Case 2

A 66-year-old female was admitted to the hospital with a history of episodic right-sided pharyngeal pain lasting for more than 5 years. The findings from MRI T2WI and 3D-TOLF revealed a close relationship between the right posterior inferior cerebellar artery (PICA) and the glossopharyngeal nerve. The preoperative procaine test yielded positive results. Additionally, the MRI T2WI showed the presence of a sac-like structure positioned ventrally to the choroid and connected medially to the foramen of Luschka (Figure 2A).

A standard retrosigmoid suboccipital approach was performed using intraoperative neurophysiological monitoring. The infrafloccular approach was used to release the lower CNs. A milky white translucent membranous cystic RL was observed wrapping around the jugular foramen area and tightly adhering to the lower CNs (Figure 2B). After excision and dissection of the RL, the right PICA was found to be ascending and exerting pressure on the REZ of CN IX (Figures 2C, D). To alleviate this pressure, the PICA was liberated and a Teflon spacer was inserted (Figure 2E).

The patient experienced a resolution of symptoms, with no recurrence during a follow-up period of over 1 year.

Discussion

Since the introduction of MVD by Jannetta for the treatment of cranial nerve disorders, it has become the mainstay of treatment for HFS and GPN (6–9). Although this technique is well-established, the literature reports an incidence of 0.5–3% for permanent cranial nerve dysfunction, such as facial palsy (10), hearing loss (11), and

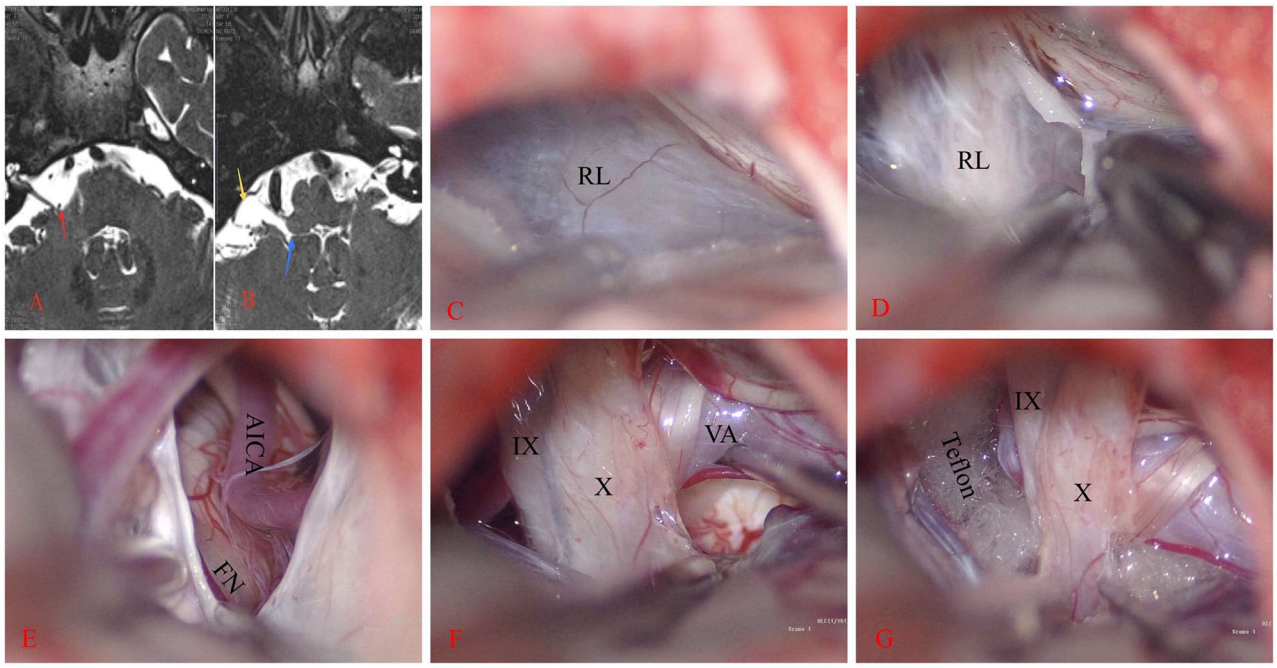

FIGURE 1
Right hemifacial spasm. **(A)** The anterior inferior cerebellar artery loop (AICA) compresses the facial nerve REZ (red arrow). **(B)** A sac-like structure on the ventral side of the flocculus (yellow arrow) is observed on T2WI. This structure communicates inwardly with the fourth ventricle through the foramen of Luschka (blue arrow). **(C, D)** A large rhomboid lip (RL) wraps around the jugular foramen and combines with the choroid to form a large lacuna. CN IX and X are located ventral to it and stick tightly. **(E–G)** After the RL is released, the vertebral artery (VA) and AICA are lifted away, revealing the REZ of the facial nerve (FN). Teflon is then placed between them.

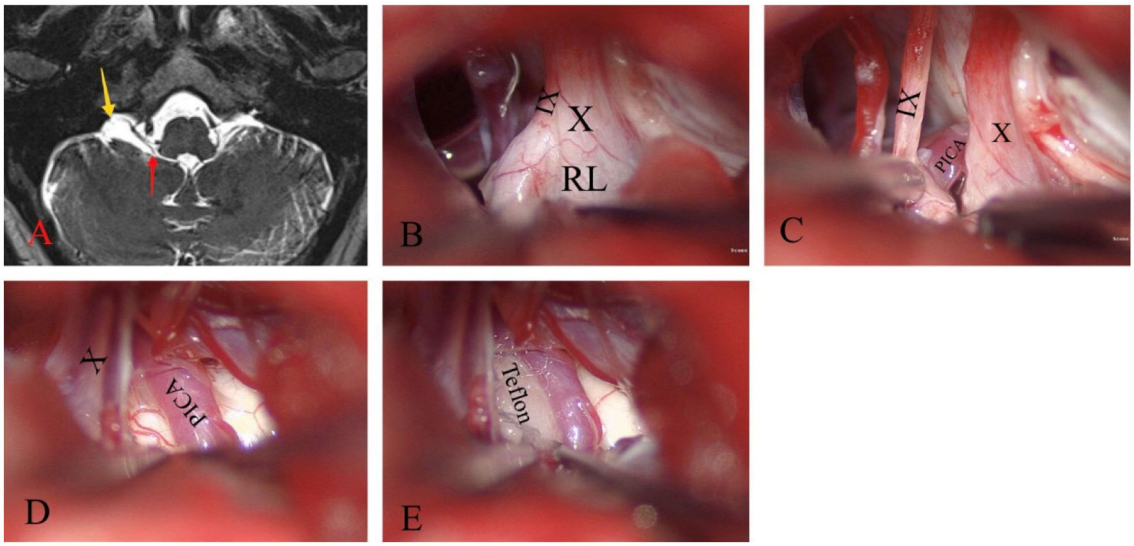

FIGURE 2
Glossopharyngeal neuralgia on the right side. **(A)** T2WI shows a sac-like structure (yellow arrow) located ventral to the flocculus that connects to the fourth ventricle through the foramen of Luschka (red arrow). **(B)** The large RL surrounds the jugular foramen and tightly adheres to the lower cranial nerves. **(C–E)** By releasing and resecting most of the RL, CN IX, CN X, and the posterior inferior cerebellar artery (PICA) were effectively exposed to compress the REZ. Teflon is then inserted between them.

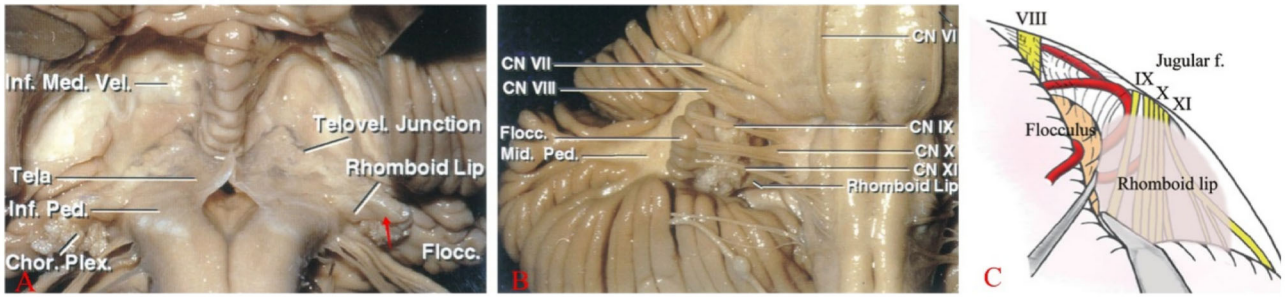

FIGURE 3
(A) The RL, a thin membranous neural structure, extends laterally from the floor of the fourth ventricle to join with the choroid plexus (Tela), forming a lacuna (red arrow) outside the lateral recess and the foramen of Luschka. **(B)** Located posterior to CNs IX, X, and XI, the RL is ventral to the recess and extends outward with the choroid plexus. **(C)** A large RL overlays the surface of the lower cranial nerves, obstructing the view of the REZ of CN VII and IX from the rear (Note: **A, B** are reproduced from *Cranial anatomy and surgical approaches* by Rhoton AL; Lippincott Williams & Wilkins, 2008. **C** is reproduced from Matsushima T. (ed): *Microsurgical Anatomy and Surgery of the Posterior Fossa*; Springer, 2015.).

lower cranial nerve deficits (12, 13). These complications may be caused by intraoperative malpractice, as well as the complexity and variability of individual anatomy, which increases the difficulty of surgery. Furthermore, inadequate knowledge and mishandling of the RL can contribute to nerve injuries. The RL is occasionally mistaken for thickened arachnoid membranes, which increases the risk of cranial nerve injuries during separation. Therefore, it is vital to clearly understand the anatomical relationship between the arachnoid membrane, RL, and the lower CNs to ensure the safety of MVD.

As the fourth ventricle migrates into the lateral recess, the floor of the fourth ventricle and the RL form the ventral wall of the lateral recess (14). The RL continues to migrate ventrally. Along with the choroid plexus, the RL forms the most lateral end of the lateral recess, creating a trap-like structure (Figure 3A). At the lateral end, the RL forms the ventral margin of the foramen of Luschka, while the choroid and its accompanying choroid plexus form the dorsal margin. CN IX and CN X are located ventrally to the RL, with the CN VII and CN VIII and the choroid located anteriorly above it (Figures 3B, C). Akiyama et al. (15) classified RL into three types: non-extension type, lateral extension type, and jugular foramen type, based on the relationship of the RL to the choroid plexus. All types of RL surround CN IX and CN X and are in contact with or locally adherent to them. The jugular foramen type adheres extremely closely to CN IX.

Although researchers have provided detailed descriptions of the microanatomy of RL, the clinical significance of RL has not yet been recognized (16). This lack of recognition may be attributed to the inadequate understanding of RL anatomy and structure. In a study conducted by Nakahara et al. (4), only 9 out of 34 patients

with HFS had visualized RL during surgery (26.5%), and only 3 cases (8.8%) could be demonstrated on preoperative MRI. On T2WI MRI, a larger RL exhibited high signal cystic manifestations ventral to the flocculus, which connected medially with the fourth ventricle through the foramen of Luschka. However, visualizing smaller RLs was challenging. A case study by Cho et al. (3) reported the misdiagnosis of a large RL as an arachnoid cyst, which highlights the importance of understanding RL anatomy and features to avoid such misdiagnoses. RL and arachnoid cysts are distinct tissue structures. The RL is visually thicker, translucent, and milky white compared to the arachnoid. Histologically, the RL has a two-layered structure with ciliated cells in the inner layer, similar to the ventricular cells at the base of the fourth ventricle, and an outer layer that consists of glial cells and neurons. In contrast, the arachnoid membrane lacks nerve cells. Anatomically, the outer arachnoid membrane accompanies the lower CNs into the jugular foramen, whereas the RL does not enter the jugular foramen.

In MVD surgery, it is important to release and separate the RL in a precise manner. Precision separation allows the surgeon to clearly view the REZ of CN VII, IX, and X while avoiding any unnecessary retraction of the lower CNs. By gently retracting the flocculus posterosuperiorly using the infrafloccular approach, the RL and the REZ of CN VII can be sufficiently visualized. However, if the RL is large or tightly adherent to CN IX and X, it becomes difficult to visualize the REZ of CN VIII, IX, and X. Improper retraction or failure to correctly identify the relationship between the RL and the lower nerves can also lead to postoperative cranial nerve injury. In patients with a large RL, considering its anatomical relationship with CN VII and IX is important. To avoid injury to the lower CNs, the RL should be patiently and carefully dissected from these cranial nerves or separated in the direction of the nerve alignment before retracting the flocculus. This allows for improved visualization of the periphery of the REZ of CN VII, IX, and X and the brainstem.

Conclusions

A thorough anatomical knowledge and meticulous dissection can help surgeons observe the structures of the foramen of Luschka region more clearly. These practices can ensure the protection of cranial nerves, thereby reducing the risk of cranial nerve injuries.

Data availability statement

The original contributions presented in the study are included in the article/supplementary material, further inquiries can be directed to the corresponding author/s.

Ethics statement

The studies involving humans were approved by Medical Ethics Committee of Nanjing Brain Hospital. The studies were conducted in accordance with the local legislation and institutional requirements. Written informed consent for participation was not required from the participants or the participants' legal guardians/next of kin in accordance with the national legislation and institutional requirements. Written informed consent was obtained from the individual(s) for the publication of any potentially identifiable images or data included in this article.

Author contributions

FD: Writing – original draft, Writing – review & editing. PL: Data curation, Writing – review & editing. XZ: Data curation, Writing – review & editing. WS: Data curation, Investigation, Writing – review & editing. YX: Investigation, Supervision, Writing – original draft. DW: Investigation, Supervision, Validation, Writing – review & editing. LG: Supervision, Validation, Writing – review & editing. XH: Supervision, Validation, Writing – review & editing. KY: Supervision, Validation, Writing – review & editing. YL: Supervision, Validation, Writing – review & editing. YZ: Funding acquisition, Supervision, Validation, Visualization, Writing – review & editing.

Funding

The author(s) declare financial support was received for the research, authorship, and/or publication of this article. This study was supported by a grant from the Jiangsu Provincial Health Commission (Grant No. M2021003).

Conflict of interest

The authors declare that the research was conducted in the absence of any commercial or financial relationships that could be construed as a potential conflict of interest.

Publisher's note

All claims expressed in this article are solely those of the authors and do not necessarily represent those of their affiliated organizations, or those of the publisher, the editors and the reviewers. Any product that may be evaluated in this article, or claim that may be made by its manufacturer, is not guaranteed or endorsed by the publisher.

References

1. Hitotsumatsu T, Matsushima T, Inoue T. Microvascular decompression for treatment of trigeminal neuralgia, hemifacial spasm, and glossopharyngeal neuralgia: three surgical approach variations: technical note. *Neurosurgery*. (2003) 53:1436–41; discussion: 42–3. doi: 10.1227/01.neu.0000093431.43456.3b

2. Funaki T, Matsushima T, Masuoka J, Nakahara Y, Takase Y, Kawashima M. Adhesion of rhomboid lip to lower cranial nerves as special consideration in microvascular decompression for hemifacial spasm: report of two cases. *Surg Neurol Int.* (2010) 1:71. doi: 10.4103/2152-7806.72581

3. Cho TG, Nam TK, Park SW, Hwang SN. Glossopharyngeal neuralgia caused by arachnoid cyst in the cerebellopontine angle. *J Korean Neurosurg Soc.* (2011) 49:284–6. doi: 10.3340/jkns.2011.49.5.284

4. Nakahara Y, Matsushima T, Hiraishi T, Takao T, Funaki T, Masuoka J, et al. Importance of awareness of the rhomboid lip in microvascular decompression surgery for hemifacial spasm. *J Neurosurg.* (2013) 119:1038–42. doi: 10.3171/2013.4.Jns121546

5. Kasimu M, Tuersun M, Maimaitituerxun Y, Abulizi W, Li S, Fulati N. Abnormal rhomboid lip and choroid plexus should be valued in microvascular decompression for vestibulocochlear diseases. *World Neurosurg.* (2023). doi: 10.1016/j.wneu.2023.10.099. [Epub ahead of print].

6. Kim MK, Park JS, Ahn YH. Microvascular decompression for glossopharyngeal neuralgia: clinical analyses of 30 cases. *J Korean Neurosurg Soc.* (2017) 60:738–48. doi: 10.3340/jkns.2017.0506.010

7. Xia L, Li YS, Liu MX, Zhong J, Dou NN, Li B, et al. Microvascular decompression for glossopharyngeal neuralgia: a retrospective analysis of 228 cases. *Acta Neurochir.* (2018) 160:117–23. doi: 10.1007/s00701-017-3347-1

8. Palanisamy D, Kyosuke M, Yasuhiro Y, Tsukasa K, Kato Y. Management of recurrent glossopharyngeal neuralgia following microvascular decompression surgery. *World Neurosurg.* (2018) 117:339–43. doi: 10.1016/j.wneu.2018.06.136

9. Nishimura S, Kubota K, Okuyama S, Matsuyama J, Kazama K, Tomii M, et al. Microvascular decompression for glossopharyngeal neuralgia in the semi-sitting position: a report of two cases. *Tohoku J Exp Med.* (2021) 254:183–8. doi: 10.1620/tjem.254.183

10. Tian W, Meng X, Zou J. Delayed facial palsy after microvascular decompression for trigeminal neuralgia. *J Coll Phys Surg Pak.* (2020) 30:344–5. doi: 10.29271/jcpsp.2020.03.344

11. Lee MH, Lee HS, Jee TK, Jo KI, Kong DS, Lee JA, et al. Cerebellar retraction and hearing loss after microvascular decompression for hemifacial spasm. *Acta Neurochir.* (2015) 157:337–43. doi: 10.1007/s00701-014-2301-8

12. Kuroi Y, Tani S, Ohbuchi H, Kasuya H. Microvascular decompression for hypoglossal nerve palsy secondary to vertebral artery compression: a case report and review of the literature. *Surg Neurol Int.* (2017) 8:74. doi: 10.4103/sni.sni_42_17

13. Amagasaki K, Kurita N, Watanabe S, Shono N, Hosono A, Naemura K, et al. Lower cranial nerve palsy after the infraflocculer approach in microvascular decompression for hemifacial spasm. *Surg Neurol Int.* (2017) 8:67. doi: 10.4103/sni.sni_8_17

14. Jean WC, Abdel Aziz KM, Keller JT, van Loveren HR. Subtonsillar approach to the foramen of luschka: an anatomic and clinical study. *Neurosurgery.* (2003) 52:860–6; discussion: 6. doi: 10.1227/01.neu.0000053146.83780.74

15. Akiyama O, Kondo A, Arai H. The rhomboid lip: anatomy, pathology, and clinical consideration in neurosurgery. *World Neurosurg.* (2019) 123:e252–8. doi: 10.1016/j.wneu.2018.11.148

16. Fukuda H, Ishikawa M, Yamazoe N. Glossopharyngeal neuralgia caused by adhesive arachnoid. *Acta Neurochir.* (2002) 144:1057–8; discussion: 8. doi: 10.1007/s00701-002-0991-9

frontiers | Frontiers in Neurology

TYPE Case Report
PUBLISHED 16 January 2024
DOI 10.3389/fneur.2023.1288546

OPEN ACCESS

EDITED BY
Ernestina Santos,
University Hospital Center of Porto, Portugal

REVIEWED BY
Tatsuro Mutoh,
Fujita Health University, Japan
Paulo Victor Sgobbi Souza,
Federal University of São Paulo, Brazil

*CORRESPONDENCE
Ying Du
✉ tdduying@fmmu.edu.cn
Wei Zhang
✉ tdzw@fmmu.edu.cn

†These authors have contributed equally to this work and share first authorship

RECEIVED 07 September 2023
ACCEPTED 27 December 2023
PUBLISHED 16 January 2024

CITATION
Zhou X, Peng A, Li C, Li L, Yao D, Hao Y, Zhao C, Yan Q, Li Y, Liu J, Liu S, Zhu W, Du Y and Zhang W (2024) Combined central and peripheral demyelination: a case report resembling encephalomyelo radiculoneuropathy.
Front. Neurol. 14:1288546.
doi: 10.3389/fneur.2023.1288546

Combined central and peripheral demyelination: a case report resembling encephalomyelo radiculoneuropathy

Xuan Zhou[1†], Ali Peng[1†], Chuan Li[1†], Lin Li[1], Dan Yao[1], Yunfeng Hao[1], Chao Zhao[1], Qi Yan[1], Ying Li[1], Juntong Liu[1,2], Shuyu Liu[1,2], Wenping Zhu[1,2], Ying Du[1*] and Wei Zhang[1*]

[1]Department of Neurology, Tangdu Hospital, Air Force Medical University, Xi'an, Shaanxi Province, China, [2]Xi'an Medical University, Xi'an, Shaanxi Province, China

Combined central and peripheral demyelination (CCPD) is an extremely rare disease characterized by inflammatory demyelination in both the central and peripheral nervous systems. Herein, we reported case of a 14-year-old teenager who initially presented with the symptoms of acute myelitis (AM). Subsequently, the patient developed symptoms consistent with Guillain-Barré syndrome (GBS), which was supported by nerve conduction studies (NCV) and cerebrospinal fluid (CSF) analysis. Throughout the course of the disease, the patient experienced abdominal pain and abnormal liver function. After a comprehensive evaluation, we determined that the abnormal liver function was a result of hepatitis E virus (HEV) infection, which may have acted as a trigger for GBS. The patient was treated with corticosteroids, intravenous immunoglobulin and Rituximab, resulting in symptom relief and clinical improvement after therapy and follow-up. This case highlights the potential responsiveness and reversibility of CCPD. Given the heterogeneous nature of CCPD, there is currently no standardized diagnostic criteria or clear consensus on its treatment. Therefore, we recommend a thorough assessment of all possibilities and the development of consolidated management guidelines based on available data for this disorder.

KEYWORDS

combined central and peripheral demyelination, acute myelitis, Guillain-Barré syndrome, HEV infection, treatment

Introduction

Inflammatory demyelination diseases encompass a broad range of disorders characterized by demyelinating lesions mediated by inflammation. These disorders typically affect either the central nervous system (CNS) or peripheral nervous system (PNS). Combined central and peripheral demyelination (CCPD) is a rare condition that manifests as simultaneous or temporally separated demyelination in both the CNS and PNS. This particular disease is not commonly encountered in clinical practice (1). Diagnosing CCPD can be challenging due to the limited knowledge available, which is primarily derived from case reports and small case series (2–5). Moreover, some cases exhibited both CNS and PNS impairment were named as Encephalomyeloradiculoneuropathy (EMRN), which is similar with CCPD. Specific biomarkers were identified in CCPD. In 2013, Kawamura et al. found that anti-neurofascin-155

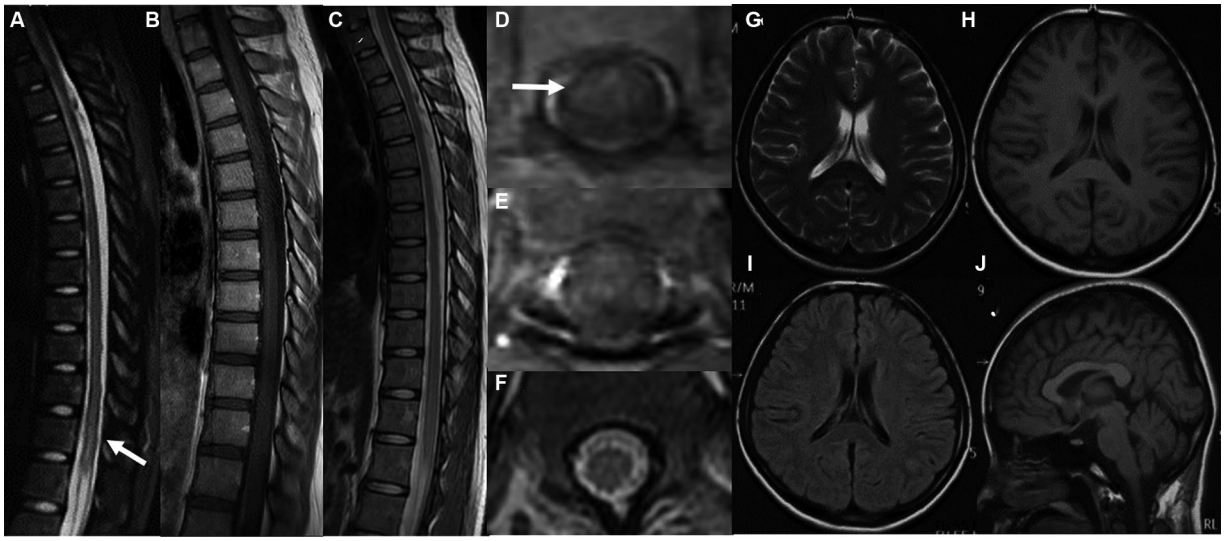

FIGURE 1
MRI images of the spinal cord both before and after therapy **(A,C,D,F)**. Gadolinium-enhanced axial T1-weighted MRI of the spinal cord **(B,E)**. MRI of the brain **(G–J)** revealed the absence of brain lesions. The sagittal T1-weighted image **(A)** and axial T1-weighted image **(D)** of the thoracic spinal cord before therapy revealed an abnormal signal in the thoracic and lumbar spinal cord (T11-L1). We did not observe obvious enhancement of spinal lesion in enhanced T1-weighted MRI **(B,E)**. After therapy, the sagittal T1-weighted image **(C)** and axial T1-weighted image **(F)** demonstrated a significant reduction in the size of the previously observed lesions.

antibodies was positive in some CCPD patients (4). Recent studies reveal some antibodies were also associated with CCPD, such as anti-neurofascin186 antibody, antigalactocerebroside and antilactosylceramide (4, 6, 22, 23). While in EMRN, anti-neutral glycosphingolipid antibodies especially anti-lactosylceramide (LacCer) antibodies were identified (25). In this case report, we present a case report of a patient manifested the symptoms of acute myelitis (AM) and Guillain-Barré syndrome (GBS). Ultimately, she was diagnosed with CCPD.

Case presentation

A 14-year-old girl with no significant medical or past history presented with weakness and tingling paresthesia in both lower extremities for 1 week. Additionally, she experienced stool and urinary retention. Prior to her presentation, she had transient abdominal pain but no fever or diarrhea. She had not received any vaccines within the past month. She was initially diagnosed with acute myelitis at a local hospital and was subsequently admitted to the neurology department of our hospital. The patient had no history of other neurological disorders, fever, weight loss, or night sweats. She also denied any changes in vision, difficulty swallowing or speaking, shortness of breath, chest pain, and loss of smell or taste sensation. Upon admission, the weakness in her lower extremities gradually worsened, while the stool and urinary retention improved. She required a wheelchair and was unable to stand up independently. A thorough examination was conducted. Initial findings and vital signs were within normal limits, and gastrointestinal, respiratory, and cardiovascular examinations were unremarkable. Neurological examination revealed that the patient was conscious, alert, and oriented. She had normal muscle bulk, but the strength of her bilateral lower extremities was graded as 2 on the muscle strength grading scale (with a maximum score of 5), with the right side being more affected than the left. Lower extremity reflexes and plantar reflex were absent, and there was hyperalgesia up to the bilateral groin.

The hemogram, liver, renal, and thyroid functions (TSH, Free T4), electrolytes (Na, K, Ca, P, Mg), muscle enzymes, vitamin B12 levels, as well as glycohemoglobin, were all within normal ranges. Virological tests (HIV, hepatitis B, hepatitis C, COVID-19) yielded negative results or fell within normal ranges. Immunological studies were conducted, and the results showed negative findings for antinuclear antibody, antiphospholipid IgM and IgG, anti-dsDNA, anticardiolipin IgM and IgG, anti-Sjogren antibody SSA and SSB, and extractable nuclear antigen. Visual-evoked potentials (VEPs) demonstrated normal P100 latencies bilaterally (right: 106 ms, left: 108 ms). SEP also exhibited normal latencies bilaterally. The CSF examination revealed normal intracranial pressure, a slightly elevated white blood cell count (20*10^6/L), and an elevated protein level (780 mg/L, normal range: 150–450 mg/L). CSF culture yielded negative results, and CSF cytology showed no malignant cells. Cerebrospinal fluid analysis indicated a normal albumin level (536 mg/L), normal IgG level (75.2 mg/L), and a normal CSF-to-serum albumin ratio (12.3). Serum albumin and serum IgG levels were also within normal ranges. Aquaporin-4, anti-MBP antibodies, and anti-MOG antibodies were not detected. CSF and blood oligoclonal bands were absent.

In the imaging assessments, Magnetic Resonance Imaging (MRI) revealed the absence of brain lesions (Figures 1G–J), while spinal cord resonance imaging and gadolinium-enhanced MRI of the spinal cord demonstrated mild cord edema, but we did not observe obvious enhancement of spinal lesion in enhanced T1-weighted MRI (Figures 1A,B,D,E). The spinal cord MRI did not indicate any manifestations of acute disseminated encephalomyelitis (ADEM) or multiple sclerosis (MS). In the early stages of treatment, the patient received methylprednisolone therapy (1,000 mg once daily) for a duration of 3 days, followed by a gradual reduction of the

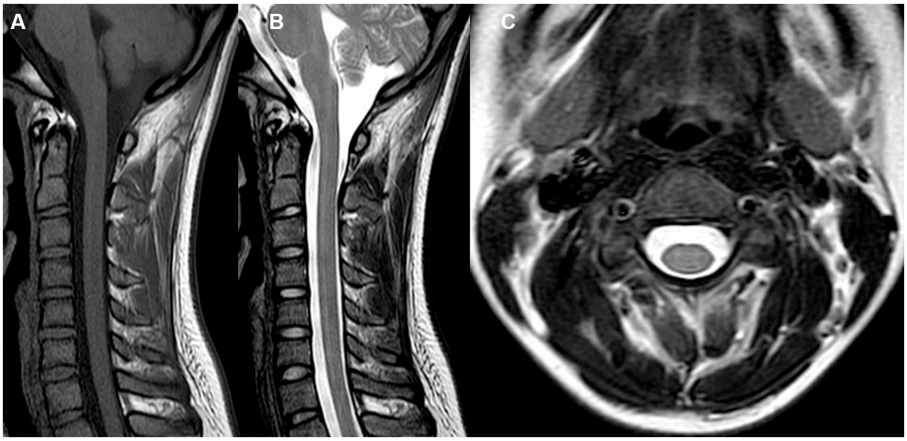

FIGURE 2
MRI images of the cervical spinal cord **(A–C)** were obtained. These included sagittal T1-weighted **(A)**, T2-weighted **(B)**, and axial T1-weighted **(C)** images. Notably, no lesions were observed in the cervical spinal cord.

methylprednisolone dosage over the course of 1 week. Subsequent to the treatment, some improvement in muscle strength was observed (lower limbs: MRC grade: 2).

However, during the course of treatment, the patient experienced abdominal pain and exhibited abnormal liver function, as indicated by elevated alanine aminotransferase (ALT) levels of 205 U/L and aspartate aminotransferase (AST) levels of 60 U/L. Notably, muscle enzyme levels remained within the normal range. Screening for Epstein–Barr Virus, Cytomegalovirus, Herpes Simplex Virus, and Herpes Zoster Virus yielded negative results. Even after receiving hepatoprotective therapy, the patient's ALT and AST levels did not return to normal. Additionally, the patient developed acute weakness in the upper limbs, which rapidly progressed to tetraplegia (bilateral lower limbs: MRC grade 2, left upper limb: MRC grade 2, and right upper limb: MRC grade 3). The patient's deep tendon reflexes remained hyporeflexic. MRI of the spinal cord revealed no lesions in the cervical spinal cord (Figure 2). Subsequently, the patient underwent a series of electromyograms (EMGs) and nerve conduction studies (NCVs). NCVs revealed peripheral neuropathy (Table 1). CSF analysis showed protein cytological dissociation, with an increased protein level of 1317.5 mg/L and a normal cell count of 4 cells/mm^3. The patient was negative for anti-glycolipid (GM1, GM2, GM3, GD1a, GD1b, GD3, GT1b, GQ1b, galactocerebroside). No oligoclonal bands were detected. The patient displayed the classic triad of weakness of extremities, albuminocytologic dissociation was observed in the CSF sample, which strongly supported the diagnosis of Guillain-Barré Syndrome (GBS). In light of the abnormal liver function, a comprehensive examination was conducted, ultimately determining that the patient's abnormal liver function was a result of HEV infection. Intravenous immunoglobulin (IVIg) was administered at a dose of 0.4 g/kg/day and continued for 5 days. The patient demonstrated some improvement after completing the course of IVIg. She regained full strength (5/5) in all muscle groups in the upper extremities and had a strength of 3/5 in the lower extremities. As liver function continued to improve, the patient received Rituximab (RTX) infusion at a dose of 100 mg, with one-week intervals for two times. At four-month follow-up, her neurological condition is stable. She experienced progressive improvement in muscle strength in all limbs and was able to briefly stand with assistance. Follow-up MRI of the spinal cord revealed evidence of lesion improvement (Figures 1C,F). NCVs indicated improvement in demyelinating polyneuropathy (Table 2).

Discussion

In this report, we present a case of CCPD in a teenage patient. Our case is notable both because the presence of central and peripheral demyelinating processes in one patient is a rare phenomenon. CCPD is characterized by demyelination affecting both the central and peripheral nervous systems. It remains unclear whether CCPD represents a distinct disorder separate from classical demyelinating diseases (6). Currently, there are no standardized criteria for diagnosing CCPD. However, a previous nationwide survey conducted in Japan established criteria for CCPD, which encompassed a diverse range of clinical manifestations involving both the CNS and PNS, such as encephalopathy, cranial neuropathy, myeloradiculoneuropathy, or Guillain-Barré syndrome (6). The synchronous occurrence of GBS and AM in CCPD appears to be rare and variable. Early-stage diagnosis of CCPD, particularly when symptoms involving both the CNS and PNS are present simultaneously, poses challenges. Published literature on cases reporting such concurrent conditions is limited. The underlying pathophysiological mechanism of CCPD remains elusive. It is uncertain whether the same antigenic target exists in both the PNS and CNS, or if there is a cross-reactive immune response to insults affecting either system (3). The immune response elicited by antecedent infections may cross-react with components of the peripheral nerves due to the sharing of common epitopes (7). Overall, CCPD encompasses a spectrum of conditions, including acute, relapsing, and chronic subtypes (4).

Anti-NF155 antibodies is a protein expressed on both central and peripheral myelin. It was first reported in CCPD cases in 2013 (4). Previous study has reported the high prevalence of anti-NF155 antibodies in CCPD (45.5–86%) (4). However, the positivity rates for anti-NF155 antibodies in CCPD differ among studies and ethnicities, some studies revealed the absent of antibody in this disorder.

10.3389/fneur.2023.1288546

TABLE 1 A summary of nerve conduction studies demonstrating demyelinating polyneuropathy.

Motor NCS					
Nerve	Site		Latency (ms)	Amplitude (mV)	Conduction velocity (m/s)
Peroneal	Right	Ankle	2.9	2.6	-
		Fibular head	9.2	2.3	48
		Popliteal	10.7	2.3	47
	Left	Ankle	3.1	3.4	-
		Fibular head	8.9	3.0	53
		Popliteal	10.4	2.9	47
Tibial	Right	Ankle	4.2	13.8	-
		Popliteal	10.8	9.8	55
	Left	Ankle	4.1	15.0	-
		Popliteal	11.2	11.8	52
Median	Right	Wrist	2.9	5.9	-
		Elbow	6.2	5.8	64
	Left	Wrist	2.8	5.8	-
		Elbow	6.2	5.6	60
Ulnar	Right	Wrist	2.4	8.2	-
		Elbow	5.5	8.1	61
		Above elbow	7.3	7.6	56
	Left	Wrist	2.4	6.3	-
		Elbow	5.3	5.9	62
		Above elbow	7.0	5.9	59
Radial	Right	Extensor indicis proprius	1.7	2.3	-
		Forearm	3.3	2.2	63
		Above elbow	4.8	2.2	67
	Left	Extensor indicis proprius	2.0	2.4	-
		Forearm	3.5	2.7	67
		Above elbow	4.9	2.4	71
Femoral	Right	Vastus medialis	5.9	0.6	-
	Left	Vastus medialis	6.4	0.7	-
Sensory NCS					
Nerve		Peak Latency (ms)	Amplitude (uV)	Conduction velocity (m/s)	
Ulnar	Right	1.7	61.5	59	
	Left	1.7	69.4	59	
Superficial	Right	1.9	16.6	58	
	Left	2.1	14.4	52	
Late responses					
Nerve		Latency (ms)			
R Tibial F-wave		49.9			
L Tibial F-wave		47.1			
R Median F-wave		23.8			
L Median F-wave		23.4			
R Ulnar F-wave		29.9			
L Ulnar F-wave		29.9			

TABLE 2 A summary of nerve conduction studies at following-up.

Motor NCS					
Nerve	Site		Latency (ms)	Amplitude (mV)	Conduction velocity (m/s)
Peroneal	Right	Ankle	3.2	1.1	-
		Fibular head	8.9	1.0	53
		Popliteal	10.0	0.9	55
	Left	Ankle	3.8	0.7	-
		Fibular head	9.4	0.5	54
		Popliteal	10.6	0.5	50
Tibial	Right	Ankle	4.2	6.1	-
		Popliteal	10.8	4.6	55
	Left	Ankle	4.4	9.2	-
		Popliteal	11.3	5.9	53
Median	Right	Wrist	2.8	8.1	-
		Elbow	6.1	8.0	62
	Left	Wrist	2.7	8.7	-
		Elbow	5.9	8.8	64
Ulnar	Right	Wrist	2.2	8.0	-
		Elbow	5.1	8.2	64
		Above elbow	6.7	8.1	63
	Left	Wrist	2.2	7.3	-
		Elbow	5.1	7.2	64
		Above elbow	6.7	6.9	63
Sensory NCS					
Nerve		Peak Latency (ms)	Amplitude (mV)	Conduction velocity (m/s)	
Nerve		Peak Latency (ms)	Amplitude (mV)	Conduction velocity (m/s)	
Ulnar	Right	1.7	80.5	57	
	Left	1.8	73.8	55	
Superficial	Right	1.8	17.4	61	
Late responses					
Nerve		Latency (ms)			
R Tibial F-wave		42.8			
L Tibial F-wave		43.2			
R Median F-wave		22.6			
L Median F-wave		23.2			

Therefore, we cannot exclude that anti-NF155 antibodies may be present in particular subgroups of patients with CCPD. So far, we are unable to demonstrate a pathophysiologic link between this case of CCPD and anti-NF155 antibody.

The manifestation of CCPD is similar with EMRN, but their pathogenesis remains to be fully elucidated. Although CCPD and EMRN both exhibit CNS and PNS impairments, the detailed pathogenesis of both disorders is still unclear at present. The clinical features of CCPD include a chronic onset, albumin-cytologic dissociation of cerebrospinal fluids, and a low frequency of oligoclonal IgG bands (OCB) positivity. In contrast, EMRN is an acute or subacute progressive disease that causes motor weakness, myelopathy, neuropathy, encephalopathy, and dysautonomia and mild CSF pleocytosis. CCPD is characterized by multifocal acquired inflammatory demyelinating sensory and motor neuropathy. While in EMRN, peripheral neuropathy is axonal, with or without demyelinating neuropathy (23, 24). Some autoantibodies, such as anti-lactosylceramide antibody, which was identified in CCPD was also found in EMRN. However, the specific biomarkers were identified for both disorders: anti-NF155 for CCPD and anti-neutral glycolipid (especially anti-lactosylceramide) for EMRN (6, 24, 27, 28). Our case exhibited some common features of EMRN such as acute motor weakness and dysautonomia, which are not common in CCPD. However, the albumin-cytological dissociation of cerebrospinal fluids and absent of OCB positivity, which is fulfilling the main features of CCPD. Ultimately, we diagnosed the case CCPD based on criteria of Ogata et al. (6). The clinical course of this case highlights the complexity of CCPD. Accurate diagnosis is crucial to ensure the patient receives the most appropriate and effective e treatment. Nerve conduction studies and spinal cord MRI are valuable diagnostic tools. Compared with previous patients with EMRN, our case had a progressing clinical course (25).

Furthermore, the patient presented the symptoms of GBS and we finally revealed HEV infection might be a trigger of GBS. GBS is a heterogeneous disease characterized by acute

immune-mediated polyneuropathies, often associated with preceding viral or bacterial infections (7, 8). Previous studies have indicated the most frequently identified infectious triggers for GBS include *Campylobacter jejuni* infection, influenza-like illnesses, cytomegalovirus, Epstein–Barr virus (EBV), and varicella-zoster virus. Additionally, hepatotropic viruses such as hepatitis A, hepatitis B, and hepatitis C have been implicated as triggering agents (9). Recently, several case reports and studies have reported an association between HEV infection and GBS (10–13). It has been suggested that HEV infection may be responsible for 5 to 11% of sporadic GBS cases in developed countries (14). A study conducted in Bangladesh further confirmed the link between HEV and GBS (15). The exact mechanism underlying GBS associated with HEV infection remains uncertain. One possibility is that HEV directly infects the peripheral nerve roots or the central nervous system, causing neural cell injury, as demonstrated by its ability to replicate in various human neuronal-derived cell lines (16). Another potential mechanism involves molecular mimicry, in which the virus indirectly triggers the disorder by sharing similar antigenic characteristics with components of the peripheral nerves (7). In our patient, who presented with symptoms of GBS and abnormal liver function, we suspected that HEV infection may have triggered the development of GBS based on previous studies (15). Notably, elevated liver enzymes, including alanine or aspartate aminotransferase, are commonly observed in GBS patients with HEV infection, occurring in approximately 75% of cases according to combined series data (17, 18). Confirmation of HEV infection can be established through etiology testing, specifically when serum anti-HEV IgG is positive. As a result, we recommend considering HEV testing in GBS patients.

Due to its rarity, the treatment of CCPD has not been thoroughly investigated. In our case, the patient underwent steroid therapy along with additional administration of IVIg therapy, resulting in a transient response (19). Subsequently, the patient received RTX and exhibited a favorable response. Although similar cases have been reported in previous literature, the optimal therapy for CCPD remains uncertain. Steroids, IVIg, and plasmapheresis have shown efficacy in treating CCPD. Acute or subacute combined CCPD has rarely been observed in adults, with documented successful treatment using plasmapheresis and IV IgG or IV corticosteroids. More recently, Rituximab has also demonstrated positive outcomes in patients with CCPD (1, 20). In another case, RTX was utilized as a third-line therapy following treatment with steroids, IVIg, and Natalizumab, resulting in clinical and radiological improvement without relapses during the 28-month follow-up period (21). Moreover, in a placebo-controlled randomized controlled trial of relapsing–remitting MS (RRMS) patients, RTX was found to drastically decrease the counts of contrast-enhancing lesions as well as volumes of T2 lesions. Furthermore, it reduced the proportion of patients with relapse at 48 weeks (RTX:20.3% vs. placebo: 40.0%) (26). Therefore, aggressive immunomodulation therapy should be considered to induce remission in patients who do not respond to these treatments.

In conclusion, the clinical presentation of CCPD exhibits significant heterogeneity, making the diagnosis challenging in clinical practice. Therefore, it is imperative to establish definitive international criteria for CCPD in larger sample sizes and across multiple centers. We recommend the utilization of MRI and electrophysiological examinations for patients suspected of having CCPD. In cases where both AM and GBS manifestations are observed, we suggest conducting anti-AQP4, MOG, and NCV assessments to achieve a precise diagnosis. Furthermore, it is crucial to exclude HEV infection in patients presenting with GBS symptoms and abnormal liver function. If patients exhibit a poor response to steroids and intravenous immunoglobulin, RTX should be considered as a secondary treatment option.

Data availability statement

The raw data supporting the conclusions of this article will be made available by the authors, without undue reservation.

Ethics statement

Written informed consent was obtained from the individual(s), and minor(s)' legal guardian/next of kin, for the publication of any potentially identifiable images or data included in this article.

Author contributions

XZ: Writing – review & editing, Writing – original draft. AP: Writing – original draft, Writing – review & editing. CL: Writing – original draft, Writing – review & editing. LL: Writing – review & editing. DY: Writing – review & editing. YH: Writing – review & editing. CZ: Writing – review & editing. QY: Writing – review & editing. YL: Writing – review & editing. JL: Writing – review & editing. SL: Writing – review & editing. WNZ: Supervision, Writing – review & editing. YD: Writing – review & editing. WIZ: Writing – review & editing, Supervision.

Funding

The author(s) declare financial support was received for the research, authorship, and/or publication of this article. This work was supported by research grants from the National Natural Science Foundation of China (81971003, 82171406, and 82271457), Shaanxi Province Health Research and Innovation Team for Cognitive Dysfunction Disease (2023TD-06), Tangdu Hospital Innovation Development Foundation (2018QYTS010, 2019QYTS002), Tangdu Hospital Clinical Research Project (2021LCYJ040), and Tangdu hospital foundation for social recruitment talent (2021SHRC011).

Acknowledgments

We thank the patient for her collaboration.

Conflict of interest

The authors declare that the research was conducted in the absence of any commercial or financial relationships that could be construed as a potential conflict of interest.

Publisher's note

References

1. Cortese A, Franciotta D, Alfonsi E, Visigalli N, Zardini E, Diamanti L, et al. Combined central and peripheral demyelination: clinical features, diagnostic findings, and treatment. *J Neurol Sci*. (2016) 363:182–7. doi: 10.1016/j.jns.2016.02.022

2. Thomas PK, Walker RW, Rudge P, Morgan-Hughes JA, King RH, Jacobs JM, et al. Chronic demyelinating peripheral neuropathy associated with multifocal central nervous system demyelination. *Brain*. (1987) 110:53–76. doi: 10.1093/brain/110.1.53

3. Zéphir H, Stojkovic T, Latour P, Lacour A, de Seze J, Outteryck O, et al. Relapsing demyelinating disease affecting both the central and peripheral nervous systems. *J Neurol Neurosurg Psychiatry*. (2008) 79:1032–9. doi: 10.1136/jnnp.2006.108290

4. Kawamura N, Yamasaki R, Yonekawa T, Matsushita T, Kusunoki S, Nagayama S, et al. Anti-neurofascin antibody in patients with combined central and peripheral demyelination. *Neurology*. (2013) 81:714–22. doi: 10.1212/WNL.0b013e3182a1aa9c

5. Alshamrani F, Alyami R, Alghanimi I, Alajaji R, Alkhaldi M, Alamri A. A new report of combined central and peripheral demyelination: a case report. *Front Neurol*. (2021) 12:730129. doi: 10.3389/fneur.2021.730129

6. Ogata H, Matsuse D, Yamasaki R, Kawamura N, Matsushita T, Yonekawa T, et al. A nationwide survey of combined central and peripheral demyelination in Japan. *J Neurol Neurosurg Psychiatry*. (2016) 87:jnnp-2014-309831–6. doi: 10.1136/jnnp-2014-309831

7. Willison HJ, Jacobs BC, van Doorn PA. Guillain-Barré syndrome. *Lancet*. (2016) 388:717–27. doi: 10.1016/S0140-6736(16)00339-1

8. Hahn AF. Guillain-Barré syndrome. *Lancet*. (1998) 352:635–41. doi: 10.1016/S0140-6736(97)12308-X

9. Grygorczuk S, Zajkowska J, Kondrusik M, Pancewicz S, Hermanowska-Szpakowicz T. Guillain-Barré syndrome and its association with infectious factors. *Neurol Neurochir Pol*. (2005) 39:230–6.

10. Kamani P, Baijal R, Amarapurkar D, Gupte P, Patel N, Kumar P, et al. Guillain-Barre syndrome associated with acute hepatitis E. *Indian J Gastroenterol*. (2005) 24:216.

11. Maurissen I, Jeurissen A, Strauven T, Sprengers D, De Schepper B. First case of anti-ganglioside GM1-positive Guillain-Barré syndrome due to hepatitis E virus infection. *Infection*. (2012) 40:323–6. doi: 10.1007/s15010-011-0185-6

12. Tse AC, Cheung RT, Ho SL, Chan KH. Guillain-Barré syndrome associated with acute hepatitis E infection. *J Clin Neurosci*. (2012) 19:607–8. doi: 10.1016/j.jocn.2011.06.024

13. Chen XD, Zhou YT, Zhou JJ, Wang YW, Tong DM. Guillain-Barré syndrome and encephalitis/encephalopathy of a rare case of northern China acute severe hepatitis E infection. *Neurol Sci*. (2014) 35:1461–3. doi: 10.1007/s10072-014-1731-7

14. Stevens O, Claeys KG, Poesen K, Saegeman V, Van Damme P. Diagnostic challenges and clinical characteristics of hepatitis E virus-associated Guillain-Barré syndrome. *JAMA Neurol*. (2017) 74:26–33. doi: 10.1001/jamaneurol.2016.3541

15. Geurtsvankessel CH, Islam Z, Mohammad QD, Jacobs BC, Endtz HP, Osterhaus AD. Hepatitis E and Guillain-Barre syndrome. *Clin Infect Dis*. (2013) 57:1369–70. doi: 10.1093/cid/cit512

16. Drave SA, Debing Y, Walter S, Todt D, Engelmann M, Friesland M, et al. Extra-hepatic replication and infection of hepatitis E virus in neuronal-derived cells. *J Viral Hepat*. (2016) 23:512–21. doi: 10.1111/jvh.12515

17. van den Berg B, van der Eijk AA, Pas SD, Hunter JG, Madden RG, Tio-Gillen AP, et al. Guillain-Barré syndrome associated with preceding hepatitis E virus infection. *Neurology*. (2014) 82:491–7. doi: 10.1212/WNL.0000000000000111

18. Fukae J, Tsugawa J, Ouma S, Umezu T, Kusunoki S, Tsuboi Y. Guillain-Barré and miller fisher syndromes in patients with anti-hepatitis E virus antibody: a hospital-based survey in Japan. *Neurol Sci*. (2016) 37:1849–51. doi: 10.1007/s10072-016-2644-4

19. Farag M, Sibtain N, Burge J, Chaudhry V, Silber E. Atypical inflammatory demyelinating syndrome with central and peripheral nerve involvement. *Mult Scler Relat Disord*. (2021) 51:102926. doi: 10.1016/j.msard.2021.102926

20. Pineda AA, Ogata K, Osoegawa M, Murai H, Shigeto H, Yoshiura T, et al. A distinct subgroup of chronic inflammatory demyelinating polyneuropathy with CNS demyelination and a favorable response to immunotherapy. *J Neurol Sci*. (2007) 255:1–6. doi: 10.1016/j.jns.2007.01.004

21. Granqvist M, Boremalm M, Poorghobad A, Svenningsson A, Salzer J, Frisell T, et al. Comparative effectiveness of rituximab and other initial treatment choices for multiple sclerosis. *JAMA Neurol*. (2018) 75:320–7. doi: 10.1001/jamaneurol.2017.4011

22. Hoshino M, Suzuki Y, Akiyama H, Yamada K, Shima S, Mutoh T, et al. Efficacy of high-dose steroid pulse therapy for anti-galactocerebroside antibody-positive combined central and peripheral demyelination. *Rinsho Shinkeigaku*. (2017) 57:747–52. doi: 10.5692/clinicalneurol.cn-000977

23. Saito K, Toru S, Shima S, Mutoh T. Anti-neutral glycolipids antibody-positive combined central and peripheral demyelination mimicking encephalomyel oradiculoneuropathy phenotype. *Clin Neurol Neurosurg*. (2018) 172:90–2. doi: 10.1016/j.clineuro.2018.06.046

24. Shima S, Kawamura N, Ishikawa T, Masuda H, Iwahara C, Niimi Y, et al. Anti-neutral glycolipid antibodies in encephalomyeloradiculoneuropathy. *Neurology*. (2014) 82:114–8. doi: 10.1212/WNL.0000000000000015

25. Nanaura H, Kataoka H, Shima S, Iwasa N, Eura N, Sugie K, et al. A patient with encephalomyeloradiculoneuropathy exhibiting a relapsing-remitting clinical course: correlation of serum and cerebrospinal fluid anti-neutral glycosphingolipids antibodies with clinical relapse. *Front Neurol*. (2018) 9:206. doi: 10.3389/fneur.2018.00206

26. Hauser SL, Waubant E, Arnold DL, Vollmer T, Antel J, Fox RJ, et al. B-cell depletion with rituximab in relapsing-remitting multiple sclerosis. *N Engl J Med*. (2008) 358:676–88. doi: 10.1056/NEJMoa0706383

27. Mutoh T, Ueda A, Niimi Y. Sphingolipid abnormalities in encephalomyeloradicu loneuropathy (EMRN) are associated with an anti-neutral glycolipid antibody. *FEBS Open Bio*. (2023) 13:1580–6. doi: 10.1002/2211-5463.13578

28. Sasaki A, Hayakawa I, Mutoh T, Abe Y. The first pediatric anti-lactosylceramide antibody-positive encephalomyeloradiculoneuropathy. *Heliyon*. (2022) 8:e10198. doi: 10.1016/j.heliyon.2022.e10198

frontiers | Frontiers in Neurology

TYPE Case Report
PUBLISHED 18 January 2024
DOI 10.3389/fneur.2023.1329541

OPEN ACCESS

EDITED BY
Giovanni Meola,
University of Milan, Italy

REVIEWED BY
Dominic D'Agostino,
University of South Florida, United States
Lucio Comai,
University of Southern California,
United States

*CORRESPONDENCE
Matthew C. L. Phillips
✉ Matthew.Phillips@waikatodhb.health.nz

RECEIVED 29 October 2023
ACCEPTED 27 December 2023
PUBLISHED 18 January 2024

CITATION
Phillips MCL, Johnston SE, Simpson P, Chang DK, Mather D and Dick RJ (2024) Time-restricted ketogenic diet in amyotrophic lateral sclerosis: a case study. *Front. Neurol.* 14:1329541. doi: 10.3389/fneur.2023.1329541

Time-restricted ketogenic diet in amyotrophic lateral sclerosis: a case study

Matthew C. L. Phillips[1]*, Samuel E. Johnston[2], Pat Simpson[3], David K. Chang[4], Danielle Mather[4] and Rognvald J. Dick[2]

[1]Department of Neurology, Waikato Hospital, Hamilton, New Zealand, [2]Older Persons and Rehabilitation Service, Waikato Hospital, Hamilton, New Zealand, [3]Department of Respiratory Medicine, Waikato Hospital, Hamilton, New Zealand, [4]Department of Speech Language Therapy, Waikato Hospital, Hamilton, New Zealand

Amyotrophic lateral sclerosis (ALS) is an incurable neurodegenerative disorder. The most devastating variant is bulbar-onset ALS, which portends a median survival of 24 months from the onset of symptoms. Abundant evidence indicates that neuron metabolism and mitochondrial function are impaired in ALS. Metabolic strategies, particularly fasting and ketogenic diet protocols, alter neuron metabolism and mitochondria function in a manner that may mitigate the symptoms of this disorder. We report the case of a 64-year-old man with a 21-month history of progressive, deteriorating bulbar-onset ALS, with an associated pseudobulbar affect, who implemented a time-restricted ketogenic diet (TRKD) for 18 months. During this time, he improved in ALS-related function (7% improvement from baseline), forced expiratory volume (17% improvement), forced vital capacity (13% improvement), depression (normalized), stress levels (normalized), and quality of life (19% improvement), particularly fatigue (23% improvement). His swallowing impairment and neurocognitive status remained stable. Declines were measured in physical function, maximal inspiratory pressure, and maximal expiratory pressure. Weight loss was attenuated and no significant adverse effects occurred. This case study represents the first documented occurrence of a patient with ALS managed with either a fasting or ketogenic diet protocol, co-administered as a TRKD. We measured improved or stabilized ALS-related function, forced expiratory volume, forced vital capacity, swallowing, neurocognitive status, mood, and quality of life. Measurable declines were restricted to physical function, maximal inspiratory pressure, and maximal expiratory pressure. Now over 45 months since symptom onset, our patient remains functionally independent and dedicated to his TRKD.

KEYWORDS

motor neuron disease, amyotrophic lateral sclerosis, neurodegeneration, energy metabolism, mitochondria dysfunction, metabolic strategy, fasting, ketogenic diet

Introduction

Amyotrophic lateral sclerosis (ALS) is an incurable neurodegenerative disorder that afflicts 4.1–8.4 out of every 100,000 people in the world (1), with the number of new cases anticipated to rise over the next 20–25 years (2). Although most patients develop limb-onset ALS, 25–30% of patients develop the more devastating bulbar-onset variant, which is associated with a median survival of 24 months from the onset of symptoms (3). Bulbar-onset ALS typically presents with dysarthria, dysphagia, or dysphonia.

Many patients also develop changes in behavior, cognition, and mood. The pathogenesis of ALS involves the degeneration and death of upper motor neurons in the brain motor cortices, lower motor neurons in the brainstem and spinal cord, and neurons in the frontotemporal regions of the brain (4). Approximately 90% of patients lack a family history and are classified as sporadic ALS, whereas the remaining 10% show a pattern of inheritance associated with a gene mutation and are classified as familial. Treatment for sporadic and familial ALS is limited and new therapies are needed.

Abundant evidence indicates that neuron metabolism and mitochondrial function are impaired in ALS (5–10). On a morphological level, mitochondria are abnormally shaped, swollen, and vacuolated (6, 11). Metabolically, human-derived motor neurons in both sporadic and familial ALS exhibit defective oxidative phosphorylation, ATP loss, and elevated levels of reactive oxygen species (9, 12). Mitochondria in ALS motor neurons also display impaired glucose metabolism, tricarboxylic acid (TCA) cycle activity, calcium buffering, axonal transport, and population dynamics (5, 10). Moreover, degradations in cell metabolism and mitochondria function have been documented in astrocytes, microglia, Schwann cells, hepatocytes, lymphocytes, and skeletal muscle cells (6). Collectively, these impairments in cell metabolism and mitochondria function culminate in a chronic bioenergetic challenge that disproportionately impacts metabolically active cells such as neurons, glia, and myocytes.

Metabolic strategies, particularly fasting and ketogenic diet protocols, alter cell metabolism and mitochondria function (13). Both strategies enhance production of the dominant blood ketone, beta-hydroxybutyrate (BHB), such that its concentration is sustained at 0.5–0.6 mmol/L or higher (14). BHB metabolism leads to an enhanced free energy of ATP hydrolysis and a greater supply of TCA cycle intermediates (15). Ketone metabolism also produces fewer reactive oxygen species and increases the production of oxidative stress resistance factors (16, 17). Importantly, fasting and ketogenic diet regimens renew the mitochondria pool by upregulating mitogenesis and mitophagy (18). Despite these beneficial effects, current clinical evidence for metabolic strategies in ALS is limited to a handful of studies involving transgenic mouse models—for example, compared with mice maintained on a normal diet, mice sustained on a ketogenic diet show preserved motor performance (19), and mice fed caprylic triglyceride (a medium-chain fatty acid that is readily metabolized into ketones) show a delayed progression of weakness, improved performance, and protection from motor neuron loss (20).

Given the collective evidence, we hypothesized that a metabolic strategy might lead to clinical benefits and improved quality of life in a patient with ALS.

Case study

We report the case of a 64-year-old male dairy farm systems stock controller of European background who presented to his general practitioner with 9 months of slurring and slowing of speech, difficulty swallowing solids, coughing when consuming liquids, intermittent sialorrhea, and constant fatigue. His family had also noted intermittent episodes of laughing and sobbing. He was referred to our motor neuron disease clinic, which occurred 9 months later due to resource constraints, by which time his bulbar symptoms had worsened leading to 10 kg of weight loss since symptom onset. Medical history included colorectal cancer (T1N0M0) 12 years previously, which was treated with a hemicolectomy, as well as a myocardial infarction 11 years previously, treated with coronary angioplasty. He had a 2-year history of chronic musculoskeletal pain afflicting both shoulders, hips, and ankles. Regular medications included aspirin and metoprolol. He was a life-long smoker (10 cigarettes a day for 50 years—he had quit 4 years previously, but recently resumed smoking due to frustration over his symptoms). There was no family history of neuromuscular disease. Socially, he lived with his wife, who was also his caregiver, and had recently retired from work due to his symptoms. On examination, our patient had a muscular build, with little body fat, and he exhibited inappropriate laughter and crying throughout the consultation. He was 160 cm in height and 72.2 kg in weight, with a calculated body-mass index of 28.2 kg/m^2. Neurological examination of the bulbar region revealed definite tongue wasting and fasciculations, a brisk jaw jerk, and spastic dysarthria. Examination of the cervical region revealed mild wasting of the bilateral supraspinatus and infraspinatus muscles and mild weakness in left shoulder abduction, elbow flexion and extension, and finger grip and abduction (all 5-/5). All limb reflexes were normal (2+) and plantar responses were normal. Electromyography of the bulbar, cervical, thoracic, and lumbosacral regions revealed moderate to severe chronic denervation (reduced recruitment and large-amplitude, long-duration motor unit action potentials) in multiple muscles in all four regions. MRI brain showed mild diffuse leukoariosis and MRI spine showed multilevel bilateral foraminal stenoses in the cervical spine, both considered normal for age by a neuroradiologist. An ALS panel analysis for mutations in 35 different genes was negative (ALS Panel, Blueprint Genetics, Espoo, Finland). Blood investigations were normal. At the 3-month follow-up, 21 months after symptom onset, our patient was diagnosed with bulbar-onset ALS with an associated pseudobulbar affect by two independent neurologists (both with neurophysiology fellowships) based on the 2020 Gold Coast criteria (21).

Given the deteriorating symptoms, riluzole was offered but our patient declined, after which an 18-month time-restricted ketogenic diet (TRKD) was presented as an option (Figure 1). The TRKD involved reducing feeding times to two meals a day. Our patient chose the timing of the two meals every day and up to 1 h was permitted per meal, ensuring that food intake was limited to 2 h per day, with fasting (allowing only water, tea, and coffee) occurring all other hours. The modified ketogenic diet was roughly 60% fat, 30% protein, 5% fiber, and 5% net carbohydrate by weight and comprised primarily of whole foods (green vegetables, meats, eggs, nuts, seeds, creams, and natural oils). Our patient was encouraged to eat to satiation at every meal and not to restrict his calorie intake. After obtaining written informed consent, we provided him with a booklet containing guidelines, recipes, and space to record daily (bedtime) blood glucose and ketone levels using a blood glucose and ketone monitor (CareSens Dual, Pharmaco Diabetes, Auckland, New Zealand). The lead investigator provided support as needed via email. Aside from the TRKD, there were no other

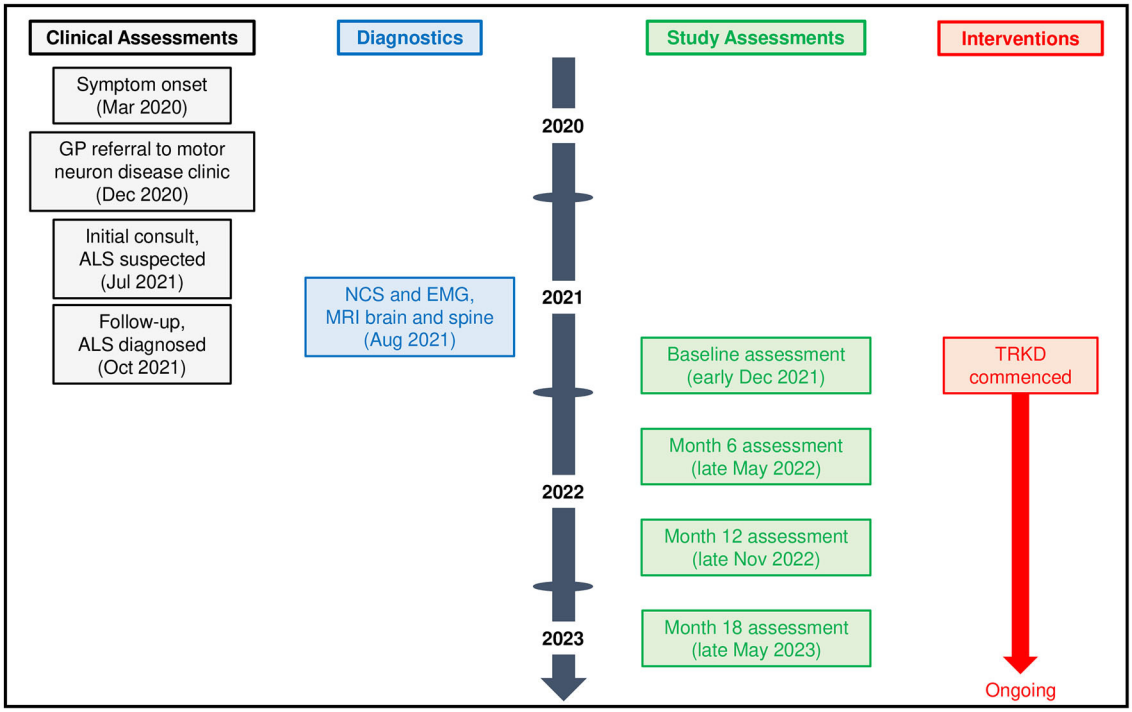

FIGURE 1
Patient timeline.

lifestyle changes and our patient continued to smoke 10 cigarettes a day.

Clinical assessments were conducted during the week preceding the start of the TRKD, with repeat assessments at 6, 12, and 18 months. Clinical assessments evaluated ALS-related function, physical function, pulmonary function, swallowing impairment, neurocognitive status, mood, and quality of life. Assessors were blinded to the intervention. ALS-related function was reported by the patient and caregiver using the Revised ALS Functional Rating Scale (ALSFRS-R) (scores range from 0 to 48, higher numbers indicate improved function) (22). Physical function was measured by a physiotherapist using the get-up-and-go, 6-min walk, and stair climb tests, with an average from two tests calculated for each measure (23–25). Pulmonary function was measured by a pulmonary clinical nurse specialist using spirometry, which assessed forced expiratory volume, forced vital capacity, maximal inspiratory pressure, and maximal expiratory pressure. Swallowing impairment was assessed by speech and language therapists with videofluoroscopic swallowing study and interpreted using the New Zealand Index for Multidisciplinary Evaluation of Swallowing (NZIMES, available at https://fliphtml5.com/nfqi/zyar/basic), which delineates the oral phase, oral transit parameters, pharyngeal phase, crico-esophageal parameters, and laryngeal parameters. Neurocognitive status was measured by a neuropsychologist using the Repeatable Battery for the Assessment of Neuropsychological Status (RBANS, with Form A used at baseline and Week 12 and Form B used at Weeks 6 and 18) (26), Processing Speed from the Wechsler Adult Intelligence Scale—Fourth Edition (27), the Trail Making Test from the Delis-Kaplan Executive Function System (28), and the Controlled Oral Word Association Test (COWAT) from the Multilingual Aphasia Examination (29) (for all tests, higher numbers indicated improved neurocognition), as well as mood using the Depression Anxiety Stress Scale (30). Quality of life was reported by the patient and caregiver using the Functional Assessment of Chronic Illness Therapy—Fatigue (FACIT-F) (scores range from 0 to 160, higher numbers indicate better quality of life) (31). Body weight and blood markers were measured at each assessment. We conducted an adverse effects questionnaire with the patient and caregiver at 6, 12, and 18 months.

During the 18-month TRKD, our patient's mean blood glucose and ketone levels were 6.52 +/- 0.91 and 0.77 +/- 0.43 mmol/L, respectively (Figure 2), with improvement or stability documented in most outcome measures (Tables 1, 2). Regarding function, the ALSFRS-R improved (42–45, representing a 7% improvement from baseline). The get-up-and-go, 6-min walk, and stair climb tests showed decline. Regarding pulmonary function, the forced expiratory volume improved (2.31–2.70 L, representing a 17% improvement), as did forced vital capacity (3.83–4.33 L, representing a 13% improvement). The maximal inspiratory and expiratory pressures declined. Baseline swallowing impairment remained stable aside from the oral phase (none to mild impairment) and laryngeal parameters (moderate to mild impairment). Despite his stabilized swallowing function, our patient opted for a radiologically inserted gastrostomy (RIG) insertion 9 months into the TRKD to mitigate symptoms of aspiration, which existed before the TRKD was implemented and were only triggered by water (to date, the RIG remains solely

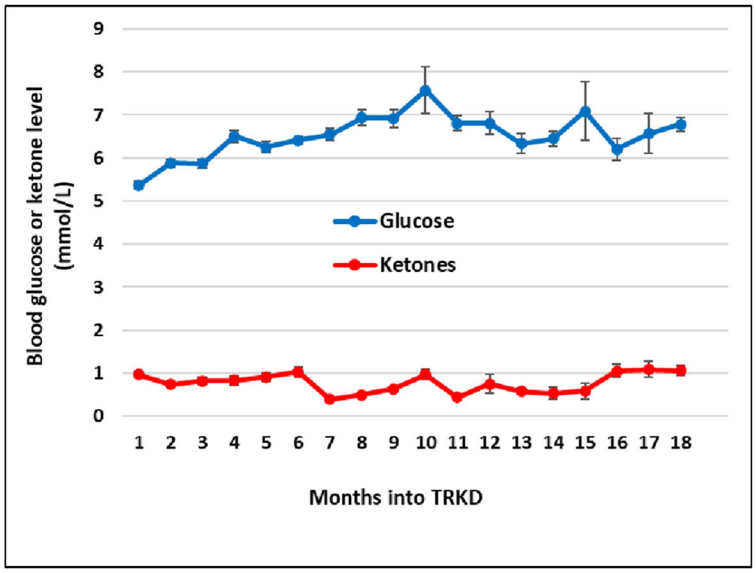

FIGURE 2
Mean monthly blood glucose and ketone (beta-hydroxybutyrate) levels during the time-restricted ketogenic diet (TRKD). Error bars indicate standard error.

used for water intake). The neurocognitive tests generally remained stable. Baseline depression and stress levels resolved (moderate to normal). Regarding quality of life, the FACIT-F improved (114–136, representing a 19% improvement), particularly fatigue as measured by the FACIT-F subscale (35–43, representing a 23% improvement). Our patient's weight was 72.2 kg at baseline and 69.0 kg at month 18. Blood investigations for hemoglobin, creatinine, liver function tests, and glycosylated hemoglobin remained normal over 18 months. Blood triglycerides increased from 1.3 to 1.6 mmol/L, high-density lipoprotein remained at 1.1 mmol/L, low-density lipoprotein increased from 3.1 to 5.4 mmol/L, and total cholesterol increased from 4.8 to 7.2 mmol/L. Our patient experienced no significant adverse effects during the TRKD and consistently mentioned enhanced energy, improved sleep, and reductions in his chronic musculoskeletal pain.

Discussion

This case study represents the first documented occurrence of a patient with ALS managed with either a fasting or ketogenic diet protocol, co-administered as a TRKD. We measured improved ALS-related function (7% improvement from baseline), forced expiratory volume (17% improvement), forced vital capacity (13% improvement), depression (normalized), stress levels (normalized), and quality of life (19% improvement), particularly fatigue (23% improvement). His swallowing impairment and neurocognitive status remained stable. Measurable declines were restricted to physical function, maximal inspiratory pressure, and maximal expiratory pressure. Weight loss was attenuated and no significant adverse effects occurred.

Although fasting and ketogenic diet protocols may individually confer metabolic benefits in ALS, they can be readily combined. Time-restricted feeding eases the burden of organizing multiple meals, which compensates for the extra time required to become familiar with a ketogenic diet, whereas the diet may improve long-term hunger (32), which increases the tolerability of the fasts. The modified ketogenic diet used here was simple, flexible, palatable, and affordable, which alleviated the restrictions that have been associated with ketogenic diets in the past (33). Regardless of whether metabolic strategies are isolated or combined, it is important to monitor blood glucose and BHB levels so that difficulties can be detected and resolved. Despite good adherence to the 18-month TRKD, our patient's mean blood glucose levels averaged 6.52 mmol/L and his BHB 0.77 mmol/L, which is in the lower range of physiological ketosis (albeit, still within range). This may relate to his body composition and the ALS process itself. Our patient's lower fat mass probably provided less fuel reserve for fasting-induced ketogenesis. Moreover, many individuals with ALS exhibit skeletal muscle hypermetabolism (5), which may constitute an adaptive response to decreased energy metabolism efficiency (34). Hypermetabolism could have increased our patient's ketone utilization, leading to lower blood levels.

During this case study, our patient improved or stabilized in most measures of function, which is consistent with TRKD-induced enhancements in neuron, glial cell, and myocyte metabolism as well as mitochondria function. The ALS community relies on the ALSFRS-R to monitor activities of daily living and disease progression (4, 22), which typically declines by 1 point per month (35). Given our patient's baseline score of 42, his score should have declined to 24 during the TRKD. Instead, it improved to 45. Although ALSFRS-R score changes do not necessarily reflect improvement (4), and the specific tests of physical function declined at the final assessment, the fact that our patient's score

10.3389/fneur.2023.1329541

TABLE 1 Outcome measures for ALS-related, physical, pulmonary, and swallowing function at baseline, 6 months, 12 months, and 18 months after commencing the time-restricted ketogenic diet (for all tests except the get-up-and-go and stair climb, higher numbers indicate improved outcomes; improved or stabilized outcomes are highlighted in blue and declines are highlighted in red).

Outcome	Baseline	Month 6	Month 12	Month 18
ALS-related function				
ALSFRS-R				
Speech	3	3	3	3
Salivation	2	2	2	3
Swallowing	3	3	3	3
Handwriting	4	4	3	4
Handling utensils	4	4	4	4
Dressing and hygiene	4	4	4	4
Turning in bed	4	4	4	4
Walking	4	4	4	4
Climbing stairs	3	4	4	4
Dyspnea	3	4	4	4
Orthopnea	4	4	4	4
Respiratory insufficiency	4	4	4	4
Total	42	44	43	45
Physical function				
Get-up-and-go (s)	6.9	6.6	6.8	7.9
6-min walk (m)	541	568	538	497
Stair climb (s)	8.9	8.3	9.3	10.5
Pulmonary function				
FEV1 (L, % predicted)	2.31, 86	2.62, 97	2.37, 88	2.70, 99
FVC (L, % predicted)	3.83, 111	3.87, 112	4.14, 120	4.33, 124
MIP (kPa, % predicted)	5.86, 70	4.10, 50	5.00, 60	4.10, 50
MEP (kPa, % predicted)	11.30, 86	12.20, 93	6.70, 51	4.10, 31
Swallowing impairment				
Oral phase	None	Mild	Mild	Mild
Oral transit parameters	None	Mild	Mild	None
Pharyngeal phase	Mild	Mild	Mild	Mild
Crico-esophageal parameters	None	None	None	None
Laryngeal parameters	Moderate	None	None	Mild

ALSFRS-R, Revised Amyotrophic Lateral Sclerosis Functional Rating Scale; FEV1, Forced Expiratory Volume; FVC, Forced Vital Capacity; MIP, Maximal Inspiratory Pressure; MEP, Maximal Expiratory Pressure.

did not decline over 18 months is potentially important. With respect to pulmonary function, forced vital capacity is arguably the most significant spirometric correlate of disease progression in ALS (36), which shows an average decline of 2–3% predicted per month (35). Given our patient's baseline of 3.83 L (111% predicted), his score should have declined to at least 2.87 L (75% predicted) during the TRKD. Instead, it improved to 4.33 L (124% predicted). Importantly, the maximal inspiratory and expiratory pressures declined during the TRKD, which is discordant with the improved forced expiratory volume and vital capacity, but these measurements should be viewed cautiously as both tests are notoriously difficult to perform and poorly predictive of respiratory capacity (37). Lastly, swallowing impairment occurs in 85–92% of patients diagnosed with bulbar-onset ALS and is associated with malnutrition, aspiration pneumonia, faster functional decline, and increased mortality (38). Importantly, our patient's swallowing function remained stable during the 18-month TRKD, with only minor variations noted in the oral phase (slightly declined) and laryngeal parameters (slightly improved), both of which can be attributed to typical variations seen from swallow to swallow.

Our patient improved or remained stable in most measures of neurocognitive status, mood, and quality of life. Although ALS is often considered a neuromuscular disorder, 50% of patients exhibit impaired executive function, language fluency,

TABLE 2 Outcome measures for neurocognitive status, mood, and quality of life at baseline, 6 months, 12 months, and 18 months after commencing the time-restricted ketogenic diet (for all tests, higher numbers indicate improved outcomes; improved or stabilized outcomes are highlighted in blue and declines are highlighted in red).

Outcome	Baseline	Month 6	Month 12	Month 18
Neurocognitive status				
RBANS (scaled score, percentile)				
Immediate memory	76, 5	76, 5	81, 10	85, 16
Visuospatial/constructional	100, 50	100, 50	105, 63	131, 98
Language	96, 39	96, 39	92, 30	92, 30
Attention	91, 27	82, 12	91, 27	85, 16
Delayed memory	98, 45	100, 50	102, 55	100, 50
Total	88, 21	86, 18	91, 27	97, 42
Processing Speed (scaled score, percentile)	97, 42	86, 18	100, 50	94, 34
Trail Making Test (scaled score, percentile)				
Visual scanning	12, 75	7, 16	10, 50	10, 50
Number sequencing	14, 91	12, 75	13, 84	11, 63
Letter sequencing	12, 75	12, 75	13, 84	12, 75
Number switching	11, 63	11, 63	10, 50	11, 63
Motor speed	11, 63	10, 50	11, 63	11, 63
COWAT (raw score, percentile)				
Phonological fluency	18, <10	18, <10	18, <10	17, <10
Semantic fluency	22, 90	21, 90	18, 75	19, 75
Mood				
Depression Anxiety Stress Scale				
Depression	Moderate	Moderate	Normal	Normal
Anxiety	Normal	Moderate	Normal	Normal
Stress	Moderate	Moderate	Normal	Normal
Quality of life				
FACIT-F (overall)	114	135	141	136
FACIT-F subscale (fatigue)	35	43	42	43

RBANS, Repeatable Battery for the Assessment of Neuropsychological Status; COWAT, Controlled Oral Word Association Test; FACIT-F, Functional Assessment of Chronic Illness Therapy - Fatigue.

or cognition due to pathology in the frontotemporal region (39, 40). The RBANS measures a variety of cognitive domains related to memory, visuospatial and constructional ability, expressive language, and attention (26). Our patient's low baseline RBANS scores (21st percentile) suggested a degree of baseline executive-type impairment, which remained stable (or improved) after the 18-month TRKD (42nd percentile). The COWAT measures verbal fluency (29). Our patient's low baseline phonological fluency scores (<10th percentile) indicated substantial language impairment at baseline, which remained stable. The ongoing stability in most of the neurocognitive tests is encouraging and may reflect TRKD-associated enhancements in neocortical neuron metabolism and mitochondria function. From the perspective of our patient and his wife, the greatest benefits associated with the TRKD related to his mood and energy levels. His moderate baseline depression and stress levels resolved. He also improved his quality of life and fatigue scores, which allowed him to maintain an active outdoors lifestyle on his farm.

During the 21 months prior to the TRKD, our patient lost 10 kg of body weight, which was concerning given that weight loss is negatively correlated with survival in ALS (7, 8). By contrast, he lost only 3.2 kg of weight during the 18-month TRKD. Although the resumption of his smoking habit may have accounted for a portion of the 10 kg of weight loss, the relative weight preservation during the TRKD hints at a weight-sparing effect. It might seem paradoxical that a strategy with the potential to induce a caloric deficit could somehow lead to a weight-sparing effect in ALS. However, the explanation may lie in a TRKD-induced increased efficiency of ATP synthesis. ALS involves the accumulation of damaged, uncoupled mitochondria (41), followed by a progressive decrease in energy metabolism efficiency, energy dissipation through thermogenesis, and ATP depletion despite failing attempts by hypermetabolism to compensate for the shortfall. Fasting may counter this process by inducing mitochondria renewal and coupling, which can increase the rate of ATP synthesis—for example, in a study involving uncoupling

protein-3 knockout mice, fasted mice showed a four-fold higher rate of ATP synthesis compared to fed mice despite no measurable difference in TCA cycle activity or whole-body energy expenditure (42). The TRKD may have increased ATP synthesis efficiency in our patient, culminating in less generated energy being "lost" and a subsequent sparing effect on muscle and fat reserves. Consistent with this hypothesis, well-designed trials have shown that simply increasing calorie intake, which would not increase metabolic efficiency, does not significantly attenuate weight loss in people with ALS (43, 44).

Given that this is a case study, we cannot draw firm conclusions regarding the mechanism of the documented improvements or potential impact of the TRKD on survival. Clinical features associated with shorter survival times include bulbar-onset ALS, older age, rapid functional decline (as measured by the ALSFRS-R), low forced vital capacity, frontotemporal dementia, and pronounced weight loss (3). Given that most of these negative prognostic features either improved or stabilized in our patient, it is reasonable to anticipate an ongoing TRKD-induced survival benefit. Alternative explanations for some of the improvements include a practice effect and a placebo effect. Although the former is possible, this seems unlikely given the lengthy 6-month time intervals between assessments. Since it is not possible to blind patients to metabolic strategies, a placebo effect may have partially contributed to the improvements.

In conclusion, this case study represents the first documented occurrence of a patient with ALS managed with either a fasting or ketogenic diet protocol, co-administered as a TRKD. We measured improved or stabilized ALS-related function, forced expiratory volume, forced vital capacity, swallowing impairment, neurocognitive status, depression, stress levels, and quality of life. Measurable declines were restricted to physical function, maximal inspiratory pressure, and maximal expiratory pressure. Our patient remains functionally independent and dedicated to his TRKD. Despite its limitations, this case study is encouraging and serves as a proof-of-concept for further studies involving metabolic strategies in ALS.

Data availability statement

The original contributions presented in the study are included in the article/supplementary material, further inquiries can be directed to the corresponding author.

Ethics statement

Ethical approval was not required for this study involving a human participant because local and institutional review boards do not require ethics approval for case reports/studies, so long as written informed consent is obtained. The study was conducted in accordance with the local legislation and institutional requirements. The participant provided written informed consent to participate in this study. Written informed consent was obtained from the individual for the publication of any potentially identifiable images or data included in this article.

Author contributions

MP: Conceptualization, Formal analysis, Methodology, Supervision, Writing—original draft, Writing—review & editing. SJ: Data curation, Writing—review & editing. PS: Data curation, Writing—review & editing. DC: Data curation, Writing—review & editing. DM: Data curation, Writing—review & editing. RD: Data curation, Formal analysis, Methodology, Writing—review & editing.

Funding

The author(s) declare that no financial support was received for the research, authorship, and/or publication of this article.

Conflict of interest

The authors declare that the research was conducted in the absence of any commercial or financial relationships that could be construed as a potential conflict of interest.

Publisher's note

References

1. Longinetti E, Fang F. Epidemiology of amyotrophic lateral sclerosis: an update of recent literature. *Curr Opin Neurol.* (2019) 32:771–6. doi: 10.1097/WCO.0000000000000730

2. Arthur KC, Calvo A, Price TR, Geiger JT, Chió A, Traynor BJ. Projected increase in amyotrophic lateral sclerosis from 2015 to 2040. *Nat Commun.* (2016) 7:12408. doi: 10.1038/ncomms12408

3. Masrori P, Van Damme P. Amyotrophic lateral sclerosis: a clinical review. *Eur J Neurol.* (2020) 27:1918–29. doi: 10.1111/ene.14393

4. Goutman SA, Hardiman O, Al-Chalabi A, Chió A, Savelieff MG, Kiernan MC, et al. Recent advances in the diagnosis and prognosis of amyotrophic lateral sclerosis. *Lancet Neurol.* (2022) 21:480–93. doi: 10.1016/S1474-4422(21)00465-8

5. Blasco H, Lanznaster D, Veyrat-Durebex C, Hergesheimer R, Vourch P, Maillot F, et al. Understanding and managing metabolic dysfunction in amyotrophic lateral sclerosis. *Expert Rev Neurother.* (2020) 20:907–19. doi: 10.1080/14737175.2020.1788389

6. Cozzolino M, Carrì MT. Mitochondrial dysfunction in ALS. *Prog Neurobiol.* (2012) 97:54–66. doi: 10.1016/j.pneurobio.2011.06.003

7. Dupuis L, Pradat P-F, Ludolph AC, Loeffler J-P. Energy metabolism in amyotrophic lateral sclerosis. *Lancet Neurol.* (2011) 10:75–82. doi: 10.1016/S1474-4422(10)70224-6

8. Guillot SJ, Bolborea M, Dupuis L. Dysregulation of energy homeostasis in amyotrophic lateral sclerosis. *Curr Opin Neurol.* (2021) 34:773–80. doi: 10.1097/WCO.0000000000000982

9. Smith EF, Shaw PJ, De Vos KJ. The role of mitochondria in amyotrophic lateral sclerosis. *Neurosci Lett.* (2019) 710:132933. doi: 10.1016/j.neulet.2017.06.052

10. Zhao J, Wang X, Huo Z, Chen Y, Liu J, Zhao Z, et al. The impact of mitochondrial dysfunction in amyotrophic lateral sclerosis. *Cells.* (2022) 11:2049. doi: 10.3390/cells11132049

11. Kong J, Xu Z. Massive mitochondrial degeneration in motor neurons triggers the onset of amyotrophic lateral sclerosis in mice expressing a mutant SOD1. *J Neurosci.* (1998) 18:3241–50. doi: 10.1523/JNEUROSCI.18-09-03241.1998

12. Singh T, Jiao Y, Ferrando LM, Yablonska S, Li F, Horoszko EC, et al. Neuronal mitochondrial dysfunction in sporadic amyotrophic lateral sclerosis is developmentally regulated. *Sci Rep.* (2021) 11:18916. doi: 10.1038/s41598-021-97928-7

13. Phillips MCL. Metabolic strategies in healthcare: a new era. *Aging Dis.* (2022) 13:655–72. doi: 10.14336/AD.2021.1018

14. VanItallie TB, Nufert TH. Ketones: metabolism's ugly duckling. *Nutr Rev.* (2003) 61:327–41. doi: 10.1301/nr.2003.oct.327-341

15. Veech RL, Chance B, Kashiwaya Y, Lardy HA, Cahill GF. Ketone bodies, potential therapeutic uses. *IUBMB Life.* (2001) 51:241–7. doi: 10.1080/152165401753311780

16. Masino SA, Ruskin DN. Ketogenic diets and pain. *J Child Neurol.* (2013) 28:993–1001. doi: 10.1177/0883073813487595

17. Shimazu T, Hirschey MD, Newman J, He W, Shirakawa K, Le Moan N, et al. Suppression of oxidative stress by β-hydroxybutyrate, an endogenous histone deacetylase inhibitor. *Science.* (2013) 339:211–4. doi: 10.1126/science.1227166

18. de Cabo R, Mattson MP. Effects of intermittent fasting on health, aging, and disease. *N Engl J Med.* (2019) 381:2541–51. doi: 10.1056/NEJMra1905136

19. Zhao Z, Lange DJ, Voustianiouk A, MacGrogan D, Ho L, Suh J, et al. A ketogenic diet as a potential novel therapeutic intervention in amyotrophic lateral sclerosis. *BMC Neurosci.* (2006) 7:29. doi: 10.1186/1471-2202-7-29

20. Zhao W, Varghese M, Vempati P, Dzhun A, Cheng A, Wang J, et al. Caprylic triglyceride as a novel therapeutic approach to effectively improve the performance and attenuate the symptoms due to the motor neuron loss in ALS disease. *PLoS ONE.* (2012) 7:e49191. doi: 10.1371/journal.pone.0049191

21. Shefner JM, Al-Chalabi A, Baker MR, Cui L-Y, de Carvalho M, Eisen A, et al. A proposal for new diagnostic criteria for ALS. *Clin Neurophysiol.* (2020) 131:1975–8. doi: 10.1016/j.clinph.2020.04.005

22. Cedarbaum JM, Stambler N, Malta E, Fuller C, Hilt D, Thurmond B, et al. The ALSFRS-R: a revised ALS functional rating scale that incorporates assessments of respiratory function. *J Neurol Sci.* (1999) 169:13–21. doi: 10.1016/S0022-510X(99)00210-5

23. Mathias S, Nayak US, Isaacs B. Balance in elderly patients: the 'get-up and go' test. *Arch Phys Med Rehabil.* (1986) 67:387–9.

24. Enright PL. The six-minute walk test. *Respir Care.* (2003) 48:783—5.

25. Bean JF, Kiely DK, LaRose S, Alian J, Frontera WR. Is stair climb power a clinically relevant measure of leg power impairments in at-risk older adults? *Arch Phys Med Rehabil.* (2007) 88:604–9. doi: 10.1016/j.apmr.2007.02.004

26. Randolph C. *Repeatable Battery for the Assessment of Neuropsychological Status (RBANS).* San Antonio, Harcourt, TX: The Psychological Corporation (1998).

27. Wechsler D. *Wechsler Adult Intelligence Scale–Fourth Edition (WAIS–IV).* San Antonio, TX: Pearson (2008).

28. Delis DC, Kaplan EF, Kramer JH. *Delis-Kaplan Executive Function System*. San Antonio, TX: Psychological Corporation. (2001).

29. Benton AL, Hamsher K, Rey GL, Sivan AB. *Multilingual Aphasia Examination (3rd ed).* Iowa City, IA: AJA Associates (1994).

30. Lovibond SH, Lovibond PF. *Manual for the Depression Anxiety Stress Scales (2nd ed.).* Sydney: Psychology Foundation of Australia (1995).

31. Yellen SB, Cella DF, Webster K, Blendowski C, Kaplan E. Measuring fatigue and other anemia-related symptoms with the functional assessment of cancer therapy (FACT) measurement system. *J Pain Symptom Manage.* (1997) 13:63–74. doi: 10.1016/s0885-3924(96)00274-6

32. Ludwig DS, Willett WC, Volek JS, Neuhouser ML. Dietary fat: from foe to friend? *Science.* (2018) 362:764–70. doi: 10.1126/science.aau2096

33. Cervenka MC, Henry BJ, Felton EA, Patton K, Kossoff EH. Establishing an adult epilepsy diet center: experience, efficacy and challenges. *Epilepsy Behav.* (2016) 58:61–8. doi: 10.1016/j.yebeh.2016.02.038

34. Konrad C, Kawamata H, Bredvik KG, Arreguin AJ, Cajamarca SA, Hupf JC, et al. Fibroblast bioenergetics to classify amyotrophic lateral sclerosis patients. *Mol Neurodegener.* (2017) 12:76. doi: 10.1186/s13024-017-0217-5

35. Atassi N, Berry J, Shui A, Zach N, Sherman A, Sinani E, et al. The PROACT database: design, initial analyses, and predictive features. *Neurology.* (2014) 83:1719–25. doi: 10.1212/WNL.0000000000000951

36. Pirola A, De Mattia E, Lizio A, Sannicolò G, Carraro E, Rao F, et al. The prognostic value of spirometric tests in amyotrophic lateral sclerosis patients. *Clin Neurol Neurosurg.* (2019) 184:105456. doi: 10.1016/j.clineuro.2019.105456

37. Caruso P, Albuquerque AL, Santana PV, Cardenas LZ, Ferreira JG, Prina E, et al. Diagnostic methods to assess inspiratory and expiratory muscle strength. *J Bras Pneumol.* (2015) 41:110–23. doi: 10.1590/S1806-37132015000004474

38. Perry BJ, Nelson J, Wong JB, Kent DM. The cumulative incidence of dysphagia and dysphagia-free survival in persons diagnosed with amyotrophic lateral sclerosis. *Muscle Nerve.* (2021) 64:83–6. doi: 10.1002/mus.27244

39. Lomen-Hoerth C, Murphy J, Langmore S, Kramer JH, Olney RK, Miller B. Are amyotrophic lateral sclerosis patients cognitively normal? *Neurology.* (2003) 60:1094–7. doi: 10.1212/01.wnl.0000055861.95202.8d

40. Ringholz GM, Appel SH, Bradshaw M, Cooke NA, Mosnik DM, Schulz PE. Prevalence and patterns of cognitive impairment in sporadic ALS. *Neurology.* (2005) 65:586–90. doi: 10.1212/01.wnl.0000172911.39167.b6

41. Dupuis L, di Scala F, Rene F, de Tapia M, Oudart H, Pradat P-F, et al. Up-regulation of mitochondrial uncoupling protein 3 reveals an early muscular metabolic defect in amyotrophic lateral sclerosis. *FASEB J.* (2003) 17:2091–3. doi: 10.1096/fj.02-1182fje

42. Cline GW, Vidal-Puig AJ, Dufour S, Cadman KS, Lowell BB, Shulman GI. In vivo effects of uncoupling protein-3 gene disruption on mitochondrial energy metabolism. *J Biol Chem.* (2001) 276:20240–4. doi: 10.1074/jbc.M102540200

43. Ludolph AC, Dorst J, Dreyhaupt J, Weishaupt JH, Kassubek J, Weiland U, et al. Effect of high-caloric nutrition on survival in amyotrophic lateral sclerosis. *Ann Neurol.* (2020) 87:206–16. doi: 10.1002/ana.25661

44. Wills A-M, Hubbard J, Macklin EA, Glass J, Tandan R, Simpson EP, et al. Hypercaloric enteral nutrition in patients with amyotrophic lateral sclerosis: a randomised, double-blind, placebo-controlled phase 2 trial. *Lancet.* (2014) 383:2065–72. doi: 10.1016/S0140-6736(14)60222-1

frontiers | Frontiers in Neurology

TYPE Case Report
PUBLISHED 18 January 2024
DOI 10.3389/fneur.2023.1281953

OPEN ACCESS

EDITED BY
Edoardo Malfatti,
Hôpitaux Universitaires Henri Mondor, France

REVIEWED BY
Aravindhan Veerapandiyan,
Arkansas Children's Hospital, United States
Vedrana Milic-Rasic,
University of Belgrade, Serbia

*CORRESPONDENCE
Dario Ronchi
✉ dario.ronchi@unimi.it

†These authors have contributed equally to this work

RECEIVED 23 August 2023
ACCEPTED 19 December 2023
PUBLISHED 18 January 2024

CITATION
Rimoldi M, Romagnoli G, Magri F, Antognozzi S, Cinnante C, Saccani E, Ciscato P, Zanotti S, Velardo D, Corti S, Comi GP and Ronchi D (2024) Case report: A novel patient presenting TRIM32-related limb-girdle muscular dystrophy. *Front. Neurol.* 14:1281953. doi: 10.3389/fneur.2023.1281953

Case report: A novel patient presenting TRIM32-related limb-girdle muscular dystrophy

Martina Rimoldi[1†], Gloria Romagnoli[1†], Francesca Magri[1], Sara Antognozzi[2], Claudia Cinnante[3], Elena Saccani[4], Patrizia Ciscato[1], Simona Zanotti[1], Daniele Velardo[1], Stefania Corti[1,5], Giacomo Pietro Comi[2,5] and Dario Ronchi[2,5]*

[1]Neuromuscular and Rare Disease Unit, Fondazione IRCCS Ca' Granda Ospedale Maggiore Policlinico, Milan, Italy, [2]Neurology Unit, Fondazione IRCCS Ca' Granda Ospedale Maggiore Policlinico, Milan, Italy, [3]Department of Radiology, Istituto Auxologico Italiano, IRCCS, Milan, Italy, [4]Neurology Unit, Department of Specialized Medicine, University Hospital of Parma, Parma, Italy, [5]Dino Ferrari Center, Department of Pathophysiology and Transplantation, University of Milan, Milan, Italy

Limb-girdle muscular dystrophy autosomal recessive 8 (LGMDR8) is a rare clinical manifestation caused by the presence of biallelic variants in the *TRIM32* gene. We present the clinical, molecular, histopathological, and muscle magnetic resonance findings of a novel 63-years-old LGMDR8 patient of Italian origins, who went undiagnosed for 24 years. Clinical exome sequencing identified two *TRIM32* missense variants, c.1181G > A p.(Arg394His) and c.1781G > A p.(Ser594Asp), located in the NHL1 and NHL4 structural domains, respectively, of the TRIM32 protein. We conducted a literature review of the clinical and instrumental data associated to the so far known 26 *TRIM32* variants, carried biallelically by 53 LGMDR8 patients reported to date in 20 papers. Our proband's variants were previously identified only in three independent LGMDR8 patients in homozygosis, therefore our case is the first in literature to be described as compound heterozygous for such variants. Our report also provides additional data in support of their pathogenicity, since p.(Arg394His) is currently classified as a variant of uncertain significance, while p.(Ser594Asp) as likely pathogenic. Taken together, these findings might be useful to improve both the genetic counseling and the diagnostic accuracy of this rare neuromuscular condition.

KEYWORDS

LGMDR8, TRIM32, limb-girdle muscular dystrophy, clinical exome sequencing, tripartite motif-containing proteins

1 Introduction

The term limb-girdle muscular dystrophy (LGMD) refers to typically non-syndromic childhood- and adult-onset group of muscular dystrophies, affecting primarily skeletal muscles, and usually associated with elevated serum creatine kinase (CK) concentration (1, 2). Patients with LGMD suffer from progressive muscle weakness and wasting, involving proximal more than distal districts, in particular muscles of the shoulder and pelvic girdles (1, 2). However, other muscle groups, such as facial, distal upper and lower limbs, may also be affected (3). In the pre-molecular era, LGMD diagnosis used to be purely clinical, and it could only be confirmed differentially once specific protein testing became available (4, 5) to exclude X-linked recessive neuromuscular disorders, such as Duchenne muscular dystrophy and Becker muscular dystrophy (1). Since the advent of molecular myology, pathogenic variants in 29 genes have been reported in distinct LGMD clinical

presentations, classified into dominant (LGMDD) or recessive (LGMDR) forms according to the pattern of inheritance, with some genes presenting both kinds of transmission (1, 2).

LGMDR8 (MIM #254110) represents the subtype 8 of the autosomal recessive type of LGMD, previously known as LGMD2H (1, 2), and initially referred to as Sarcotubular Myopathy when first described in the Hutterite population of Manitoba, in North America (6–9). This subtype of LGMDR can display clinical heterogeneity, with symptom onset ranging between the first and the fourth decade of life (10). The clinical course is progressive, and severity goes from absence of symptoms to muscular weakness with atrophy (11, 12), possibly requiring the use of a wheelchair.

Biallelic variants in the *TRIM32* gene, on chromosome 9q33, have been associated with LGMDR8, which is caused by the homonymous protein deficiency (2). *TRIM32* encodes the member 32 of the TRIpartite Motif-containing (TRIM) ubiquitin E3 ligase family, which ubiquitinates several muscle substrates, including sarcomeric proteins (13). However, the specific effect on the muscle of the so far identified *TRIM32* variants has not been fully clarified yet. Bioinformatic modeling suggests these variants may cause a potential misfolding of the TRIM32 protein, especially at the level of the C-terminal domain, leading to pathogenic consequences on the muscle physiology (14). Beside the first variant – c.1459G > A, p.(Asp487Asn) – identified in the Hutterite population with a founder effect (6, 7, 9), additional 25 variants of *TRIM32* have been described to date in other 41 non-Hutterite LGMDR8 patients, worldwide (11, 13, 15–28).

Here, we present the novel case of an Italian 63-years-old man, who experienced progressive muscle weakness since the age of 39, and only received a molecular diagnosis 24 years later. He is the first LGMDR8 case in literature to be identified as compound heterozygous for two *TRIM32* missense variants, whose pathogenicity has not been clarified yet. We describe his clinical, histopathological, muscle magnetic resonance imaging (MMRI) and molecular findings, against the backdrop of other 52 LGMDR8 patients harboring biallelic *TRIM32* variants (Table 1; Figure 1A), reported across 19 published studies (7, 11, 13, 15–30).

2 Methods

The study was approved by the institutional review board of the Fondazione IRCCS Ca' Granda Ospedale Maggiore Policlinico, Milan (Italy). The patient provided written informed consent for all aspects of the study. All the details related to data collection and analysis are available in Supplementary material. Clinical, histological, immunohistochemical, MMRI, and molecular data from the proband were integrated within our literature review of additional 52 LGMDR8 patients, carrying biallelic *TRIM32* variants (Table 1; Figure 1A).

As far as the literature review is concerned, the following terms were searched through PubMed in May 2023, filtering for human studies, abstract and full-text availability in English: "((trim32) AND (lgmdr8)) OR (limb-girdle muscular dystrophy recessive 8)." We included publications reporting patients of any age, and providing clinical, instrumental, and molecular characterization, with the latter clearly specifying the presence of *TRIM32* biallelic variants, either carried in homozygosis or compound heterozygosis. We applied exclusion criteria at both molecular and clinical levels: (1) the identification of monoallelic *TRIM32* variants led to the exclusion of the heterozygous patients; (2) among the patients carrying *TRIM32* variants biallelically, we excluded those cases clearly showing a non-LGMDR8 phenotype, such as the Bardet-Biedl syndrome type 11 (BBS11).

3 Results

3.1 Case report

A 63-year-old man came to our attention presenting with progressive muscle weakness and difficulty in climbing the stairs, since the age of 39. The patient was born to non-consanguineous parents, had a typical psychomotor development, and a negative family history of neuromuscular disorders. He stopped running in 12-month time from symptom onset, developing a waddling gait and inability to walk long distances by the age of 53. Serum CK levels were persistently increased over the years, ranging between 600 and 3,000 U/L (with 350 U/L representing the upper normal limit in men); his cardiopulmonary examination was always unremarkable.

A muscle biopsy of the vastus lateralis, collected at the age of 40, revealed dystrophic changes, such as severe fibroadipose replacement, predominance of type 2 fibers, increased fiber size variability, and presence of necrotic fibers with macrophagic invasion. Furthermore, there was evidence of numerous splitting fibers, subsarcolemmal and intracytoplasmic vacuoles containing finely granular material, without the presence of sarcotubular aggregates (Figures 2A–D). Immunohistochemistry showed desmin and myotilin accumulations within muscle fibers, as well as increased p62 detection compared to control muscles (Figures 2E–G). Electromyography (EMG) and electroneurography (ENG), performed at the early stage of the disease, showed a myopathic pattern of the quadriceps femoris, supporting the diagnosis of a pelvic girdle myopathy (clinical timeline is displayed in Figure 1B). The primary hypothesis of a putative involvement of the *DMD* gene, possibly responsible for Becker muscular dystrophy, was ruled out by Sanger sequencing and MLPA analysis, at the time of symptom onset.

His last physical examination revealed bilateral hypotrophy of the anterior compartment of the thigh and of the gastrocnemius, winged scapula, and selective weakness of pectoral, upper and lower limb muscles, causing waddling gait and bilateral foot drop. He was able to climb the stairs and stand up from a seated position only with the use of external aids. The patient reported to have recently experienced mild weakness of the upper limbs, and right thigh myalgias, with no cramps nor myoglobinuria. He did not complain of dysphagia or dysphonia. The most recent CK dosage was 2,400 U/L, in line with his previous values.

Following the neuromuscular visit, a muscle MRI scan was performed for the first time in 24 years of disease duration. This revealed diffuse morphological changes in several muscles of the upper and lower limbs (Supplementary Figure 1), with a severe fibroadipose degeneration involving the shoulder and pelvic girdles. In particular, the fatty infiltration pattern of the pelvic girdle and of the thigh muscles showed relative sparing of rectus

TABLE 1 Summary of the 26 TRIM32 variants carried biallelically by the 53 LGMDR8 patients (including our case) reported in the literature.

Variant	ACMG Class	Protein domain	*N*	Age at onset (years)	Age at last visit (years)	CPK (U/L)	Neuromuscular semiology	MMRI	EMG/ ENG	Muscle biopsy	Cardio-pulmonary involvement	Notes on ethnicity/family	Reference
c.35dupA p.(Asp12Glufs*44)	n/a	pre-RING	1	25	49	1,684	LL > UL and P weakness; progressive; cleft lip and palate; bilateral pes cavus; lumbar lordosis	FR	M and NG	M	Normal	Indian; with BR parents	Chandrasekharan et al. (19)
c.59G > T p.(Cys20Phe)	3	RING	1	25	30	1,708	LL > UL and G weakness; C pseudohypertrophy	n/p	n/p	n/p	n/a	n/a	Chakravorty et al. (17)
c.115_116insT p.(Cys39Leufs*17)	n/a	RING	3	30–40	30–40	n/a	dLL and P weakness (3); BBs signs (2)	FR	n/p	D (1); n/p (2)	Normal	Spanish/Australian family; with BR parents	Servián-Morilla et al. (26)
c.459_462dup p.(Arg155Asnfs*29)	5	CC	1	10	40	1,450	LL, pUL, F and G weakness; progressive; WB since 30	n/a	n/p	M	Normal	Turkish	Johnson et al. (21)
c.467T > C p.(Leu156Pro)	3	CC	2	27; 36	43; 54	926; 1,500	LL, pUL and G weakness (2); progressive (2); muscle atrophy and WB at 53 (1); pseudohypertrophy (1)	n/p	n/p	M	n/a	Brothers	Mair et al. (22)
c.488T > C p.(Leu163Pro)	3	CC	2	3; 32	21; 40	6,500; 398	L and G weakness (2); progressive (2); WA at 20 (1)	atrophy and FR	n/p	M; D	Normal (1); n/a (1)	Pakistani (1); Persian (1)	Johnson et al. (21)
c.574dup p.(Glu192Glyfs*7)	5	CC	2	30; 30	56; 48	802; 443	L, G, A and PS weakness; WB since late 40s	atrophy and FR	n/p	D	Mild aberrant contraction (1)	Belgian	Johnson et al. (21)
c.650A > G p.(Asn217Ser)	3	inter CC-NHL1	4	20–67	57–67	n/a	L and G weakness (3); asymptomatic (1); FD (1); progressive (4); WA at 58 (1)	focal FR	n/p	D (2); n/p (2)	Normal	Spanish/Australian family	Servián-Morilla et al. (26)
c.691del p.(Ala231Glnfs*21)	5	inter CC-NHL1	1	early 30s	42	1,844	P and LL weakness; progressive	atrophy and FR	n/p	D	Normal	British	Johnson et al. (21)
c.872T > G p.(Ile291Ser)	3	inter CC-NHL1	1	19	48	120	L and G weakness; progressive; WA at 42	atrophy and FR	n/p	M	Normal	Persian	Johnson et al. (21)
c.1108del p.(Met370Cysfs*10)	4	NHL1	1	early 30s	42	1,844	P and LL weakness; progressive	atrophy and FR	n/p	D	Normal	British	Johnson et al. (21)

(Continued)

10.3389/fneur.2023.1281953

TABLE 1 (Continued)

Variant	ACMG Class	Protein domain	*N*	Age at onset (years)	Age at last visit (years)	CPK (U/L)	Neuromuscular semiology	MMRI	EMG/ ENG	Muscle biopsy	Cardio-pulmonary involvement	Notes on ethnicity/family	Reference
c.1163C > T p.(Ala388Val)	3	NHL1	2	30; 30	56; 48	802; 443	L, G, A and PS weakness; WB since late 40s	atrophy and FR	n/p	D	Mild aberrant contraction (1)	Belgian	Johnson et al. (21)
c.1181G > A p.(Arg394His)	4	NHL1	3	45; 30s; 39	53; 64; 63	500; n/a; 600; 2,400	pL (3), G (3), and NF (1) weakness; pL (2) and LL (1) atrophy; retractions (1); myalgia (2); paresthesia (1); WS (2); FD (1); progressive (3); WB since 60s (1); WA at 50 (1) and 63 (1)	n/a (1); n/p (1); atrophy and FR (1)	n/p (2); M (1)	D (1); M (2)	RBBB (1); LV hypertrophy (1); FVC 41% (1)	British (1); Italian (2)	Johnson et al. (21) (1); Saccone et al. (11) (1); our case
c.1184T > C p.(Ile395Thr)	3	NHL1	1	14	65	125	pL and G weakness; progressive	n/p	n/p	n/p	Aortic valve stenosis; RI and NIV	with BR parents	Ten Dam et al. (27)
c.1459G > A p.(Asp487Asn)	5	NHL3	14	0-8 (5); 20-31 (5); n/a (4)	7–15 (7); 23; 33–40 (5); 54	117–276 (5); 1,055–2,030 (5); 5–20x (3); n/a (1)	L (10), G (8), NF (4), F (2) and A (2) weakness; asymptomatic (4); pL atrophy (4); C pseudohypertrophy (2); C atrophy (1); +Gower's sign (2); myalgia and fatigue (3); WS (1); progressive (4); WB at 53 (1)	n/p (12); atrophy and FR (2)	n/p (13); M (1)	M (7); D (1); n/p (6)	n/a (9); normal (5)	German brothers (2); Hutterite brothers (2); Hutterite family (7); Bosnian Serbian (1); Serbian (1); Hutterite (1)	Schoser et al. (29) (4); Frosk et al. (7) (7); Johnson et al. (21) (2); Liewluck et al. (30) (1)
c.1560delC p.(Cys521Valfs*13)	5	inter NHL3-NHL4	3	<10 (2); 37	40; 36; 44	860; 460; 1–2.5x	myalgia and paresthesia (2); L, G and F weakness (3); WB at 40 (2); F and pL atrophy (3); C pseudohypertrophy (2)	n/p (3)	M and NG	M (2); n/p (1)	Respiratory involvement (1)	Sweden (2); Croatian (1)	Borg et al. (15) (2); Saccone et al. (11) (1)
c.1603delC p.(Leu535Serfs*21)	5	inter NHL3-NHL4	1	30	40	400	LL > UL and P weakness; WS; WA at 40	n/p	M	M	n/a	non-Hutterite	Nectoux et al. (23)
c.1700A > G p.(His567Arg)	3	NHL4	2	24; 27	30	610; 427	L, G and NF weakness; progressive; fatigue; LL hypotrophy; +Gowers' sign	atrophy and FR	M	M	n/a	Chinese sisters	Guan et al. (20)

(Continued)

10.3389/fneur.2023.1281953

TABLE 1 (Continued)

Variant	ACMG Class	Protein domain	*N*	Age at onset (years)	Age at last visit (years)	CPK (U/L)	Neuromuscular semiology	MMRI	EMG/ ENG	Muscle biopsy	Cardio-pulmonary involvement	Notes on ethnicity/family	Reference
c.1701_1703del p.(Phe568del)	3	NHL4	4	20–67	57–67	n/a	L and G weakness (3); asymptomatic (1); FD (1); progressive (4); WA at 58 (1)	focal FR	n/p	D (2); n/p (2)	Normal	Spanish/Australian family	Servián-Morilla et al. (26)
c.1753_1766dup p.(Ile590Leufs*38)	5	NHL4	1	25	52	744	L and G weakness; myalgia; progressive	n/p	M	M	Normal	Turkish; with BR parents	Cossée et al. (16)
c.1771G > A p.(Val591Met)	2	NHL4	3	teens	n/a	n/a	FD first sign (3); L and G weakness (3); ankle contractions (3); progressive (3); WA at 30 (1)	diffuse FR	n/p	D (2); n/p (1)	Normal	Spanish/Australian family (3); with BR parents (1)	Servián-Morilla et al. (26)
c.1781G > A p.(Ser594Asn)	3	NHL4	2	46; 39	66; 63	4x; 2,400	L and G weakness (2); scapular G (1), pL and LL (1) atrophy; C pseudohypertrophy (1); rigid spine (1); WS (1); FD (1); myalgia (1); progressive (2); WA at 63 (1)	diffuse atrophy and FR	n/p (1); M (1)	M	Normal	Italian	Panicucci et al. (25); our case
c.1786C > G p.(Arg596Gly)	3	NHL4	1	14	42	≤2,000	L, PS and P weakness; progressive; scoliosis; joint laxity; WA since mid-30s	n/a	n/p	M	Atrial septal aneurysm	Italian	Johnson et al. (21)
c.1837C > T p.(Arg613*)	4	NHL5	2	34; 25	45; 35	317; 2x	pL, G and A weakness; progressive	n/a (1); atrophy and FR (1)	n/p (1); M (1)	M (2)	Mitral and tricuspid valve regurgitation (1)	Polish (1); n/a (1)	Johnson et al. (21) (1); Neri et al. (24) (1)
c.1855C > T p.(Pro619Ser)	3	NHL5	1	school age	28	746.81	pL, G and T weakness; pL atrophy; progressive; +Hoover's sign	atrophy and FR	M	n/p	LV contraction alteration	Azerbaijani	Marchuk et al. (13)

ACMG class, TRIM32 structural domain, clinical phenotypes, and instrumental findings, are provided for each listed variant. Please note that compound heterozygous patients appear twice (hence N > 53). The color coding refers to the TRIM32 structural domains and intermediate regions displayed in Figure 3B. A, abdominal; ACMG, American College of Medical Genetics and Genomics; BBs, Bardet-Biedl syndrome; BR, blood-related; C, calve; CC, coiled-coil; CPK, creatine phosphokinase; d, distal; D, dystrophic; EF, ejection fraction; EMG/ENG, electromyography/electroneurography; F, facial; FD, foot drop; FR, fatty replacement; FVC, Forced Vital Capacity; G, girdle; L, limb; LV, left ventricle; M, myopathic; MMRI, muscle magnetic resonance imaging; N, number of patients; NF, neck flexor; NG, neurogenic; NIV, non-invasive ventilation; n/a, not available; n/p, not performed; p, proximal; P, pelvic; PS, paraspinal; RBBB, right bundle branch block; RI, respiratory insufficiency; T, tongue; UL/LL, upper/lower limb; WA, walking aids; WB, wheelchair bound; WS, winged scapula.

10.3389/fneur.2023.1281953

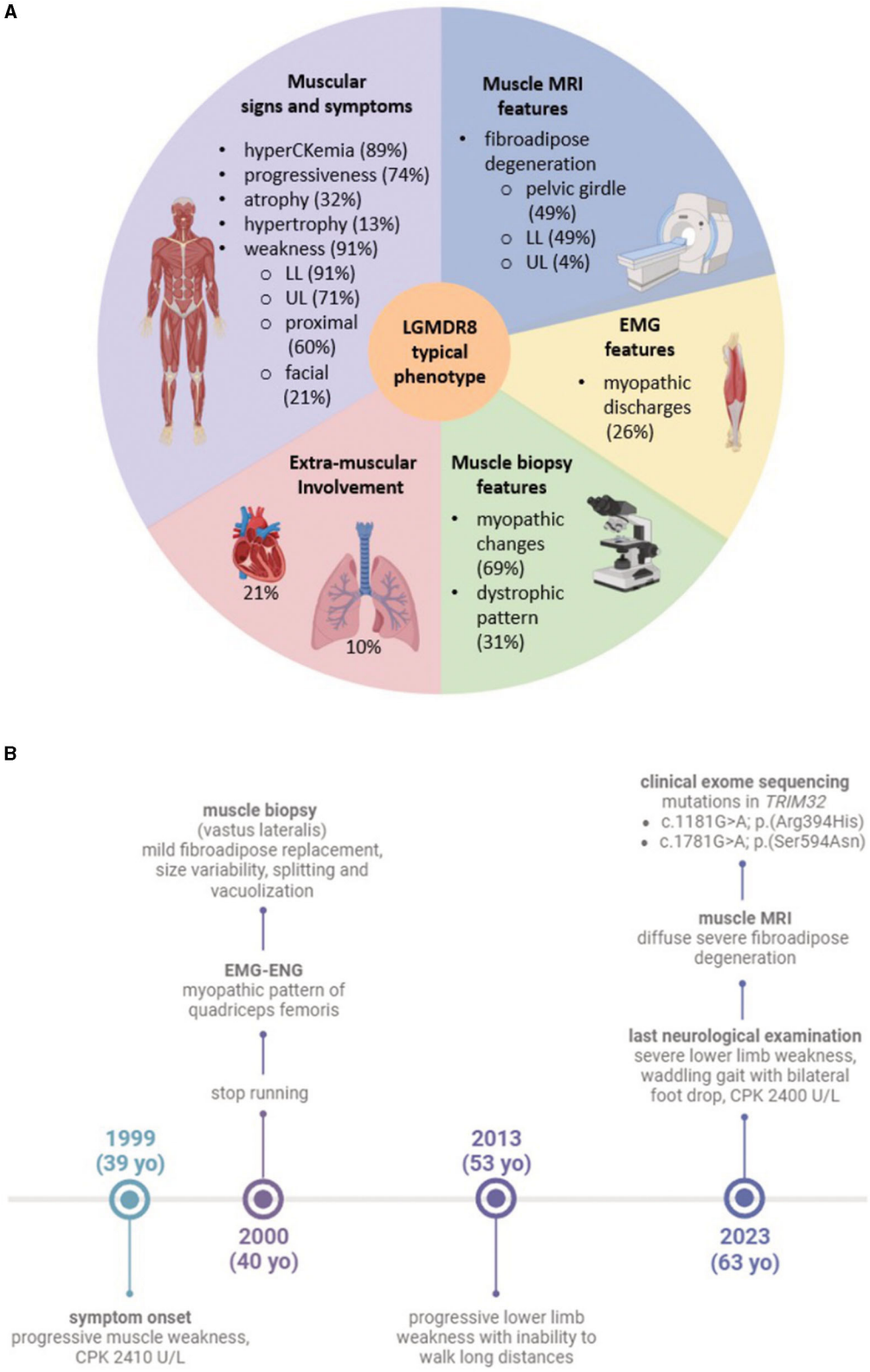

FIGURE 1
(A) Graphic of the typical LGMDR8 phenotype. The five sections summarize the most frequent clinical and instrumental features, drawn from the analysis of the 53 LGMDR8 *TRIM32*-mutated patients (including our case) reported in the literature; **(B)** timeline highlighting our patient's clinical history and diagnostic work-up. Figures **(A, B)** were created with BioRender.com.

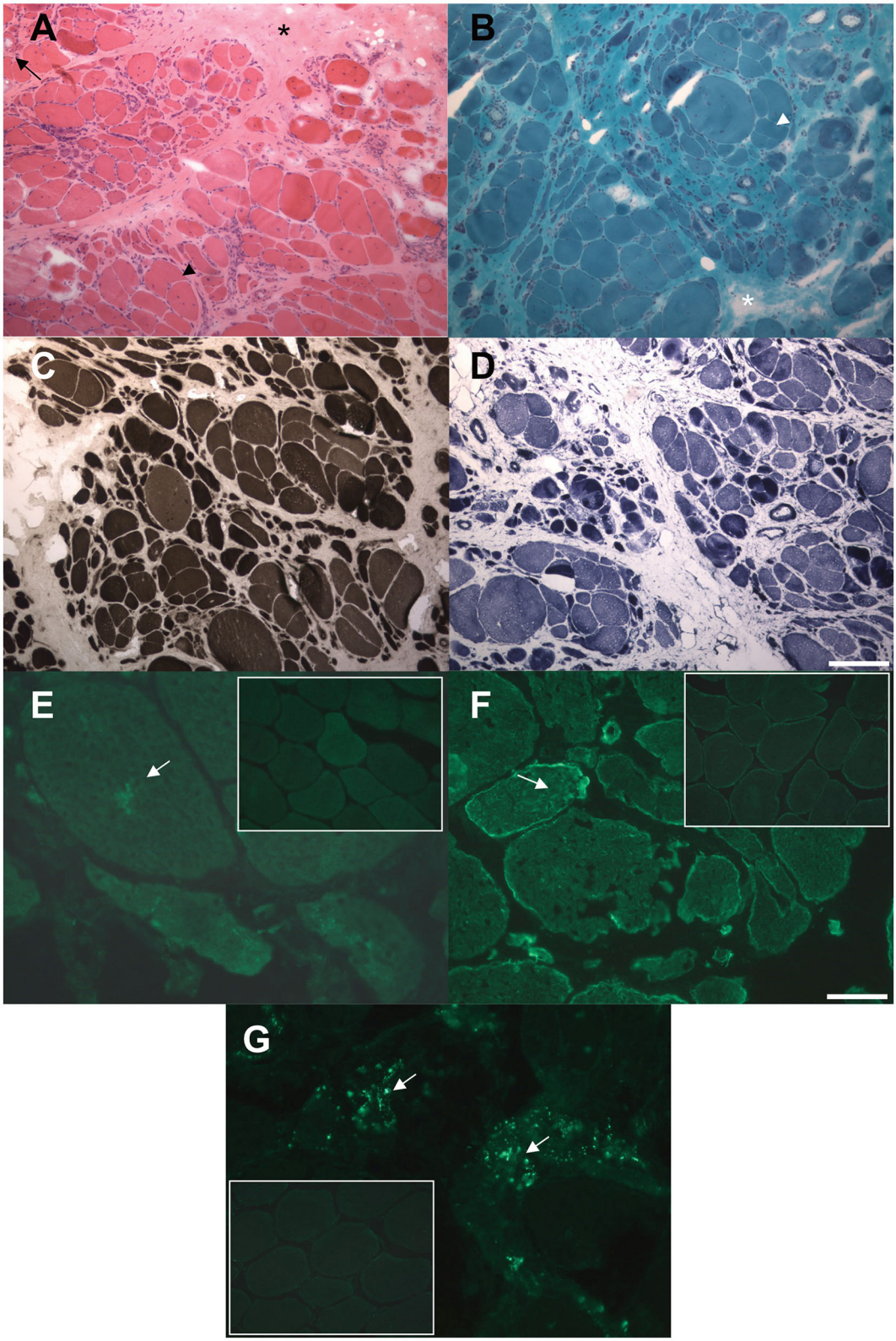

FIGURE 2
Histological and immunohistochemical findings in muscle biopsy. **(A, B)** Hematoxylin and eosin **(A)** and modified Gomori trichrome **(B)** stains showing markedly increased fiber size variability, central nuclei, severe fibro-adipose replacement (asterisks), splitting fibers (arrowheads), internal vacuoles (arrow). **(C)** ATPase pH 9.4 stain showing predominant type 2 (darker) fibers atrophy. **(D)** NADH-TR stain showing preserved oxidative enzymes activity in most of the observed fibers, with darker stain of the atrophic fibers. **(E, F)** Immunofluorescence assay showing increased intracellular accumulation of myotilin **(E)** and desmin **(F)** proteins compared to control muscles (small frames). **(G)** Immmunofluorescence assay showing increased cytoplasmic p62 signal compared to control muscle (small frame). Scale bars: 100 μm **(A–D)** 25 μm **(E–G)**.

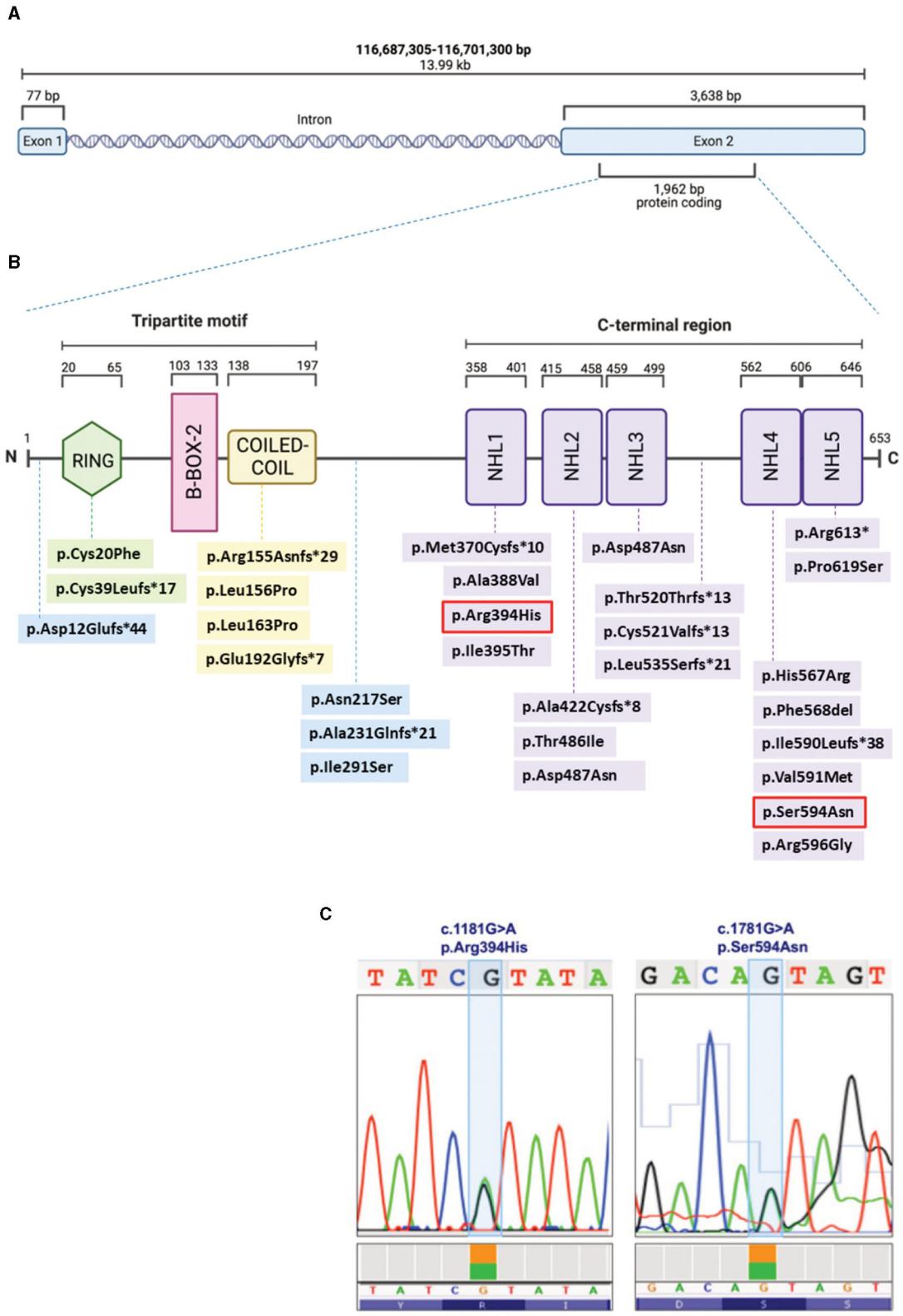

FIGURE 3
Schematic representation of the *TRIM32* gene **(A)** and TRIM32 protein **(B)**, displaying the structural domains and intermediate regions with the LGMDR8-associated biallelic variants (that are listed with the same color coding in Table 1). The two variants (c.1181G > A, p.Arg394His; c.1781G > A, p.Ser594Asn) carried by our patient are outlined in red **(B)** and also shown in the chromatograms **(C)**. Figures **(A, B)** were created with BioRender.com.

femoris, gracilis, sartorius, and the short head of biceps femoris. The most affected compartments of the thigh were the medial and the posterior ones, with a diffuse bilateral hypotrophy, which was mostly symmetric. Dystrophic changes were also present at the level of the leg muscles, with relative sparing of the flexor hallucis longus, flexor digitorum longus and tibialis posterior muscles. As for the shoulder girdle, there was diffuse fatty degeneration, with relative sparing of the right supraspinatus, as well as of the trapezius, infraspinatus and pectoralis muscles, bilaterally. At the upper arm level, the most affected muscle was the triceps brachii, followed by the deltoid muscle. In contrast to what shown by the MMRI, clinical examination of the upper limbs was normal, with MRC score being 5 in all districts, except for pectoral muscles, where MRC score was 4 bilaterally.

To make the definitive diagnosis of LGMDR8, a Clinical Exome Sequencing was performed at our center, revealing the presence of two heterozygous *TRIM32* variants (Figures 3B, C): c.1181G > A/p.(Arg394His), and c.1781G > A/p.(Ser594Asp). These were already described by Saccone et al. (11) and Panicucci et al. (25), and classified as class 4 (likely pathogenic) and class 3 (of uncertain significance) variants, respectively, according to the ACMG (American College of Medical Genetics and Genomics) criteria (Figure 3). Proband's parents or relatives were not available for segregation testing.

3.2 Literature review

We conducted a literature review of the clinical data related to 26 *TRIM32* variants, carried biallelically (in either compound heterozygosis or homozygosis) by 53 LGMDR8 patients (included our proband). Clinical and instrumental findings extracted from the 20 extant studies are reported in Table 1, and a visual summary of the LGMDR8 typical phenotype, based on the literature, is displayed in Figure 1A (7, 11, 13, 15–30).

The 91% (48/53) of the LGMDR8 patients described in the literature suffered from muscle weakness, usually self-reported as difficulty in walking/running and climbing the stairs. The upper limbs were involved in 71% of the patients (34/48), whereas proximal muscles (including those of the scapular girdle) were affected in 60% (29/48) of the cases. Other reported muscular symptoms were myalgias (11/53), exercise-intolerance (7/53), fatigue/fatigability (5/53), paresthesia (3/53), ankle contraction (3/53), muscle stiffness (1/53) and cramps (1/53). Physical examination also revealed lower limb (calves or quadriceps) hypertrophy in 13% (7/53) of the patients, and atrophy/hypotrophy (mainly affecting the lower limbs) in 32% (17/53) of them. Scapular winging was also reported in 13% (7/53) of the cases, and one patient presented with a scapuloperoneal phenotype (30). Finally, a small group of patients (5 out of 53), aged 4–33 years, did not complain of any muscle symptoms, and their neurological evaluation showed no signs of muscular impairment (7, 26). The clinical course showed progressiveness in 74% (39/53) of the cases. In this sub-group of progressive LGMDR8, 21% (8/39) of the patients needed unilateral (3/39) or bilateral (5/39) aids for walking, after 5–24 years of disease duration; while 23% (9/39) of them were wheelchair-bound at an age ranging from 30 to 70 years, after 8–40 years of disease progression. An EMG study was performed in 26% (14/53) of the LGMDR8 patients, who typically showed a myopathic pattern; neurogenic electromyographic changes were also reported in one-third of these cases.

Cardiac and respiratory involvement is not a frequent presentation in LGMDR8, but there might be cardiorespiratory alterations in some cases. Cardiological examination (electrocardiography and/or echocardiography) and spirometry testing were reported normal in 77% (30/39) of the patients with available cardiorespiratory data. The remaining 23% (9/39) showed some respiratory (10%, 4/39) and/or cardiac abnormalities (21%, 8/39), such as respiratory insufficiency and violations of myocardial conduction (Table 1).

MMRI studies of the lower limbs were described in 49% (26/53) of the cases [our patient; (13, 19, 21, 24–28)]. Their images showed fibroadipose degeneration, with preferential affection of the posterior thigh compartment and selective sparing of specific muscles. Upper limb MMRI findings have been rarely reported in the LGMDR8 literature [our case; (28)]. Wei at al. (28) described a minimal fatty infiltration without a distinct involvement pattern; conversely, our patient's MMRI showed diffuse fibroadipose replacement of the shoulder girdle, and involvement of the high arm, with selective sparing of specific muscles.

Histological findings were reported in 39 patients: 69% (27/39) of the biopsies showed nonspecific myopathic changes, whereas the remaining 31% (12/39) displayed a clearly dystrophic pattern, with two cases presenting both myopathic and neurogenic features. Immunohistochemical analysis of our patient's biopsy showed accumulations of desmin and myotilin, that are muscle-relevant targets of the TRIM32 ubiquitin ligase activity, alongside dysbindin, actin, α-actinin and tropomyosin (14). Similar findings were also observed in another LGMDR8 patient (25), who was homozygous for the c.1781G > A, p.(Ser594Asn) *TRIM32* variant, also carried by our proband. Furthermore, a certain degree of autophagy alteration has been observed in muscle samples from LGMDR8 patients: reduced levels of p62 and LC3II were described by Servián-Morilla et al. (26), whereas an increased p62 signal was detected in the muscle biopsy of our patient. Further investigations are therefore needed to elucidate TRIM32 pathways in autophagy regulation, and whether autophagy is up- or down-regulated in LGMDR8 (14).

4 Discussion

The TRIM family includes RING E3 ubiquitin ligases sharing a common evolutionary origin and a similar structure of the N-terminal RING domain as well as of the NHL repeats at the C-terminus.

In the TRIM32 653-amino-acid-long protein (Figure 3B), the N-terminal conserved tripartite motif consists of: (1) a RING structural domain (20–65 amino acids), which confers catalytic activity by interacting with the E2, and by promoting ubiquitin transfer; (2) a single type 2 B-box structural domain (103–133 amino acids), which possibly enhances the E3 RING domain activity (31) and modulates the rate of poly-ubiquitin chain synthesis (32); and (3) the Coiled-Coil structural domain (138–197 amino acids), which mediates dimerization and oligomerization

(14). The C-terminus consists of five (or six) NHL repeats of about forty residues each (358–401, 415–458, 459–499, 562–605, 606–646), that are involved in protein binding and in mediating higher order self-association and homomultimerization (14).

Looking at the clinical features and genotypes of the 53 patients from our literature review, a clear genotype-phenotype correlation did not emerge. Interestingly, Guan and coauthors (20) recently analyzed 86 *TRIM32*-mutated patients from the literature, highlighting a correlation of the *TRIM32* variants exclusively impacting on the NHL domains, with a lower age at onset and higher CK levels, compared to subjects carrying variants outside the NHL regions. A gender effect was also observed, with a lower age of symptom onset, and higher CK levels, in males than in females (20). However, their analysis included both LGMDR8 and BBS11 patients, carrying bi- or monoallelic *TRIM32* variants (20), and this may explain the different results from our review, which instead specifically focused on LGMDR8-associated *TRIM32* biallelic variants.

To date, 50% (13/26) of the *TRIM32* variants (Table 1) considered to be causative for LGMDR8 (when present biallelically, either in homozygosis or in compound heterozygosis) are located in one of the five NHL repeats, like in the case of our patient. However, LGMDR8-causing *TRIM32* variants have been recently identified also in non-NHL domains (RING and Coiled-Coil), as well as in the intermediate regions outside the structural domains, like the pre-RING region (19), inter-CoiledCoil-NHL1 (26), and inter-NHL3-NHL4 (21). These findings dismantled the initial hypothesis of a selective involvement of the NHL domains in the LGMDR8 pathogenesis (14). In particular, the RING domain was found to be mutated (p.Cys20Phe, p.Cys39Leufs*17) in 4 LGMDR8 patients reported independently by Chakravorty et al. (17) and Servián-Morilla et al. (26). Additional 4 variants have been identified also in the Coiled-Coil domain (p.Arg155Asnfs*29; p.Leu156Pro; p.Leu163Pro; p.Glu192Glyfs*7) of other 7 LGMDR8 patients, described by Johnson et al. (21) and Mair et al. (22). The only TRIM32 structural domain which seems not to be involved in the LGMDR8 pathogenesis is the B-box-2. To date, the only noted B-box-2 variant is p.(Pro130Ser), which is, in fact, associated with BBS11 (33). BBS11 is a multisystemic disorder with no skeletal muscle involvement, characterized by obesity, polydactyly, retinal dystrophy and kidney abnormalities. Interestingly, despite LGMDR8 and BBS11 being two distinct disorders, some of the LGMDR8 patients (26) carrying the truncating variant, p.Cys39Leufs*17, in the RING domain, showed typical BBS11 systemic symptoms in addition to the LGMDR8 muscular presentation. A putative explanation for the presence of such different *TRIM32*-related phenotypes might be that RING and B-Box-2 domains have less muscular specificity and a more pleiotropic activity than the Coiled-Coil domain and the NHL repeats, that instead seem to mediate more muscle-specific functions.

Our patient carried a likely pathogenic variant in the NHL1 domain, and a variant of uncertain significance in the NHL5 domain. The NHL1 variant, p.(Arg394His), was previously reported in homozygosis in two LGMDR8 patients by Saccone et al. (11) and Johnson et al. (21); whereas the NHL5 variant, p.(Ser594Asp), was described in homozygosis in one patient by Panicucci et al. (25). Clinical, histological, and imaging features of our proband were very similar to the ones described in the patient carrying the NHL5 variant (25). As for the other two cases carrying the same NHL1 variant harbored by our patient, one had analogous muscular presentation and progressiveness of the disease (21), whereas the second patient, unlike our proband, presented with additional cardiorespiratory symptoms (11). Interestingly, two of these three cases were of Italian origins (11, 25), like our patient.

5 Conclusions

We presented a novel LGMDR8 patient of Italian origins, caused by two *TRIM32* missense variants for the first time described in compound heterozygosis, and previously reported in homozygosis in three independent patients (11, 21, 25). This case report provided new evidence in support of the pathogenicity of both p.(Arg394His) and p.(Ser594Asp) variants, that are not yet classified as pathogenic. We also defined the typical LGMDR8 phenotype associated with the so far identified 26 *TRIM32* variants, by performing a literature review of clinical and instrumental data related to 53 LGMDR8 patients. All these findings, taken together, might potentially be of help in improving both the diagnostic accuracy and the genetic counseling of this rare neuromuscular disease.

Data availability statement

The raw data supporting the conclusions of this article will be made available by the authors, without undue reservation.

Ethics statement

The studies involving humans were approved by Fondazione IRCCS Ca' Granda Ospedale Maggiore Policlinico. The studies were conducted in accordance with the local legislation and institutional requirements. The participants provided their written informed consent to participate in this study. Written informed consent was obtained from the individual(s) for the publication of any potentially identifiable images or data included in this article.

Author contributions

MR: Data curation, Investigation, Writing—original draft. GR: Data curation, Investigation, Writing—original draft. FM: Investigation, Writing—review & editing. SA: Methodology, Visualization, Writing—original draft. CC: Investigation, Methodology, Writing—original draft. ES: Methodology, Writing—original draft. PC: Methodology, Writing—original draft. SZ: Methodology, Writing—original draft. DV: Methodology, Writing—original draft. SC: Writing—review & editing. GC: Writing—review & editing. DR: Conceptualization, Data curation, Investigation, Methodology, Supervision, Writing—original draft, Writing—review & editing.

Funding

The author(s) declare financial support was received for the research, authorship, and/or publication of this article. This study was (partially) funded by Italian Ministry of Health - Current research IRCCS Ca' Granda Ospedale Maggiore Policlinico and by SEQMD project (IRCCS Cà Granda Ospedale Maggiore Policlinico, PI: GC).

Acknowledgments

This work was promoted within the European Reference Network (ERN) for Rare Neuromuscular Diseases. We thank the Associazione Centro Dino Ferrari for its support.

Conflict of interest

The authors declare that the research was conducted in the absence of any commercial or financial relationships that could be construed as a potential conflict of interest.

Publisher's note

All claims expressed in this article are solely those of the authors and do not necessarily represent those of their affiliated organizations, or those of the publisher, the editors and the reviewers. Any product that may be evaluated in this article, or claim that may be made by its manufacturer, is not guaranteed or endorsed by the publisher.

Supplementary material

The Supplementary Material for this article can be found online at: https://www.frontiersin.org/articles/10.3389/fneur.2023.1281953/full#supplementary-material

References

1. Angelini C. LGMD. Identification, description and classification. *Acta Myol.* (2020) 39:207–17. doi: 10.36185/2532-1900-024

2. Straub V, Murphy A, Udd B, group Lws. 229th ENMC international workshop: limb girdle muscular dystrophies - nomenclature and reformed classification Naarden, the Netherlands, 17-19 March 2017. *Neuromuscul Disord.* (2018) 28:702–10. doi: 10.1016/j.nmd.2018.05.007

3. Magri F, Nigro V, Angelini C, Mongini T, Mora M, Moroni I, et al. The italian limb girdle muscular dystrophy registry: relative frequency, clinical features, and differential diagnosis. *Muscle Nerve.* (2017) 55:55–68. doi: 10.1002/mus.25192

4. Hoffman EP, Brown Jr RH, Kunkel LM. Dystrophin: the protein product of the Duchenne muscular dystrophy locus. *Cell.* (1987) 51:919–28. doi: 10.1016/0092-8674(87)90579-4

5. Koenig M, Hoffman EP, Bertelson CJ, Monaco AP, Feener C, Kunkel LM. Complete cloning of the Duchenne muscular dystrophy (DMD) cDNA and preliminary genomic organization of the DMD gene in normal and affected individuals. *Cell.* (1987) 50:509–17. doi: 10.1016/0092-8674(87)90504-6

6. Frosk P, Weiler T, Nylen E, Sudha T, Greenberg CR, Morgan K, et al. Limb-girdle muscular dystrophy type 2H associated with mutation in TRIM32, a putative E3-ubiquitin-ligase gene. *Am J Hum Genet.* (2002) 70:663–72. doi: 10.1086/339083

7. Frosk P, Del Bigio MR, Wrogemann K, Greenberg CR. Hutterite brothers both affected with two forms of limb girdle muscular dystrophy: LGMD2H and LGMD2I. *Eur J Hum Genet.* (2005) 13:978–82. doi: 10.1038/sj.ejhg.5201436

8. Jerusalem F, Engel AG, Gomez MR. Sarcotubular myopathy. A newly recognized, benign, congenital, familial muscle disease. *Neurology.* (1973) 23:897–906. doi: 10.1212/WNL.23.9.897

9. Shokeir MH, Kobrinsky NL. Autosomal recessive muscular dystrophy in manitoba hutterites. *Clin Genet.* (1976) 9:197–202. doi: 10.1111/j.1399-0004.1976.tb01568.x

10. Shieh PB, Kudryashova E, Spencer MJ. Limb-girdle muscular dystrophy 2H and the role of TRIM32. *Handb Clin Neurol.* (2011) 101:125–33. doi: 10.1016/B978-0-08-045031-5.00009-8

11. Saccone V, Palmieri M, Passamano L, Piluso G, Meroni G, Politano L, et al. Mutations that impair interaction properties of TRIM32 associated with limb-girdle muscular dystrophy 2H. *Hum Mutat.* (2008) 29:240–7. doi: 10.1002/humu.20633

12. Weiler T, Greenberg CR, Zelinski T, Nylen E, Coghlan G, Crumley MJ, et al. A gene for autosomal recessive limb-girdle muscular dystrophy in manitoba hutterites maps to chromosome region 9q31-q33: evidence for another limb-girdle muscular dystrophy locus. *Am J Hum Genet.* (1998) 63:140–7. doi: 10.1086/301925

13. Marchuk M, Dovbonos T, Makukh H, Semeryak O, Sharhorodska Y. Sarcotubular myopathy due to novel *TRIM32* mutation in association with multiple sclerosis. *Brain Sci.* (2021) 11:1020. doi: 10.3390/brainsci11081020

14. Lazzari E, Meroni G. TRIM32 ubiquitin E3 ligase, one enzyme for several pathologies: from muscular dystrophy to tumours. *Int J Biochem Cell Biol.* (2016) 79:469–77. doi: 10.1016/j.biocel.2016.07.023

15. Borg K, Stucka R, Locke M, Melin E, Ahlberg G, Klutzny U, et al. Intragenic deletion of TRIM32 in compound heterozygotes with sarcotubular myopathy/LGMD2H. *Hum Mutat.* (2009) 30:E831–44. doi: 10.1002/humu.21063

16. Cossée M, Lagier-Tourenne C, Seguela C, Mohr M, Leturcq F, Gundesli H, et al. Use of SNP array analysis to identify a novel TRIM32 mutation in limb-girdle muscular dystrophy type 2H. *Neuromuscul Disord.* (2009) 19:255–60. doi: 10.1016/j.nmd.2009.02.003

17. Chakravorty S, Nallamilli BRR, Khadilkar SV, Singla MB, Bhutada A, Dastur R, et al. Clinical and genomic evaluation of 207 genetic myopathies in the Indian subcontinent. *Front Neurol.* (2020) 11:559327. doi: 10.3389/fneur.2020.559327

18. Chan GHJ, Ong PY, Low JJH, Kong HL, Ow SGW, Tan DSP, et al. Clinical genetic testing outcome with multi-gene panel in Asian patients with multiple primary cancers. *Oncotarget.* (2018) 9:30649–60. doi: 10.18632/oncotarget.25769

19. Chandrasekharan SV, Sundaram S, Malaichamy S, Poyuran R, Nair SS. Myoneuropathic presentation of limb girdle muscular dystrophy R8 with a novel TRIM32 mutation. *Neuromuscul Disord.* (2021) 31:886–90. doi: 10.1016/j.nmd.2021.06.003

20. Guan Y, Liang X, Li W, Lin W, Liang G, Xie H, et al. TRIM32 biallelic defects cause limb-girdle muscular dystrophy R8: identification of two novel mutations and investigation of genotype-phenotype correlation. *Skelet Muscle.* (2023) 13:10. doi: 10.1186/s13395-023-00319-x

21. Johnson K, De Ridder W, Töpf A, Bertoli M, Phillips L, De Jonghe P, et al. Extending the clinical and mutational spectrum of *TRIM32*-related myopathies in a non-Hutterite population. *J Neurol Neurosurg Psychiatry.* (2019) 90:490–3. doi: 10.1136/jnnp-2018-318288

22. Mair D, Biskup S, Kress W, Abicht A, Brück W, Zechel S, et al. Differential diagnosis of vacuolar myopathies in the NGS era. *Brain Pathol.* (2020) 30:877–96. doi: 10.1111/bpa.12864

23. Nectoux J, de Cid R, Baulande S, Leturcq F, Urtizberea JA, Penisson-Besnier I, et al. Detection of TRIM32 deletions in LGMD patients analyzed by a combined strategy of CGH array and massively parallel sequencing. *Eur J Hum Genet.* (2015) 23:929–34. doi: 10.1038/ejhg.2014.223

24. Neri M, Selvatici R, Scotton C, Trabanelli C, Armaroli A, De Grandis D, et al. A patient with limb girdle muscular dystrophy carries a TRIM32 deletion, detected by a novel CGH array, in compound heterozygosis with a nonsense mutation. *Neuromuscul Disord.* (2013) 23:478–82. doi: 10.1016/j.nmd.2013.02.003

25. Panicucci C, Traverso M, Baratto S, Romeo C, Iacomino M, Gemelli C, et al. Novel *TRIM32* mutation in sarcotubular myopathy. *Acta Myol.* (2019) 38:8–12.

26. Servián-Morilla E, Cabrera-Serrano M, Rivas-Infante E, Carvajal A, Lamont PJ, Pelayo-Negro AL, et al. Altered myogenesis and premature senescence underlie human TRIM32-related myopathy. *Acta Neuropathol Commun.* (2019) 7:30. doi: 10.1186/s40478-019-0683-9

27. Ten Dam L, de Visser M, Ginjaar IB, van Duyvenvoorde HA, van Koningsbruggen S, van der Kooi AJ. Elucidation of the genetic cause in dutch limb girdle muscular dystrophy families: a 27-year's journey. *J Neuromuscul Dis.* (2021) 8:261–72. doi: 10.3233/JND-200585

28. Wei XJ, Miao J, Kang ZX, Gao YL, Wang ZY, Yu XF. A novel homozygous exon2 deletion of TRIM32 gene in a Chinese patient with sarcotubular myopathy: a case report and literature review. *Bosn J Basic Med Sci.* (2021) 21:495–500. doi: 10.17305/bjbms.2020.5288

29. Schoser BG, Frosk P, Engel AG, Klutzny U, Lochmüller H, Wrogemann K. Commonality of TRIM32 mutation in causing sarcotubular myopathy and LGMD2H. *Ann Neurol.* (2005) 57:591–5. doi: 10.1002/ana.20441

30. Liewluck T, Tracy JA, Sorenson EJ, Engel AG. Scapuloperoneal muscular dystrophy phenotype due to TRIM32-sarcotubular myopathy in South Dakota Hutterite. *Neuromuscul Disord.* (2013) 23:133–8. doi: 10.1016/j.nmd.2012.09.010

31. Micale L, Chaignat E, Fusco C, Reymond A, Merla G. The tripartite motif: structure and function. *Adv Exp Med Biol.* (2012) 770: 11–25. doi: 10.1007/978-1-4614-5398-7_2

32. Lazzari E, El-Halawany MS, De March M, Valentino F, Cantatore F, Migliore C, et al. Analysis of the Zn-binding domains of TRIM32, the E3 ubiquitin ligase mutated in limb girdle muscular dystrophy 2H. *Cells*. (2019) 8:254. doi: 10.3390/cells8030254

33. Chiang AP, Beck JS, Yen HJ, Tayeh MK, Scheetz TE, Swiderski RE, et al. Homozygosity mapping with SNP arrays identifies TRIM32, an E3 ubiquitin ligase, as a Bardet-Biedl syndrome gene (BBS11). *Proc Natl Acad Sci U S A.* (2006) 103:6287–92. doi: 10.1073/pnas.0600158103

frontiers | Frontiers in Neurology

TYPE Case Report
PUBLISHED 29 January 2024
DOI 10.3389/fneur.2024.1306264

OPEN ACCESS

EDITED BY
Giovanni Meola,
University of Milan, Italy

REVIEWED BY
Natalie Winter,
Hertie Institute for Clinical Brain Research (HIH), Germany
Wee Lam,
Singapore General Hospital, Singapore

*CORRESPONDENCE
Xueyuan Li
lixueyuan2000@163.com

RECEIVED 03 October 2023
ACCEPTED 15 January 2024
PUBLISHED 29 January 2024

CITATION
Shi F, Zhou X and Li X (2024) Neuralgic amyotrophy with multiple hourglass-like constrictions of anterior interosseous nerve: a case report.
Front. Neurol. 15:1306264.
doi: 10.3389/fneur.2024.1306264

Neuralgic amyotrophy with multiple hourglass-like constrictions of anterior interosseous nerve: a case report

Fangling Shi, Xiaoling Zhou and Xueyuan Li*

Department of Hand Surgery, Ningbo No.6 Hospital, Ningbo, China

Hourglass-like constrictions (HLCs) of peripheral nerves in the upper extremity were a rare form of neuralgic amyotrophy, often characterized by the sudden onset of pain in the shoulder or arm, followed by muscle weakness and amyotrophy, with limited sensory involvement. We present a case of multiple HLCs of the anterior interosseous nerve (AIN) in a 22-year-old female with left upper arm pain, finger numbness, and limited activity for 1 month. Physical examination showed weakness of the left index flexor digitorum profundus and flexor pollicis longus, with mild hypoesthesia in the first three fingers and the radial half of the ring finger. Electromyography suggested a median nerve (mainly AIN) lesion. Ultrasonographic imaging of the median nerve shows AIN bundle swelling and multiple HLCs at left upper arm. Despite conservative treatment, which included 15 days of steroid pulse therapy, Etoricoxib, and oral mecobalamin, the patient still complained of extreme pain at night without relief of any symptoms. Operation was recommended for this patient with thorough concerns of surgical advantages and disadvantages. During surgery, a total of 7 HLCs were found in her median nerve along and above the elbow joint. Only Interfascicular neurolysis was performed because the nerve constrictions were still in the early stage. The pain was almost relieved the next day. One month after surgery, she could bend her thumb and index fingers, although they were still weak. 4 months after the surgery, she was able to bend affected fingers, with muscle strength M3 level. At the same time, her fingers had fewer numbness symptoms. There was still controversy regarding treatment strategy; however, early diagnosis and surgical treatment for nerve HLCs might be a better choice to promote nerve recovery.

KEYWORDS

neuralgic amyotrophy, Parsonage-Turner syndrome, brachial neuritis, surgery, neurolysis

Introduction

Neuralgic amyotrophy, also known as brachial neuritis or Parsonage-Turner syndrome, is characterized by the sudden onset of pain in the shoulder or arm, followed by muscle weakness and amyotrophy, with limited sensory involvement (1–3). The etiology of neuralgic amyotrophy is still unclear. The pathology points toward certain autoimmune processes, induced by a viral infection or activated in an immunosuppressed state, or an allergic mechanism, leading to inflammation of selected peripheral nerves (4, 5).

With the application of high-resolution peripheral nerve imaging including, ultrasound and MRI, the presence of HLCs of involved nerves or nerve fascicles is increasingly recognized in patients with neuralgic amyotrophy (6), and patients with HLCs usually have poor recovery with residual symptoms or paresis (7). Ultrasound has the advantage of being noninvasive and cost-effective, providing important value in monitoring the progress of affected nerves (6, 8).

We achieved good clinical recovery in a neuralgic amyotrophy patient with multiple HLCs in the AIN by early surgical intervention. We discussed the early diagnosis and treatment strategy based on this special case. Written consent for publication of this case report was obtained from the patient herself.

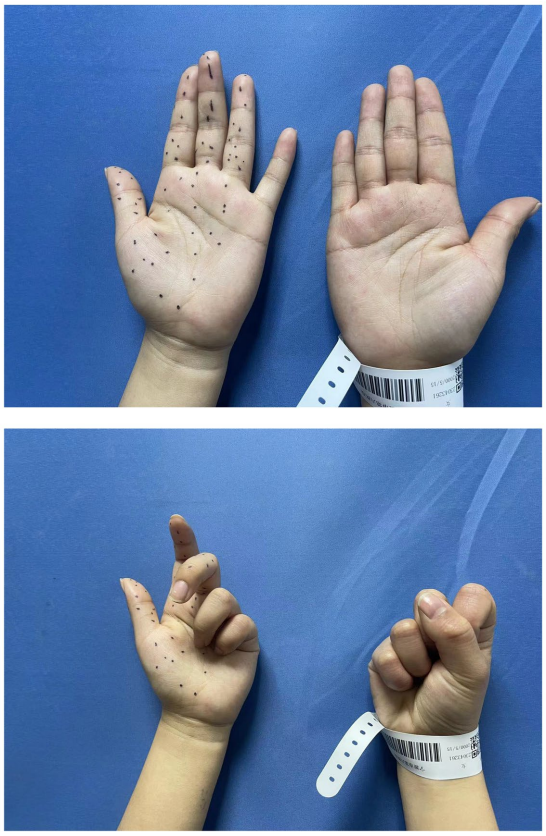

FIGURE 1
Preoperative physical examination showed the strength of the left flexor pollicis longus and index flexor digitorum profundus was MRC 2, with mild hyperesthesia in 1–4 digits.

Case report

History and examination

A 22-year-old woman complained of extreme pain in her left upper arm and numbness in her fingers after carrying heavy acrylic plates. There was no family history of nervous system or musculoskeletal disease. Initially, she was unaware of the severity of the condition. She chose to stay at home and take a rest. However, her pain and weakness showed no signs of recovery, with obvious flexion weakness of her thumb and index finger within 2 weeks. Half a month after the onset of the disease, ultrasound examination at a local hospital revealed edema of the median nerve accompanied by constrictions. One month following the onset, she came to our outpatient clinic. The patient presented with a forced left elbow flexion position due to severe pain. Physical examination showed a severe paresis of the left flexor pollicis longus and index flexor digitorum profundus muscles (strength 2 on the Medical Research Council (MRC) scale), a moderate paresis for the middle flexor digitorum profundus (MRC 3), biceps brachii, flexor carpi radialis, and abductor pollicis brevis muscles (MRC 3–4), with mild hypesthesia first three fingers and the radial half of the ring finger (Figure 1). The rest of muscle strength, tendon reflexes, Tinel's sign and neck examination were unremarkable.

At first, we adopted conservative treatment for the patient including 2 weeks of steroid pulse therapy (1 mg/kg), etoricoxib and oral mecobalamin. However, the patient still complained of extreme pain described as shooting and drilling at night. Therefore, electromyography (EMG) and ultrasound examination were performed when she came to the clinic again.

The EMG results showed that the abductor pollicis brevis, flexor pollicis longus, flexor carpi radialis, and biceps brachii exhibited fibrillation potentials and positive sharp waves, indicating AIN and musculocutaneous nerve both involvement. The conduction velocity of Median nerve was 53 m/s and the compound muscle action potential (cMAP) of the biceps muscle, as shown in EMG, was 10.5 mV (Table 1).

TABLE 1 Patient's electromyography results.

Muscle	Fibrillation potentials	Positive sharp waves	cMAP	Lat
Abductor pollicis brevis	+	+	1.3	4.3
Flexor pollicis longus	+	+	—	—
Flexor carpi radialis	+	+		
Biceps brachii	+	+	10.5	10.8

Detected nerves	cMAP(Left)	Lat(Left)	cMAP(Right)	Lat(Right)
Lateral antebrachial cutaneous nerve	42.3	1.4	40.1	1.3
Superficial radial nerve	58.7	1.7	—	—
Median nerve	18.4	3.1	43.1	3.1

Ultrasound examination of the median nerve showed nerve bundle swelling and multiple HLCs of left upper arm (Figure 2). Magnetic resonance imaging was not performed.

Surgery

The Median nerve was exposed through 2 incisions in front of the elbow joint. Inspection of the median nerve revealed that nerve fascicles (mainly AIN) were partially swollen and hardened due to inflammatory thickening of the epineurium proximal to the medial epicondyle.

After the thickened epineurium had been opened, multiple HLCs lesions along with AIN bundle were exposed. One of the fascicles showed 4 HLCs and other fascicles showed 3 HLCs (Figure 3).

During surgery, a total of 7 HLCs were found at 10.5, 9.5, 9.0, 6.0, 2.0, 1.5 and 0 cm proximal to the medial epicondyle (Figure 3) in her AIN bundle and without any visible source of external compression. During surgical intervention, nerve epineurium and part of the interfascicular nerve were released and electrical stimulation was performed on the median nerve. A total of 1 mL Compound Betamethasone was injected underneath the affected AIN epineurium.

Postoperative course

After surgery, the left elbow was immobilized at 135° position with splint for 2 weeks. The next day, the patient's pain was almost relieved. One month after surgery, she was able to bend her thumb and index fingers actively, although still weak (MRC 2). 4 months after the surgery, she was able to bend her thumb and index finger (MRC 3). At the same time, her fingers were less numbed.

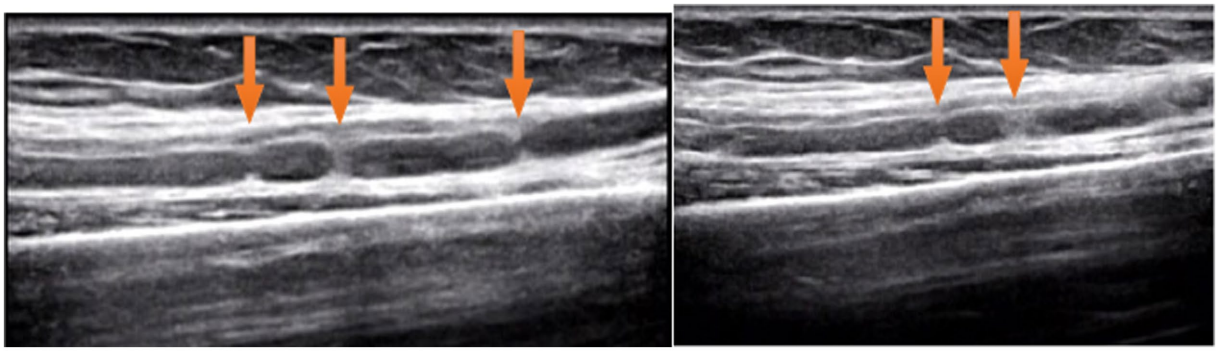

FIGURE 2
The longitudinal ultrasound image shows multiple HLCs of AIN (arrow).

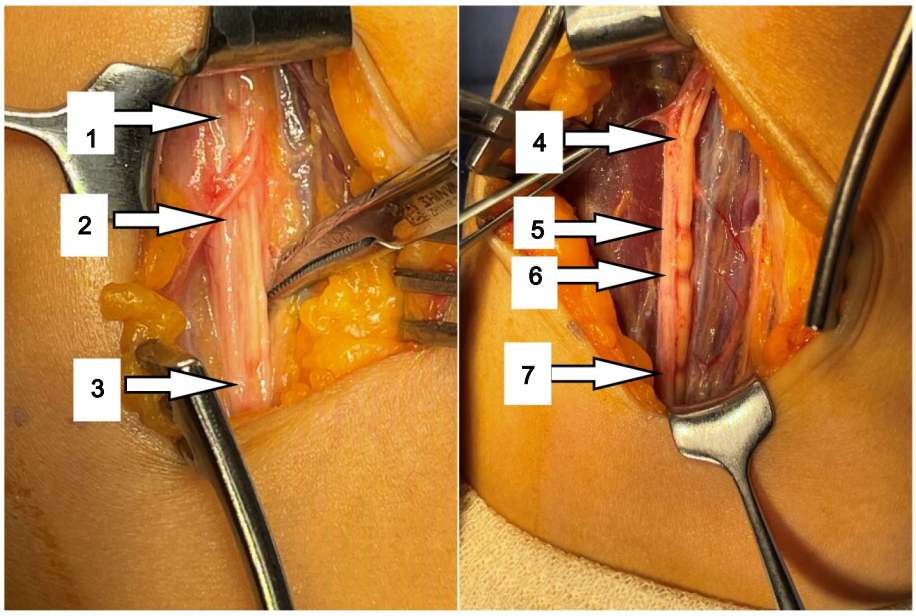

FIGURE 3
Multiple HLCs had been observed in the affected AIN during the operation (arrow).

Discussion

The structural pathology of HLCs has been described in numerous cases of neuralgic amyotrophy, affecting various nerves including AIN, PIN, musculocutaneous nerve, suprascapular nerve and posterior cord (9). Recent progress in research on high-resolution imaging has effectively improved the understanding and early diagnosis of neuralgic amyotrophy (4, 6, 8). Moreover, Peripheral nerve surgery is gradually recognized as a routine treatment for neuralgic amyotrophy with HLCs (4, 5, 7, 10). In this case, we diagnosed AIN nerve constrictions early using ultrasound and performed surgical procedures after 2 weeks of conservative treatment, avoiding further progression of nerve constriction.

For decades, the diagnosis of neuralgic amyotrophy has been mainly based on specific symptoms, such as acute intense pain around the shoulder girdle followed by muscle weakness and amyotrophy (3, 4, 11). In the early stage of neuralgic amyotrophy, EMG may indicate that 2 or more nerves are involved. The EMG characteristics in this case indicated nerve axonal injury and compared with sensory nerves, mainly the axons of the motor nerves were damaged. The clinical features of this case include severe pain and acute muscle weakness, which are consistent with the clinical diagnosis of neuralgic amyotrophy. One month after the onset of the disease, electromyography showed that AIN was severely damaged, with partial axonal damage of the musculocutaneous nerve.

High-resolution peripheral nerve imaging such as MRI and ultrasound technology are considered valuable tools for the diagnosis of neuralgic amyotrophy based on the pathologic basis of HLC (2, 12, 13). Arányi et al. reported abnormal ultrasound findings in 74% of neuralgic amyotrophy patients and classified abnormalities as swelling without constriction, swelling with incomplete constriction, swelling with complete constriction, and fascicular entwinement (14, 15). However, there are few reports of HLC in patients with early-stage neuralgic amyotrophy. Paolo et al. described 39 patients with neuralgic amyotrophy, of which 29 had the presence of HLCs detected by ultrasound within 1 month of onset and recommended using ultrasound as the first-line complementary tool within the first 2 weeks after symptom onset (6). In this case, at 2 weeks of onset, ultrasound examination revealed edema and HLCs in the patient's AIN, and at 4 weeks of onset, there were no signs of improvement in the AIN. Ultrasonography showed that the AIN above the elbow joint had obvious swelling with multiple HLCs.

Neuralgic amyotrophy was previously considered a rare self-limited disease with good prognosis (16). Recent publications suggested that the incidence of neuralgic amyotrophy was severely underestimated, and its actual incidence rate is 1/1000 per year (17). Treatment includes early administration of corticosteroids, appropriate pain management, and physiotherapy. Pan et al. explored the nerves of patients with persistent palsy and no signs of clinical recovery and found that HLC lesion in the nerve is the pathological basis of brachial neuritis (7). On the basis of poor clinical recovery and HLCs, Pan et al. consider surgical intervention as a treatment option to deal with those patients who do not respond to conservative treatment after several months (7).

However, there was still controversy regarding treatment strategy and timing of surgical intervention. In this particular case, operation was recommended with thorough concerns about surgical advantages and disadvantages as there is no significant improvement after conservative treatment, and more importantly, the ultrasound confirmed the presence of constriction in the nerve bundles which usually predicts poor recovery. The intraoperative findings highly coincided with the results of preoperative ultrasound. Interfascicular neurolysis and fascicle stimulation were performed because the nerve constrictions were still in the early stage and the nerve constrictions were incomplete, except the 6th and 7th constrictions were 80% constriction. After interfascicular neurolysis, the nerve structure was still continuous and acceptable.

In this case, even though we discovered HLCs in AIN early on, the patient still recovered poorly after conservative treatment. However, we believed that early diagnosis is important to allow prompt neurolysis surgery that was beneficial for the patient's functional recovery. During neurolysis, the pressure inside the perineurium and between the interfascicular nerve bundles was released. Local Betamethasone was injected beneath the perineurium to prevent further edema. Fortunately, the patient's symptoms were relieved in a short period.

Kim et al. (18) speculated that delay of the surgery, age of the patient, and method of surgical treatment indicated poor prognosis. Therefore, if there is a clear diagnosis indicating the presence of HLCs and poor recovery after conservative treatment, surgical treatment is the best choice to avoid further narrowing of the affected nerves and promote functional recovery.

The selection of surgical methods is based on the results of intraoperative nerve stimulation, personal experience of the surgeon, and the basis of the degrees of constriction found at surgical exploration (7). Severity of constriction was also defined by Gstoettner according to the percentage of nerve/fascicle thinning: $\leq$25% thinning was classified as mild, 25–75% as moderate and $\geq$75% as severe constriction (4). In complete constriction cases, interfascicular neurolysis only was not recommended, and patients should undergo neurorrhaphy. In this case, the 6th and 7th contractions in Figure 3 are severe, but we believe that functional recovery was still possible by neurolysis since the constriction was not complete and this case was still in its early stages. The prognosis of this patient confirmed our hypothesis.

For neuralgic amyotrophy, early diagnosis and surgical treatment for nerve hourglass-like constrictions might be a better choice to promote nerve recovery speed. Neurolysis helps reduce pressure in the nerves, restore muscle function, and shorten the course of the disease in the early stages.

Data availability statement

The original contributions presented in the study are included in the article/supplementary material, further inquiries can be directed to the corresponding author/s.

Ethics statement

Ethical approval was not required for the study involving humans in accordance with the local legislation and institutional requirements. Written informed consent to participate in this study was not required from the participants or the participants' legal guardians/next of kin in accordance with the national legislation and the institutional

requirements. Written informed consent was obtained from the individual(s) for the publication of any potentially identifiable images or data included in this article.

Author contributions

FS: Data curation, Software, Writing – original draft. XZ: Methodology, Supervision, Writing – review & editing. XL: Project administration, Supervision, Writing – original draft, Writing – review & editing.

Funding

The author(s) declare financial support was received for the research, authorship, and/or publication of this article. This study was supported by Ningbo Medical Science and Technology Project (2021Y55), Ningbo Science Technology Planning Project (2022S058) and Ningbo Top Medical and Health Research Program (No. 2022020506).

Conflict of interest

The authors declare that the research was conducted in the absence of any commercial or financial relationships that could be construed as a potential conflict of interest.

Publisher's note

All claims expressed in this article are solely those of the authors and do not necessarily represent those of their affiliated organizations, or those of the publisher, the editors and the reviewers. Any product that may be evaluated in this article, or claim that may be made by its manufacturer, is not guaranteed or endorsed by the publisher.

References

1. Firmino GF, Schulze ML, Schlindwein MAM, Rampeloti B, Gonçalves MVM, Maçaneiro CH, et al. Neuralgic Amyotrophy: its importance in orthopedics practice. *Spine Surg Related Res*. (2021) 5:232–7. doi: 10.22603/ssrr.2021-0014

2. Ijspeert J, Janssen RMJ, van Alfen N. Neuralgic amyotrophy. *Curr Opin Neurol*. (2021) 34:605–12. doi: 10.1097/WCO.0000000000000968

3. van Alfen N. Clinical and pathophysiological concepts of neuralgic amyotrophy. *Nat Rev Neurol*. (2011) 7:315–22. doi: 10.1038/nrneurol.2011.62

4. Gstoettner C, Mayer JA, Rassam S, Hruby LA, Salminger S, Sturma A, et al. Neuralgic amyotrophy: a paradigm shift in diagnosis and treatment. *J Neurol Neurosurg Psychiatry*. (2020) 91:879–88. doi: 10.1136/jnnp-2020-323164

5. Pan Y, Wang S, Zheng D, Tian W, Tian G, Ho PC, et al. Hourglass-like constrictions of peripheral nerve in the upper extremity. *Neurosurgery*. (2014) 75:10–22. doi: 10.1227/NEU.0000000000000350

6. Ripellino P, Arányi Z, van Alfen N, Ventura E, Peyer AK, Cianfoni A, et al. Imaging of neuralgic amyotrophy in the acute phase. *Muscle Nerve*. (2022) 66:709–14. doi: 10.1002/mus.27732

7. Pan Y-w, Wang S, Tian G, Li C, Tian W, Tian M. Typical brachial neuritis (Parsonage-Turner syndrome) with hourglass-like constrictions in the affected nerves. *J Hand Surg Am*. (2011) 36:1197–203. doi: 10.1016/j.jhsa.2011.03.041

8. Wang T, Qi H, Wang Z, Zhang L, Cui L, Liu L, et al. The role of ultrasonography in diagnosis of neuralgic amyotrophy. *Skelet Radiol*. (2022) 52:1305–11. doi: 10.1007/s00256-022-04253-9

9. Nakagawa Y, Hirata H. Hourglass-like constriction of the brachial plexus in the posterior cord: a case report. *Neurosurgery*. (2018) 82:E1–e5. doi: 10.1093/neuros/nyx171

10. Ochi K, Horiuchi Y, Tazaki K, Takayama S, Matsumura T. Surgical treatment of spontaneous anterior interosseous nerve palsy: a comparison between minimal incision surgery and wide incision surgery. *J Plast Surg Hand Surg*. (2013) 47:213–8. doi: 10.3109/2000656X.2012.753079

11. van Alfen N, van Engelen BG. The clinical spectrum of neuralgic amyotrophy in 246 cases. *Brain*. (2006) 129:438–50. doi: 10.1093/brain/awh722

12. Cignetti NE, Cox RS, Baute V, McGhee MB, van Alfen N, Strakowski JA, et al. A standardized ultrasound approach in neuralgic amyotrophy. *Muscle Nerve*. (2022) 67:3–11. doi: 10.1002/mus.27705

13. Sneag DB, Saltzman EB, Meister DW, Feinberg JH, Lee SK, Wolfe SW. MRI Bullseye sign: an indicator of peripheral nerve constriction in parsonage-turner syndrome. *Muscle Nerve*. (2017) 56:99–106. doi: 10.1002/mus.25480

14. Arányi Z, Csillik A, Dévay K, Rosero M, Barsi P, Böhm J, et al. Ultrasonographic identification of nerve pathology in neuralgic amyotrophy: enlargement, constriction, fascicular entwinement, and torsion. *Muscle Nerve*. (2015) 52:503–11. doi: 10.1002/mus.24615

15. ArÁnyi Z, Csillik A, DéVay K, Rosero M, Barsi P, BÖhm J, et al. Ultrasonography in neuralgic amyotrophy: sensitivity, spectrum of findings, and clinical correlations. *Muscle Nerve*. (2017) 56:1054–62. doi: 10.1002/mus.25708

16. Parsonage MJ, Turner JW. Neuralgic amyotrophy; the shoulder-girdle syndrome. *Lancet*. (1948) 1:973–8.

17. van Alfen N, van Eijk JJ, Ennik T, Flynn SO, Nobacht IE, Groothuis JT, et al. Incidence of neuralgic amyotrophy (Parsonage Turner syndrome) in a primary care setting--a prospective cohort study. *PLoS One*. (2015) 10:e0128361. doi: 10.1371/journal.pone.0128361

18. Kim W, Kang SH, An JY. Posterior interosseous fascicular constriction within the radial nerve in a diabetic patient with bilateral neuralgic Amyotrophy: a case report. *Front Neurol*. (2021) 12:12. doi: 10.3389/fneur.2021.701571

frontiers | Frontiers in Neurology

TYPE Case Report
PUBLISHED 09 February 2024
DOI 10.3389/fneur.2024.1340694

OPEN ACCESS

EDITED BY
Daniele Orsucci,
Unità di Neurologia,
Azienda Usl Toscana Nord Ovest, Italy

REVIEWED BY
Riccardo Cristofani,
University of Milan, Italy
Gianni Sorarù,
University of Padua, Italy
Masahisa Katsuno,
Nagoya University Hospital, Japan
Atsushi Hashizume,
Nagoya University, Japan

*CORRESPONDENCE
Haruna Akanuma
akaharu@fmu.ac.jp

RECEIVED 18 November 2023
ACCEPTED 26 January 2024
PUBLISHED 09 February 2024

CITATION
Akanuma H, Kadowaki S and Kanai K (2024) Case report: Klinefelter syndrome may protect against the development of spinal and bulbar muscular atrophy.
Front. Neurol. 15:1340694.
doi: 10.3389/fneur.2024.1340694

Case report: Klinefelter syndrome may protect against the development of spinal and bulbar muscular atrophy

Haruna Akanuma[1]*, Suguru Kadowaki[2] and Kazuaki Kanai[1]

[1]Department of Neurology, Fukushima Medical University School of Medicine, Fukushima, Japan, [2]Department of Neurology, Ohta General Hospital Foundation, Ohta Nishinouchi Hospital, Kōriyama, Japan

Spinal and bulbar muscular atrophy (SBMA) is an X-linked recessive motor neuron disease caused by the expansion of cytosine-adenine-guanine (CAG) repeats in the androgen receptor (AR) gene. It is thought that the nuclear translocation of abnormal AR proteins following binding to testosterone triggers the onset of the disease. We report the case of a patient who had SBMA coincident with Klinefelter syndrome. He developed SBMA symptoms rapidly after receiving androgen replacement therapy for Klinefelter syndrome. No cases of coincident SBMA and Klinefelter syndrome have been reported, and if confirmed by further patients in future, that androgen hormones are strongly associated with the development and progression of SBMA in fact in humans.

KEYWORDS

testosterone, spinal and bulbar muscular atrophy, Klinefelter syndrome, androgen replacement therapy, leuprorelin

Introduction

Spinal and bulbar muscular atrophy (SBMA) is an X-linked recessive motor neuron disease caused by the expansion of CAG repeats in the androgen receptor (AR) gene (1). It is thought that the nuclear translocation of abnormal AR proteins following binding to testosterone triggers the onset of the disease (2). Suppression of testosterone by luteinizing hormone-releasing hormone (LHRH) analogs can disrupt the pathomechanisms of the disease (3), and it has been used clinically as a treatment for SBMA (4). Klinefelter syndrome is caused by a supernumerary X chromosome in an XY male as a result of the meiotic nondisjunction of the X chromosome (5). Males with Klinefelter syndrome often have decreased serum testosterone concentrations and elevated luteinizing hormone and follicle-stimulating hormone levels. Testosterone supplementation is used to treat some symptoms of Klinefelter syndrome that result from abnormal hormone levels (6). Here, we present a patient who had Klinefelter syndrome who developed SBMA symptoms rapidly after receiving androgen replacement therapy.

Case presentation

The patient was a 49-year-old man. At the age of 38, he developed muscle spasms and muscle twitching in the extremities and abdomen. He visited a neurology clinic at the age of 40,

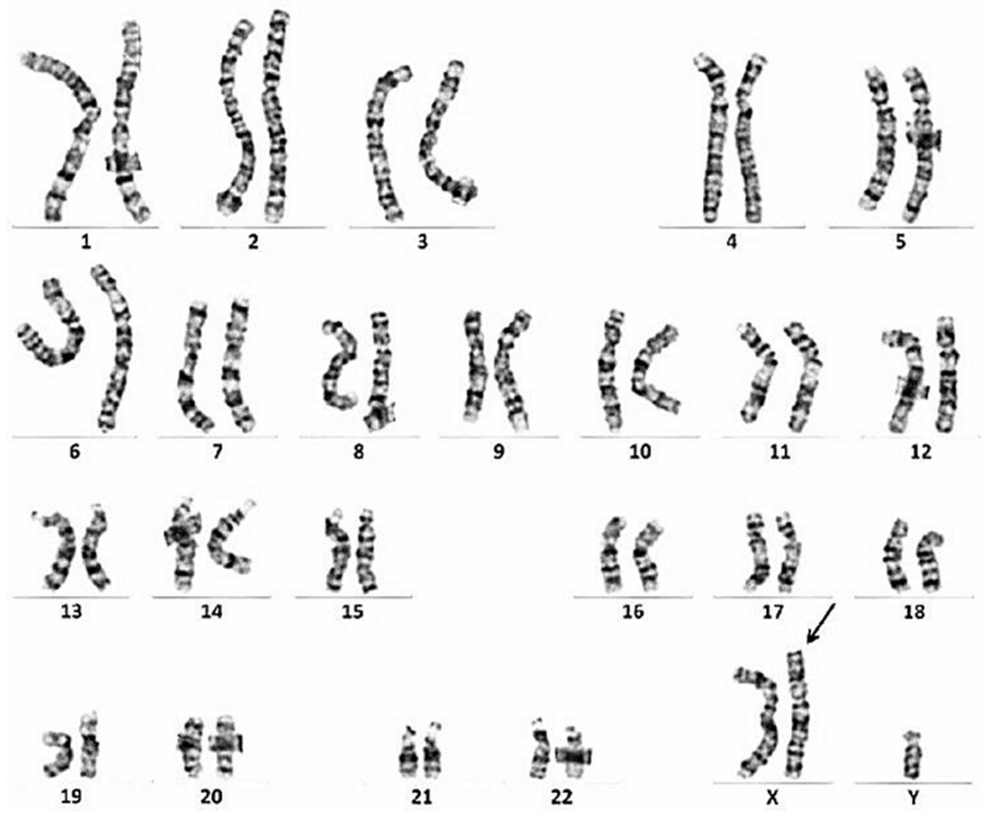

FIGURE 1
Chromosome analysis reveals an abnormal karyotype 47, XXY.

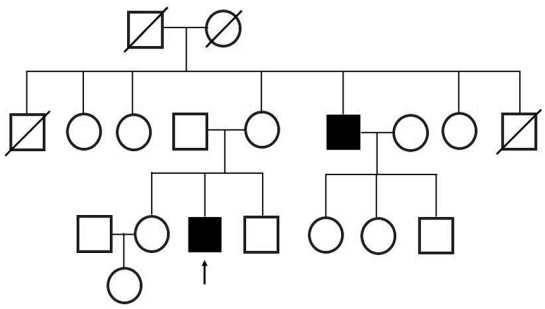

FIGURE 2
Family tree. The patient's maternal uncle was diagnosed with SBMA.

at which time stiff-person syndrome was initially suspected. Although a thorough examination was performed, the cause was undetermined. At that visit, his serum creatine kinase (CK) levels were within normal limits (221 IU/L, reference value: 62–287 IU/L). At the age of 46, he complained of infertility and was examined by a urologist. He was found to have severe atrophy of the testes as well as azoospermia. Chromosome analysis revealed an abnormal karyotype 47, XXY and he was diagnosed with Klinefelter syndrome (Figure 1). His serum total testosterone level at this time was 295.3 ng/mL (reference value: 142.4–923.1 ng/mL), which was at the lower limit of normal. However, his luteinizing hormone level was 21.89 mIU/mL (reference value: 0.1–8.7 mIU/mL) and follicle-stimulating hormone level was 23.95 mIU/mL (reference value: <0.3–13.8 mIU/mL), which were both above the upper limit of normal. Thus, androgen replacement therapy was initiated to treat Klinefelter syndrome. At the age of 48, he developed postural instability and tremors in the upper limbs. He visited the neurology clinic again, at which time Parkinson's disease was suspected and a thorough examination was performed; however, there were no notable abnormalities other than an elevated serum CK level of 487 U/L. Shortly thereafter, his knees began to buckle more frequently, and he could no longer climb stairs without a handrail. The frequency of muscle spasms also increased and occurred daily. He visited our department for a detailed examination at age 48.

At the time of his visit to our department, physical and neurological examinations indicated gynecomastia, tongue atrophy, postural tremors in both upper extremities, proximal muscle weakness, and loss of tendon reflexes in the extremities. He complained of subjective muscle twitching, but no fasciculation was visible. During this initial visit, we noticed that he had a family history of SBMA: his maternal uncle was diagnosed with SBMA at age 47 and was treated with LHRH analogs (Figure 2).

Blood tests revealed an elevated serum CK level of 610 IU/L (reference value: 59–248 IU/L), and total testosterone level of 6.45 ng/mL (reference value: 1.71–8.71 ng/mL). Nerve conduction studies showed a decreased amplitude of sensory nerve action potentials and needle electromyography showed a markedly increased amplitude of

Abbreviations: SBMA, Spinal and bulbar muscular atrophy; AR, Androgen receptor; LHRH, Luteinizing hormone-releasing hormone; CK, Creatine kinase.

motor unit potentials. Electrocardiography showed Brugada-type ST-segment elevation. Genetic testing revealed expanded CAG repeats ($n = 46$) in the AR gene, and he was diagnosed as a coincidental case of SBMA and Klinefelter syndrome. Only one peak was detected in the polymerase chain reaction test using capillary electrophoresis, indicating that both alleles of the AR gene had the same expanded CAG repeats (Figure 3).

Shortly thereafter, androgen replacement therapy was discontinued and the LHRH agonist leuprorelin was started for the treatment of SBMA. Since that time, his symptoms have remained stable, his CK levels have trended downward, and his testosterone is now at a castrate level (Figure 4).

Discussion

SBMA (1) is thought to be caused by a gain-of-function mutation in the AR gene, which results in mutant AR proteins binding to testosterone and translocating from the cytoplasm to the nucleus, where these mutant proteins accumulate and induce cytotoxicity in motor neurons and skeletal muscle (2, 7). It is thought that the binding of testosterone to the AR protein is necessary for the onset of SBMA (2). Thus, women with an AR gene with expanded CAG repeats do not develop the disease and are asymptomatic because their testosterone levels are much lower than those of men. It was reported that even women who are homozygous for an AR gene with expanded CAG repeats have only minor symptoms and do not develop SBMA (8). The administration of testosterone in a transgenic mouse model was shown to trigger the development of SBMA (2). To the best of our knowledge, no direct evidence of this mechanism of action has been shown in male patients with SBMA or carrier women with an AR gene with expanded CAG repeats.

As far as we are aware, no cases of coincident SBMA and Klinefelter syndrome have been reported (9). We hypothesize that the androgen replacement therapy for Klinefelter syndrome may have triggered the development of SBMA. The patient had relatively low serum androgenic hormone levels before starting androgen replacement treatment, probably as a result of Klinefelter syndrome. In addition, tremor is the first and most frequent symptom in male patients with SBMA, but less frequent in female patients (10). In the current patient, only mild muscle spasms and muscle twitching were observed before the initiation of androgen replacement therapy, which is similar to the symptoms observed in female carriers (8, 11). Furthermore, although it was reported that a decrease in serum creatinine levels precedes the onset of motor symptoms by approximately 15 years in male patients with SBMA, no decrease in serum creatinine levels was observed in this patient. After administrating testosterone, this patient developed tremors and weakness, which resembled the results shown in a transgenic mouse model (2). This suggests that testosterone induces the development of subclinical SBMA in patients with Klinefelter syndrome.

In this case, the protective effect of Klinefelter syndrome against the development of SBMA may be explained by low testosterone levels suppressing the translocation of AR to the nucleus, rather than owing to the low testosterone levels *per se*. This is because a previous case report showed that a transgender patient with SBMA who had been using spironolactone for a long time to achieve gender

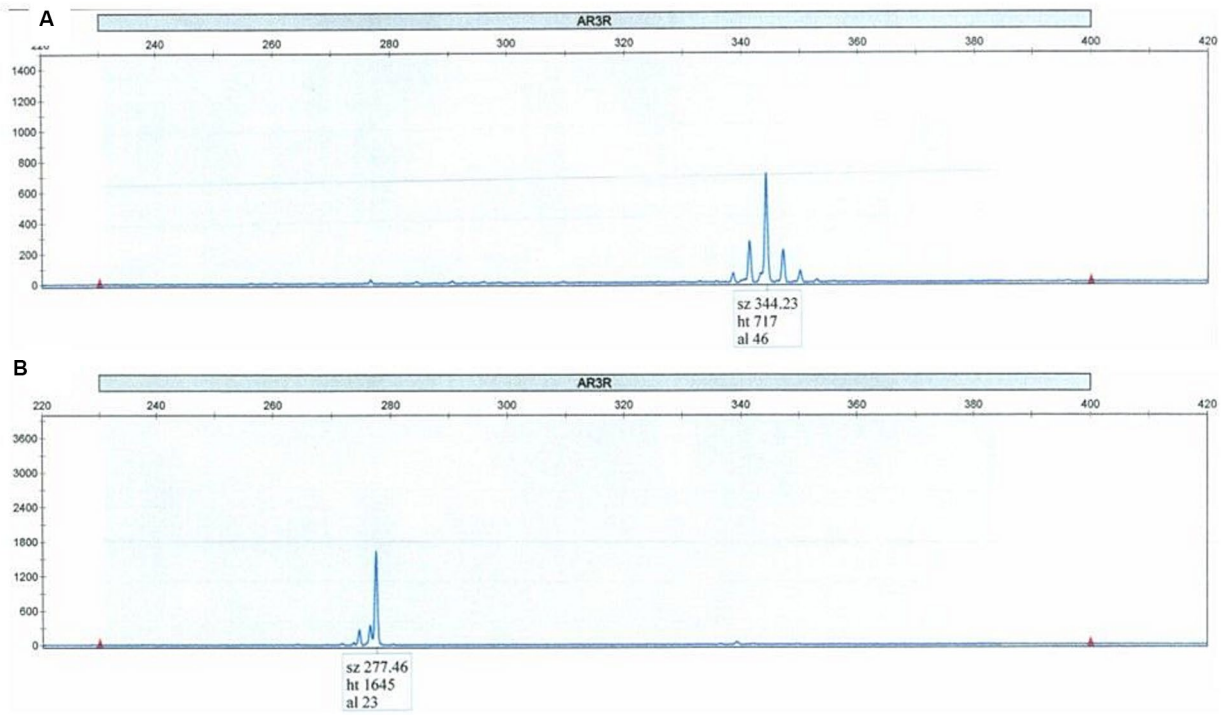

FIGURE 3
Polymerase chain reaction test using capillary electrophoresis **(A)** shows the expansion of 46 CAG repeats. Only one peak was detected, indicating that both alleles of the AR gene had the same expanded CAG repeats. Normal control is shown in the lower panel **(B)**.

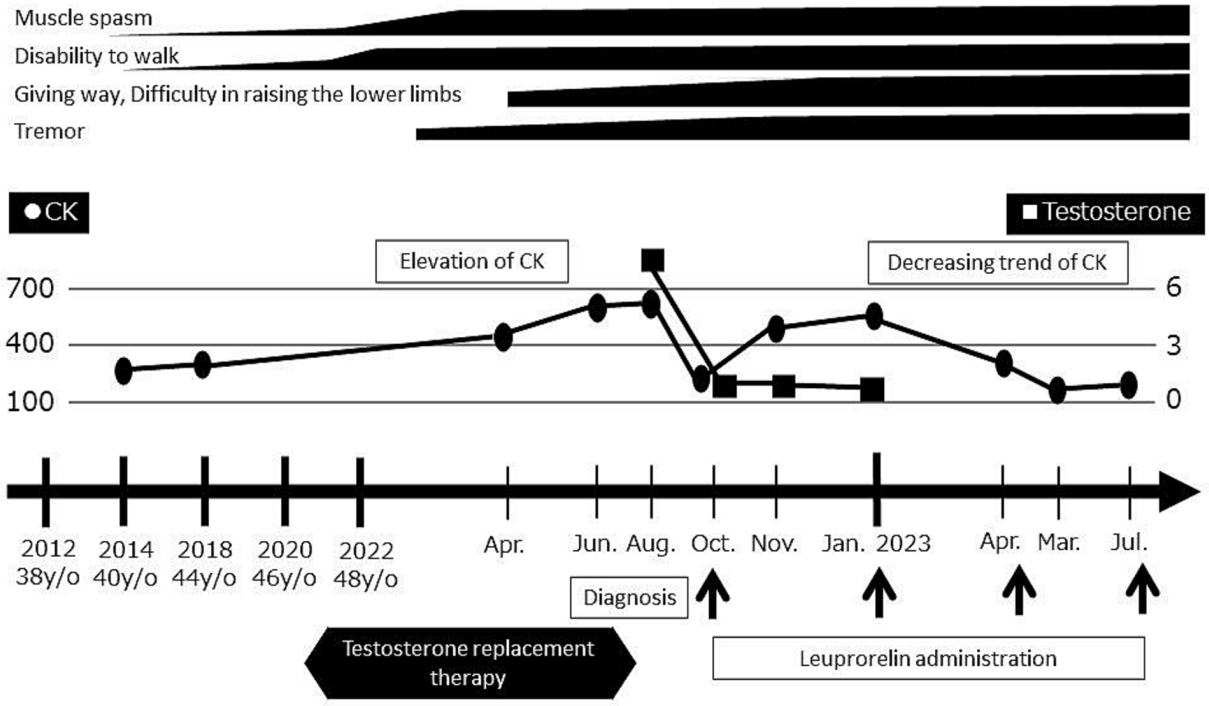

FIGURE 4
Timeline of evaluations and diagnosis. Serum CK levels and motor symptoms worsened after the initiation of androgen replacement therapy. Upon the discontinuation of androgen replacement therapy and initiation of leuprorelin, the serum CK levels decreased and symptoms became stable.

reassignment developed SBMA despite having low levels of serum testosterone (12). In that report, it was discussed that the action of spironolactone as a partial agonist or selective AR modulator led to the development of SBMA. The results of these two case reports are consistent with those of a study that showed the efficacy of LHRH analogs and the ineffectiveness of androgen antagonists in an SBMA mouse model (13). This is interesting because it demonstrates that the pathology of the human disease and that of the mouse model are consistent.

The karyotype of this patient was 47, XXY and the AR gene was located on the X chromosome indicating this patient had two alleles of the AR gene with abnormally expanded CAG repeats; thus, the expression level of the abnormal AR protein may also be high. Therefore, the initiation of testosterone replacement therapy in this patient may have caused an earlier and more severe onset of symptoms by promoting a higher degree of nuclear translocation of the abnormal AR protein bound to testosterone. Although it was reported that excess X chromosome inactivation occurs in the majority of cells in Klinefelter syndrome (11, 12), 15%–30% of the genes on the inactivated X chromosome escape inactivation (13). At this time, the extent to which the AR gene is expressed or inactivated in patients with Klinefelter syndrome is unknown. Further cell biological studies will be necessary to examine this problem.

To the best of our knowledge, this is the first report of a patient who had coincident SBMA and Klinefelter syndrome and provides the first direct evidence that testosterone triggers SBMA in patients. This case provides new and interesting insights into the role of testosterone in the pathomechanism of SBMA development.

Data availability statement

The raw data supporting the conclusions of this article will be made available by the authors, without undue reservation.

Ethics statement

Written informed consent was obtained from the individual for the publication of any potentially identifiable images or data included in this article.

Author contributions

HA: Writing – original draft. SK: Writing – review & editing. KK: Writing – review & editing.

Funding

The author(s) declare that no financial support was received for the research, authorship, and/or publication of this article.

Acknowledgments

The authors thank Shelby King and J. Ludovic Croxford from Edanz (https://jp.edanz.com/ac) for editing a draft of this manuscript.

Conflict of interest

SK was employed by Ohta General Hospital Foundation.

The remaining authors declare that the research was conducted in the absence of any commercial or financial relationships that could be construed as a potential conflict of interest.

Publisher's note

All claims expressed in this article are solely those of the authors and do not necessarily represent those of their affiliated organizations, or those of the publisher, the editors and the reviewers. Any product that may be evaluated in this article, or claim that may be made by its manufacturer, is not guaranteed or endorsed by the publisher.

Supplementary material

The Supplementary material for this article can be found online at: https://www.frontiersin.org/articles/10.3389/fneur.2024.1340694/full#supplementary-material

References

1. La Spada AR, Wilson EM, Lubahn DB, Harding AE, Fischbeck KH. Androgen receptor gene mutation in X-linked spinal and bulbar muscular atrophy. *Nature*. (1991) 352:77–9. doi: 10.1038/352077a0

2. Katsuno M, Adachi H, Kume A, Li M, Nakagomi Y, Niwa H, et al. Testosterone reduction prevents phenotypic expression in a transgenic mouse model of spinal and bulbar muscular atrophy. *Neuron*. (2002) 35:843–54. doi: 10.1016/s0896-6273(02)00834-6

3. Tanaka F, Katsuno M, Banno H, Suzuki K, Adachi H, Sobue G. Current status of treatment of spinal and bulbar muscular atrophy. *Neural Plast*. (2012) 2012:284. doi: 10.1155/2012/369284

4. Hashizume A, Katsuno M, Suzuki K, Hirakawa A, Hijikata Y, Yamada S, et al. Long-term treatment with leuprorelin for spinal and bulbar muscular atrophy: natural history-controlled study. *J Neurol Neurosurg Psychiatry*. (2017) 88:1026–32. doi: 10.1136/jnnp-2017-316015

5. Gravholt CH, Chang S, Wallentin M, Fedder J, Moore P, Skakkebæk A. Klinefelter syndrome: integrating genetics, neuropsychology, and endocrinology. *Endocr Rev*. (2018) 39:389–423. doi: 10.1210/er.2017-00212

6. Chang S, Skakkebæk A, Gravholt CH. Klinefelter syndrome and medical treatment: hypogonadism and beyond. *Hormones*. (2015) 14:531–48. doi: 10.14310/horm.2002.1622

7. Hashizume A, Fischbeck KH, Pennuto M, Fratta P, Katsuno M. Disease mechanism, biomarker and therapeutics for spinal and bulbar muscular atrophy (SBMA). *J Neurol Neurosurg Psychiatry*. (2020) 91:1085–91. doi: 10.1136/jnnp-2020-322949

8. Schmidt BJ, Greenberg CR, Allingham-Hawkins DJ, Spriggs EL. Expression of X-linked bulbospinal muscular atrophy (Kennedy disease) in two homozygous women. *Neurology*. (2002) 59:770–2. doi: 10.1212/wnl.59.5.770

9. Caballero PE. Klinefelter's syndrome associated with progressive muscular atrophy simulating Kennedy's disease. *Ann Indian Acad Neurol*. (2012) 15:227–9. doi: 10.4103/0972-2327.99730

10. Ishihara H, Kanda F, Nishio H, Sumino K, Chihara K. Clinical features and skewed X-chromosome inactivation in female carriers of X-linked recessive spinal and bulbar muscular atrophy. *J Neurol*. (2001) 248:856–60. doi: 10.1007/s004150170069

11. Zhao LY, Li P, Yao CC, YX TRHT, Chen YZZZ, Li Z. Low XIST expression in Sertoli cells of Klinefelter syndrome patients causes high susceptibility of these cells to an extra X chromosome. *Asian J Androl*. (2023) 25:662–73. doi: 10.4103/aja202315

12. Mahyari E, Guo J, Lima AC, Lewinsohn DP, Stendahl AM, Vigh-Conrad KA, et al. Comparative single-cell analysis of biopsies clarifies pathogenic mechanisms in Klinefelter syndrome. *Am J Hum Genet*. (2021) 108:1924–45. doi: 10.1016/j.ajhg.2021.09.001

13. Sun Z, Fan J, Wang Y. X-chromosome inactivation and related diseases. *Genet Res*. (2022) 2022:1391807. doi: 10.1155/2022/1391807

frontiers | Frontiers in Neurology

TYPE Case Report
PUBLISHED 04 March 2024
DOI 10.3389/fneur.2024.1340693

OPEN ACCESS

EDITED BY
Giovanni Meola,
University of Milan, Italy

REVIEWED BY
Edoardo Malfatti,
Hôpitaux Universitaires Henri Mondor, France
Chiara Fiorillo,
University of Genoa, Italy

*CORRESPONDENCE
Stefania Corti
✉ stefania.corti@unimi.it
Dario Ronchi
✉ dario.ronchi@unimi.it

†These authors have contributed equally to this work

RECEIVED 18 November 2023
ACCEPTED 22 February 2024
PUBLISHED 04 March 2024

CITATION
Piga D, Rimoldi M, Magri F, Zanotti S, Napoli L, Ripolone M, Pagliarani S, Ciscato P, Velardo D, D'Amico A, Bertini E, Comi GP, Ronchi D and Corti S (2024) Case report: A novel *ACTA1* variant in a patient with nemaline rods and increased glycogen deposition. *Front. Neurol.* 15:1340693. doi: 10.3389/fneur.2024.1340693

Case report: A novel *ACTA1* variant in a patient with nemaline rods and increased glycogen deposition

Daniela Piga[1†], Martina Rimoldi[2,3†], Francesca Magri[1], Simona Zanotti[2], Laura Napoli[2], Michela Ripolone[2], Serena Pagliarani[1], Patrizia Ciscato[2], Daniele Velardo[2], Adele D'Amico[4], Enrico Bertini[4], Giacomo Pietro Comi[1,5], Dario Ronchi[1,5*†] and Stefania Corti[2,5*†]

[1]IRCCS Fondazione Cà Granda Ospedale Maggiore Policlinico, Neurology Unit, Milan, Italy, [2]IRCCS Fondazione Cà Granda Ospedale Maggiore Policlinico, Neuromuscular and Rare Disease Unit, Milan, Italy, [3]IRCCS Fondazione Cà Granda Ospedale Maggiore Policlinico, Medical Genetics Unit, Milan, Italy, [4]Unit of Neuromuscular and Neurodegenerative Disorders, Bambino Gesu' Children's Research Hospital, IRCCS, Rome, Italy, [5]Department of Pathophysiology and Transplantation, Dino Ferrari Center, University of Milan, Milan, Italy

Background: Congenital myopathies are a group of heterogeneous inherited disorders, mainly characterized by early-onset hypotonia and muscle weakness. The spectrum of clinical phenotype can be highly variable, going from very mild to severe presentations. The course also varies broadly resulting in a fatal outcome in the most severe cases but can either be benign or lead to an amelioration even in severe presentations. Muscle biopsy analysis is crucial for the identification of pathognomonic morphological features, such as core areas, nemaline bodies or rods, nuclear centralizations and congenital type 1 fibers disproportion. However, multiple abnormalities in the same muscle can be observed, making more complex the myopathological scenario.

Case presentation: Here, we describe an Italian newborn presenting with severe hypotonia, respiratory insufficiency, inability to suck and swallow, requiring mechanical ventilation and gastrostomy feeding. Muscle biopsy analyzed by light microscopy showed the presence of vacuoles filled with glycogen, suggesting a metabolic myopathy, but also fuchsinophilic inclusions. Ultrastructural studies confirmed the presence of normally structured glycogen, and the presence of minirods, directing the diagnostic hypothesis toward a nemaline myopathy. An expanded Next Generation Sequencing analysis targeting congenital myopathies genes revealed the presence of a novel heterozygous c.965 T > A p. (Leu322Gln) variant in the *ACTA1* gene, which encodes the skeletal muscle alpha-actin.

Conclusion: Our case expands the repertoire of molecular and pathological features observed in actinopathies. We highlight the value of ultrastructural examination to investigate the abnormalities detected at the histological level. We also emphasized the use of expanded gene panels in the molecular analysis of neuromuscular patients, especially for those ones presenting multiple bioptic alterations.

KEYWORDS

***ACTA1*, skeletal muscle rods, glycogen storage, nemaline myopathy, case report**

1 Introduction

Congenital myopathies are a group of rare congenital genetic muscle disorders, that primarily affect the structure and the function of skeletal muscles, leading to hypotonia and muscle weakness (1–3). Mutations in various genes with a crucial role in muscle development, maintenance, and contraction, have been associated with different phenotypic and histological expressions of these disorders. Because of their wide genetic and clinical heterogeneity, next-generation sequencing (NGS) has been increasingly used for their diagnosis in recent years (3–6).

While the current classification of congenital myopathies remains subject to an ongoing evaluation, because of the constant discovery of additional genes, the diagnostic algorithm still relies on muscle biopsy findings (3, 7, 8). In fact, in reference Centers for neuromuscular disorders, despite the growing tendency toward a gene-first approach in the diagnostic assessment of such complex clinical scenarios, muscle biopsy data remain crucial in orienting and/or confirming the definitive diagnoses. Among congenital myopathies, Nemaline Myopathy (NM) features the presence of nemaline bodies (NBs), that are rod-shaped structures within muscle fibers (9–11). These rods consist in protein inclusions containing Z-line proteins, and they are likely to contribute to disrupt muscle function, leading to sarcomeric dysfunction and muscle weakness (1, 12–15).

Although nemaline bodies can be considered pathognomonic features of NMs (8, 12, 16, 17), their presence does not rule out the possibility of alternative diagnoses, including acquired conditions (18). Therefore, the identification of rod-shaped structures should prompt the molecular analysis of genes associated with NM, together with those underlying other genetic forms (18).

Congenital NM has been associated with causative variants in 14 genes encoding for sarcomeric components, and for auxiliary proteins involved in the regulation of sarcomeric functions, stability, or turnover (3, 19). Deleterious variants in *ADSSL1*, *CFL2*, *KLHL40*, *KLHL41, LMOD3*, *MYO18B*, *MYPN*, *NEB* and *TNNT3* are recessively inherited, while molecular defects in *KBTBD13* display a dominant inheritance. Finally, *ACTA1*, *TPM2*, *TPM3* and *TNNT1* genes are associated with recessive or dominant NM forms. Most of NM patients present mutations in *NEB* (50% of cases) or *ACTA1* (20–30% of patients), with *ACTA1* variants representing the most common defect in patients with congenital onset or severe presentations (20–22).

ACTA1 gene encodes for the skeletal muscle 42 kDa alpha-actin protein, whose main function is to interact with myosin during muscle contraction. Mutations in the *ACTA1* gene can disrupt the normal structure and function of the alpha-actin-1 protein, resulting in muscle weakness, hypotonia (low muscle tone), and various muscular conditions collectively referred to as "actinopathies" (23–25). Muscle biopsies of NM patients might display a rich repertoire of pathological alterations, including cores, nemaline and intranuclear bodies, actin accumulations, fiber-type disproportion, dystrophic features, and zebra bodies.

Here, we report the case of a neonatal patient, who presented clinical features of congenital myopathy and glycogen accumulations on histological and ultrastructural analyses of the muscle. The identification of nemaline bodies at electron microscopy oriented the investigation toward the discovery of a *de novo*, novel heterozygous variant in the *ACTA1* gene.

2 Case presentation

The patient is the second-born child to non-consanguineous healthy parents of Italian origins (Supplementary Figure 1). He was born at full term through a vaginal delivery, following a pregnancy characterized by reduced fetal movements. At birth, the baby displayed significant hypotonia and lacked spontaneous movements and breathing activity. APGAR score was 4, 6 and 8 at 1st, 5th, and 10th minute, respectively. The newborn was immediately intubated and provided with invasive mechanical ventilation. Due to his severe general conditions, the patient was promptly transferred to the Neonatal Intensive Care Unit of our hospital for further examinations and treatments. During his hospital stay, the baby required continuous mechanical ventilation. He also showed difficulties in facial expressions, sucking, swallowing, and general voluntary movements. Furthermore, a bilateral cryptorchidism was observed. When he was 54 days old, a tracheostomy and percutaneous gastrostomy were performed, following which the baby displayed a steady growth curve, with an appropriate weight gain.

Routine biochemical profiles on multiple occasions, comprehensive of Creatine phosphokinase (CPK) dosage, returned physiological results. Ophthalmological and cardiological evaluation, with the latter including electrocardiography (ECG) and echocardiography, revealed no abnormalities. Auditory brainstem response (ABR) testing showed bilateral high auditory thresholds, higher on the right side, without brainstem dysfunction; a follow-up Brainstem Auditory Evoked Response (BAER) testing was therefore recommended at 3 months of life, and this turned out to be normal.

Electromyography (EMG) showed a widespread muscle damage, suggesting a myogenic suffering, mainly involving the proximal regions of both upper al lowerlimbs.

Electroencephalogram (EEG) displayed a global alteration of the cerebral organization, with slow wave abnormalities, and absence of sleep phase transition.

Muscle biopsy was performed on right quadriceps, at 9 days of age. Histological analyses showed a great variability in fiber size, with a slight prevalence of type 1 fibers, and a 15% of hypotrophic fibers estimated to belong to both types of fibers. Several fibers showed the presence of cytoplasmic and subsarcolemmal optically empty vacuoles, sometimes of conspicuous size, and intracytoplasmic fuchsinophilic granulations (Figure 1). In particular, by analyzing semithin sections, we estimated the presence of rods in 14.6% of the fibers. Nuclear centralization, degenerative fibers with augmented connective tissue, fiber splittings and increased acid phosphatase staining were not observed. Analysis on semithin sections showed that the vacuoles were PAS positive, indicating an increased glycogen content (Figure 2), and suggesting a glycogen storage disease; in fact, the histopathological features resembled branching or debranching enzyme deficiency (Autosomal Recessive Glycogen Storage Disease type 4 or 3, respectively). These findings prompted the molecular analysis of the genes implied in muscle glycogen storage disorders, such as *GBE1* and *AGL*, without conclusive results. The subsequent ultrastructural analyses by electron microscopy confirmed the presence of extensive glycogen collections, leading to significant alterations in muscle architecture (Figure 3A). In addition, several cytoplasmic rods of variable size were found in some muscle fibers

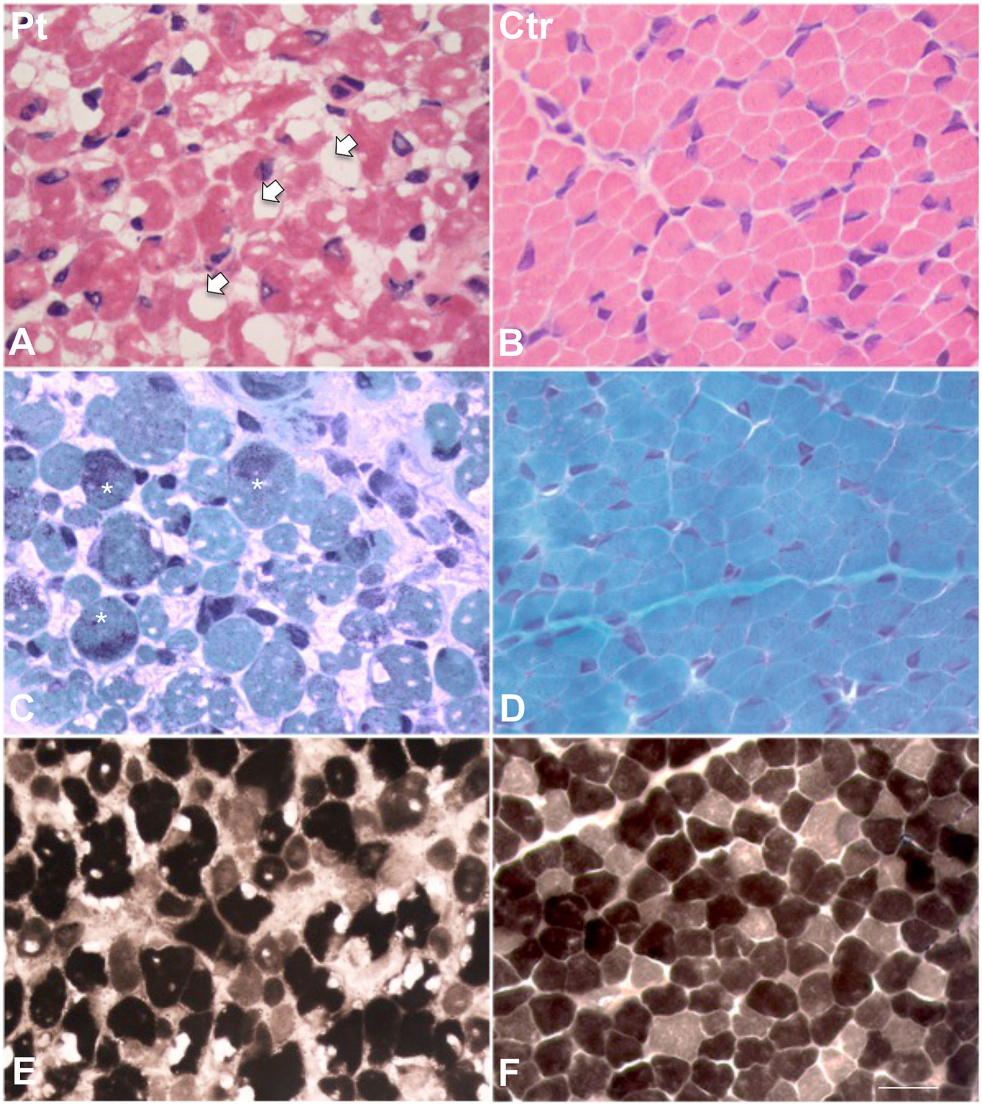

FIGURE 1
Histological findings in muscle biopsy. H&E stain in our patient **(A)** showed a great variability in fiber size. Several fibers showed the presence of cytoplasmic and subsarcolemmal optically empty vacuoles, sometimes of conspicuous size (arrows). **(B)** H&E stain in age-matched healthy control. **(C)** MGT stain in our patient showed the presence of intracytoplasmic fuchsinophilic granulations (asterisks). **(D)** MGT stain in age-matched healthy control. **(E)** ATPase pH 9.4 in our patient and **(F)** in age-matched control. Scale bar 10 μm.

(Figures 3B–D). Fibers with area of compartmentalization for nemaline rods (Figure 3E) and glycogen granules (Figure 3F) were also observed.

To better understand such complex histological findings, additional genetic investigations were conducted. NGS sequencing analysis of a panel of genes involved in congenital myopathies revealed the presence of a novel heterozygous c.965 T > A p.(Leu322Gln) variant in the *ACTA1* gene (NM_001100.3) (Figure 4A). The absence of the variant in Patient's parents supported the hypothesis of its *de novo* origin (Figure 4B). The variant was not found in available population databases (GnomAD MAF:0), and it is currently classified as likely pathogenic, according to the ACMG guidelines (criteria PP3-strong, PM1 and PM2). All the interrogated *in silico* prediction tools unanimously assigned a pathogenic behavior to this novel variant, which would affect an evolutionary conserved residue (Figure 4C) located in the large domain of actin, subdomain 3 (amino acids 270–337) (Figure 4D).

Eventually, the baby was discharged at 3 months and 6 days of age, with home mechanical ventilation and enteral nutrition through a gastrostomy pump. The patient is nowadays 6 years old, and he is currently nourished through a PEG tube, and yet presenting an important drooling, for which he is treated with anticholinergic drugs. He still requires continuous assisted ventilation, and his cardiological follow-up continues to show no abnormalities. He utilizes a tilting postural system for sitting, with anti-gravity support for the upper limbs. He also uses positioning braces for the lower limbs and a half-day corset, especially for seated activities. On the cognitive side, he demonstrates good abilities in attention and sensory orientation, and adequate interactive and communicative skills.

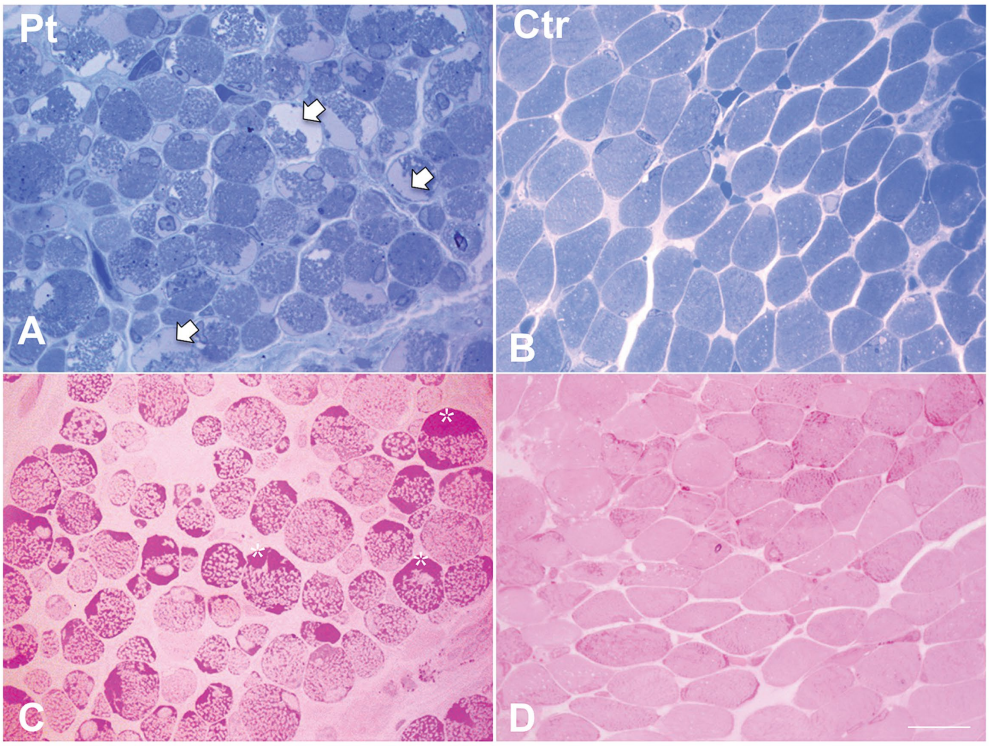

FIGURE 2
Histological findings in muscle biopsy. Toluidine blue stained semithin section in our patient **(A)** showed cytoplasmic and subsarcolemmal pale staining storage material (arrows). **(B)** Toluidine blue stained semithin section in age-matched healthy control. **(C)** PAS stain in our patient showed increased subsarcolemmal glycogen content (asterisks). **(D)** PAS stain in age-matched healthy control. Scale bar 10 µm.

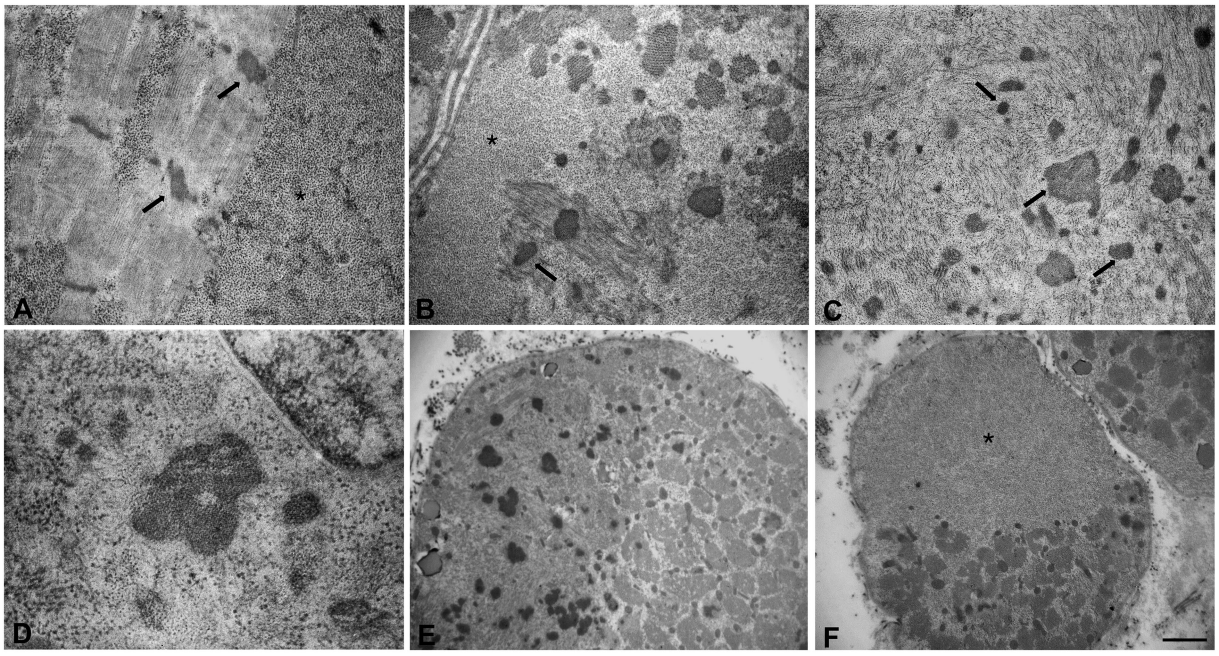

FIGURE 3
Ultrastructural analyses of the muscle sample by electron microscopy. **(A)** Glycogen granules accumulated among the myofibrils and initial thickening of Z line (arrows). **(B,C)** Large glycogen collections localized at the subsarcolemmal level and at intracytoplasmic sites, several nemaline rods of variable size and shape (arrows), myofibrillar disorganization. **(D)** High magnification of a nemaline rod and glycogen granules. **(E,F)** Fibers with areas of compartmentalization. **(E)** In the left area the muscle fiber contains several nemaline rods. **(F)** In the upper area the muscle fiber is completely replaced by glycogen. Scale bars **(A–C)**: 0.8 µm, **(D)**: 0.5 µm. **(E,F)**: 3.3 µm. **(A,B,F)** Asterisks indicate large glycogen collections.

10.3389/fneur.2024.1340693

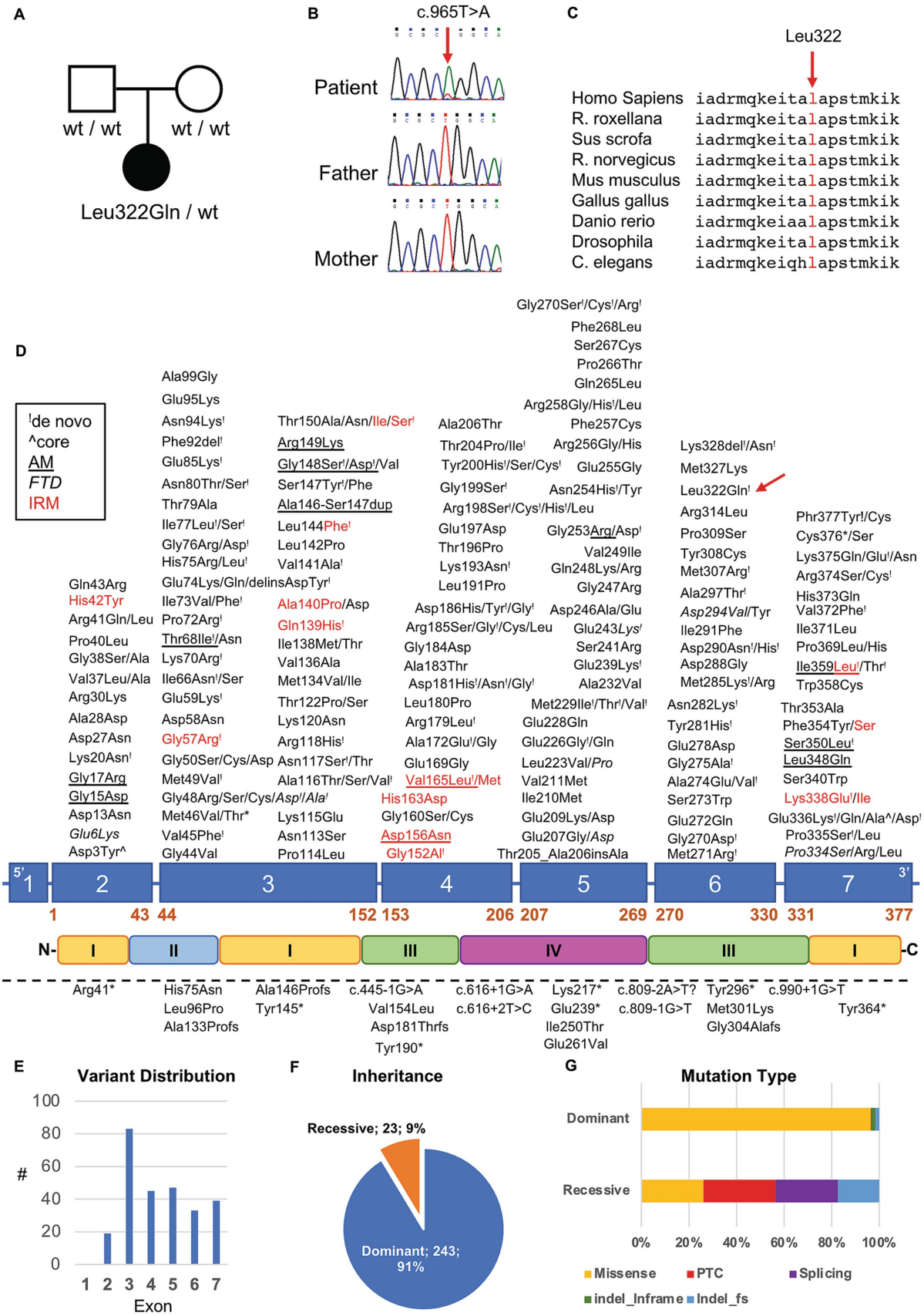

FIGURE 4
Genetic studies in our patient. **(A)** Pedigree of the family. Black symbol indicates the affected patient. **(B)** Sequence electropherograms showing the presence of the heterozygous c.965 T > A *ACTA1* variant in the patient but not in his parents suggesting *de novo* occurrence of the variant.

(Continued)

FIGURE 4 (Continued)

(C) Evolutionary conservation of the affected residue across species. **(D)** Diagram showing the structure of *ACTA1* gene and protein. Dominant and recessive variants are indicated above and under the diagram, respectively. "!" symbol indicates a variant in which *de novo* occurrence was suspected or demonstrated; red color indicates variant associated with intranuclear rod myopathy (IRM); italic style is used for variant associated with fiber type disproportion, the underlined style is used for variants associated with muscle description of homogeneous filamentous inclusions containing actin; the "^" symbol was used to indicate variants found in patients with muscle fibers presenting core regions with no contractile material or mitochondria. Dashed lines indicate the presence of a large genomic deletion. **(E–G)** Distribution of *ACTA1* variants based on their exonic location **(E)**, inheritance pattern **(F)** and mutational types **(G)**.

3 Discussion and conclusion

We describe a novel proband presenting with a severe congenital myopathy, due to a novel *ACTA1* molecular defect.

Pathogenic variants in *ACTA1* are most commonly *de novo* dominant missense mutations (90% of defects), and lead to severe NM pathology by dominant-negative effect (26) (Figures 4E–G). Rarely, *ACTA1* variants can be recessively inherited in NM patients with intrauterine onset. These variants belong to a heterogenous type of mutations that include missense substitutions, and variants predicted to alter the reading frame, or to result in truncated forms of the protein. Biallelic *ACTA1* variants might allow (24) or not (27) the expression of skeletal muscle actin, whereas the expression of the homologous cardiac actin (encoded by *ACTC1*) is generally preserved. Even if cardiac involvement is not typical of NM, dilated or hypertrophic cardiomyopathy may also be present, particularly in association with specific mutations of *ACTA1* (3, 28, 29).

Additional clinical presentations may be associated with *ACTA1* variants, and these are usually reflected by specific alterations observed at the muscle biopsy, such as: core-like areas, fiber-type disproportion, intranuclear rods, actin-containing filamentous inclusions, and zebra bodies. Some of these abnormalities are suspected to be mutation-specific, supporting the definition of a spectrum of congenital myopathies related to actin dysfunction (23).

To date, more than 250 *ACTA1* pathogenic variants have been reported as pathogenic, spanning all the coding exons of the gene, hence affecting the entire 3D structure of the encoded actin protein (20, 24, 30). Several variants associated with congenital myopathy are known to be located in close proximity to the proposed actin–tropomyosin contact sites (31). The novel amino acid change described in this report would also impinge in the same region. Amino-acidic changes have been demonstrated to increase the aggregation of actin, potentially leading to nemaline rods (26). Nevertheless, a prediction of the pathogenic effect for *ACTA1* variants is complicated by the dynamic nature of the protein (limiting the efficacy of structural modeling), and by the presence of several actin binding proteins, that can influence several aspects of actin's function and turnover, through allosteric interactions. The partial knowledge of these aspects hampers genotype–phenotype correlations and the design of innovative therapies.

Clinically, the *ACTA1*-related NM often exhibits severe congenital forms leading to respiratory failure with death within the first year of life, though mild or childhood onset forms have also been reported (20, 32).

In early-onset NM linked to *ACTA1* variants, affected newborns present with floppy appearance due to neonatal hypotonia and severe congenital muscle weakness impairing the achievement of developmental milestones (2, 20). The weakness also affects the respiratory muscles, leading to breathing difficulties within the first hours of life. In many cases, patients require tracheostomy for mechanical ventilation. In addition to this, weakness can impair swallowing and feeding, contributing to poor weight gain. Consequently, some affected patients necessitate tube feeding and gastrostomy.

Joint contractures, facial weakness with high-arched palate, fine and gross motor delays, skeletal deformities, such as clubfeet, pectus excavatum or scoliosis, and muscle atrophy are not so uncommon (3, 18, 20, 32). Antenatal presentation, with reduced fetal movements and quantitative alteration of the amniotic fluid, have also been reported (20).

Inter- and intrafamilial clinical variability has been described in individuals with NM due to *ACTA1* pathogenic variants (30). Despite the abovementioned phenotypic variability, a correlation seems to emerge between the position of the mutation and its clinical and histological presentations (31–33). Interestingly, in a recent cohort study (20), patients harboring biallelic null *ACTA1* variants showed an increased life expectancy; this outcome was explained by the higher expression levels of cardiac alpha-actin in muscle samples. Cardiac alpha-actin is the main alpha-actin form in skeletal muscle during embryonic development, and it is then replaced by skeletal muscle alpha-actin around birth (20). The total absence of skeletal muscle alpha-actin in the skeletal muscles of these NM patients (due to the presence of biallelic null *ACTA1* variants), probably led to an increased expression of cardiac alpha-actin after birth, which might have contributed to a less severe disease course.

Our patient presented a typical congenital form of NM due to *ACTA1* mutations, with severe and generalized skeletal muscle weakness, hypotonia and lack of spontaneous movements. Disease onset was antenatal, since reduced fetal movements were reported during pregnancy. At birth, the patient immediately required assisted ventilation and nutrition. He also presented bilateral cryptorchidism, which is often reported in other forms of congenital myopathies (3). Repeated cardiological assessments excluded structural and functional anomalies. Nowadays our patient, who is 6-year-old, is still ventilated and fed with gastrostomy but no cardiological impairment has been so far observed. He displays adequate interactive and communicative skills.

A preliminary histological assessment disclosed a significant accumulation of PAS-positive material, while intracytoplasmic fuchsinophilic granulations were observed only in less than 10% of the fibers. This observation initially led to the suspicion of a glycogen storage disorder (GSD) and, consequently, to perform specific analyses on *GBE1* and *AGL*, ruling out the presence of pathogenic variants in both genes. These negative results prompted us to focus more accurately on the fuchsinophilic granulations, that were therefore studied also at the ultrastructural level. This further analysis confirmed

increased glycogen content, but also revealed the presence of nemaline rods within fibers, often scattered in the glycogen. In addition, we observed a disorganized sarcomeric architecture with myofibrillar disarray, a finding which is more frequently seen in patients with more severe clinical presentations. Indeed, the degree of severity of sarcomeric disorganization is acknowledged as a more reliable prognostic marker compared to the percentage of positive fibers for nemaline bodies (34). In fact, the complete or partial absence of the typical nemaline rods is not uncommon, especially in newborns, since the detection of these rod-shaped structures depends on the time of sampling as well as on the muscle analyzed. Moreover, in neonatal cases, the physiological small dimension of muscle fibers, further reduced by atrophy or hypotrophy, can complicate the observation (20, 35).

Therefore, the employment of ultrastructural analyses is a helpful approach for the detection of these pathological structures.

Interestingly, accumulations of glycogen were also observed in the muscle biopsies from other patients carrying *ACTA1* mutations (10, 36, 37). However, there are conflicting opinions on whether glycogen storage might be a consistent feature of the *ACTA1*-related NM. Notably, glycogen accumulation was observed in the muscles of 11 NM patients with pathogenic variants in *ACTA1*, but ultrastructural confirmation was obtained in only three of them (35). In contrast, a recent in-depth examination of muscle biopsies from other 10 subjects with congenital or pediatric clinical onset did not disclose this finding (20). Moreover, a correlation between glycogen accumulation and the site or type of molecular defects is also missing. Glycogen accumulation is not typically observed in other forms of congenital myopathy, including those linked to the most frequent *NEB* mutations (34). Furthermore, *ACTA1* mouse models, that nicely recapitulate several aspects of human myopathology, also fail to show increased glycogen content (38, 39).

A defect in energy utilization has been hypothesized as possible mechanism underlying such glycogen accumulations in *ACTA1*-mutated muscles (40). In support of this hypothesis, a downregulation of the genes involved in glucose and glycogen metabolism was observed in muscle biopsies collected from 12 NM patients, and, interestingly, one of them was *ACTA1* mutated (40).

The impaired breakdown of glycogen could be the consequence of altered activity of glycogen phosphorylase, the main contributor of cytosolic glycogen lysis. This enzyme was found to interact with structural muscle proteins, including alpha actinin and F-actin (41). Alpha-actinin deficiency has been associated with increased glycogen content in a mouse model (42). Finally, we cannot exclude that pathological changes acting in the muscle of patients harboring *ACTA1* pathogenic variants could influence phosphorylase regulation by post-translational or epigenetic mechanisms (43).

To date, there is no availability of any specific pharmacological treatments for NM, and this is mainly due to the complexity of the clinical and histological presentations of the disease, which makes the definition of a phenotype–genotype correlation and the development of targeted therapies utterly challenging.

The possibility to predict the clinical course of NM based on genotype could enhance the clinical management and thereby the outcomes of the affected patients. Appropriate medical management, including physical respiratory and nutritional support, where needed, can play a pivotal role in improving the quality of life for individuals with this condition (33, 44, 45). Muscle mass augmenting exercise seem to be beneficial for patients with certain *ACTA1* mutations (10, 46). Several studies of *ACTA1*-NM mouse models demonstrated the ameliorating effects on the clinical course of specific factors inducing fiber hypertrophy (i.e., myostatin inhibitors), as well as of dietary tyrosine supplementation, hence suggesting potential targets for *ACTA1* disease therapies (47, 48). In a *ACTA1*-NM mouse model harboring the His40Tyr variant, Lindqvist and colleagues (49) performed intramuscular injections of recombinant adeno-associated viral vectors with a myosin transgene able to facilitate muscle contraction. When present, the transgene leads to restoration of the intrinsic force-generating capacity and avoids fiber atrophy.

In addition, other studies evaluated the therapeutic effects of the use of small molecules modulating calcium release from troponin C. These substrates are able to sensitize the contractile apparatus to Ca2+, subsequently activating troponin, with the result of improving muscle contraction in neuromuscular disorders, including *ACTA1*-related disease (23, 46, 50). Finally, Sztal and colleagues revealed a less severe manifestation of the *ACTA1*-NM due to an increase in transcriptional activity of an actin paralogue in a zebrafish disease model (51).

Our report highlights the clinical utility of electron microscopy to drive and support molecular testing. Nowadays, the diagnosis of inherited neuromuscular disorders usually relies on NGS protocols that are performed soon after clinical and instrumental examinations, bypassing the need for invasive muscle biopsy procedures. However, molecular testing and muscle biopsy are not mutually exclusive. For example, in neonatal and infantile-onset congenital hypotonia, muscle biopsy can often lead to a precise diagnosis alone or facilitate the orientation of the genetic testing. In the pediatric population of neuromuscular patients, the diagnostic yield was higher when genetic testing was matched with muscle biopsy findings (52). Congenital myopathies in particular show the highest degree of agreement between muscle biopsies findings and genetic results (53).

Data availability statement

The raw data supporting the conclusions of this article will be made available by the authors, without undue reservation.

Ethics statement

The studies involving humans were approved by "Comitato Etico Milano Area 2 Fondazione IRCCS Ca' Granda Ospedale Maggiore Policlinico" (Milan, Italy). The studies were conducted in accordance with the local legislation and institutional requirements. Written informed consent for participation in this study was provided by the participants' legal guardians/next of kin. Written informed consent was obtained from the minor(s)' legal guardian/next of kin for the publication of any potentially identifiable images or data included in this article.

Author contributions

DP: Conceptualization, Data curation, Writing – original draft. MaR: Conceptualization, Data curation, Writing – original

draft. FM: Writing – review & editing. SZ: Writing – review & editing. LN: Writing – review & editing. MiR: Writing – review & editing. SP: Writing – review & editing. PC: Writing – review & editing. DV: Writing – review & editing. AD'A: Writing – review & editing. EB: Writing – review & editing. GC: Writing – review & editing. DR: Conceptualization, Data curation, Investigation, Writing – original draft, Writing – review & editing. SC: Writing – review & editing.

Funding

The author(s) declare that financial support was received for the research, authorship, and/or publication of this article. This study was partially funded by Italian Ministry of Health – Current research IRCCS Cà Granda Ospedale Maggiore Policlinico.

Acknowledgments

We thank the Associazione Centro Dino Ferrari for its support. We also thank the "Bank of muscle tissue, peripheral nerve, DNA and cell culture," member of Telethon network of Genetic Biobanks, at Fondazione IRCCS Ca' Granda, Ospedale Maggiore Policlinico, Milano, Italy. This work is promoted within the European Reference Network for Neuromuscular Diseases (ERN-NMD), MS as HCP Representative for the Italian ERN-NMD.

Conflict of interest

The authors declare that the research was conducted in the absence of any commercial or financial relationships that could be construed as a potential conflict of interest.

Publisher's note

Supplementary material

The Supplementary material for this article can be found online at: https://www.frontiersin.org/articles/10.3389/fneur.2024.1340693/full#supplementary-material

References

1. Goebel HH, Anderson JR, Hübner C, Oexle K, Warlo I. Congenital myopathy with excess of thin myofilaments. *Neuromuscul Disord*. (1997) 7:160–8. doi: 10.1016/S0960-8966(97)00441-0

2. Colombo I, Scoto M, Manzur AY, Robb SA, Maggi L, Gowda V, et al. Congenital myopathies: natural history of a large pediatric cohort. *Neurol Int*. (2015) 84:28–35. doi: 10.1212/WNL.0000000000001110

3. Cassandrini D, Trovato R, Rubegni A, Lenzi S, Fiorillo C, Baldacci J, et al. Congenital myopathies: clinical phenotypes and new diagnostic tools. *Italian J Pediat*. (2017) 43:101. doi: 10.1186/s13052-017-0419-z

4. Boycott KM, Vanstone MR, Bulman DE, MacKenzie AE. Rare-disease genetics in the era of next-generation sequencing: discovery to translation. *Nat Rev Genet*. (2013) 14:681–91. doi: 10.1038/nrg3555

5. Bowdin SC. The clinical utility of next-generation sequencing in the neonatal intensive care unit. *CMAJ*. (2016) 188:786–7. doi: 10.1503/cmaj.160490

6. François-Heude MC, Walther-Louvier U, Espil-Taris C, Beze-Beyrie P, Rivier F, Baudou E, et al. Evaluating next-generation sequencing in neuromuscular diseases with neonatal respiratory distress. *Eur J Paediat Neurol*. (2021) 31:78–87. doi: 10.1016/j.ejpn.2021.01.011

7. Tubridy N, Fontaine B, Eymard B. Congenital myopathies and congenital muscular dystrophies. *Curr Opin Neurol*. (2001) 14:575–82. doi: 10.1097/00019052-200110000-00005

8. North KN, Wang CH, Clarke N, Jungbluth H, Vainzof M, Dowling JJ, et al. Approach to the diagnosis of congenital myopathies. *Neuromuscul Disord*. (2014) 24:97–116. doi: 10.1016/j.nmd.2013.11.003

9. Buxmann H, Schlösser R, Schlote W, Sewell A, Nowak KJ, Laing NG, et al. Congenital nemaline myopathy due to ACTA1-gene mutation and carnitine insufficiency: a case report. *Neuropediatrics*. (2001) 32:267–70. doi: 10.1055/s-2001-19122

10. Ilkovski B, Cooper ST, Nowak K, Ryan MM, Yang N, Schnell C, et al. Nemaline myopathy caused by mutations in the muscle α-skeletal-actin gene. *Am J Hum Genet*. (2001) 68:1333–43. doi: 10.1086/320605

11. Sparrow JC, Nowak KJ, Durling HJ, Beggs AH, Wallgren-Pettersson C, Romero N, et al. Muscle disease caused by mutations in the skeletal muscle alpha-actin gene (ACTA1). *Neuromuscular Disord*. (2003) 13:519–31. doi: 10.1016/S0960-8966(03)00101-9

12. Barohn RJ, Jackson CE, Kagan-Hallet KS. Neonatal nemaline myopathy with abundant intranuclear rods. *Neuromuscul Disord*. (1994) 4:513–20. doi: 10.1016/0960-8966(94)90092-2

13. Goebel HH, Warlo I. Gene-related protein surplus myopathies. *Mol Genet Metab*. (2000) 71:267–75. doi: 10.1006/mgme.2000.3064

14. Corbett MA, Robinson CS, Dunglison GF, Yang N, Joya JE, Stewart AW, et al. A mutation in α-tropomyosinslow affects muscle strength, maturation and hypertrophy in a mouse model for nemaline myopathy. *Hum Mol Genet*. (2001) 10:317–28. doi: 10.1093/hmg/10.4.317

15. Joureau B, de Winter JM, Conijn S, Bogaards SJP, Kovacevic I, Kalganov A, et al. Dysfunctional sarcomere contractility contributes to muscle weakness in ACTA1-related nemaline myopathy (NEM3). *Ann Neurol*. (2018) 83:269–82. doi: 10.1002/ana.25144

16. Schröder JM, Durling H, Laing N. Actin myopathy with nemaline bodies, intranuclear rods, and a heterozygous mutation in ACTA1 (Asp154Asn). *Acta Neuropathol*. (2004) 108:250–6. doi: 10.1007/s00401-004-0888-1

17. Hutchinson DO, Charlton A, Laing NG, Ilkovski B, North KN. Autosomal dominant nemaline myopathy with intranuclear rods due to mutation of the skeletal muscle ACTA1 gene: clinical and pathological variability within a kindred. *Neuromuscular Disord*. (2006) 16:113–21. doi: 10.1016/j.nmd.2005.11.004

18. North KN, Ryan MM. Nemaline Myopathy – RETIRED CHAPTER, FOR HISTORICAL REFERENCE ONLY In: MP Adam, GM Mirzaa, RA Pagon, SE Wallace, LJ Bean and KW Grippet al, editors. *GeneReviews®*. Seattle (WA): University of Washington, Seattle (1993)

19. Clarkson E, Costa CF, Machesky LM. Congenital myopathies: diseases of the actin cytoskeleton. *J Pathol*. (2004) 204:407–17. doi: 10.1002/path.1648

20. Labasse C, Brochier G, Taratuto AL, Cadot B, Rendu J, Monges S, et al. Severe ACTA1-related nemaline myopathy: intranuclear rods, cytoplasmic bodies, and enlarged perinuclear space as characteristic pathological features on muscle biopsies. *Acta Neuropathol Commun*. (2022) 10:101. doi: 10.1186/s40478-022-01400-0

21. Laitila JM, McNamara EL, Wingate CD, Goullee H, Ross JA, Taylor RL, et al. Nebulin nemaline myopathy recapitulated in a compound heterozygous mouse model with both a missense and a nonsense mutation in Neb. *Acta Neuropathol Commun*. (2020) 8:18. doi: 10.1186/s40478-020-0893-1

22. Yin X, Pu C, Wang Z, Li K, Wang H. Clinico-pathological features and mutational spectrum of 16 nemaline myopathy patients from a Chinese neuromuscular center. *Acta Neurol Belg*. (2022) 122:631–9. doi: 10.1007/s13760-020-01542-9

23. Nowak KJ, Ravenscroft G, Laing NG. Skeletal muscle α-actin diseases (actinopathies): pathology and mechanisms. *Acta Neuropathol*. (2013) 125:19–32. doi: 10.1007/s00401-012-1019-z

24. O'Grady GL, Best HA, Oates EC, Kaur S, Charlton A, Brammah S, et al. Recessive ACTA1 variant causes congenital muscular dystrophy with rigid spine. *Eur J Hum Genet*. (2015) 23:883–6. doi: 10.1038/ejhg.2014.169

25. Zukosky K, Meilleur K, Traynor BJ, Dastgir J, Medne L, Devoto M, et al. Association of a novel ACTA1 mutation with a dominant progressive scapuloperoneal myopathy in an extended family. *JAMA Neurol*. (2015) 72:689–98. doi: 10.1001/jamaneurol.2015.37

26. Ilkovski B. Evidence for a dominant-negative effect in ACTA1 nemaline myopathy caused by abnormal folding, aggregation and altered polymerization of mutant actin isoforms. *Hum Mol Genet*. (2004) 13:1727–43. doi: 10.1093/hmg/ddh185

27. Nowak KJ, Sewry CA, Navarro C, Squier W, Reina C, Ricoy JR, et al. Nemaline myopathy caused by absence of α-skeletal muscle actin. *Ann Neurol*. (2007) 61:175–84. doi: 10.1002/ana.21035

28. Kaindl A, Ruschendorf F, Krause S, Goebel H, Koehler K, Becker C, et al. Missense mutations of ACTA1 cause dominant congenital myopathy with cores. *J Med Genet*. (2004) 41:842–8. doi: 10.1136/jmg.2004.020271

29. D'Amico A, Graziano C, Pacileo G, Petrini S, Nowak KJ, Boldrini R, et al. Fatal hypertrophic cardiomyopathy and nemaline myopathy associated with ACTA1 K336E mutation. *Neuromuscul Disord*. (2006) 16:548–52. doi: 10.1016/j.nmd.2006.07.005

30. Lehtokari VL, Gardberg M, Pelin K, Wallgren-Pettersson C. Clinically variable nemaline myopathy in a three-generation family caused by mutation of the skeletal muscle alpha-actin gene. *Neuromuscular Disord*. (2018) 28:323–6. doi: 10.1016/j.nmd.2017.12.009

31. Feng JJ, Marston S. Genotype–phenotype correlations in ACTA1 mutations that cause congenital myopathies. *Neuromuscular Disord*. (2009) 19:6–16. doi: 10.1016/j.nmd.2008.09.005

32. Moreno CAM, Abath Neto O, Donkervoort S, Hu Y, Reed UC, Oliveira ASB, et al. Clinical and histologic findings in ACTA1-related nemaline myopathy: case series and review of the literature. *Pediatr Neurol*. (2017) 75:11–6. doi: 10.1016/j.pediatrneurol.2017.04.002

33. Wallgren-Pettersson C, Bushby K, Mellies U, Simonds A. 117th ENMC workshop: ventilatory support in congenital neuromuscular disorders — congenital myopathies, congenital muscular dystrophies, congenital myotonic dystrophy and SMA (II) 4–6 April 2003, Naarden, the Netherlands. *Neuromuscular Disord*. (2004) 14:56–69. doi: 10.1016/j.nmd.2003.09.003

34. Malfatti E, Romero NB. Nemaline myopathies: state of the art. *Revue Neurol*. (2016) 172:614–9. doi: 10.1016/j.neurol.2016.08.004

35. Ryan MM, Ilkovski B, Strickland CD, Schnell C, Sanoudou D, Midgett C, et al. Clinical course correlates poorly with muscle pathology in nemaline myopathy. *Neurol Int*. (2003) 60:665–73. doi: 10.1212/01.WNL.0000046585.81304.BC

36. Lim DS, Roberts R, Marian AJ. Expression profiling of cardiac genes in human hypertrophic cardiomyopathy: insight into the pathogenesis of phenotypes. *J Am Coll Cardiol*. (2001) 38:1175–80. doi: 10.1016/S0735-1097(01)01509-1

37. Nguyen MAT, Hardeman EC. Mouse models for thin filament disease In: NG Laing, editor. *The sarcomere and skeletal muscle disease*. New York, NY: Springer (2008). 66–77.

38. Crawford K, Flick R, Close L, Shelly D, Paul R, Bove K, et al. Mice lacking skeletal muscle actin show reduced muscle strength and growth deficits and die during the neonatal period. *Mol Cell Biol*. (2002) 22:5887–96. doi: 10.1128/MCB.22.16.5887-5896.2002

39. Ravenscroft G, Jackaman C, Bringans S, Papadimitriou JM, Griffiths LM, McNamara E, et al. Mouse models of dominant ACTA1 disease recapitulate human disease and provide insight into therapies. *Brain*. (2011) 134:1101–15. doi: 10.1093/brain/awr004

40. Sanoudou D, Haslett JN, Kho AT, Guo S, Gazda HT, Greenberg SA, et al. Expression profiling reveals altered satellite cell numbers and glycolytic enzyme transcription in nemaline myopathy muscle. *Proc Natl Acad Sci U S A*. (2003) 100:4666–71. doi: 10.1073/pnas.0330960100

41. Chowrashi P, Mittal B, Sanger JM, Sanger JW. Amorphin is phosphorylase; phosphorylase is an alpha-actinin-binding protein. *Cell Motility*. (2002) 53:125–35. doi: 10.1002/cm.10059

42. Quinlan KGR, Seto JT, Turner N, Vandebrouck A, Floetenmeyer M, Macarthur DG, et al. α-Actinin-3 deficiency results in reduced glycogen phosphorylase activity and altered calcium handling in skeletal muscle. *Hum Mol Genet*. (2010) 19:1335–46. doi: 10.1093/hmg/ddq010

43. Migocka-Patrzałek M, Elias M. Muscle glycogen phosphorylase and its functional partners in health and disease. *Cells*. (2021) 10:883. doi: 10.3390/cells10040883

44. Wallgren-Pettersson C, Laing NG. 109th ENMC international workshop: 5th workshop on nemaline myopathy, 11th–13th October 2002, Naarden, the Netherlands. *Neuromuscular Disord*. (2003) 13:501–7. doi: 10.1016/S0960-8966(03)00007-5

45. Wang CH, Dowling JJ, North K, Schroth MK, Sejersen T, Shapiro F, et al. Consensus statement on standard of care for congenital myopathies. *J Child Neurol*. (2012) 27:363–82. doi: 10.1177/0883073812436605

46. Nguyen MAT, Joya JE, Kee AJ, Domazetovska A, Yang N, Hook JW, et al. Hypertrophy and dietary tyrosine ameliorate the phenotypes of a mouse model of severe nemaline myopathy. *Brain*. (2011) 134:3516–29. doi: 10.1093/brain/awr274

47. Tinklenberg J, Meng H, Yang L, Liu F, Hoffmann RG, Dasgupta M, et al. Treatment with ActRIIB-mFc produces myofiber growth and improves lifespan in the Acta1 H40Y murine model of nemaline myopathy. *Am J Pathol*. (2016) 186:1568–81. doi: 10.1016/j.ajpath.2016.02.008

48. Tinklenberg JA, Siebers EM, Beatka MJ, Meng H, Yang L, Zhang Z, et al. Myostatin inhibition using mRK35 produces skeletal muscle growth and tubular aggregate formation in wild type and TgACTA1D286G nemaline myopathy mice. *Hum Mol Genet*. (2018) 27:638–48. doi: 10.1093/hmg/ddx431

49. Lindqvist J, Levy Y, Pati-Alam A, Hardeman EC, Gregorevic P, Ochala J. Modulating myosin restores muscle function in a mouse model of nemaline myopathy. *Ann Neurol*. (2016) 79:717–25. doi: 10.1002/ana.24619

50. Russell AJ, Hartman JJ, Hinken AC, Muci AR, Kawas R, Driscoll L, et al. Activation of fast skeletal muscle troponin as a potential therapeutic approach for treating neuromuscular diseases. *Nat Med*. (2012) 18:452–5. doi: 10.1038/nm.2618

51. Sztal TE, McKaige EA, Williams C, Ruparelia AA, Bryson-Richardson RJ. Genetic compensation triggered by actin mutation prevents the muscle damage caused by loss of actin protein. *PLoS Genet*. (2018) 14:e1007212. doi: 10.1371/journal.pgen.1007212

52. Yang K, Iannaccone S, Burkhalter LS, Reisch J, Cai C, Schindel D. Role of nerve and muscle biopsies in pediatric patients in the era of genetic testing. *J Surg Res*. (2019) 243:27–32. doi: 10.1016/j.jss.2019.04.085

53. Veneruso M, Fiorillo C, Broda P, Baratto S, Traverso M, Donati A, et al. The role of muscle biopsy in diagnostic process of infant hypotonia: from clinical classification to the genetic outcome. *Front Neurol*. (2021) 12:735488. doi: 10.3389/fneur.2021.735488

frontiers | Frontiers in Neurology

TYPE Case Report
PUBLISHED 23 April 2024
DOI 10.3389/fneur.2024.1342844

OPEN ACCESS

EDITED BY
Giovanni Meola,
University of Milan, Italy

REVIEWED BY
Idris Long,
University of Science Malaysia (USM), Malaysia
José Damián Carrillo-Ruiz,
General Hospital of Mexico, Mexico

*CORRESPONDENCE
Haijuan Zhang
✉ 1376724925@qq.com
Ziyu Ye
✉ yeziyu_edu@163.com
Linfang Zhao
✉ tigeryeah2022@163.com

†These authors have contributed equally to this work

RECEIVED 22 November 2023
ACCEPTED 02 April 2024
PUBLISHED 23 April 2024

CITATION
Wang C, Liu Y, Li L, Zhang H, Ye Z and Zhao L (2024) The efficacy of electroacupuncture for cervical nerve edema and movement disorder caused by the brachial plexus injury: a case report. *Front. Neurol.* 15:1342844. doi: 10.3389/fneur.2024.1342844

The efficacy of electroacupuncture for cervical nerve edema and movement disorder caused by the brachial plexus injury: a case report

Chao Wang[1†], Yingjun Liu[1†], Lu Li[1], Haijuan Zhang[1*], Ziyu Ye[2*] and Linfang Zhao[1*]

[1]The Third Affiliated Hospital of Zhejiang Chinese Medical University, Hangzhou, China, [2]Guangzhou University of Chinese Medicine, Guangzhou, China

The brachial plexus injury (BPI) is one of the most severe types of peripheral nerve injuries, often caused by upper limb traction injury. In clinic, the surgery is widely used to treat the BPI. However, surgery may need to be performed multiple times at different stages, which carries risks and brings heavy economic burden. In non-surgical treatment, splinting, local injection of corticosteroids, and oral corticosteroids can achieve significant short-term benefits, but they are prone to recurrence and may cause complications of mechanical or chemical nerve damage. In this report, we present a case of a 46-year-old female patient with BPI. The patient had difficulty in raising, flexing and extending of the left upper limb, and accompanied with the soreness and pain of neck and shoulder. After 3 months of EA treatment, a significant reduction in the inner diameter of the left C5 to C7 root at the outlet of brachial plexus nerve was detected by musculoskeletal ultrasound, and the soreness and pain in the left neck and shoulder were significantly reduced. The soreness and pain in the left neck and shoulder did not recur for 2 years.

Case summary: The patient is a 46-year-old female with BPI. She experienced difficult in lifting, flexing and extending of the left upper limb, which accompanied by soreness and pain in the left neck and shoulder. After 3 months of EA treatment, the patient's pain and limb's movement disorder was improved. After 2 years of follow-up, the patient's left neck and shoulder showed no further pain.

Conclusion: EA has shown satisfied efficacy in BPI, improving limb restrictions and relieving pain in patients for at least 2 years.

KEYWORDS

brachial plexus injury, electroacupuncture, cervical nerve edema, movement disorder, case report

Introduction

Brachial plexus injury (BPI) is one of the most common peripheral nerve injuries and is a disabling condition closely associated with trauma, fractures, and cervical spondylosis (1). The impairment of limb function significantly affects the patients' work and daily life (2). The brachial plexus is composed of the C5 to C8 cervical nerves and the anterior branch of the T1 thoracic nerve (3). Any nerve injury involving the brachial plexus is referred to be BPI.

Excessive traction is one of the major mechanisms leading to BPI, which happened on 95% of BPI patients and even more (4). Previous studies have shown that surgical intervention is considered to be the final solution for clinical management of BPI, but it carries high risks and costs (5). In non-surgical treatments, local corticosteroid injections, splinting, and oral corticosteroids have shown significant short-term benefits but are prone to recurrence and may lead to complications such as mechanical or chemical nerve damage (6). Therefore, selecting the optimal treatment approach for BPI is crucial. Electroacupuncture (EA) for BPI has been proven to be clinically effective with less adverse reactions, low long-term recurrence rates, and is considered as the best conservative treatment option for patients who unwilling to undergo surgery (4, 7). Current cases mostly use electromyography, computed tomography (CT), and other examinations to evaluate BPI, but the full data of brachial plexus edema, pain, limb motor, and mood throughout the treatment is not reported yet.

Currently, CT myelography is the gold standard for diagnosing BPI. However, some patients are afraid of the side effects of CT myelography (such as radiation, bleeding, infection, low-pressure headaches, allergies, etc.), and therefore refuse this examination (8). Magnetic resonance imaging (MRI) is more expensive and takes a longer time to perform the examination, and the patient is needed to keep calm in order to obtain clear imaging. Similarly, ultrasound can be used to evaluate almost all peripheral neuropathies without any radiation damage. But it is of high quality, low price, timely, and effective. It can clearly observe the shape and movement of the brachial plexus nerves, and can locate nerve entrapment (9).

Although early diagnosis and treatment of BPI play a very important role in effectively improving the prognosis, unexpected situations often occur, such as delays and unexpected situations happening in treatment and aggravation of symptoms after some treatments (10). This article will present a case of BPI, in which the patient was injured twice after brachial plexus injury, and her symptoms worsened after undergoing rehabilitation and massage. The patient was assessed by the musculoskeletal ultrasound examination in different time points. Finally, she received EA to relieve his symptoms, and no recurrence happened after two years of follow-up.

Case presentation

The patient was a 46-year-old female who experienced a strain in the left shoulder, resulting in difficulty in raising, flexing and extending of the left upper limb for 2 weeks. Subsequently, the patient's left shoulder pain worsened during dancing, and then she was diagnosed as BPI at the local hospital. Cervical spine X-ray in the lateral view revealed osteophyte formation at the C4-C6 vertebra and stenosis of the C4/5 intervertebral space. The patient received the rehabilitation and massage, but the symptoms worsened, and spontaneous twitching (Supplementary Video 1) in the left shoulder appeared. Further test revealed subacromial bursitis and a small cystic lesion in the proximal humerus of the left shoulder, as well as supraspinatus tendonitis on the ipsilateral side. As the condition gradually worsened, the patient was diagnosed with depression and anxiety symptoms, and accompanied by insomnia. As medications such as escitalopram, ibuprofen, and clonazepam were prescribed, the emotional disorder and insomnia of the patient were improved, while which didn't have significant effect on the pain and movement disorder (Table 2). In June 2020, the patient was admitted and the multi-disciplinary treatment was arranged for her.

After the physical examination, we found that the bilateral neck muscles were tense, which were accompanied with pain (Table 2) and restricted neck movement. Besides, the patient also appeared positive for paravertebral tenderness in the cervical 3–7 spinous process, positive for tenderness in the upper corner of the left scapula, and positive for left brachial plexus traction test. However, the results of both intervertebral foraminal compression test and neck rotation test are negative. The muscle tension of the limbs, muscle strength of the right upper limb, and tendon reflexes in both upper limbs are normal. The examination on muscle strength test of the left upper limb is uncooperative. Besides, the bilateral Hoffmann sign are negative.

Musculoskeletal ultrasound of the brachial plexus showed an increased inner diameter at the left C5 to C7 nerve root outlet compared to the right side, with uneven internal echoes and enhanced nerve sheath echoes. The inner diameter at the C5 nerve root outlet was approximately 0.44 cm, at the C6 nerve root exit was approximately 0.46 cm, and at the C7 nerve root exit was ~0.43 cm (Figure 1).

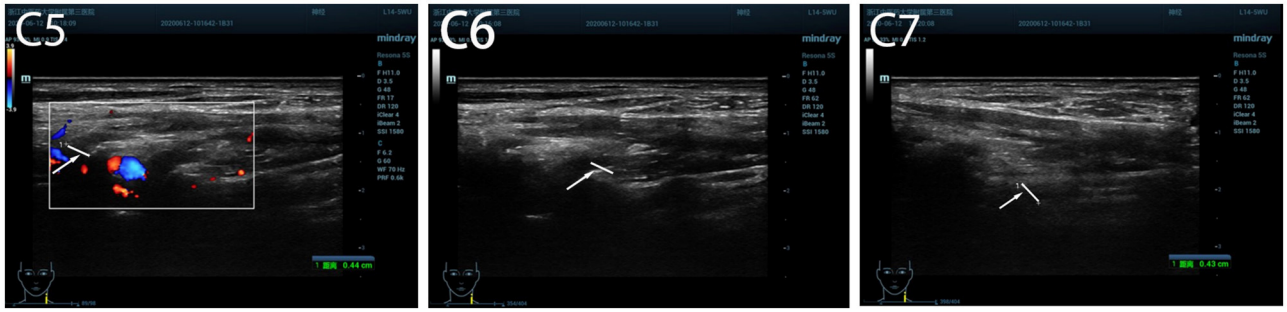

FIGURE 1
The inner diameter of cervical nerve root at C5, C6 C7 before treatment.

In order to further confirm the diagnosis, the patient underwent other tests. All blood tests, including the routine blood test, blood biochemical, electrolyte and metabolic profiles, were normal. The result of CT on the brain suggested no evidence of intracranial hemorrhage or territory infarction. The MRI of left shoulder revealed that left-sided cystic degeneration of the upper end of the humerus and left supraspinatus tendon disease. The electromyography of left upper limb shows no abnormalities. Thus, the patient was clearly diagnosed with BPI.

This patient was treated with stainless steel acupuncture needles (size: 0.25 mm × 40 mm) inserted into a depth of approximately 1.5 cun. Acupuncture was performed at acupoints, namely Jiaji (EX-B2), Jianyu (LI15), Jianliao (SJ14), Binao (LI14), Hegu (LI4) and Waiguan (SJ5) (Table 1). Connect one pair of positive and negative electrodes of the electrical stimulation device to Jianyu (LI15) and Jianliao (SJ14), and connect the other pair of positive and negative electrodes to Jiaji (EX-B2) upper and lower points bilaterally (Supplementary Figure 1). Set the knob of the electrical stimulation device (HANS-200A) to zero, select mode of continuous wave with a frequency of 2 Hz (11). Then, turn on the power, adjust the intensity gradually until the patient can tolerate it, based on the occurrence of rhythmic muscle contractions locally. Each session lasts for 30 min. After treatment, turn off the power, remove the electrodes, and withdraw the needle. Treat once every 2 days, continuously for 3 months.

TABLE 1 The framework of the acupuncture point prescription.

Acupoints	Locations
Jiaji (EX-B2)	Bilateral side to the posterior midline of the cervical spine, 0.5 cun apart from the 1st to 7th cervical spinous process
Jianyu (LI15)	Anterior and inferior to the acromion, in the depression between the acromion and the greater tuberosity of the humerus
Jianliao (SJ14)	In a depression appears posterior and inferior to the acromion when the arm is abducted.
Binao (LI14)	On the outside of the arm, at the insertion point of the deltoid muscle, 7 cun above Quchi point
Hegu (LI4)	Between the first and second metacarpals, and at the midpoint of the radial side of the second metacarpal

After 3 months of EA treatment, the ultrasound of brachial plexus showed that the inner diameter of the left C5 to C7 nerve root exits was relatively wider than the right side, with uneven internal echoes and enhanced nerve sheath echoes. The inner diameter at the C5 nerve root exit on the left side was approximately 0.38 cm, at the C6 nerve root outlet was approximately 0.39 cm, and at the C7 nerve root outlet was approximately 0.36 cm (Figure 2). Compared with pre-treatment, the inner diameter of the left C5 to C7 brachial plexus nerve root outlet was significantly reduced, the pain of the patient's left neck and shoulder was significantly relieved (Table 2), and the movement disorder of limbs was improved (Table 2, Supplementary Video 2).

After 2 years of follow-up, it was found that the inner diameter of the left C5 to C7 nerve root outlet was relatively wider than the right side, with even internal echoes and normal nerve sheath echoes. The inner diameter at the C5 nerve root outlet on the left side was approximately 0.30 cm, at the C6 nerve root outlet was approximately 0.38 cm, and at the C7 nerve root outlet was approximately 0.33 cm (Figure 3). Compared with the musculoskeletal ultrasound on BPI patient 2 years ago, the inner diameter of the left C5 to C7 brachial plexus nerve root outlet narrowed, and the patient did not experience a recurrence of soreness and pain (Table 2) in the left neck and shoulder, and the movement of limbs and emotion disorder restored to normal (Tables 2, 3). The timeline of this case report is shown in Figure 4.

Discussion

EA is a treatment in Traditional Chinese Medicine (TCM) that combines acupuncture to electrotherapy (12, 13). It regulates the physiological functions and disease state of the body by applying electrical stimulation at specific acupuncture points. EA analgesia mainly involves in inhibiting afferent spinal cord signals, mediating the release of substances (such as TNF-α), participating in axonal reflexes and nerve impulse regulation, thereby reducing pain sensation (14). Furthermore, EA has been shown to improve the microenvironment of the injured nervous system by increasing levels of endogenous neurotrophic factors and reducing inflammation, thereby rebuilding neuronal circuits,

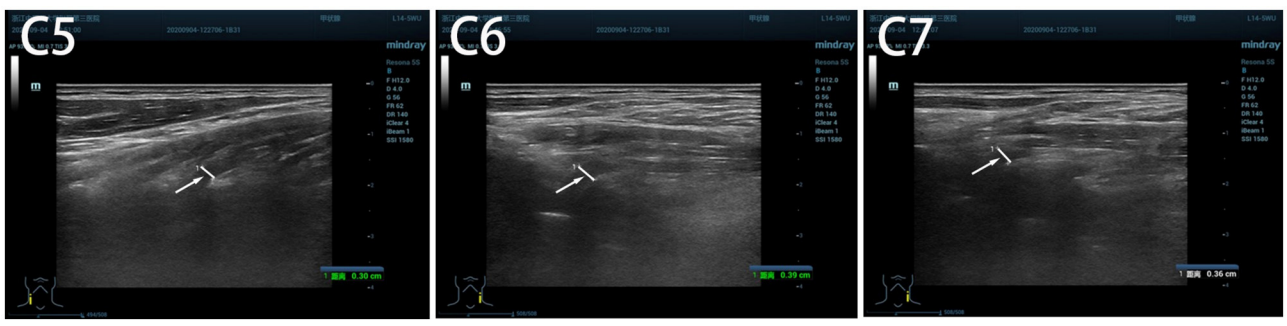

FIGURE 2
The inner diameter of cervical nerve root at C5, C6, C7 after 3 months' treatment.

restoring motor and sensory functions (15, 16). In addition, EA can reduce stroke-related nerve damage by promoting angiogenesis, alleviating inflammatory response, and regulating the blood-brain barrier (BBB) (17, 18). Some studies have proposed different mechanism of EA such as a decrease of C nerve fibers response in the spinal cord after repeated PNM in the sciatic or tibial nerve division in induced neuropathic nerves in cats (19). Although there is currently controversy over the mechanism of EA, the different EA parameters can produce a marked effect in specific situation. Clinical trials have shown improvements in strength, pain, and range of motion after the shoulder treated by EA (20, 21). The application of EA on neurogenic pain has shown that the ectopic emission signal of the damaged nerve is reduced, which translates into a reduction in pain perception (22), but evidence on this mechanism remains insufficient and further research is needed.

The BPI is one of the more serious peripheral nerve injury diseases, with partial or even complete loss sensorimotor function of the upper limbs as the main manifestation (23). The prevalence of the disease is increasing year by year, mainly caused by motor vehicle accidents, especially motorcycle traffic accidents (24) and traction injuries during neonatal delivery (25), which is seriously affecting people's daily life. There are a few case reports about BPI treated by acupuncture, but few papers are related to EA. In this case report, we observed the morphology of brachial plexus in different time points through musculoskeletal ultrasound which can directly reflect the damage and recovery of nerves. Meanwhile, we also estimated the pain and emotion of patient with BPI due the closed relationship between them. Different to previous reports, we have selected a middle-aged female patient who have experienced two traumatic injuries on brachial plexus, and their symptoms have worsened after other treatments. Thus, the process of their illness and changes are relatively complex. This case is about a 46-year-old female patient with brachial plexus damage and mixed cervical spondylosis, accompanied with poor lift, limited flexion and extension, spontaneous twitching of her left upper extremity, and pain in the left neck and shoulder treated with the EA. Musculoskeletal ultrasound in this case report revealed a significant reduction in the edema of brachial plexus nerve root. And the soreness, pain, and movement disorder in the left neck and shoulder were significantly reduced by the EA. During a two-year follow-up, the symptoms of BPI did not recur, and emotion disorder returned to normal. Based on the meridian theory and clinical practice experience of TCM, the acupuncture points such as Jiaji (EX-B2), Jianyu (LI15), Jianliao (SJ14), Binao (LI14), Hegu (LI4) and Waiguan (SJ5) were selected according to the local and remote therapeutic effect in the therapy of acupuncture. These acupuncture points are located in the distribution area of brachial plexus, blood vessels and tissues. The electrostimulation on these points can increase local blood circulation, repair nerve conduction (26, 27), and promote tissue repair. Meanwhile, EA is proved to decrease the edema of nerve (28) that is as same as what reported in this case report. The strength of the EA is the satisfactory effect on pain and motion which can last for 2 years without recurrence. Moreover, it is worth noting that the patient experienced local subcutaneous bleeding during the treatment, but the patient agreed to continue treatment only after communicating with the patient.

However, there were some limitations in this case report. Firstly, due to the number of cases involved in this case report is merely one, the evidence of the EA effectiveness is one-sided. Secondly, this case is under a specific situation, and no general conclusions can be drawn. Besides, the ultrasonic system and ultrasound technician in this report was changed within 2 years, which may lead to some biased results. In addition, since the patient had been taking analgesics and mood drugs, the impact of the medication on BPI patients could not be thoroughly excluded.

TABLE 2 The assessment of pain and mood.

Time points	VAS	HAMA	HAMD
Before admission	6	10	12
3 months after admission	2	8	9
2 years after treatment	0	7	6

TABLE 3 The assessment on the range of shoulder motion.

Time points	Forward flexion	Active abduction	Active external rotation
Before admission	60	90	23
3 months after admission	125	130	75
2 years after treatment	145	143	83

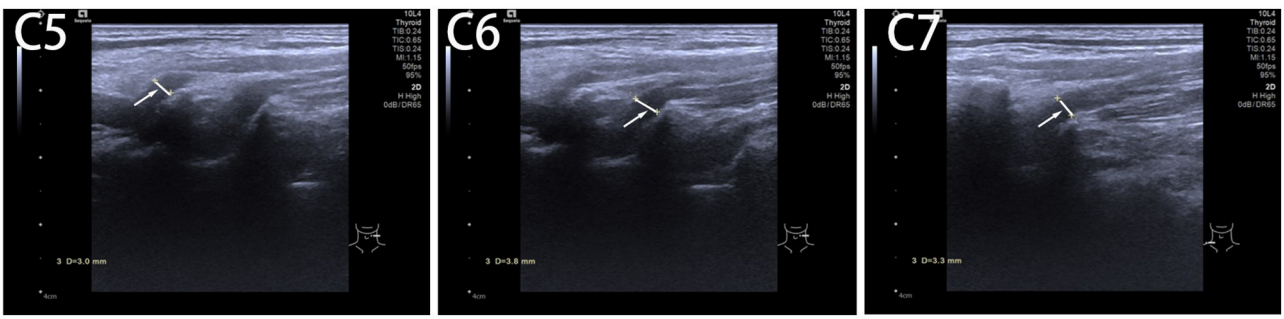

FIGURE 3
The inner diameter of cervical nerve root at C5, C6 C7 after 2 years of follow-up.

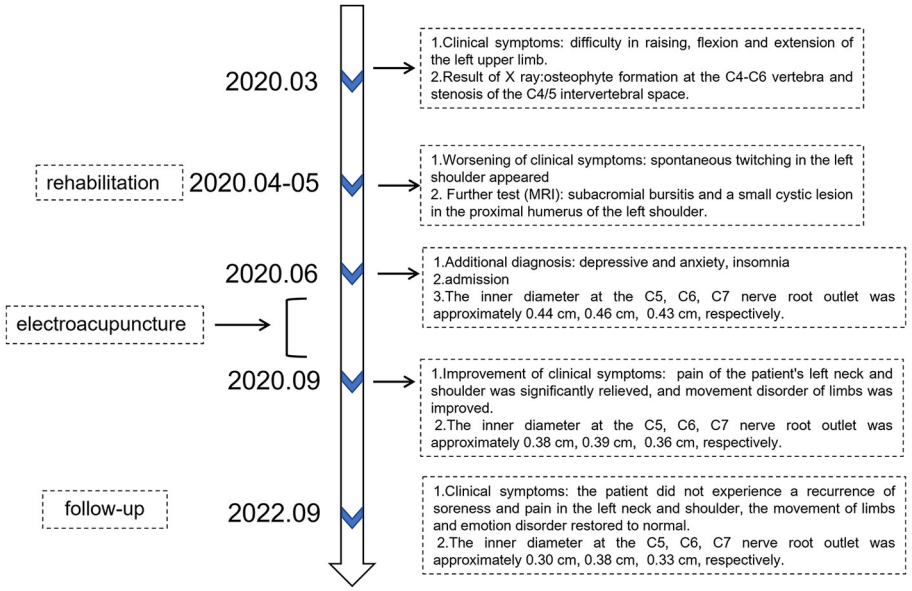

FIGURE 4
The timeline of disease course.

The musculoskeletal ultrasound, as one of the assessment methods, can provide more objective clinical evidence for the promotion of EA in future research. However, musculoskeletal ultrasound is still a maneuver-dependent tool, repeated measurement must be conducted to avoid bias. The current treatment duration and optimal parameters for EA treatment of BPI still require more in-depth studies to elucidate.

Conclusions

After 3 months of EA treatment, pain and joint function are improved for patients with BPI. And after 2 years, the patient did not experience a recurrence of soreness and pain in the left neck and shoulder. We understand that this study focuses only on the changes in the clinical symptom and musculoskeletal ultrasound, the bias of the results still can't be avoided. We hope that this case report can provide some theoretical bases for further exploring the clinical evidence of EA for BPI in the future.

Data availability statement

The original contributions presented in the study are included in the article/Supplementary material, further inquiries can be directed to the corresponding authors.

Ethics statement

The studies involving humans were approved by Third Affiliated Hospital of Zhejiang Chinese Medical University. The studies were conducted in accordance with the local legislation and institutional requirements. The participants provided their written informed consent to participate in this study. Written informed consent was obtained from the individual(s) for the publication of any potentially identifiable images or data included in this article.

Author contributions

CW: Writing – original draft. YL: Writing – original draft. LL: Methodology, Writing – review & editing. HZ: Writing – original draft. ZY: Investigation, Writing – review & editing. LZ: Conceptualization, Writing – review & editing.

Funding

The author(s) declare financial support was received for the research, authorship, and/or publication of this article. This work was mainly supported by Zhejiang Traditional Chinese Medicine Science and Technology Plan Project (No.2023ZL078) and secondarily supported by Scientific Research Project of Zhejiang Traditional Chinese Medicine University (No. 2022JKZKTS47).

Conflict of interest

The authors declare that the research was conducted in the absence of any commercial or financial relationships that could be construed as a potential conflict of interest.

Publisher's note

All claims expressed in this article are solely those of the authors and do not necessarily represent those of

their affiliated organizations, or those of the publisher, the editors and the reviewers. Any product that may be evaluated in this article, or claim that may be made by its manufacturer, is not guaranteed or endorsed by the publisher.

Supplementary material

The Supplementary Material for this article can be found online at: https://www.frontiersin.org/articles/10.3389/fneur.2024.1342844/full#supplementary-material

References

1. Gutkowska O, Martynkiewicz J, Urban M, Gosk J. Brachial plexus injury after shoulder dislocation: a literature review. *Neurosurg Rev.* (2020) 43:407–23. doi: 10.1007/s10143-018-1001-x

2. de Santana Chagas AC, Wanderley D, de Oliveira Ferro JK, Alves de Moraes A, Morais de Souza FH, da Silva Tenório A, et al. Physical therapeutic treatment for traumatic brachial plexus injury in adults: A scoping review. *PM&R.* (2022) 14:120–50. doi: 10.1002/pmrj.12566

3. Gilcrease-Garcia BM, Deshmukh SD, Parsons MS. Anatomy, imaging, and pathologic conditions of the brachial plexus. *RadioGraphics.* (2020) 40:1686–714. doi: 10.1148/rg.2020200012

4. Wang J, Wei L, Li G, Bao Y, Tang Y, Zhang L, et al. Electroacupuncture for brachial plexus injury caused by fracture of the right greater tuberosity of the humerus and dislocation of the right shoulder joint: a case report. *Acupunct Med.* (2022) 40:484–6. doi: 10.1177/09645284221085578

5. Arzillo S, Gishen K, Askari M. Brachial plexus injury: treatment options and outcomes. *J Craniofacial Surg.* (2014) 25:1200. doi: 10.1097/SCS.0000000000000841

6. Op de Coul LS, Bleeker S, de Groot JH, Nelissen RGHH, Steenbeek D. Elbow flexion contractures in neonatal brachial plexus palsy: A one-year comparison of dynamic orthosis and serial casting. *Clin Rehabil.* (2023) 37:72–85. doi: 10.1177/02692155221121011

7. Hou A-L, Zheng M-X, Hua X-Y, Huo B-B, Shen J, Xu J-G. Electroacupuncture-related metabolic brain connectivity in neuropathic pain due to brachial plexus avulsion injury in rats. *Front Neural Circuits.* (2020) 14:35. doi: 10.3389/fncir.2020.00035

8. Agarwal P, Mittal S, Sharma D. Diagnosis and management of adult BPI: results of first 50 cases. *J Clini Orthopaedics Trauma.* (2021) 12:166–71. doi: 10.1016/j.jcot.2020.06.036

9. Haber HP, Sinis N, Haerle M, Schaller H-E. Sonography of brachial plexus traction injuries. *Am J Roentgenol.* (2006) 186:1787–91. doi: 10.2214/AJR.04.1861

10. Chang C-Y, Wu Y-T, Chen L-C, Chan R-C, Chang S-T, Chiang S-L. Massage-induced brachial plexus injury. *Phys Ther.* (2015) 95:109–16. doi: 10.2522/ptj.20130487

11. Zhang W-T, Jin Z, Cui G-H, Zhang K-L, Zhang L, Zeng Y-W, et al. Relations between brain network activation and analgesic effect induced by low vs. high frequency electrical acupoint stimulation in different subjects: a functional magnetic resonance imaging study. *Brain Res.* (2003) 982:168–78. doi: 10.1016/S0006-8993(03)02983-4

12. Tu J-F, Yang J-W, Shi G-X, Yu Z-S, Li J-L, Lin L-L, et al. Efficacy of intensive acupuncture versus sham acupuncture in knee osteoarthritis: a randomized controlled trial. *Arthritis Rheumatol.* (2021) 73:448–58. doi: 10.1002/art.41584

13. Mawla I, Ichesco E, Zöllner HJ, Edden RAE, Chenevert T, Buchtel H, et al. Greater somatosensory afference with acupuncture increases primary somatosensory connectivity and alleviates fibromyalgia pain via insular γ-aminobutyric acid: a randomized neuroimaging trial. *Arthritis Rheumatol.* (2021) 73:1318–28. doi: 10.1002/art.41620

14. Shi G-X, Tu J-F, Wang T-Q, Yang J-W, Wang L-Q, Lin L-L, et al. Effect of electro-acupuncture (EA) and manual acupuncture (MA) on markers of inflammation in knee osteoarthritis. *J Pain Res.* (2020) 13:2171–9. doi: 10.2147/JPR.S256950

15. Guan J, Geng W-Q, Li Y, Liu G-Y, Ding L-B, Liu Y-J, et al. Decreased synovial fluid biomarkers levels are associated with rehabilitation of function and pain in rotator cuff tear patients following electroacupuncture therapy. *Med Sci Monit.* (2020) 26:e923240–1-e923240-10. doi: 10.12659/MSM.923240

16. Chassot M, Dussan-Sarria JA, Sehn FC, Deitos A, de Souza A, Vercelino R, et al. Electroacupuncture analgesia is associated with increased serum brain-derived neurotrophic factor in chronic tension-type headache: a randomized, sham controlled, crossover trial. *BMC Complement Altern Med.* (2015) 15:144. doi: 10.1186/s12906-015-0664-x

17. Yu N, Wang Z, Chen Y, Yang J, Lu X, Guo Y, et al. The ameliorative effect of bloodletting puncture at hand twelve Jing-well points on cerebral edema induced by permanent middle cerebral ischemia via protecting the tight junctions of the blood-brain barrier. *BMC Complement Altern Med.* (2017) 17:470. doi: 10.1186/s12906-017-1979-6

18. Xing Y, Yang S-D, Wang M-M, Dong F, Feng Y-S, Zhang F. Electroacupuncture alleviated neuronal apoptosis following ischemic stroke in rats via midkine and ERK/JNK/p38 signaling pathway. *J Mol Neurosci.* (2018) 66:26–36. doi: 10.1007/s12031-018-1142-y

19. Hanai F. Effect of electrical stimulation of peripheral nerves on neuropathic pain. *Spine.* (2000) 25:1886. doi: 10.1097/00007632-200008010-00005

20. Lo M-Y, Wu C-H, Luh J-J, Wang T-G, Fu L-C, Lin J-G, et al. The effect of electroacupuncture merged with rehabilitation for frozen shoulder syndrome: a single-blind randomized sham-acupuncture controlled study. *J Formosan Med Assoc.* (2020) 119:81–8. doi: 10.1016/j.jfma.2019.03.012

21. Shin S, Yang SP Yu A, Yoo J, Lim SM, Lee E. Effectiveness and safety of electroacupuncture for poststroke patients with shoulder pain: study protocol for a double-center, randomized, patient- and assessor-blinded, sham-controlled, parallel, clinical trial. *BMC Complement Altern Med.* (2019) 19:58. doi: 10.1186/s12906-019-2468-x

22. Qu Z, Liu L, Zhao L, Xu X, Li Z, Zhu Y, et al. Prophylactic electroacupuncture on the upper cervical segments decreases neuronal discharges of the trigeminocervical complex in migraine-affected rats: an in vivo extracellular electrophysiological experiment. *J Pain Res.* (2020) 13:25–37. doi: 10.2147/JPR.S226922

23. Wu KY, Spinner RJ, Shin AY. Traumatic brachial plexus injury: diagnosis and treatment. *Curr Opin Neurol.* (2022) 35:708–17. doi: 10.1097/WCO.0000000000001124

24. Kaiser R, Waldauf P, Haninec P. Types and severity of operated supraclavicular brachial plexus injuries caused by traffic accidents. *Acta Neurochir.* (2012) 154:1293–7. doi: 10.1007/s00701-012-1291-7

25. Van der Looven R, Le Roy L, Tanghe E, Samijn B, Roets E, Pauwels N, et al. Risk factors for neonatal brachial plexus palsy: a systematic review and meta-analysis. *Dev Med Child Neurol.* (2020) 62:673–83. doi: 10.1111/dmcn.14381

26. Li H, Yu L, Ye D, Chang L, Zhao F, Wang H, et al. Rehabilitation training combined with Jiaji electroacupuncture can promote the recovery of muscle group function and improve the quality of life in patients with upper limb peripheral nerve injury. *J Healthc Eng.* (2021) 2021:e3621568. doi: 10.1155/2021/3621568

27. Lan X, Zhang X, Zhou G, Wu C, Li C, Xu X. Electroacupuncture reduces apoptotic index and inhibits p38 mitogen-activated protein kinase signaling pathway in the hippocampus of rats with cerebral ischemia/reperfusion injury. *Neural Regen Res.* (2017) 12:409–16. doi: 10.4103/1673-5374.202944

28. Ahn SM, Kim YR, Shin Y-I, Ha KT, Lee S-Y, Shin HK, et al. Therapeutic potential of a combination of electroacupuncture and trkb-expressing mesenchymal stem cells for ischemic stroke. *Mol Neurobiol.* (2019) 56:157–73. doi: 10.1007/s12035-018-1067-z

frontiers | Frontiers in Neurology

TYPE Case Report
PUBLISHED 09 May 2024
DOI 10.3389/fneur.2024.1346353

OPEN ACCESS

EDITED BY
Giovanni Meola,
University of Milan, Italy

REVIEWED BY
Jan T. Groothuis,
Radboud University Medical Centre, Netherlands
Hua Liu,
The Affiliated Hospital of Southwest Jiaotong University, China

*CORRESPONDENCE
Zhiyou Cai
✉ caizhiyou@ucas.ac.cn

RECEIVED 29 November 2023
ACCEPTED 11 April 2024
PUBLISHED 09 May 2024

CITATION
Liu S, Sun H, Wang S, Liao J, Yang X and Cai Z (2024) Isolated unilateral brachial plexus injury following carbon monoxide intoxication: a case report and literature review.
Front. Neurol. 15:1346353.
doi: 10.3389/fneur.2024.1346353

Isolated unilateral brachial plexus injury following carbon monoxide intoxication: a case report and literature review

Shu Liu[1,2,3,4,5], Houchao Sun[4,5], Shengyuan Wang[1,2,3,4,5], Jincheng Liao[1,2,3,4,5], Xu Yang[4,5] and Zhiyou Cai[1,2,3,4,5]*

[1]Chongqing Medical University, Chongqing, China, [2]Chongqing Institute of Green and Intelligent Technology, Chinese Academy of Sciences, Chongqing, China, [3]Chongqing School, University of Chinese Academy of Sciences, Chongqing, China, [4]Department of Neurology, Chongqing General Hospital, Chongqing, China, [5]Chongqing Key Laboratory of Neurodegenerative Diseases, Chongqing University, Chongqing, China

Carbon monoxide (CO) is a gas that has no odor or color, making it difficult to detect until exposure leads to coma or death. CO poisoning is one of the most common and deadly poisonings around the world. CO poisoning is a common and often fatal form of poisoning worldwide. A toxic effect of CO is tissue hypoxia, which leads to systemic complications. Additionally, there may be severe neurological symptoms and delayed complications following CO poisoning. However, peripheral neuropathy is relatively rare after CO poisoning. Previously, only one case of unilateral plexopathy after CO poisoning, accompanied by rhabdomyolysis and cognitive dysfunction, has been reported. In this report, an isolated unilateral brachial plexopathy following CO intoxication is described. A key mechanism in this case may be CO-induced spinal cord ischemia. Immediate administration of hyperbaric oxygen therapy (HBOT) is crucial to prevent peripheral neuropathy after acute CO intoxication. Hyperbaric oxygen therapy (HBOT) should be administered immediately after acute CO intoxication to prevent peripheral neuropathy. Additionally, peripheral neuropathy following acute CO intoxication may benefit from consistent rehabilitation training.

KEYWORDS

carbon monoxide intoxication, peripheral neuropathy, hyperbaric oxygen therapy, spinal cord ischemia, rehabilitation training

Introduction

Carbon monoxide (CO) is a gas that is both colorless and odorless, making it difficult to detect. Its potential danger lies in its ability to cause coma or even death without being noticed. CO poisoning is a common and fatal type of poisoning that is widespread across the globe. The toxicity of CO leads to tissue hypoxia, resulting in a range of systemic and neurological complications. However, the occurrence of peripheral neuropathy following CO poisoning is relatively uncommon and typically affects younger individuals.

10.3389/fneur.2024.1346353

TABLE 1 Motor nerve conduction study and sensory nerve conduction study in the patient after carbon monoxide intoxication.

Nerve	Dl	Amp	Dis	Vel
	mS	mV	mm	m/s
MNCS				
Axillaris left				
Erb-Del.	8.85	1.19		
Medianus left				
Erb-Del.	3.67	12.5		
Medianus left				
Wrist-APB	3.27	20.1		
Elb-APB	6.72	18.1	195	56.5
Elb-F	25.8	0.55		
Musculocutaneous left				
Erb-Biceps	8.41	0.29		
Musculocutaneous right				
Erb-Tricep	4.67	24.8		
Radialis left				
Erb-Tricep	4.45	19.7		
Ulnaris left				
Wrist-ADM	2.42	13.1		
Elbow-ADM	5.33	12.9	195	67
Stim 1-F	21.1	2.3		
Stim 2-F	20.3	2.7		
SNCS				
Medianus left				
Wrist-DigII	2.6	17.6	170	65.4
Ulnaris left				
Wrist-DigV	1.96	46.9	120	61.2

MNCS, motor nerve conduction study; Dl, distal latency; Amp, amplitude; Dis, distance; Vel, velocity; Erb, elbow; Del, deltoid; APB, abductor pollicis brevis; ADM, abductor digiti minimi; Sti, stimulation; SNCS, sensory nerve conduction study.

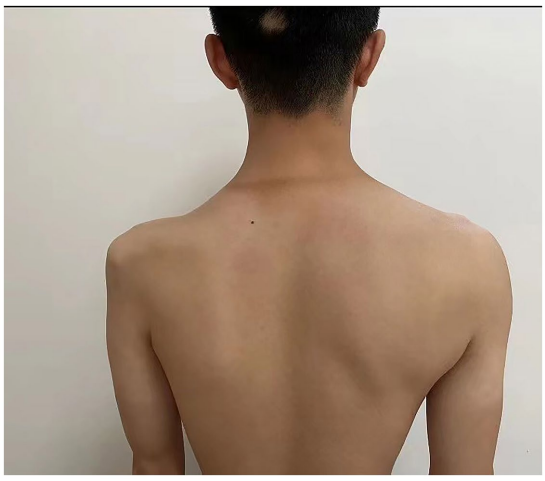

FIGURE 1
The muscle profile of the patient.

Case report

On 11 February 2022, a 31-year-old man was found unconscious by his wife after sleeping in a closed car for approximately 7 h. He was admitted to the hospital and diagnosed with acute CO poisoning. Blood tests showed an elevated level of carbon monoxide hemoglobin (13.8%). Brain magnetic resonance imaging (MRI) revealed small, slightly brighter signals in the bilateral basal ganglia. After being in a coma for about 12 h, he regained consciousness without any cognitive deficits. However, he woke up with weakness in his left upper arm and limited movement of the limb.

The patient's left arm was paralyzed, as indicated by a grade 1 muscle test on the medical research council (MRC) scale during neurological examination. There was also reduced sensation to temperature, pain, and vibration in the distal region of the left arm, and absent deep tendon reflexes in the left upper arm. Ultrasonic examination showed swelling of the left median and radial nerves in the forearm and upper arm. A motor nerve conduction study indicated normal motor conduction velocity (MCV) for the left ulnar, median, and radial nerves, but a decreased compound muscle action potentials (CMAP) amplitude for the left axillary and musculocutaneous nerves. Sensory conduction velocity (SCV) for the left median and ulnar nerves fell within the normal range (Table 1). Needle electromyography revealed abnormal spontaneous activities, including positive sharp waves and fibrillation potentials, in the left deltoid, biceps brachii, and triceps brachii (Table 2). Electrophysiological interpretation suggested severe abnormalities in the upper branches and moderate abnormalities in the middle branches, indicating the presence of left brachial plexopathy involving the upper and middle branches. After receiving around 80 sessions of hyperbaric oxygen therapy (HBOT) once daily for 90 min each session, and undergoing rehabilitation training including exercise training, low-frequency pulsed electrical therapy, ultrasound therapy, as well as acupuncture, massage, electroacupuncture, and acupoint injection, the patient returned to the hospital for a follow-up examination 70 days after the CO poisoning incident. There was a slight improvement in the restricted movement of his left upper limb. Manual muscle tests revealed an MRC grade of 3 in the muscle groups of the left upper arm, including the left biceps brachii, triceps brachii, brachialis, brachioradialis, and deltoid. Sensation to pinprick and light touch in the left upper limb was present. Additionally, the patient did not show any other long-term effects. However, significant atrophy of the left deltoid and biceps muscles was noted (Figure 1). Compared to the initial admission, the re-examination of the cerebral MRI showed no significant changes. The sensory nerve conduction study revealed decreased nerve conduction velocity and amplitude in the left radial nerves (Table 3). Motor nerve conduction was normal, except for highly decreased motor amplitude in the left axillary and musculocutaneous nerves (Table 4). Besides, the N20 latency of the left median nerve is normal, but the amplitude is relatively lower compared to the right side, suggesting abnormal left upper limb somatosensory evoked potentials (SEP). The electrophysiological conclusion for this readmission indicated left incomplete brachial plexopathy.

The patient's subsequent examination findings remained largely unchanged from the initial assessment. However, we conducted a comprehensive magnetic resonance imaging (MRI) of the entire spine for the patient. The results revealed a long strip of high signal intensity in the left region of the cervical medulla at the 4/5 intervertebral space level (Figure 2). Throughout his current

hospital stay, the patient has been receiving ongoing rehabilitation training and HBOT.

Discussion

Carbon monoxide (CO) is known to have toxic effects on various systems in the body, including the central nervous system, cardiovascular system, respiratory system, hematological system, metabolic and endocrinological system, musculoskeletal system, and sensory systems such as vision and hearing. While there have been numerous reports on the effects of CO poisoning on the cardiovascular system and central nervous system, such as memory loss, encephalopathy, speech difficulties and Parkinson's-like symptoms, however, there is a limited amount of research available specifically focusing on the development of peripheral neuropathies in CO poisoning cases.

To the best of our knowledge, a comprehensive clinical study on peripheral neuropathy following CO poisoning has been conducted. The study examined 2,759 patients with acute CO poisoning between 1976 and 1982, and 23 individuals (11 men and 12 women, with a mean age of 29.3) were diagnosed with peripheral neuropathy through electrophysiological detection. Among these patients, 14 had sensory symptoms, 8 had mixed symptoms, and only one had isolated motor symptoms. The majority of cases involved the lower extremities, with only two cases affecting other areas. The study also revealed that peripheral neuropathy following CO poisoning primarily affected young individuals, and all patients recovered within a period of 3 to 6 months (1). Furthermore, Rahmani et al. (2) reported a case of a 42-year-old man who experienced reversible bilateral brachial plexus injury following acute CO poisoning. The patient showed a favorable prognosis after receiving HBOT. Gi-Young Park et al. (3) reported a case of unilateral brachial plexopathy accompanied by impaired cognitive function after CO intoxication. Electrophysiological interpretation indicated an incomplete brachial plexopathy with axonal involvement. The 45-year-old patient exhibited a poor prognosis, with no significant improvement in left upper extremity weakness and cognitive function even after 11 months of CO intoxication. Other articles have also documented cases of peripheral neuropathy following CO intoxication, including sciatic neuropathy and rhabdomyolysis, motor and sensory peripheral neuropathy, and unilateral diaphragmatic paralysis.

The exact underlying mechanisms of peripheral neuropathy following CO poisoning are still uncertain. However, there are four potential mechanisms that could contribute to this condition: hypoxia and subsequent ischemia caused by CO, nerve compression, the cytotoxic effects of CO, and petechial hemorrhages. CO induces hypoxia by forming carboxyhemoglobin (COHb) and binding to heme-containing proteins, particularly cytochrome c oxidase and myoglobin. Additionally, CO binds to heme proteins in platelets, leading to the release of nitric oxide (NO). Increased levels of NO result in the production of peroxynitrite (ONOO), which impairs mitochondrial function and exacerbates tissue hypoxia (Figure 3) (4). The central nervous system is particularly susceptible to the effects of ischemia and hypoxia. The thoracic spinal cord receives blood supply from the radiculomedullary arteries, which originate from a few intercostal arteries branching from the subclavian artery and aorta. Impairment of blood flow through these arteries can pose a significant risk of ischemia due to limited collateralization in the thoracic vascular region. Additionally, the watershed effect, which occurs when two streams of blood flowing in opposite directions meet, is common in the spinal cord's vascular system. The midthoracic area exhibits the maximum watershed effect due to the greatest distance between radicular arteries (5). In this case, a long strip of high T2 signal was observed in the left part of the cervical medulla at the level of the 4/5 intervertebral space. An abnormal signal intensity was also present in the left cervical spinal cord, correlating with the clinical symptoms and signs. A disk protrusion was noted at that level, although it did not compress the spinal cord sufficiently to cause brachial plexus injury. The patient was found lying in the driver's seat with his head tilted to the left by his wife. It is possible that spondylogenic compression myelopathy (possibly due to ischemia) may have been related to the unconscious patient's position in the car. Therefore,

TABLE 2 Electromyographic findings in the patient after carbon monoxide intoxication.

Spontaneous activities			
Muscle	Explanation	Fib	PSW
Right Biceps	Normal	0/10	0/10
Right Deltoid	Normal	0/10	0/10
Right Vastus	Normal	0/10	0/10
Left Vastus	Normal	0/10	0/10
Left ADM	Normal	0/10	0/10
Left Abd pollicis brevis	Normal	0/10	0/10
Left Triceps		2/10	0/10
Left Biceps	Loss of MU	6/10	6/10
Left Deltoid	Loss of MU	6/10	6/10

Fib, fibrillation potential; PSW, positive sharp wave; ADM, abductor digiti minimi; Abd, abductor.

TABLE 3 Sensory nerve conduction study in the patient when readmission.

Nerve/Part	Site	Onset Lat	Peak Lat	Amp	Distance	Velocity
		ms	ms	mm	mm	m/s
Left median nerve—middle finger						
Wtist	DigIII	2.4	3.18	56.4	125	52
Left ulnar nerve—Little finger						
Wrist	DigV	2.08	2.81	31.5	100	48
Left radial nerve—anatomical snuff box (Forearm)						
Forearm	Wrist	2.19	2.92	14.0	95	43

Lat, latency; Dig, digiti; Amp, amplitude.

TABLE 4 Motor nerve conduction study in the patient when readmission.

Nerve/Part	Muscle	Latency	Amplitude	Distance	Velocity
		ms	mV	mm	m/s
Left radial nerve—EIP					
Forearm	EIP	2.34	3.3		
Spiral Gr	EIP	3.7	3.6	80	59
Left median nerve—Abductor pollicis brevis					
Wrist	Abductor pollicis brevis	3.23	9.4		
Elbow	Abductor pollicis brevis	6.25	10.9	160	53
Left ulnar nerve—ADM					
Wrist	Abductor digiti minimi	2.66	10.9		
Elbow	Abductor digiti minimi	5.1	9.0	160	65
Left axillary nerve—Deltoid					
Erb's	Deltoid	2.92	8.9	190	
Left musculocutaneous nerve—Biceps					
Erb's	Biceps	4.79	1.6	302	
Right axillary nerve—Deltoid					
Erb's	Deltoid	3.44	28		
Right musculocutaneous nerve—Biceps					
Erb's	Biceps	3.96	9.1		
Right radial nerve—EIP					
Forearm	EIP	2.60	8.9		
Spiral Gr	EIP	4.01	9.2	95	68

EIP, extensor indicis proprius; Erb, elbow; ADM, abductor digiti minimi.

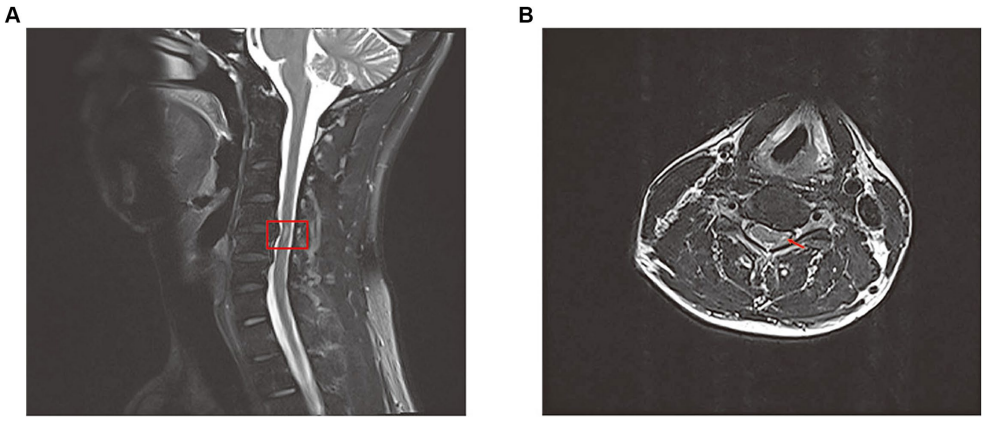

FIGURE 2
Total spine magnetic resonance image(MRI) revealed long strip T2 high signal in the left part of the cervical medulla at the level of the 4/5 intervertebral space on sagittal position **(A)** and cross section **(B)**.

we suspect that spinal cord ischemia caused by CO intoxication may be a key mechanism in the development of left brachial plexopathy. Additionally, nerve compression and the cytotoxic effects of CO should also be taken into consideration.

In our case, a young man experienced isolated unilateral brachial plexus injury following acute CO poisoning, with incomplete improvement after nearly 3 months. This represents the second reported case of unilateral brachial plexopathy following CO intoxication in the literature thus far.

Conclusion

The main mechanism behind unilateral brachial plexopathy following CO poisoning may be the ischemia of the spinal cord. Therefore, it is crucial to promptly address the hypoxia caused by CO through treatments like HBOT and normobaric 100% oxygen therapy to prevent peripheral neuropathy after acute CO intoxication. Additionally, consistent participation in rehabilitation training may play a significant role in the treatment of peripheral neuropathy following acute CO poisoning.

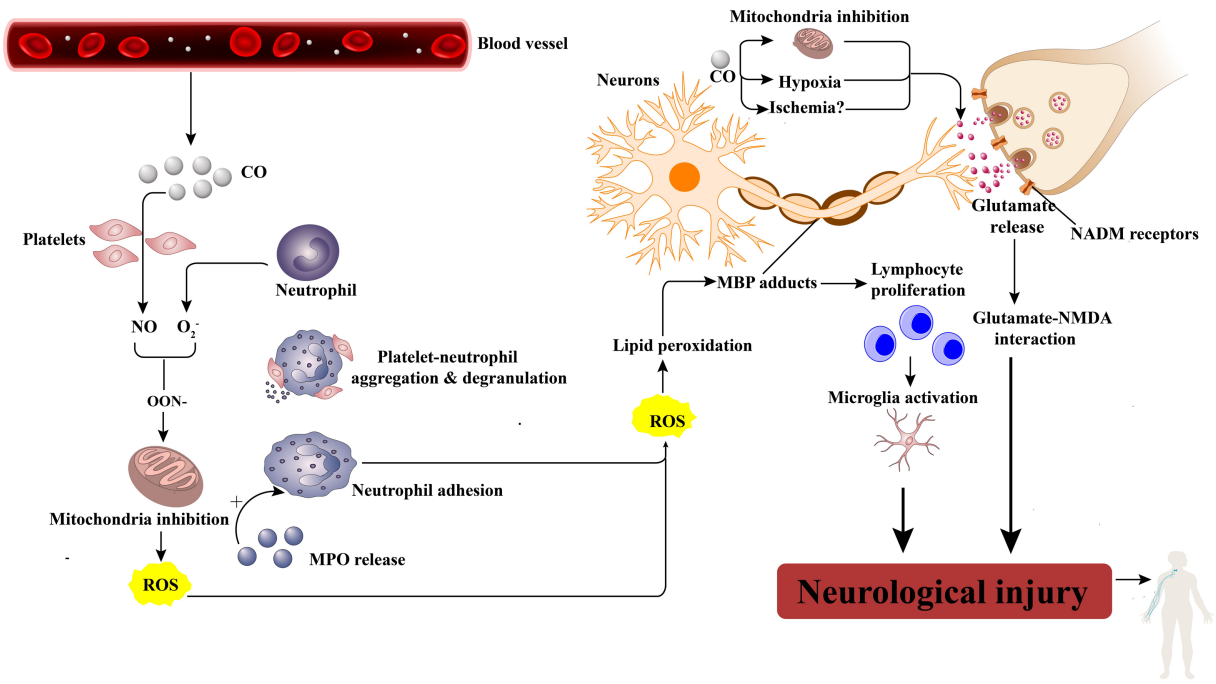

FIGURE 3
CO leads to neurologic injury. CO activates platelets by displacing platelet nitric oxide (NO) from surface hemoproteins. NO reacts with oxygen free radicals ($O2^-$) to produce peroxynitrite (ONOO2), which inhibits mitochondrial function and produces reactive oxygen species(ROS). Besides, activated neutrophils by NO will degranulate and release myeloperoxidase (MPO), which causes more neutrophil activation and adhesion, thereby causing cellular damage as well as lipid peroxidation, specifically on myelin basic protein (MBP). When peroxidated, MBP forms adducts that cause lymphocyte proliferation, microglia activation, and, finally, neurologic injury. Moreover, the general effects of hypoxia and the effect of CO toxicity directly on mitochondria cause glutamate release, which activates N-methyl-D-aspartate (NMDA) receptors, further leading to neurologic injury.

Data availability statement

The original contributions presented in the study are included in the article/supplementary material, further inquiries can be directed to the corresponding author.

Ethics statement

The studies involving humans were approved by the Institutional Review Board at Chongqing General Hospital. The studies were conducted in accordance with the local legislation and institutional requirements. Written informed consent for participation was not required from the participants or the participants' legal guardians/next of kin in accordance with the national legislation and institutional requirements. Written informed consent was obtained from the individual(s) for the publication of any potentially identifiable images or data included in this article.

Author contributions

SL: Conceptualization, Formal analysis, Visualization, Writing – original draft, Writing – review & editing. HS: Formal analysis, Writing – review & editing. SW: Formal analysis, Visualization, Writing – review & editing. JL: Visualization, Writing – review & editing. XY: Visualization, Writing – review & editing. ZC: Funding acquisition, Supervision, Writing – review & editing.

Funding

The author(s) declare that financial support was received for the research, authorship, and/or publication of this article. This work was supported by the Foundation of Capacity Improvement in Neurology Department of Chongqing (ZS03174).

Acknowledgments

The authors would like to acknowledge that this article has been published as a preprint on Research Square at the following DOI: https://doi.org/10.21203/rs.3.rs-2364878/v1.

Conflict of interest

The authors declare that the research was conducted in the absence of any commercial or financial relationships that could be construed as a potential conflict of interest.

Publisher's note

All claims expressed in this article are solely those of the authors and do not necessarily represent those of their affiliated organizations, or those of the publisher, the editors and the reviewers. Any product that may be evaluated in this article, or claim that may be made by its manufacturer, is not guaranteed or endorsed by the publisher.

References

1. Choi IS. A clinical study of peripheral neuropathy in carbon monoxide intoxication. *Yonsei Med J*. (1982) 23:174–7. doi: 10.3349/ymj.1982.23.2.174

2. Rahmani M, Belaidi H, Benabdeljlil M, Bouchhab W, El Jazouli N, El Brini A, et al. Bilateral brachial plexus injury following acute carbon monoxide poisoning. *BMC Pharmacol Toxicol*. (2013) 14:61. doi: 10.1186/2050-6511-14-61

3. Park GY, Kwon DR, Jung WB. Unilateral brachial plexus injury following carbon monoxide intoxication: a case report. *Medicine*. (2018) 97:e11699. doi: 10.1097/MD.0000000000011699

4. Chenoweth JA, Albertson TE, Greer MR. Carbon Monoxide Poisoning. *Crit Care Clin*. (2021) 37:657–72. doi: 10.1016/j.ccc.2021.03.010

5. Martirosyan NL, Feuerstein JS, Theodore N, Cavalcanti DD, Spetzler RF, Preul MC. Blood supply and vascular reactivity of the spinal cord under normal and pathological conditions. *J Neurosurg Spine*. (2011) 15:238–51. doi: 10.3171/2011.4.SPINE10543

Frontiers in Neurology

Explores neurological illness to improve patient care

The third most-cited clinical neurology journal explores the diagnosis, causes, treatment, and public health aspects of neurological illnesses. Its ultimate aim is to inform improvements in patient care.

Discover the latest Research Topics

See more →

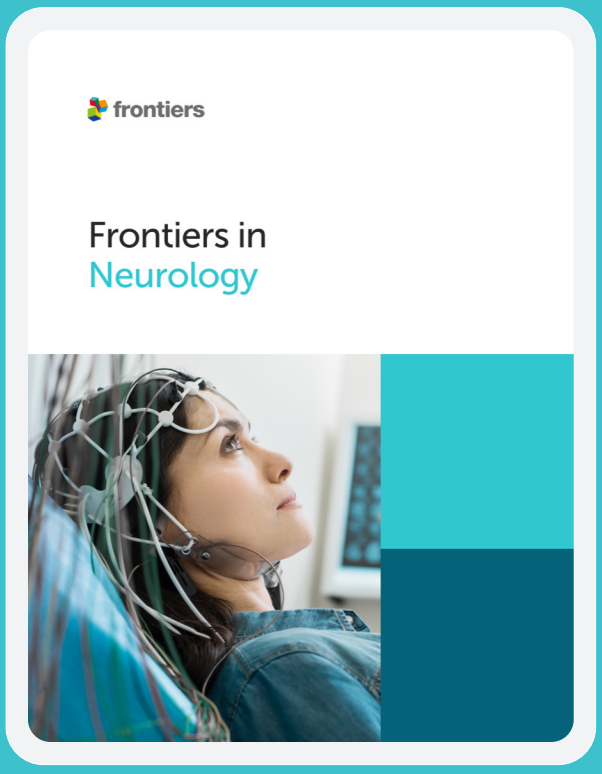

Frontiers

Avenue du Tribunal-Fédéral 34
1005 Lausanne, Switzerland
frontiersin.org

Contact us

+41 (0)21 510 17 00
frontiersin.org/about/contact